THE DEVELOPMENT AND ASSESSMENT OF A FIXED DOSE COMBINATION TABLET OF RANITIDINE AND METRONIDAZOLE

by

Loti David King'ori

A Thesis Submitted to Rhodes University
in Fulfilment of the Requirements for the Degree of

MASTER OF SCIENCE (PHARMACY)

January 2011

Faculty of Pharmacy
RHODES UNIVERSITY
Grahamstown
South Africa

ABSTRACT

The oral route of drug administration is convenient since it is acceptable to most patients and the manufacturing processes used to produce tablets and capsules are relatively simple when compared to those used to manufacture other types of dosage forms. Metronidazole (MTZ) and Ranitidine (RTD) have been used in combination, as part of triple therapy for the treatment of ulcers. However the use of large numbers of tablets and long duration of therapy makes adherence to drug treatment challenging for patients. Therefore the formulation of a fixed dose combination (FDC) of MTZ and RTD may improve patient adherence to therapy and consequently may reduce morbidity and mortality due to ulcers.

A stability indicating HPLC method for the simultaneous analysis of MTZ and RTD was developed and validated according to the International Conference on Harmonization (ICH) guidelines. The method was sensitive, selective, precise, accurate and linear.

Preformulation studies were performed on the active pharmaceutical ingredients (API) alone and in combination with potential excipients. Differential scanning calorimetry (DSC) studies revealed a potential interaction between MTZ and RTD, however the interaction was not apparent following IR analysis of the same samples. DSC analyses of the API in combination with potential excipients revealed that the compounds were compatible with most materials with the exception of a binary mixture of RTD and Dibasic calcium phosphate (DCP) that exhibited a potential interaction. Thermal gravimetric analysis (TGA) of MTZ and RTD revealed that both compounds exhibited thermal stability. The Carrs Index (CI) and Hausner Ratio (HR) values of MTZ and RTD indicated that both compounds exhibited poor flow and compressibility properties, whereas the CI and HR values for (Microcrystalline cellulose) MCC and DCP indicated better flowability and compressibility characteristics.

Direct compression and wet granulation processes were assessed to identify a suitable method of manufacture of FDC tablets of MTZ and RTD. The blends were evaluated using bulk and tapped density and the resultant tablets were evaluated for weight uniformity, crushing strength, tensile strength and disintegration time. The wet granulation method of manufacture produced tablets that showed acceptable pharmacotechnical properties: this approach was therefore used as the method of manufacture of FDC tablets of MTZ and RTD.

Tablet formulations comprised of API, *viz.* MTZ and RTD and different compositions of MCC, DCP, Sodium starch glycolate (SSG) and Croscarmellose sodium (CCS), were manufactured in order to screen for an appropriate diluent and disintegrant composition for use in response surface studies. Assays of tablet content and *in vitro* drug release were undertaken using the validated HPLC method. Tablets in which MCC and CCS were used appeared to produce better assay and dissolution results as compared to those manufactured using DCP and SSG. Consequently a formulation comprised of MCC and CCS was selected and used in studies in which the effect(s) of level two formulation and composition changes as described in the Scale and Post Approval Changes for Immediate Release (SUPAC-IR) Guidelines on tablet disintegration and *in vitro* release were assessed. A Box-Behnken statistical design was used for the investigation of the effect of input factors, *viz.* CCS, (Polyvinyl pyrollidone K30) PVP-K30 and magnesium stearate on measured responses, *viz.* disintegration time and percent drug release in 10 minutes (Q_{10}). CCS appeared to have an inverse linear relationship on disintegration time and a linear relationship with the Q_{10} for MTZ and RTD, whereas PVP-K30 and magnesium stearate appeared to have an antagonistic effect on the measured responses. Furthermore CCS and magnesium stearate exhibited an interaction that had an agonistic effect on the Q_{10} value for RTD. A numerical optimization

approach was used to predict a formulation composition that would produce tablets that exhibited a disintegration time and Q_{10} values for MTZ and RTD that fell within the constraints set in our laboratory. The resultant model was found to be accurate and had a percent prediction error of < 5% for all measured response variables.

FDC tablets of MTZ and RTD have been successfully produced. The disintegration of the tablet and dissolution of the API were within compendial specifications and the tablets are of suitable quality and have the potential to be further investigated to reduce the pill burden in the treatment of ulcers.

ACKNOWLEDGEMENTS

I would like to express my sincere gratitude to the following people:
My supervisor, Professor R. B. Walker for his, guidance, support and patience throughout this research,

The Head and Dean of the Faculty of Pharmacy at Rhodes University Professor R. B. Walker for the opportunity to conduct this research and provision of laboratory space, equipment and facilities during the course of this research,

Mr T. Samkange, Mr L. Purdon, Mr C. Nontyi, Ms L. Emslie, Mr D. Morley and Ms. S. Morley for their technical assistance during my studies.

Dr F. A. Chaibva for providing thoughtful ideas and assistance in understanding the concept of Statistical Design of Experiment and Response Surface Methodology,

Dr W. K. M. Kasongo, Dr S. M. M. Khamanga, my colleagues in the BRG, the Faculty of Pharmacy and Department of Chemistry for their support, encouragement and making the duration of my study pleasurable and fun,

My parents, Mr and Mrs D.K. Mollel for their financial support throughout my studies and to my siblings Nengai, Esuvat, Baraka and relatives for their financial support during my holiday and who believed in me in moments that I thought things fell apart,

The warden at Gavin Relly Post Graduate Village, Professor L. Juma, fellow Sub-warden, Ms G. Kasere, and my friend Mr T. Mutengwa (Beef) who helped me with my sub-warden responsibilities during the course of my research.

STUDY OBJECTIVES

Metronidazole (MTZ) and ranitidine (RTD) are used as part of triple therapy in the management of ulcers. The desired clinical outcome when treating uncomplicated ulcers is dependent on patient adherence to pharmacotherapy. However drug therapy in the treatment of ulcers may require the administration of a large number of tablets and is dependent on the severity of the condition. Treatment may be as short as seven days or as long as one month and consequently adherence to drug therapy becomes challenging. RTD is used as an alternative to proton pump inhibitors for the treatment of ulcer in patients that cannot tolerate proton pump inhibitors and is also used as a second line treatment of ulcers. Therefore the development of a FDC tablet of MTZ and RTD may improve patient adherence to therapy and consequently reduce morbidity and mortality due to ulcers.

The objectives of this study were therefore:

i. To develop and validate a sensitive high performance liquid chromatographic method to quantitate MTZ and RTD in pharmaceutical dosage forms.
ii. To conduct preformulation studies to determine the compatibility of excipients and API in FDC tablet formulations.
iii. To develop and optimize a suitable method of manufacture of FDC tablets of MTZ and RTD.
iv. To conduct preliminary formulation studies to identify a suitable formulation composition(s) that could be used for response surface studies.
v. To determine the impact of formulation and composition changes as described in SUPAC-IR Guidelines on the disintegration time and *in vitro* release characteristics of MTZ and RTD FDC tablets.
vi. To use RSM to optimize the disintegration time and *in vitro* release characteristics of MTZ and RTD from the tablets.

TABLE OF CONTENTS

LIST OF FIGURES

LIST OF TABLES

LIST OF ACRONYMS

ACN	Acetonitrile
ANOVA	Analysis of Variance
API	Active Pharmaceutical Ingredient
ATR	Attenuated Total Reflectance
BCS	Biopharmaceutics Classification System
BP	British Pharmacopoeia
BUA	Blend Uniformity Analysis
cAMP	Cyclic Adenosine Monophosphate
C^{14}	Carbon 14
CCD	Central Composite Design
CCS	Croscarmellose Sodium
CI	Carr's Index
CNS	Central Nervous System
DCP	Dibasic Calcium Phosphate
DNA	Deoxyribose Nucleic Acid
DOE	Design of Experiment
DSC	Differential Scanning Calorimetry
DTA	Differential Thermal Analysis
EGA	Evolve Gas Analysis
EGD	Evolve Gas Detection
FDA	Food and Drug Authority
FDC	Fixed Dose Combination
FT-IR	Fourier Transform Infrared
GLC	Gas Liquid Chromatography
GORD	Gastro Oesophageal Reflux Disease
H_2	Histamine 2
HPLC	High Performance Liquid Chromatography
HR	Hausner Ratio
ICH	International Conference on Harmonization
ID	Internal Diameter
IE	Ion Exchange

IR	Immediate Release (in context of tablet preparation)
IR	Infrared (in context of spectrophotometry)
IS	Internal Standard
IST	Isothermal Stress Testing
LOD	Limit of Detection
LOQ	Limit of Quantitation
LLC	Liquid Liquid Chromatography
MCC	Microcrystalline Cellulose (in context of excipients)
MCC	Medicine Control Council (in context of regulatory authority)
MeOH	Methanol
MTZ	Metronidazole
NADH	Nicotine Adenine Dinucleotide
NP	Normal Phase
PE	Prediction Error
PFOR	Pyruvate Ferrodoxine Oxido Reductase
PPI	Proton Pump Inhibitors
PRESS	Predicted Residual Error Sum of Squares
PVP	Polyvinylpyrrolidone
PVP-K30	Povidone K30
RP	Reversed Phase
RSD	Relative Standard Deviation
RSM	Response Surface Methodology
$\mathbf{R_s}$	Resolution
$\mathbf{R_t}$	Retention time
RTD	Ranitidine
SE	Size Exclusion
SEM	Scanning Electron Microscopy
SODF	Solid Oral Dosage Form
SSG	Sodium Starch Glycolate
SUPAC	Scale Up and Post Approval Change
TFDA	Tanzania Food and Drug Authority
TGA	Thermogravimetric Analysis
TLC	Thin Layer Chromatography

USP	United States Pharmacopoeia
UV	Ultra Violet
XRPD	X-Ray Powder Diffraction
ZES	Zollinger Ellison Syndrome

CHAPTER ONE
A REVIEW OF RANITIDINE AND METRONIDAZOLE

1.1 INTRODUCTION

Gastric and duodenal ulcers are conditions in which the mucosal membranes of the stomach and duodenum become ulcerated as a result of excessive gastric acid secretion and in which the degree of mucus protection provided to the mucosa is limited [1]. The exact aetiology of the disease is not known, however it has been reported that infection with *Helicobacter pylori*, chronic use of non-steroidal anti-inflammatory drugs, cigarette smoking, alcohol abuse and stress are contributing factors [2-4].

Two types of ulcers are known to exist *viz*. acute and chronic. Acute ulceration is easily managed and usually does not give rise to serious complications. However, chronic ulceration is more serious, due to the persistence of the ulcer, potential for haemorrhage, perforation or stenosis formation and/or the potential for malignant changes to the membrane structure of the gut [1]. As with any other disease, early diagnosis and treatment may significantly reduce morbidity and consequently mortality.

The management of ulcers depends on the degree of ulceration and associated complications. Pharmacotherapy is usually sufficient for the treatment of acute and mild cases of ulcers, however surgery may be considered if a patient fails to respond to treatment, or if there is malignancy or if bleeding occurs frequently [5]. The current approach to the management of ulcerous conditions aims at relieving the pain and discomfort associated with the condition, and to prevent the recurrence and complications of the disease. In South Africa the treatment for ulcers consists of administration of a proton pump inhibitor and one antibiotic which could be clarithromycin 500 mg twice daily or amoxicillin 1000 mg per day in combination with metronidazole (MTZ) as a 400 mg twice daily dose for a period of seven days [6]. If a proton pump inhibitor is contraindicated for any reason, an alternative regimen that includes the use of ranitidine (RTD) 300 mg daily for seven days in addition to administration of bismuth subcitrate in doses of 120 mg six hourly for seven days and one of the aforementioned antibiotics in combination with MTZ [6]. In the latter regimen a patient will have to take nine to eleven tablets per day for the duration of therapy which may vary between seven days and a month depending on severity of the condition. Since

pharmacotherapy entails taking a large number of tablets, patient adherence to therapy is often compromised with the result that morbidity and mortality may increase.

In comparison to combination therapy, fixed-dose combination (FDC) therapy has been shown to improve patient adherence [7]. The formulation of a fixed-dose combination tablet of RTD and MTZ for the management of ulcers may therefore improve patient adherence since the number of tablets that have to be taken on a daily basis may be reduced from eleven to seven or nine depending on the course of antibiotic that is taken.

1.2 PHYSICOCHEMICAL PROPERTIES OF RANITIDINE AND METRONIDAZOLE

1.2.1 RANITIDINE

1.2.1.1 Description

RTD hydrochloride is a white to yellowish crystalline powder with little or no odour [8]. It exists in two major polymorphic forms, *viz.* Forms 1 and 2 in addition to a series of pseudo polymorphic forms [9]. The chemical name for RTD is (*N*-(2[({5-[(dimethylamino) methyl]-2-furanyl}methyl)thio]ethyl}-*N′*-methyl-2-nitro-1,1-ethenediamine hydrochloride) and the chemical structure is depicted in Figure 1.1.

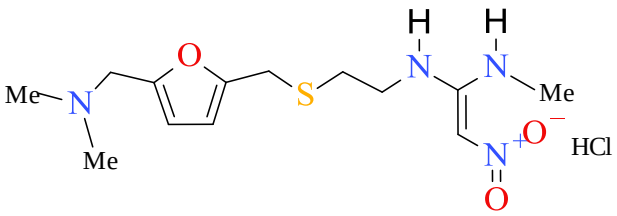

Figure 1.1 Chemical structure of RTD, $C_{13}H_{22}N_4O_3S.HCl$ (MW=350.869)

1.2.1.2 Solubility

RTD is very soluble in water [8,10]. The solubility of RTD in different solvents is listed in Table 1.1.

Table 1.1 Solubility of RTD in various solvents. Adapted from [8]

Solvent	Solubility
Acetic acid	Freely soluble
Water	Very soluble
Methanol	Soluble
Ethanol	Sparingly soluble
Ethylacetate	Very slightly soluble
Isopropanol	Very slightly soluble
Dioxane	Insoluble
Chloroform	Insoluble

1.2.1.3 pH of solution

The pH of a 1 % w/v solution of RTD is 4.5-6 [10].

1.2.1.4 pK_a

The dissociation constants of RTD determined by spectrophotometric and potentiometric pH titration at 25ºC were 1.89 and 8.65 respectively [11,12].

1.2.1.5 Melting range

The melting range of RTD depends on the polymorphic form from which the compound was crystallized. RTD crystals derived from polymorph Form 1 have a melting range of 135-136ºC and crystals derived from polymorph Form 2 have a melting range of 143-144ºC [8].

1.2.1.6 Ultraviolet absorption spectrum

An ultraviolet scan of a 0.00064 % w/v solution of RTD depicted in Figure 1.2 revealed two absorption maxima at a wavelength of 229 nm (ε = 20779) and 313 nm (ε = 19123). The scan was generated using a Lamba 25 UV/VIS Spectrometer (Perkin Elmer® Ltd, Beaconsfield, England) at a scan speed of 480 nm min^{-1}

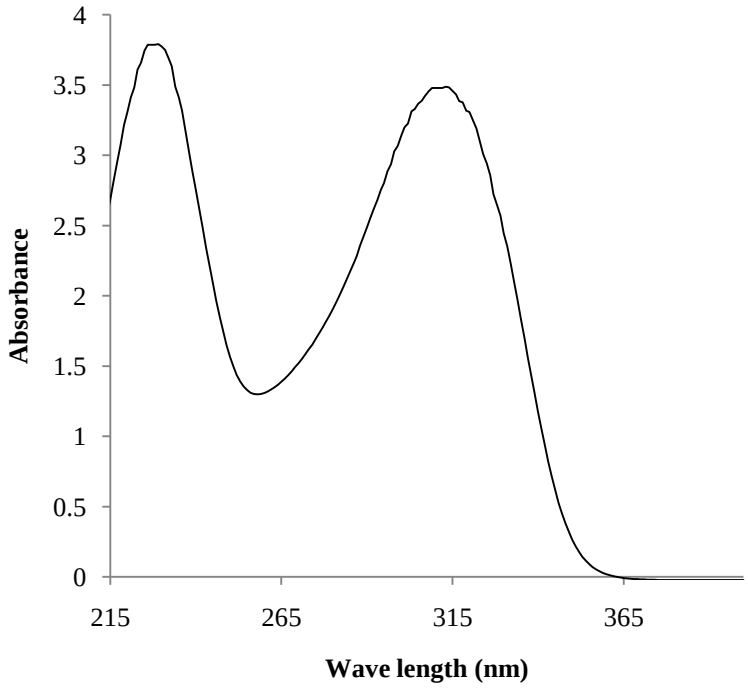

Figure 1.2 UV absorption spectrum of RTD in water generated at a scan rate of 480 nm min^{-1}

1.2.1.7 Infrared spectrum

The infrared (IR) spectrum of RTD powder was generated using a Spectrum 100 Fourier transform-infrared (FT-IR) attenuated total reflectance (ATR) spectrometer (Perkin Elmer® Ltd Beaconsfield, England). The IR spectrum was obtained at a 4000-650 cm^{-1} wave-number range, 4 scans and at a resolution of 4 cm^{-1}. The typical IR spectrum of RTD is depicted in Figure 1.3 and the absorption band assignments are shown in Table 1.2 [8].

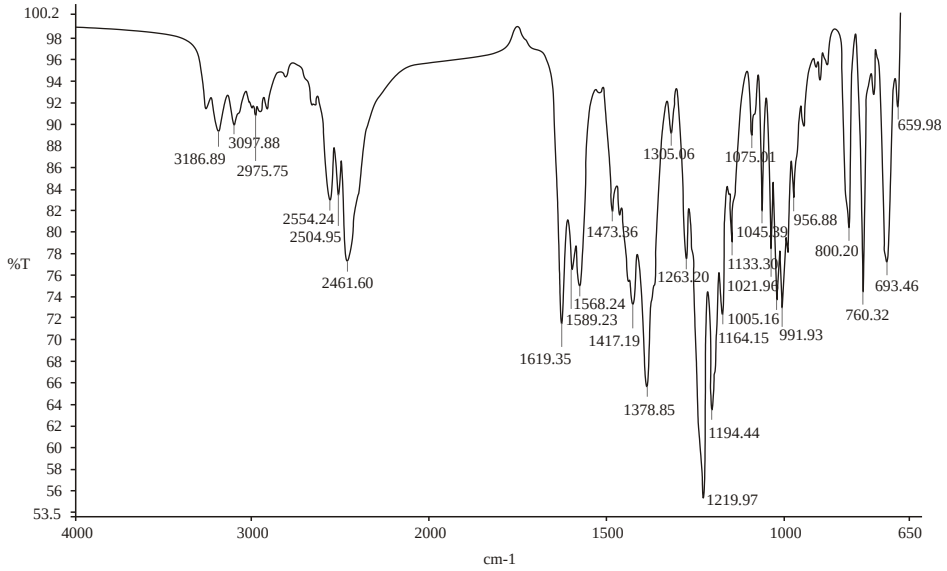

Figure 1.3 IR spectrum of RTD generated at 4 scans and resolution of 4 cm^{-1}

Table 1.2 IR absorption band assignments

Bands (cm^{-1})	**Assignment**
1080-1360	CN; C-N stretch
2560-2640	$H\text{-}N^{+}R_3$; N^{+}-H stretch
3020-3100	CH; C-H stretch

1.2.1.8 Stability

RTD degrades readily when exposed to moisture, light and heat [8,10,13]. RTD powder is susceptible to degradation when incubated in 0.1 M solution of sodium hydroxide (NaOH) and when incubated in a 3% v/v hydrogen peroxide (H_2O_2) solution complete degradation of the drug occurred [14]. Similar results have also been reported following stability testing of RTD tablets and parenteral solutions under conditions of different temperature, light exposure and storage times [15].

When RTD powder was incubated with 0.1 M of hydrochloric acid (HCl) in a tightly sealed amber-coloured bottle for 24 h, no degradation was observed when the samples were analyzed using high performance liquid chromatography (HPLC) [14].

1.2.1.9 Clinical pharmacology

1.2.1.9.1 Mode of action

Histamine is produced by mast cells located in the stomach which secrete gastric acid following activation of the gastric parietal cells. Histamine binds to histamine-2 (H_2) receptors located on the parietal cells resulting in an increase in levels of adenylcyclase, cyclic-AMP (cAMP) and intracellular calcium ultimately causing gastric acid secretion [16]. RTD is a H_2 receptor antagonist that competes with histamine for the H_2-receptor sites thereby, blocking histamine accessibility to the receptor reversibly, reducing acid secretion consequently lowering gastric acidity [5,16].

1.2.1.9.2 Clinical use

RTD has been used clinically for the management of gastro-oesophageal reflux disease (GORD), Zollinger-Ellison Syndrome (ZES) and ulcers since 1981 [8]. Furthremore, RTD is also used preoperatively to prevent acid reflux and aspiration during surgery [17-19]. Unlike cimetidine, RTD has a superior side-effects profile, exhibits fewer drug interactions and requires less frequent administration to exert a therapeutic effect [5,6,16,18].

1.2.1.9.3 Side effects and interactions

Generally $H\text{-}_2$ receptor antagonists are well tolerated with the exception of cimetidine [5,16,20]. The most common side effects associated with the use of RTD are diarrhoea, dizziness, somnolence, headache, rash and reversible hepatitis with or without jaundice [16,18,20].

Unlike cimetidine, RTD when administered at therapeutic doses does not inhibit the cytochrome P450 microsomal enzyme system, which makes it less likely to interact with other drugs that are metabolized or transported by this pathway [5,10,18,20]. However, with the exception of famotidine, all H_2-receptor antagonists increase the bioavailability of ethanol by inhibition of gastric first-pass metabolism [16]. RTD increases the bioavailability of alcohol through facilitation of gastric emptying and reduction in first-pass metabolism as consequence of saturation of alcoholdehydrogenase [20,21].

An increase in plasma levels of acetaminophen was observed when it was co-administered with RTD due to the inhibition of acetaminophen glucuronyltransferase preventing hepatic first-pass metabolism [22].

1.2.1.9.4 High risk groups

To date there have been no reported cases of risk when RTD was administered to pregnant women and nursing mothers however, RTD should only be administered to this group when it is absolutely necessary since it crosses the placenta and is secreted in breast milk [16,23-25].

In geriatric patients, RTD has been known to cause central nervous system (CNS) dysfunction of which the most common symptoms include slurred speech, delirium and depression [5,6,16,18]. These side effects are transient and usually disappear when a change to treatment with an alternate H_2-receptor antagonist is made. Chronic use of RTD has also been associated with vitamin B_{12} deficiency in geriatric patients [26], therefore long-term use in this patient group should be evaluated frequently.

A dose adjustment for RTD in patients with renal impairment is necessary to avoid the risk of toxicity [5,6,16,18,18].

There is a paucity of information relating to the safety of RTD in paediatric patients [18], therefore dose adjustment on a weight basis is of paramount importance since the presence of immature organs make these patients vulnerable to toxicity.

1.2.1.10 Clinical pharmacokinetics

1.2.1.10.1 Dosage

RTD is available in different dosage forms such as tablets of 75 mg, 150 mg and 300 mg strength, syrup of 150 mg/10ml strength and an intravenous (IV) injection of 50 mg/2ml strength [6].

The normal adult dose of RTD for the treatment of ulcers is 150 mg twice daily or 300 mg at night for 4-8 weeks [6,27,28], followed by once-daily dose of 150 mg as maintenance therapy [6]. IV infusion can be used if a patient is nauseous or vomiting and the recommended IV dose is 50 mg in 0.9 % m/v saline or 5% m/v dextrose solutions infused over 2 h [6,18].

The treatment of ZES requires the use of large doses [16] of between 600-900 mg on daily basis [6]. This is usually sufficient for treatment when surgery is not indicated. However, depending on severity of the condition, doses of up to 6 g daily may be required [6].

For the relief of symptoms in patients presenting with hyperacidity and heartburn, a dose of 75 mg administered 30 min before meals is usually sufficient to relieve the condition and in paediatric patients, 2-4 mg/kg administered orally twice daily via the oral route has proven effective [6].

For prevention of acid reflux and aspiration during surgery, a dose of RTD of 150 mg administered orally 12 h and 2 h prior to surgery is recommended [18,29]

1.2.1.10.2 Absorption

RTD is well absorbed following oral administration with bioavailability ranging between 30-88% [6,8,16,30], although in paediatric patients following oral administration to children aged between 3.5-16 years the bioavailability was approximately 48% [31]. The plasma concentration versus time profile of RTD following oral administration of 150 mg shows two peak concentrations [8,32] with the first and second peak occurring within 1.1±0.4 h and 3±0.0 h, with a maximum serum concentration (C_{max}) of 313±93.55ng/ml and 296±68.01 ng/ml at each time respectively [32]. The administration of RTD with food or antacids has been shown to delay absorption and therefore the time to peak concentration is delayed although the total therapeutic effect remaining unchanged [18,33]

1.2.1.10.3 Distribution

Following oral or parenteral administration approximately 15% of the RTD administered binds to plasma proteins [6,34]. The approximate volume of distribution of RTD is 0.1-1.9 l/kg and the distribution half-life is 6.1±0.9 min. [8,16,30,35]. The distribution,

absorption and excretion of C^{14} labelled RTD in rats following parenteral administration were monitored and relatively high concentrations of radio-labelled RTD were concentrated in the kidneys, liver and gastro-intestinal tract whereas lower concentrations were observed in the brain [36]. Similar results in which the concentration of RTD in the cerebro-spinal fluid of healthy subjects was 3.3-5.0% that in plasma have been reported [8].

RTD has been detected in breast milk with resultant concentrations higher than those found in serum [37]. Following multiple dose administration to breast-feeding mothers the minimum concentration in milk occurred between 1 and 2 h following dosing and the maximum concentration was observed at the end of the 12-hour dosing interval [37].

1.2.1.10.4 Metabolism

Rantidine is susceptible to both oxidative and demethylation reactions and the sites at which these reactions occur are highlighted in Figure 1.4.

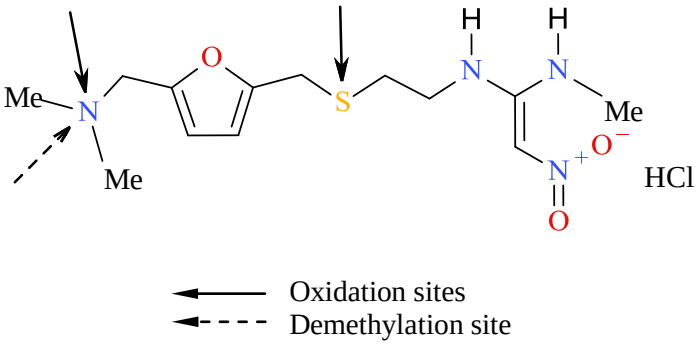

Figure 1.4 Oxidation and demethylation sites of RTD

Metabolic studies of RTD performed using isolated dog and rat hepatocytes revealed that, RTD is metabolised to desmethylranitidne (Figure 1.5 I), RTD S-oxide (Figure 1.5 II), RTD N-oxide (Figure 1.5 III) and two unidentified minor metabolites [8,30,38]. When RTD is administered intravenously and orally alone, 1.3±0.3% of the intravenous dose and 2.6±0.2% of the oral dose are converted to the desmethyl metabolite [8].

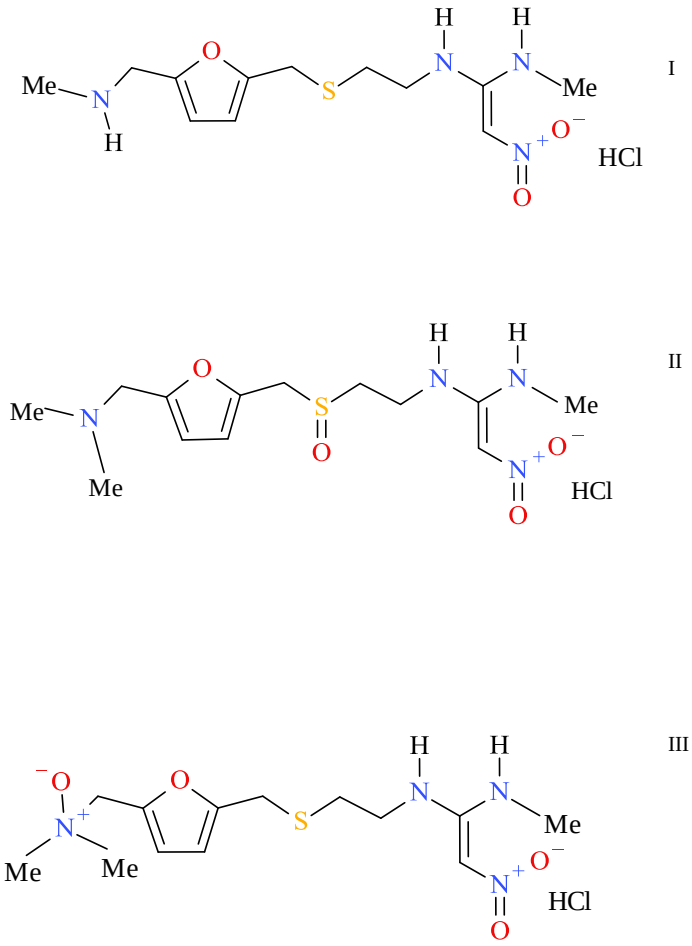

Where,

I = DesmethylRTD
II = RTD S-oxide
III = RTD N-oxide

Figure 1.5 Metabolites of RTD

1.2.1.10.5 Elimination

RTD is primarily excreted as an unchanged (30-70%) drug in urine [30,34,39]. The elimination half-life of RTD is 1.9±0.1 hours and the plasma clearance is 709±62 ml/min [8,34] indicating that dose adjustment in patients presenting with renal dysfunction is necessary. The pharmacokinetics and pharmacodynamics of RTD in subjects with varying degrees of renal impairment have been investigated and reported that a dose reduction of up to 66% for patients with creatinine clearance of 50 ml/min results in sub-therapeutic concentration [40]. Therefore, to avoid therapeutic failure, a dose reduction by 50% in patient with a creatinine clearance of <10 ml/min should be sufficient to produce the desired therapeutic effect with safety [41].

1.2.2 METRONIDAZOLE

1.2.2.1 Description

MTZ is a white or yellowish crystalline powder, odourless and bitter to taste [42,43]. The chemical name is 1-(2-hydroxyethyl)-2-methyl-5-nitroimidazole and the chemical structure is depicted in Figure 1.6.

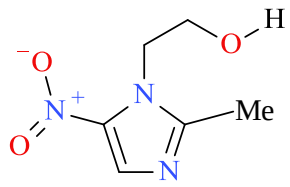

Figure 1.6 Chemical structure of MTZ ($C_6H_9N_3O_3$ MW=171.16)

1.2.2.2 Solubility

The solubility of MTZ at 22ºC in monobasic potassium phosphate (KH_2PO_4) buffer solution of pH 1.2 is 64.8 mg/ml [44]. The solubility of MTZ in other solvents at 25ºC is summarized in Table 1.3.

Table 1.3 Solubility of MTZ in various solvents [42]

Solvent	Solubility (mg/ml)
Water	10.5
Methanol	32.5
Ethanol	15.4
Chloroform	3.8
Heptane	<0.01

1.2.2.3 pK_b

The base dissociation constant (pK_b) of MTZ determined by UV spectrophotometry is 11.47 [45].

1.2.2.4 pH of a solution

The pH of a 0.1% m/v aqueous solution of MTZ determined at 20°C ranged between 5.62-5.69.

1.2.2.5 Ultraviolet absorption spectrum

An ultraviolet scan of a 0.06% m/v solution of MTZ in methanol acidified with 0.05 M sulphuric acid revealed an absorption maximum at a wavelength of 275 nm (ε=13774) that is similar to a lambda max of 274 nm reported for MTZ in an acidified methanol solution [42]. The scan was generated using a Lambda 25 UV/VIS Spectrometer (Perkin Elmer® Ltd Beaconsfield, England) at a scan rate of 480 nm min^{-1} as depicted in Figure 1.7.

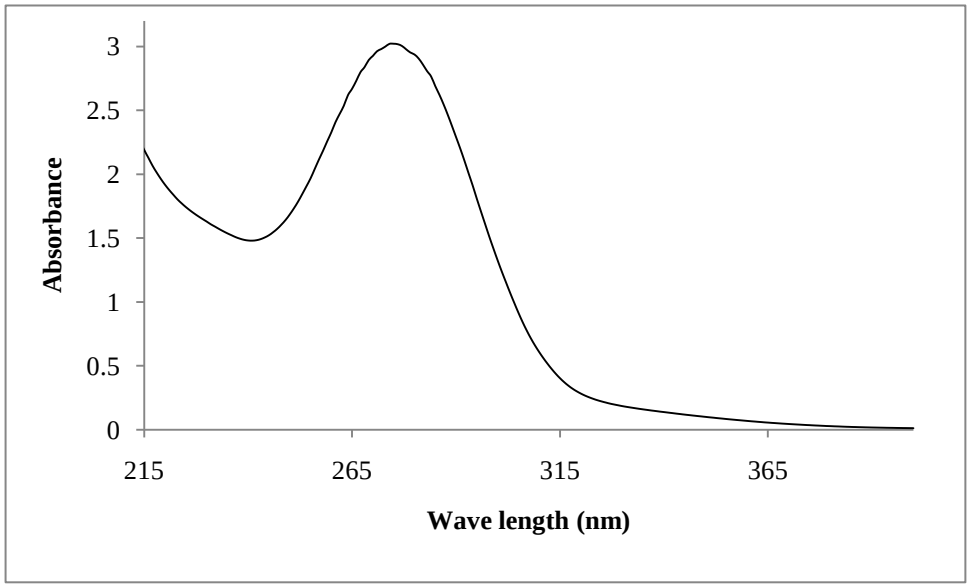

Figure 1.7 UV spectrum of MTZ in acidified methanol generated at a scan rate of 480 nm min^{-1}

1.2.2.6 Infrared spectrum

The IR absorption spectrum of MTZ was determined using a Spectrum 100 FT-IR Spectrometer with Universal ATR Sampling Accessory (Perkin Elmer® Ltd Beaconsfield, England). The spectrum was generated in the range between 4000-650 cm^{-1} wave numbers, 4 scans and at a resolution of 4 cm^{-1}. A similar IR absorption spectrum of MTZ reference standard compressed in potassium bromide pellet has been reported [42]. The IR spectrum of

MTZ is depicted in Figure 1.8 and the band assignments for the absorption spectrum are summarized in Table 1.4.

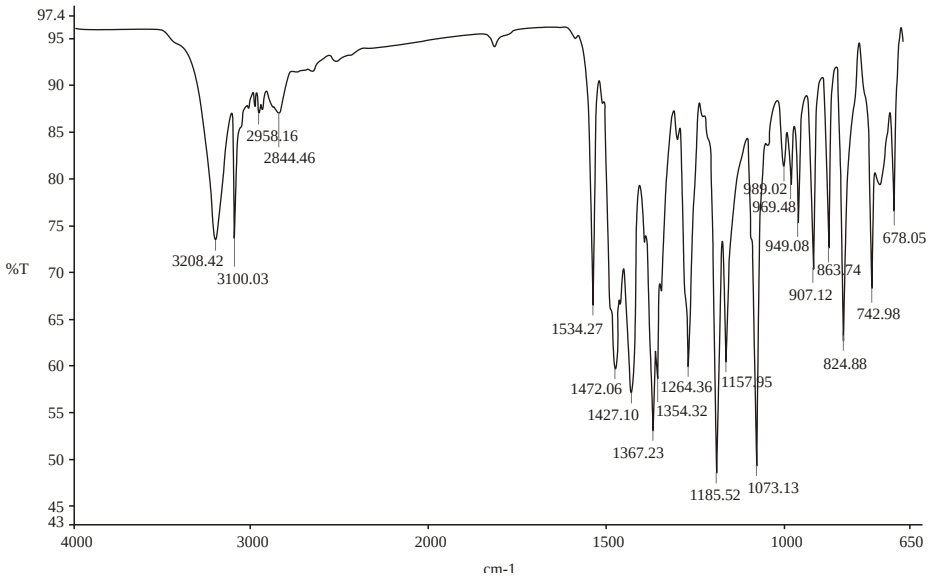

Figure 1.8 Infrared spectrum of MTZ generated at 4 scans and resolution of 4 cm^{-1}

Table 1.4 Absorption bands assignments. Adapted and modified from [42]

Band (cm^{-1})	**Assignment**
3200-3550	OH stretch
3020-3100	C=CH; C-H stretch
1538;1350	NO_2; N-O stretch
970-1250	C-OH; C-O stretch
830	C-NO_2; C-N stretch

1.2.2.7 Stability

MTZ is a photo labile 5-nitroimidazole derivative and must be protected from light [46]. The degradation reaction involves several rearrangements of the 5-nitroimidazole structure as shown in Figure 1.9, and requires substitution on the ring nitrogen-1(N^1) with functional group other than hydrogen [47]. N^1 unsubstituted MTZ can decompose in a similar fashion following prolonged heating in 1.5 M NaOH with copper catalysis [48]. Basic solutions can be used to distinguish between the substituted and unsubsituted N^1 5-nitroimidazole and the degradation of MTZ in de-ionized water following irradiation with ultraviolet light at 254 nm and 200-400 nm has been reported [49].

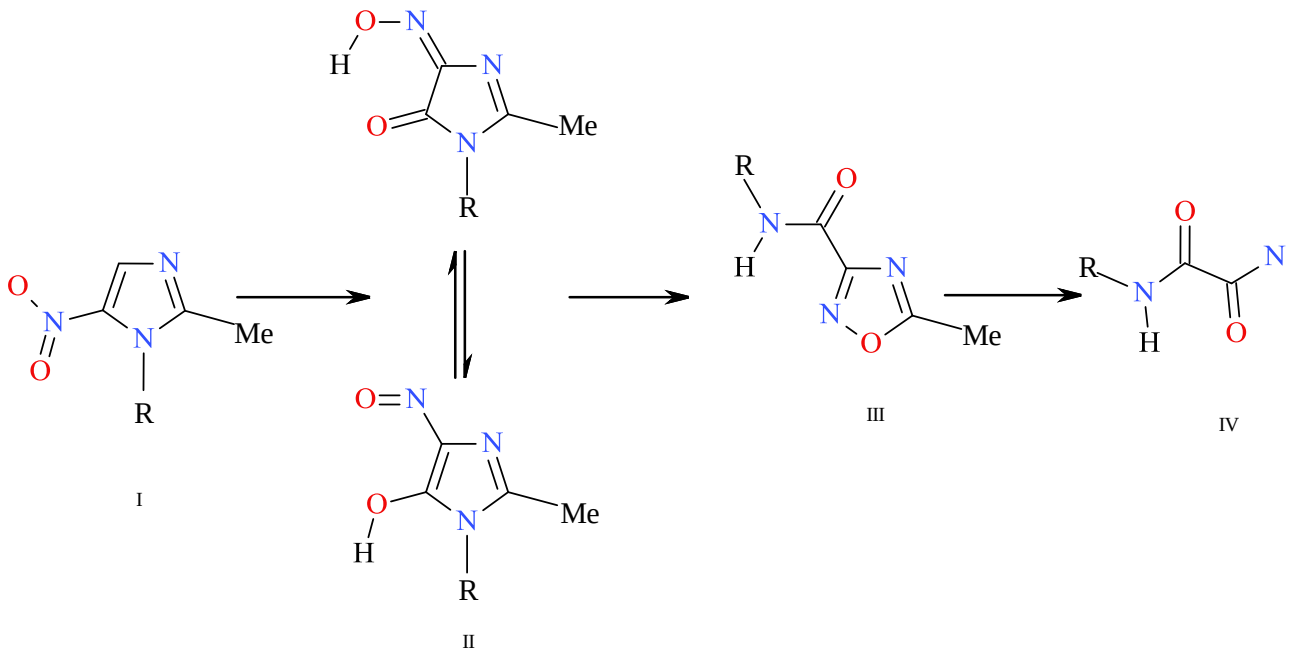

Where,

R = CH_2CH_2OH
I = MTZ
II = 2-imidazoline-4,5-dione-4-oxime
III = 1,2,4-oxidiazole-3-carboxamide
IV = oxamide

Figure 1.9 MTZ degradation scheme, redrawn from [50]

As with any N^1-subsituted 5-nitroimidazole, acid, alkaline hydrolysis of MTZ follows first-order reaction kinetics with the reaction taking place in two phases *viz*. initially forming nitrite ions after which degradation of the parent compound occurs [51]. It has been reported that, alkaline hydrolysis of MTZ produces ammonia and acetic acid whereas an amine with at least one hydrogen atom is formed in acidic and alkaline hydrolytic conditions [51]. The degradation products of MTZ alkaline hydrolysis are shown in Figure 1.10.

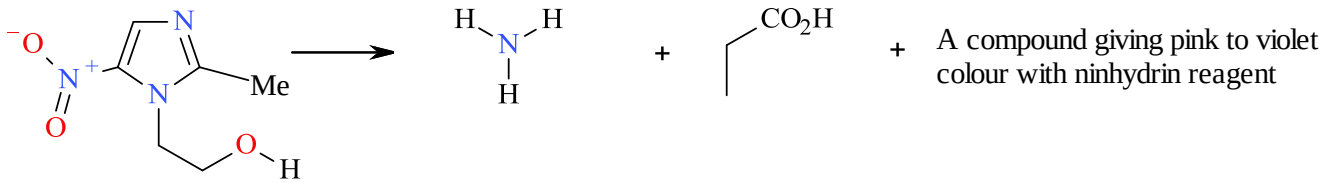

Figure 1.10 Alkaline hydrolytic degradants of MTZ, redrawn from [52]

1.2.2.8 Clinical pharmacology

1.2.2.8.1 Mode of action

MTZ has a similar mode of action to other 5-nitroimidzoles and the antimicrobial activity depends on the formation of an intermediate toxic metabolite in the cells of susceptible protozoa and bacteria [53]. The drug enters the cell of susceptible protozoa or anaerobic bacteria by passive diffusion. The nitro functional group is chemically reduced by ferrodoxin to form a nitro radical that binds to deoxyribose nucleic acid (DNA) and consequently causes inhibition of nucleic acid synthesis [54,55]. The mechanism of action of MTZ is depicted in Figure 1.11.

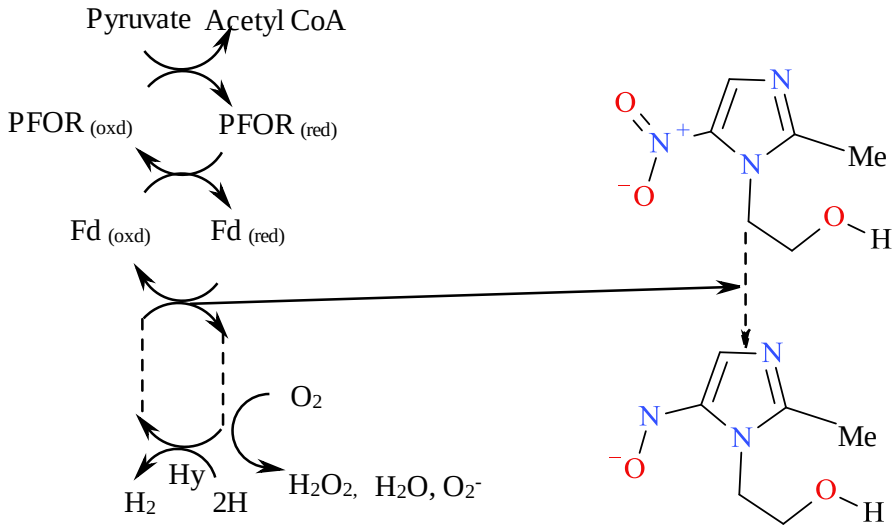

Where,

Oxd= oxidised
Red= reduced
Hy = Hydrogenase

Figure 1.11 MTZ activation scheme. Adapted and modified from [56]

1.2.2.8.2 Spectrum of activity

The spectrum of activity of MTZ in bacteria depends on the presence of a ferrodoxin-linked dehydrogenase associated mechanism in the cell, which is a common metabolic activity in most obligate anaerobic microorganisms such as the *Bacteroides* and *Clostridium* species

[43,57,58]. MTZ is also active against protozoal species such as *Balantidium coli, Blastocystis hominis, Entamoeba histolytica, Giardia lamblia and Trichomona vaginalis* [43,53,58] and facultative anaerobes such as *Gardnella vaginalis* and *Helicobacter pylori* [43].

1.2.2.8.3 Resistance

Anaerobic gram-negative bacterial resistance to MTZ is extremely low with less than 1% of the *Bacteroides* species showing resistance [59]. However a better understanding of the mechanism by which resistance is developed is of importance, since an increase in the number of resistant strains of anaerobic bacteria and protozoa will lead to treatment failure. The resistant strains of *Bacteroides fragilis* have plasmid encoded genes that are transferred to sensitive strains by conjugation [56]. These strains of microorganism have low levels of pyruvate ferrodoxine oxidoreductase (PFOR), an enzyme that is responsible for the reduction of ferrodoxin (Fd) and decarboxylation of pyruvate to form acetyl CoA as shown in Figure 1.11 [56,60]. The decreased level of PFOR consequently results in low levels of reduced Fd, thereby compromising the formation of the nitro radical that is responsible for the inhibition of nucleic acid synthesis [56].

The existence of resistant strains of *Helicobacter pylori* to MTZ have been reported [61]. The resistance in these strains can be attributed to the low activity of nicotinamide adenine dinucleiotide (NADH) oxidase and NADH nitroreductase in comparison to that in sensitive strains [61]. Similar results were observed in studies in which the resistance of *Helicobacter, Bacteroides, Clostridium, Giardia, Entamoeba* and *Trichomonads* were investigated at a molecular level and all resistant strains had altered or reduced levels of the proteins responsible for drug activation [62].

1.2.2.8.4 Clinical use

MTZ is used to treat infections caused by anaerobic bacteria and protozoa. It is also reported to have a radio-sensitising effect on hypoxic tumour cells [43,63]. It is clinically indicated for treatment of susceptible protozoal infections such as balantidiasis, amoebiasis, giardiasis, trichomoniasis and *Blastocytis hominis* infection [43,53,58,64].

MTZ is also used for treatment and prophylaxis of anaerobic bacterial infections such as bacterial vaginosis, acute necrotising ulcerative gingivitis, pelvic inflammatory disease, antibiotic associated colitis, tetanus and infections caused by *Bacteroides fragilis* [43,58].

MTZ is indicated for the treatment of meningitis, endocarditis, brain abscess and septicaemia caused by susceptible anaerobic bacteria [58]. In addition, also it is used for the eradication of *Helicobacter pylori* infections in peptic ulcer disease, treatment of guinea worm infection, Crohn's disease, hepatic encephalopathy and prophylaxis of infections following bowel surgery [43,58].

1.2.2.8.5 Side effects and interactions

The most common side effects of MTZ are dose related and include headache, nausea, dry mouth or a metallic taste in the mouth. Infrequent side effects include diarrhoea, vomiting, constipation, weakness, dizziness, ataxia, insomnia and passing of dark urine [43,53,58,64]. Moderate neutropenia and thrombocytopenia have also been reported following administration of MTZ [43,53]. Rare side effects associated with the use of MTZ include cholestatic hepatitis, pancreatitis, jaundice, or thrombophlebitis following intravenous infusion. Cases of CNS side effects such as seizures, ataxia and reversible encephalopathy have also been reported [43,53,58]. Irreversible encephalopathy in a 38-year-old woman was attributed to treatment with a high dose of MTZ [65].

MTZ is known to cause a disulfuram-like reaction when taken concomitantly with alcohol. Phenytoin and phenobarbital have been reported to accelerate the metabolism of MTZ with a consequent reduction in effectiveness [43,53,58,64]. MTZ also potentiates the anticoagulant effects of coumarin type anticoagulants such as warfarin and it also known to reduce the excretion of lithium and therefore has the potential to cause lithium toxicity [43,64]. Cimetidine has been reported to increase the plasma levels of MTZ by decreasing MTZ clearance, consequently increasing the risk of neurological side effects [43,53,64].

MTZ and its hydroxy metabolite are mutagenic to bacterial cells, however, *in vivo* and *in vitro* studies performed on mammalian cells did not reveal any mutagenic effect [43,53]. In spite of this finding, lymphocyte mutation was observed in sheep following treatment with MTZ in therapeutic doses of 1 g per day for 10 days [66]. As there is insufficient data relating

to genotoxicity of MTZ in humans, evidence of carcinogenicity is still unclear and the question of whether MTZ is carcinogenic in humans remains unanswered [43,66].

1.2.2.8.6 High risk groups

The mutagenic effect of MTZ on bacterial cells and some mammalian cells still poses a question relating to safe use of MTZ in pregnant women. A meta-analysis study has concluded that there is no risk of teratogenicity to the foetus following MTZ administration to pregnant women [67]. Nonetheless cases of signal association between vaginal administration of MTZ during pregnancy and congenital hydrocephalus have been reported [68]. Similarly treatment with MTZ during pregnancy and the occurrence of adrenal neuroblastoma in infants has also been reported [69]. Although the use of MTZ during pregnancy is still questionable it has been suggested that risk assessment of the teratogenic potential and trichomoniasis and bacterial vaginosis perinatal outcome should be undertaken, prior to use [70].

MTZ is secreted in breast milk giving the milk a bitter taste and consequently impairing feeding [43]. It is therefore recommended that breast feeding to be discontinued for 12-24 h following single-dose therapy [43,64].

Geriatric patients are prone to the risk of developing blood dyscrasias due to the long-term use of high doses of MTZ [64]. Therefore blood level monitoring is advised for geriatric patients placed on MTZ therapy for longer than 10 days. Furthermore dose adjustments maybe necessary in patients with impaired hepatic function [43,64], a condition that is likely to be prevalent in this patient group.

1.2.2.9 Clinical pharmacokinetics

1.2.2.9.1 Dosage

MTZ is administered in different dosage forms including solid, semi-solid, suspension and infusion technologies. Tablets are usually taken with or after food, however it is usually preferred that MTZ be taken with food to minimize gastro-intestinal irritation [43,53]. In suspensions, MTZ benzoate should be taken at least an hour before food, after which it is

hydrolysed in the gastro intestinal tract to release MTZ that is subsequently absorbed. MTZ can be applied topically as a cream or gel, administered rectally as a suppository or parenterally as an infusion of MTZ or MTZ hydrochloride [43].

The ultimate dose to be administered is dependent on the type and severity of infection to be treated and whether that infection is parasitic or bacterial in origin.

In order to treat amoebiasis effectively, MTZ is administered orally in doses of 400-800 mg three times daily for 5-10 days [43,64]. The paediatric dose to be administered depends on the age of the patient. Children aged between one to three years receive 100-200 mg three times daily, children aged between three and seven years receive 100-200 mg four times daily and children aged between seven and ten years receive 200-400 mg three times daily [43,64]. An alternate approach may be to use a dose of 35-50 mg/kg in divided doses for 5-10 days.

The treatment of giardiasis requires a dose of 2 g daily to be given orally for three consecutive days or 400 mg three times daily for 5 days. For paediatric patients children aged between 1-3 years receive 500 mg per day, children aged between three and seven years receive 600-800 mg per day and children aged between seven and ten years receive 1 g per day for three days. An alternate approach may be to use a dose of 15 mg/kg daily in divided doses for 5-7 days [43,64].

For the treatment of trichomoniasis MTZ can be administered as a single oral dose of 2 g or as a two-day course in divided doses of 800 mg and 1200 mg in the morning and evening respectively [43,64]. Alternatively 200 mg three times daily or 400 mg twice daily for seven days may be administered. In paediatric patients children aged between one and three years receive 50 mg three times daily, children aged between three and seven years receive 100 mg twice daily and children aged between seven and ten years receive 100 mg three times daily for seven days. An alternate approach may be to use a dose of 15 mg/kg daily in divided doses for seven days [43,64].

The treatment regimen for the management of bacterial vaginosis is similar to that for the management of trichomoniasis or by application of 0.75% w/w gel at a dose of 5 g once or twice daily for 5 days [43].

For the treatment of anaerobic bacterial infections MTZ is administered at an initial oral dose of 800 mg followed by 400 mg 8 hourly for seven days or, as an intravenous infusion of 500 mg (5 mg/ml) at a rate of 5 ml/min every 8 h. An alternate approach may be to use suppositories at a dose of 1 g every 8 h for three days, followed by 1 g every 12 h after which treatment continues by oral therapy [43,64]. For paediatric patients a dose of 7.5 mg/kg administered orally or intravenously every 8 h has proved to be effective. An alternate regimen may be to use suppositories at dose of 125 mg for children less than one year, 250 mg for children aged between one and five years and 500 mg for children aged between five and ten every 8 h for three days and twice daily there after [43].

For the post-operative prophylaxis of anaerobic bacterial infections in patients who have undergone bowel surgery, the doses are similar to those used for treatment but MTZ is usually used in combination with an aminoglycoside or betalactam antibiotic [43,71,72].

The treatment of peptic ulcers with MTZ is used in combination with an acid suppressant or inhibitor and an antibiotic. The regimens that are recommended for use have been described in the introduction of this chapter.

For the treatment of rosacea the topical application of a thin film of MTZ gel 0.75% w/w has proven effective [43,73,74].

1.2.2.9.2 Absorption

MTZ is almost completely absorbed following oral administration with a C_{max} of approximately 6-12 µg/ml being achieved within 1-3 h of dosing [42,43,53,64]. Food may delay the absorption of MTZ but total absorption remains unaffected [43]. Rectal absorption of MTZ is slower than that observed following oral administration with a resultant bioavailability of 60-80%. The C_{max} following rectal administration is half that achieved following an oral dose of MTZ [43,64] with adequate concentrations attained within 3 h after insertion of the dosage form [64].

Vaginal absorption following administration of pessaries is poor with a resultant bioavailability of 20-25% and a C_{max} of 2 µg/ml [43]. Despite the poor bioavailability it was

concluded that intravaginal application was as effective as the oral dose in the treatment of bacterial vaginosis [75].

1.2.2.9.3 Distribution

Following absorption, MTZ is widely distributed in body tissues and fluids with the intracellular concentration rapidly reaching extracellular levels, [43,53,58,64]. Similarly the distribution of C^{14} MTZ in rats following administration of an oral dose revealed that MTZ was rapidly absorbed and equilibration between blood and most tissues was rapid [76]. MTZ enters the foetal circulation rapidly and less than 20% of the drug is bound to plasma proteins [43,53]. The approximate volume of distribution at steady state ranges between 0.5-1.1 l/kg [77].

1.2.2.9.4 Metabolism

The metabolism of MTZ occurs in the liver as a result of side chain oxidation and glucuronidation of the parent drug [43]. The oxidative metabolites are 1-(2-hydroxyethyl)-2-hydroxymethyl-5-nitroimidazole which possesses antimicrobial activity of 30-65% that of the parent compound [77] and 2-methyl-5-nitroimidazole-1-acetic acid [42,43,58]. The metabolism of MTZ in man and dogs was similar [78]. However following oral dosing, only the parent drug and the active metabolite were detected in vaginal fluids [42]. The metabolism of MTZ in human liver microsomes accounts for 75% of the intrinsic clearance of MTZ [79].

1.2.2.9.5 Elimination

The major route of elimination of MTZ from the body is via urinary excretion with 10-20% unchanged drug present in urine and 6-15% of MTZ excreted in faeces. The elimination half-life of MTZ is approximately 7.5-8 h and is slightly longer for the hydroxymetabolite [43,53,58,58,64]. However, in infants the elimination half-life has been reported to range between 25-109 h [43]. Upadhyaya *et al* [80] observed results that are close to the lower range previously reported [43], an elimination half-life of 22.3-22.5 h was observed in neonatal patients following administration of 7.5 mg/kg MTZ as an infusion. The half-life of

MTZ is prolonged in infants due to their under developed renal and hepatic function, but as the infant matures, the half-life values are reduced closer to those observed in adults [81].

The elimination of active metabolites is prolonged in patients with renal dysfunction and there are no reports of toxicity in these cases, consequently dose adjustments in renal dysfunction may not be necessary [77].

1.3 CONCLUSION

In sub-Saharan Africa, gastric and duodenal ulcer disease has mostly been associated with *Helicobacter pylori* infection [82]. The infection with *Helicobater pylori* accounts for 10-15% of gastric and duodenal ulcers cases, where 80% of the population in the developing countries have shown evidence of *Helicobater pylori* infection [82]. Thus eradication of *Helicobacter pylori* constitutes a fundamental part in the treatment of ulcers since it reduces the risk of recurrence and complications of the disease [83].

Triple therapy is a common approach for the management and treatment of uncomplicated ulcers. Nonetheless the pill burden and duration of therapy makes adherence a challenge with a consequence of potentiating morbidity and even mortality. RTD and MTZ have been used in combination as a part of triple therapy, however, with the discovery of proton pump inhibitors (PPI) in 1981 [84] the role of RTD in triple therapy has become minimal.

Even though PPI are effective and safe, they exhibit large inter-patient variability with respect to their pharmacokinetics and some have the propensity to interact with other drugs [85]. Furthermore, the use of PPI for treatment of ulcers is more expensive compared to the use of H_2-receptor antagonist [86]. In contrast RTD does not show such activity and variability. In South Africa RTD is used as second line therapy in the management of ulcers or as an alternate drug for patients in which the use of PPI are contraindicated [6]. Therefore the development of a FDC of RTD and MTZ may help reduce the pill burden for patients and consequently reduce morbidity and mortality. In addition, the cost of treatment and medication error may be reduced following the use of FDC formulation.

Therefore the objective of the work has been to manufacture FDC for these two drugs, and in the process develop an analytical method for the quantitation of these drugs in pharmaceutical dosage forms.

RTD and MTZ have similar physiochemical properties such as hydrophilicity and crystallinity which makes them good candidates for formulating a FDC solid dosage form of these compounds. In addition the similarity of physiochemical properties facilitates the selection of an appropriate analytical technique for the simultaneous analysis of these compounds, since variation of analytical conditions may not be required to ensure the production of accurate and precise results.

CHAPTER TWO
HPLC METHOD DEVELOPMENT AND VALIDATION

2.1 INTRODUCTION

2.1.1 Historical background

Chromatography is a technique used to separate compounds in a complex matrix into the constituent parts of that mixture. It is estimated that at least 5% of the chemical research conducted in the United States of America (USA) in 2003 involved some form of chromatographic technique [87]. Chromatography was first described by Mikhail Semenovich Tswett in 1901, he used liquid-adsorption chromatography with calcium carbonate ($CaCO_3$) as an adsorbent and a petrol ether ethanol mixture as eluant to achieve separation of the constituents of chlorophyll, xanthophyll and carotenoid from leaves [88,89]. In 1931 the method reported by Tswett was used successfully to purify xanthophylls on a $CaCO_3$ adsorption chromatographic column [88]. This application led to the emergence of different chromatographic techniques such as partition chromatography consisting of liquid-liquid chromatography (LLC) and gas-liquid chromatography (GLC), paper chromatography (PC), thin layer chromatography (TLC) and ion exchange chromatography (IEC). Braithwaite and Smith [90] published a review of commonly used chromatographic techniques as summarized in Figure 2.1.

2.1.2 Overview

Different chemical and spectroscopic analytical methods have been used for the analysis of MTZ and RTD in pharmaceutical dosage forms or biological fluids such as plasma and urine. However most of these methods report the analysis of a single compound at any one time from a sample matrix. Despite the rapid advancement in analytical technology and techniques, HPLC is still the preferred tool for the analyses of active pharmaceutical ingredients (API) and products as reported in most official compendia [91]. The objective of this study was to develop an HPLC method for the simultaneous determination of RTD and MTZ in pharmaceutical solid dosage forms.

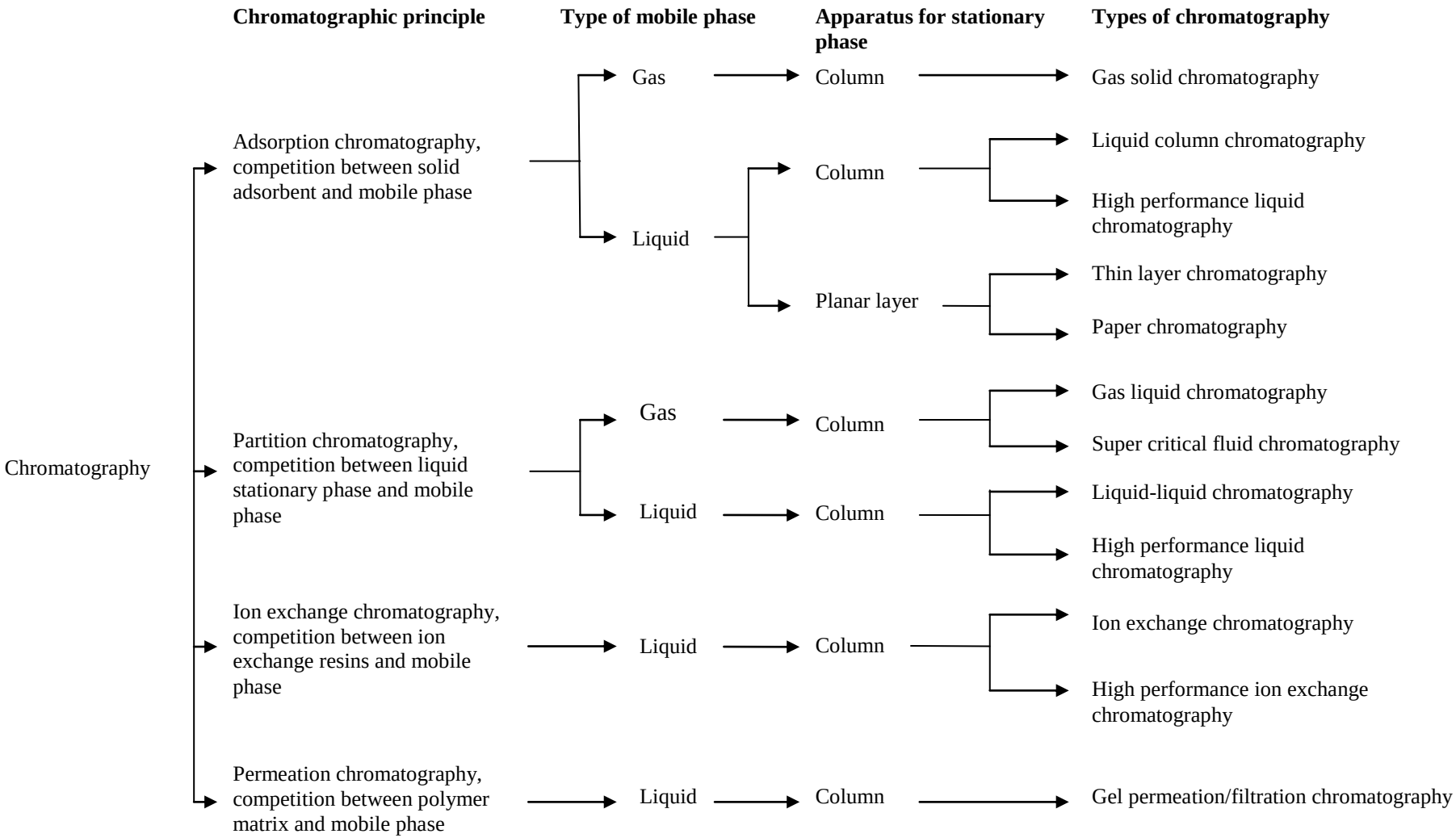

Figure 2.1 Classification of chromatographic techniques. Adapted from [91]

2.1.3 Classification of HPLC

The development of liquid chromatography that has taken place over approximately thirty years has resulted in the development of a technique that is currently known as HPLC. However, the principles of HPLC have remained the same as those for liquid chromatography with the exception that automated sample injection, continuous solvent pumping and reusable stationary phases or columns have become the norm [92].

HPLC techniques can be classified into four types *viz.* normal phase (NP), reversed-phase (RP), ion exchange (IE) and size exclusion (SE) chromatography, with each technique defined according to the dominating molecular interaction and forces that prevail in the separation process [89,90].

2.1.3.1 Normal Phase-HPLC (NP-HPLC)

NP-HPLC makes use of polar interactions between an analyte in a mixture and the stationary phase to achieve an effective separation. As with any other liquid chromatographic method, the analyte is in continuous competition with molecules of the mobile phase for adsorption sites located on the stationary phase. Therefore the stronger the interaction between an analyte and the stationary phase the longer the time that the analyte is retained on the column and *vice versa* [89].

In NP-HPLC the backbone of the stationary phase is usually comprised of porous silica oxide (SO_2) or aluminium oxide (Al_2O_3) with hydroxyl (OH) group linkages covering the surface of the stationary phase, thereby ensuring the presence of polar surface [89]. The mobile phase for NP-HPLC technique is mainly comprised of non-polar solvents such heptane and hexane and small quantities of polar components, such as MeOH and ethanol, may sometimes be added to produce optimum resolution and retention conditions for the compounds to be separated [93]. NP-HPLC has been shown to be a superior technique for the separation of complex mixtures, however, it is not without shortcomings, which include, but are not limited to, limitations in solvent choices, lengthy equilibration times and limited sample applicability. Consequently this has led to the development of bonded-phase chromatography [94], also known as reversed-phase HPLC (RP-HPLC).

2.1.3.2 Reversed-phase HPLC (RP-HPLC)

RP-HPLC is a commonly used chromatographic technique in pharmaceutical sciences research and accounts for 90% of all low molecular weight compound analyses [89]. RP-HPLC uses a non-polar stationary phase in conjunction with a polar mobile phase, although the addition of non-polar mobile phase fractions is not uncommon when required to achieve an adequate separation. The stationary phase is comprised of a hydrocarbon chain of varying carbon lengths, chemically bonded to the silica backbone or support. The silica support can also be bonded chemically to different functional groups such as amino, cyanopropyl, ethers and diols to produce polar stationary phases such as for NP-HPLC. Alternatively ion-exchange functional groups such as sulphonic acid, amino and quaternary ammonium may be used and these are similar to those applied in IE-HPLC [90,95].

The retention of analyte(s) in RP-HPLC occurs primarily through dispersive forces such as hydrophobic or van der Waal's interactions [89]. Analyte(s) interact differently with the stationary phase depending on their polarity, resulting in longer and shorter retention times for non-polar and polar compounds respectively [89,92]. The retention of analyte(s) also depends on the polarity of the eluant, the more polar the eluant the longer the retention of nonpolar compounds and *vice versa*. In RP-HPLC the retention of hydrophobic analyte(s) on a stationary phase increases with increasing polarity and the strength of the eluant [92,96]. Despite the capability for using RP-HPLC for the analysis of different compounds, the pH of a mobile phase remains the major complication in sample separation, therefore it is recommended that analyses are performed with an eluant pH in the range 2.0-8.5 as hydrolysis or cleavage of the stationary phase may occur at extremes of the pH range [90,96].

2.1.3.3 Ion exchange HPLC (IE-HPLC)

IE-HPLC is commonly used for the separation of biological materials such as nucleic acid, amino acids and/or sugars [93,97]. Furthermore, inorganic samples known to have poor detectability and organic samples with poor UV absorptivity have been successfully separated using IE-HPLC [97]. IE-HPLC has also been used in preparative separations of analyte(s) by evaporation of volatile buffers such as ammonium acetate and ammonium formate [98] without adulteration of the analyte(s) [93,96].

The stationary phase in IE-HPLC is similar to those used for RP-HPLC with the exception of the bonded groups. In IE-HPLC the bonded phase is comprised of quaternary ammonium or amine functional groups for the separation of anions, or carboxylate or sulphonate groups for the separation of cations [93,96]. The retention of analyte(s) in IE-HPLC occurs through the exchange of ions between a charged stationary phase and counter ions of the analyte(s) of interest in the mobile phase, held at a specific pH and ionic strength [93,97]. As a result anionic or acidic analyte(s) are separated using anion-exchange columns as described in Equation 2.1 and separation of cations or protonated basic analyte(s) is achieved by using cation-exchange columns as described in Equation 2.2 [96].

$$X^- + R^+Cl^- \leftrightarrow X^-R^+ + Cl^- \qquad \textbf{Equation 2.1}$$

$$\boldsymbol{X^+ + R^-K^+ \leftrightarrow X^+R^- + K^+} \qquad \textbf{Equation 2.2}$$

Where,

R^+= anion exchange stationary phase
R^- = cation exchange stationary phase
X^+ = cationic analyte
X^- = anionic analyte

The separation of ionisable analyte(s) depends on the pH and ionic strength of the eluant [93,97]. Acidic analyte(s) lose proton(s) as the pH of the mobile phase increases, whereas basic analyte(s) gain proton(s) as the pH of the mobile phase decreases. Therefore as the pH of the mobile phase increases the retention time of acidic compounds will decrease and the retention for basic material will increase and *vice versa*. However this is true for only certain ranges of pH, specifically those that are similar to the pK_a values of the analyte(s) of interest [93]. Furthermore, incorporation of sufficient buffer salt at appropriate concentrations in the mobile phase is essential for the maintenance of an optimal pH for the effective separation of compounds of interest [93,96,99].

2.1.3.4 Size exclusion-HPLC (SE-HPLC)

SE-HPLC is also known as gel permeation chromatography (for organic mobile phases) or gel filtration chromatography (for aqueous mobile phases) [100]. SE-HPLC is a separation technique in which the relative size or hydrodynamic volume of macromolecules with respect to the pore shape and size of the stationary phase is critical to achieving a suitable separation [93]. The elution of larger molecules is achieved through the void volume of the column

whilst smaller molecules, depending on their relative size, are eluted through the pores of the column particles. As a result smaller molecules take longer to elute due to their permeation in and through the stationary phase [101-104].

SE-HPLC has been used for the separation of biological samples such as immunoglobulin, for sample clean-up, to separate monomers, dimers, trimers and larger aggregates of protein and polysaccharide [105], for the estimation of molecular mass and separation of reaction products from reaction mixtures amongst others [101].

SE-HPLC can be used over a wide range of mobile phase conditions since an effective separation requires minimal analyte(s) and stationary phase interaction, and is primarily dependant on the size of the molecule rather than enthalpic interactions as in NP, RP and IE HPLC [106]. Furthermore, the need to apply gradient elution is not necessary in SE-HPLC due to the nature of the separation mechanism (size or hydrodynamic volume) and consequently the instrumentation is simpler since no special pumping mechanism is required to produce a solvent gradient in comparison to other HPLC techniques [104].

2.2 ANALYTICAL METHODS FOR THE ANALYSIS OF RANITIDINE AND METRONIDAZOLE

The initial conditions used for the development of an HPLC method for the simultaneous analysis of RTD and MTZ were selected from published HPLC methods that had been used for the analysis of these compounds alone or in combination with each other. A summary of the conditions reported are listed in Table 2.1.

Table 2.1 Summary of HPLC conditions for the analysis of ranitidine and metronidazole

Analyte(s)	Sample matrix	Column	Mobile phase	Flow rate	Detector	Retention time	Reference
RTD: MTZ	Human plasma	Shim-pack C_{18}: 5µm 300 x 4.6 mm	10% v/v acetonitrile (ACN) in 10mM phosphate buffer; pH= 3.5	1 ml/min	UV 315 nm	6.4 min: 9.7 min respectively	[107]
RTD	Raw material	YMC-Pack ODS-AM: 5µm 150 x 4.6 mm	43% v/v methanol (MeOH) in 10mM SDS, 50mM phosphate buffer; pH 6.8	1 ml/min	UV 228 nm	27.0 min	[108]
RTD	Dosage forms	Phenomenex® Luna II column Agilent: 5µm 250 x 4.6 mm	10% v/v ACN in 10mM phosphate buffer; pH 7.1	1 ml/min	UV 230 nm	5.4 min	[14]
RTD	Human plasma	Symmetry® C_{18} : 5µm 150x 3.9 mm	12% v/v ACN in 50mM phosphate buffer; pH= 6.5	1 ml/min	UV 313 nm	2.8 min	[109]
RTD	Blood	µBondapak™ C_{18}: 10µm 150 x 3.9 mm	8% v/v ACN in 10mM phosphate buffer; pH= 5.1	2.5 ml/min	UV 330 nm	5.0 min	[110]
MTZ	Raw material	Waters Spherisorb® C_{18}: 5µm 250 x 4.6 mm	ACN: Water (14:86)% v/v	1 ml/min	UV 310 nm	7.6 min	[111]
MTZ	Blood	Hypersil ODS: 5µm 150x 4.6 mm	10% v/v ACN in 50 mM phosphate buffer containing 0.1% triethylamine ; pH=7	1 ml/min	UV 317 nm	6.7 min	[112]
MTZ	Human plasma	Merck Lichrosphere® 100 RP 18: 5µm 125 x 4 mm	15% v/v ACN in 10mM phosphate buffer; pH= 4.7	1 ml/ min	UV 318 nm	2.6 min	[113]
MTZ	Tissue	Zorbax SB-phenyl: 5µm 150 x 4.6 mm	15% v/v MeOH in 10mM phosphate buffer; pH= 4.0	1 ml/ min	UV 313 nm	9.2 min	[114]

It is evident that the majority of methods reported for the analysis of RTD and MTZ have been selected for their determination in biological samples and that there is a dearth of analytical methods for the analysis of these API in raw materials and pharmaceutical dosage forms [14,107,108,110-113]. The majority of the methods use RP-HPLC with C_{18} or C_8 stationary phases or, on rare occasions, a phenyl support has been used to achieve a separation [115]. The retention times for both compounds is in general $\leq$ 10 min, however a retention time as long as 27 min has been reported for MTZ [108].

The most commonly used organic modifier and buffer solution for mobile phase preparation has been ACN, and mono-basic potassium phosphate and the pH of the buffer ranged between 3.5-7.1 and the ACN content between 5-14% v/v [14,107-109,111,115,116]. Where ACN was not used in the mobile phase MeOH has been used [108,114].

The separation of molecules that ionize is best achieved in systems in which the mobile phase is buffered (§ 2.1.3.3). RTD is a weak acid (§ 1.2.1.4) and MTZ a weak base (§ 1.2.2.3), therefore buffer systems have been necessary to achieve suitable separation of these compounds [14,107-110,115,116] although a mobile phase in which no buffer was used has been reported for the analysis of MTZ raw material [111].

Ultraviolet (UV) absorption spectroscopy has been used for the detection of these compounds at wavelengths of between 228-230 nm or 315-330 nm for RTD and wavelengths of between 310-342 nm for MTZ [111,115]. In one instance, a wavelength of 274 nm was used for the detection of MTZ benzoate [116].

The published studies provide sufficient data on the chromatographic conditions for the analysis of RTD and MTZ in a variety of sample matrices (Table 2.1). Consequently these conditions were used as a starting point for the development and selection of an appropriate HPLC technique for simultaneous analysis of MTZ and RTD in raw material, powder blends and dosage forms. Therefore a RP-HPLC method using UV detection was selected as the preferred analytical tool for the quantitation of RTD and MTZ during formulation development and assessment studies.

2.3 EXPERIMENTAL

2.3.1 Materials and reagents

RTD, MTZ and ornidazole were purchased from Sigma Aldrich (St Louis, Missouri, USA). ACN (UV cutoff 200 nm) and MeOH (UV cutoff 215 nm) were purchased from Romil Ltd (Waterbeach, Cambridge, United Kingdom). Sodium hydroxide pellets and potassium dihydrogen orthophosphate were purchased from Merck Chemicals Ltd (Modderfontein, Gauteng, South Africa) and triethylammine was procured from SaarChem Pty Ltd (Krugersdorp, Gauteng, South Africa).

HPLC grade water for buffer and sample preparation was purified using a Milli-RO® 15 water purification system (Millipore Co., Bedford, Massachusetts, USA) that consisted of a Super C® carbon cartridge, two ion-X® ion exchange cartridges and an Organex-Q® cartridge. The water was filtered through a 0.22 µm Millipak® stack filter (Millipore, Bedford, Massachusetts, USA) prior to use.

2.3.2 HPLC system

The modular HPLC system consisted of a model P100 dual piston solvent delivery module (Thermo Separation Products, San Jose, California, USA), a model AS100 autosampler (Thermo Separation Products, San Jose, California, USA) fitted with a Rheodyne® Model 7010 injector (Rheodyne, Reno, Nevada, USA), a fixed volume 20 µl loop and a Gastight® 250 µl Model 1725 syringe (Hamilton Co., Reno, Nevada, USA). A linear UV/VIS-500 Model 6200-9060 detector (Linear Instrument Co., California, USA) and Spectra Physics SP 4600 integrator (Thermo Separation Products, San Jose, California, USA) were used for detection and data collection respectively. Separation was achieved on a Nova-Pak® C_{18} 60 Å 4 µm, 3.9 x 150 mm cartridge column (Waters Association, Milford, Massachusetts, USA) at 22±0.5°C.

2.3.2.1 Column selection

The selection of a suitable column for RP-HPLC analyses is dependent in part on the physiochemical properties of the analyte(s) of interest as these determine the nature and

magnitude of the interactive forces that are involved between analyte(s) and the stationary phase to achieve a suitable separation [89,92,96,101].

As indicated in § 1.2 RTD is a weak acid and MTZ is a weak base and their physiochemical properties have been described in detail in Chapter One. Following evaluation of the physiochemical properties of these compounds and a review of the relevant literature, a RP C_{18} column was selected for use in this study, despite operating pH limitations and the silanol effect usually observed when analysing basic molecules with silica based stationary phases [89,90].

The resolution and peak height of a response for a compound of interest on a chromatogram are dependent in part on the particle size and diameter of the material used for the stationary phase [117]. Columns with particles of particle size ranging between 3-10 µm have been reported to be an excellent compromise in terms of resolution, resultant back pressure and column lifetime and the best results have been reported when using columns with stationary phases of particle size diameter of 5 µm [96]. Although the risk of column plugging is increased with smaller particle sizes [96,118] the benefits of using such materials outweigh the limitations, therefore a column with 4 µm particle size diameter was selected for use in these studies.

The choice of a specific length and internal diameter of a column depends on the requirements for analysis. In general a range of between 3-4.6 mm for the internal diameter (id) and a length of 150 mm is considered adequate for normal analytical applications, whilst larger diameter columns have mostly been reserved for preparative purification of samples [96]. Narrow bore columns have improved separation and reduced solvent consumption and reports suggest that solvent consumption may decrease four times when a 2.1 mm id column is used in comparison to when a 4.6 mm id column is used [96]. Therefore a column with 3.9 mm id, 150 mm length and 4 µm particle size was selected for use in these studies.

The interaction of an analyte(s) with the stationary phase depends on the diffusivity of the analyte(s) through the pores of the column particles [118]. Columns with a larger pore size usually exhibit poor interactions between small dimension analyte molecules or particles due to a reduced relative surface area [96,118]. For routine analysis of molecules of < 2000 Da, a pore size of between 70-120 Å has been reported to be effective [96].

Following evaluation of the factors related to column performance and the review of literature, a Nova-Pak® C_{18} 60 Å 4 µm, 3.9 id x 150 mm HPLC cartridge column (Waters Association, Milford, Massachusttes, USA) was selected for the development of a RP-HPLC UV method for the simultaneous analysis of RTD and MTZ in pharmaceutical dosage forms.

2.3.2.2 Internal Standard (IS) selection

Quantitative analyses of finished products usually require sample preparation that often results in sample loss as a direct consequence of the extensive sample manipulation prior to analysis. Furthermore, biological samples usually require pre-treatment prior to analysis and the pre-treatment process often results in sample loss [96,119]. In addition, instrumental variation such as variability in flow rate and injection volume may result in variability in detector response to the same concentration of an analyte(s). Therefore to compensate for these deficiencies, an internal standard (IS) may be added to calibration and sample solutions to reduce analytical method variability [96,120].

A suitable IS should be well resolved from all components of a mixture and have a retention time close to that of the compound(s) of interest and, if possible, a similar chemical structure to facilitate detection [96,120]. Furthermore, the response factor of an IS must be of the same order of magnitude as the compounds which are to be analyzed [121] and must also be stable under the analytical conditions used to achieve an effective separation [122].

Frequently used IS for the analysis of RTD include procainamide or metoclorpromide [110] whereas for MTZ, tinidazole [112-114], ornidazole and phenylpropanolamine hydrochloride have been used [112].

Ornidazole was selected as the preferred IS since it exhibits a similar structure to MTZ, does not elute close to the analytes *viz.* MTZ and RTD and is readily available.

2.3.2.3 Preparation of stock solutions

Stock solutions of RTD (100 µg/ml), MTZ (100 µg/ml) and IS (100 µg/ml) were prepared by accurately weighing 10±0.05 mg of each compound using a Model AG135 Mettler Toledo top-loading analytical balance (Mettler Instruments, Zurich, Switzerland) and quantitatively

transferring each to a separate 100 ml A-grade volumetric flask. Each sample was dissolved in a mixture of MeOH:water (80:20) % v/v followed by sonication for 1 min using a Model B-12 Ultrasonic bath (Branson Cleaning Equipment Co., Shelton, Connecticut, USA). Aliquots from each stock solution were harvested and transferred to 5 ml A-grade volumetric flasks to produce mixture solutions of MTZ, RTD and the IS. The resultant mixture solutions were serially diluted using MeOH:water (80:20) to produce RTD:MTZ solutions of concentration 1:2.5, 2:5, 4:10, 6:15, 8:20 µg/ml respectively and that for the IS of 40 µg/ml.

2.3.2.4 Preparation of buffers

Phosphate buffer (50 mM) was prepared by accurately weighing 6.8 g of potassium dihydrogen orthophosphate into a 1000 ml A-grade volumetric flask and adding 2 ml triethylamine, and the solution was made up to volume with HPLC water. The buffer pH was adjusted to 6.7 using 0.1 M sodium hydroxide solution and the pH was monitored using a Crison GLP 21 pH-meter (Crison Instruments, Barcelona, Spain). The pH of the buffer solution was adjusted prior to the addition of organic modifier to avoid imprecise pH measurement due to drift of electrode response that is attributed to the presence of an organic modifier [96].

2.3.2.5 Preparation of mobile phase

The mobile phase was comprised of ACN 9% v/v in phosphate buffer at a pH of 6.7 containing 0.2% triethylamine. The mobile phase was degassed under vacuum using a Model A-25 Eyela Aspirator (Tokyo Rikakikai Co., Tokyo, Japan) and filtered through a 0.45 µm Durapore® HVLP membrane filter (Millpore Co., Billerica, Massachusetts, USA) prior to use.

2.4 RESULTS AND DISCUSSION

2.4.1 Effect of organic solvent composition

The retention time (R_t) and resolution (R_s) of RTD, MTZ and the IS were significantly influenced by the ACN content of the mobile phase as shown in Figure 2.2 and Table 2.2 respectively.

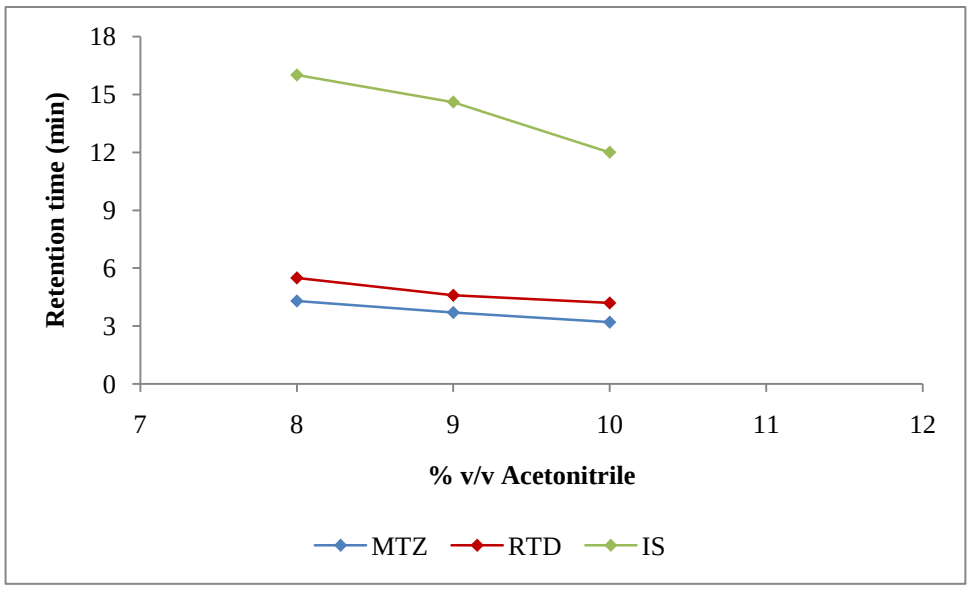

Figure 2.2 The effect of organic solvent composition on the R_t of MTZ, RTD and IS

Table 2.2 The effect of ACN content on peak R_s

ACN content (%) v/v	R_s
8	4.3
9	3.3
10	1.8

The R_t of MTZ, RTD and IS were 3.7, 4.6 and 14.6 min respectively when ACN was used at 9% v/v in the buffer. A reduction in the ACN content to 8% v/v in the buffer had an impact on the R_s between MTZ and RTD which changed to 4.3 from a value of 3.3 when 9% v/v ACN was included in the mobile phase as shown in Table 2.2. Furthermore the R_t of the IS increased to 16 min and consequently the run time had to be increased to 19 min. This change may be due to the decrease in competition between ACN molecules and IS molecules for the adsorbent sites on the stationary phase as a result of the low concentration of organic modifier. When the ACN content was increased to 10% v/v the R_s between MTZ and RTD changed to 1.8 and the R_t of the IS decreased to approximately 12 min. This may be due to

displacement of analyte molecules from the adsorbent sites on the stationary phase as a consequence of an increase in ACN concentration. The FDA recommends that the resolution between peaks of interest be not less than 2 [123]. Therefore, despite the optimal run time achieved at 10% v/v ACN content, the best compromise for resolution and the analytical run time was obtained at a concentration of 9% v/v ACN.

2.4.2 Effect of buffer molarity

In general buffer concentration has a relatively minor effect on the retention times of ionic sample when using reversed-phase chromatographic methods [96]. The effect of buffer molarity on the R_t of RTD is depicted in Figure 2.3.

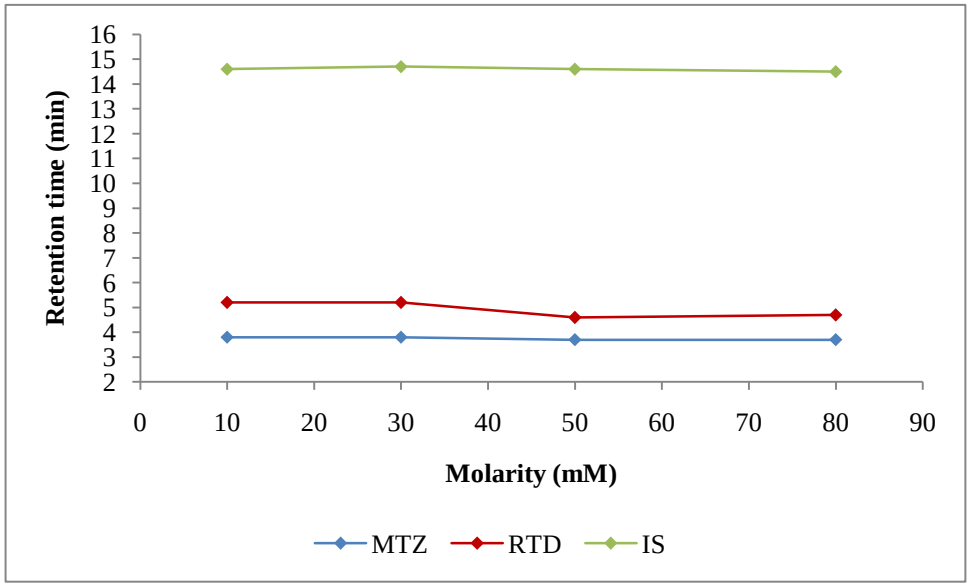

Figure 2.3 The effect of buffer molarity on the R_t of MTZ, RTD and IS

The results show that a change in the buffer molarity had an effect on the R_t of RTD whilst the R_t of MTZ and the IS were not as significantly affected. Increasing the molarity of a buffer from 10 to 50 mM resulted in a decrease in the R_t of RTD from 5.2 to 4.6 min. This may be due to an increase in competition between the buffer anions and RTD for the silanol sites as a consequence of the high buffer concentration. Furthermore, increasing the buffer concentration to 80 mM resulted in no change in the R_t of RTD.

2.4.3 Effect of triethylamine

The separation of basic compounds using silica-based stationary phases is often associated with changes in peak asymmetry and peak tailing due to what is known as the "silanol" effect. However the use of buffers in the mobile phase may sometimes alleviate the problem with varying degrees of success and that is dependent on the basicity of the analyte of interest [96,124].

The addition of triethylamine to a mobile phase has been reported to improve peak asymmetry and separation efficiency for basic compounds [96,125,126]. The addition of triethylamine to the mobile phase reduced peak tailing for RTD more efficiently than changes of the buffer molarity as described in Table 2.3.

Table 2.3 The effect of triethlyamine on peak tailing factor

Buffer molarity (mM)	**Peak tailing factor**
10	3.5
50	1.8
50*	1.25

*Buffer solution contains 0.2% v/v triethylamine

The peak tailing factor at 10 mM and 50 mM mobile phase buffer concentrations were 3.5 and 1.8 respectively, and on addition of 0.2% triethylamine to a mobile phase containing 50 mM buffer solution the peak tailing factor was reduced to 1.25. This may be due to preferential attachment of triethlyamine molecules to the acidic hydrogen atoms located on the silanol ends of the stationary phase backbone. A peak tailing factor of ≤ 2 is considered acceptable for routine quantitative analyses [123] and the addition of triethlyamine was necessary for the accurate quantitation of MTZ and RTD.

2.4.4 Effect of buffer pH

The pH of the buffer used to prepare the mobile phase had a significant effect on the R_t of RTD as depicted in Figure 2.4.

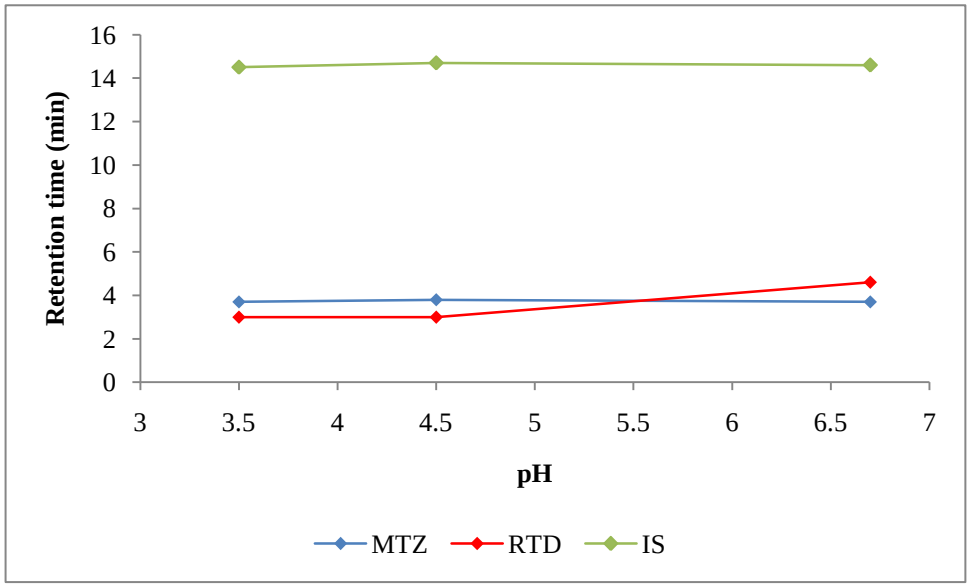

Figure 2.4 Effect of buffer pH on the retention time of MTZ, RTD and IS

A change in pH from 3.5 to 4.5 had no effect on the R_t of MTZ and RTD. However at a pH of 6.7 the R_t of RTD changed to 4.6 min with better resolution between MTZ and RTD being achieved.

2.4.5 Effect of flow rate

In general flow rate has an effect on the analytical run time. The effect of mobile phase flow rate on analytical run time is described in Table 2.4.

An increase in the flow rate of the mobile phase facilitates shorter analytical run times. Increasing the flow rate from 1 to 1.5 ml/min resulted in a change in the analytical run time from 20 to 18 min. Increasing the flow rate to 2 ml/min facilitated analytical run times of 16 min, whereas a flow rate of 2.5 ml/min resulted in a 14 min analytical run time. Despite the short analytical run time observed at a flow rate of 2.5 ml/min, the 3.9 mm id of the column was not suitable for the flow rate (2.5 ml/min). Therefore with respect to the id of the column, a flow rate of 2 ml/min resulted in an optimal analytical run time since flow rates of 1.0-2.0 ml/min are recommended for columns with id of 3.9 mm [127].

Table 2.4 The effect of mobile phase flow rate on analytical run time

Flow rate (ml/min)	Analytical run time (min)
1.0	20
1.5	18
2.0	16
2.5	14

2.4.6 Chromatographic conditions

The final HPLC chromatographic conditions for the simultaneous analysis of MTZ and RTD are summarized in Table 2.5 and a typical chromatogram obtained with these conditions is depicted in Figure 2.5.

Table 2.5 Chromatographic conditions

Column	C_{18} Nova-Pak® 4 µm 3.9 x 150 mm cartridge
Flow	2 ml/min
Injection volume	20 µL
Detection	317 nm
Temperature	22 ± 0.5°C
Mobile phase	ACN: 50 mM buffer pH 6.7 (9:91) %v/v containing 0.2% v/v triethylamine
Detector sensitivity	0.005 AUFS
Chart speed	2.5 mm min^{-1}

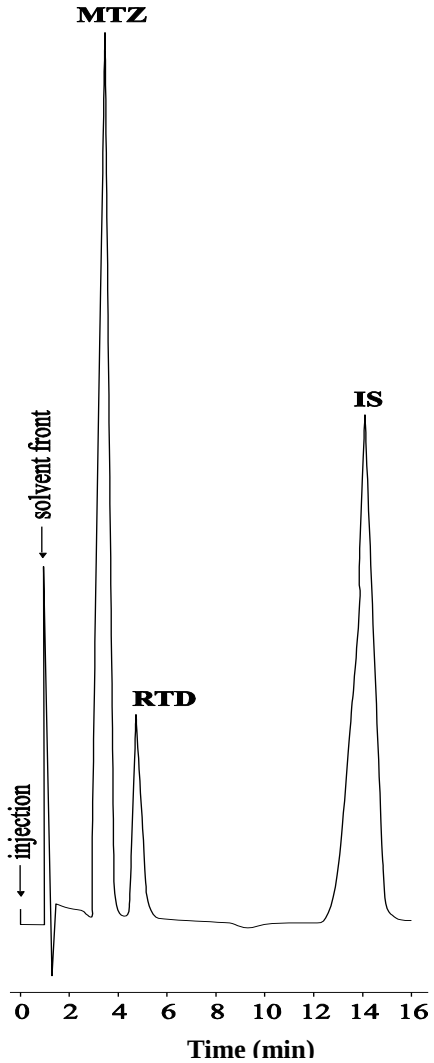

Figure 2.5 Typical chromatogram of MTZ, RTD and IS at a concentration of 10, 4 and 40 µg/ml respectively obtained using the conditions described in Table 2.4

2.5 METHOD VALIDATION

2.5.1 Introduction

Reliable and reproducible analytical methods are critical for the assessment of quality of a starting material, intermediate and finished product in the pharmaceutical, cosmetic, chemical and food industries. However many of the analytical methods fail to produce the expected results when different environmental conditions, instrumentation, equipment or different analysts are used. To minimise the issues encountered due to variability of this nature, it is of paramount importance that analytical methods are validated prior to implementation [96,128]. The validation of analytical methods is an integral part of the requirements for submission of analytical methods to regulatory authorities such as Food and Drug Administration (FDA), Tanzania Food and Drug Authority (TFDA), Medicine Control Council (MCC) and compendia such as the United States Pharmacopoeia (USP) and the British Pharmacopoeia (BP) amongst others [128]. The types of studies performed for method validation depends on the goal(s) of the specific analytical method under investigation. For instance methods developed for the trace analysis of materials requires a different approach and acceptance criteria in comparison to major component analysis. However at the early stages of method development specificity, accuracy, precision, range and linearity studies of the analytical method must be considered [96,129].

2.5.2 Linearity and range

The linearity of an analytical method describes whether the response of an analyte(s) in relation to the concentration of that analyte is linear [129]. The acceptability of linearity data depends on the correlation coefficient (R^2) generated following least square linear regression analysis of analyte response versus analyte concentration. An R^2 value of > 0.999 is generally acceptable for major component assay [96,128]. For assay purposes linearity studies are performed at 50%, 75%, 100%, 125% and 150% of the target levels for analyte that exhibit linear response at these concentrations [96,128].

The range of an analytical method is the interval between the upper and lower concentrations of an analyte for which the accuracy, precision and linearity are within acceptable limits [96,128].

The linearity and range for the analysis of RTD and MTZ were established by plotting the peak height ratios of MTZ/IS and RTD/IS versus the concentration of MTZ and RTD respectively as summarized in Table 2.6.

Table 2.6 The resultant peak height ratios as function of concentration

MTZ			RTD		
Concentration (µg/ml) (n=5)	**Average peak height ratio**	**% RSD**	**Concentration (µg/ml) (n=5)**	**Average peak height ratio**	**% RSD**
2.5	0.22±0.005	2.56	1	0.05±0.001	3.10
5.0	0.42±0.015	3.62	2	0.12±0.004	3.92
10.0	0.86±0.024	2.78	4	0.25±0.004	1.72
15.0	1.27±0.033	2.61	6	0.37±0.013	3.52
20.0	1.66±0.049	2.97	8	0.49±0.016	3.39

The equation of the line and R^2 for MTZ was $y = 0.0832x + 0.0171$ and 0.9995 respectively and that for RTD was $y = 0.0626x - 0.0024$ and 0.9995 respectively. The respective calibration curves for MTZ and RTD are depicted in Figures 2.6 and 2.7 respectively. The resultant curve for MTZ was linear at concentrations of 2.5, 5, 10, 15, and 20 µg/ml and that for RTD at concentrations of 1, 2, 4, 6, and 8 µg/ml.

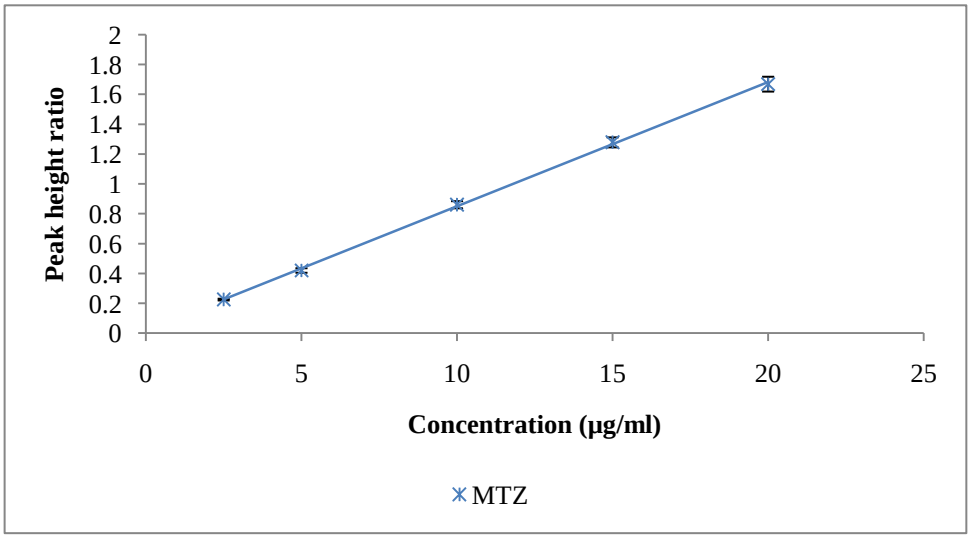

Figure 2.6 Range and linearity curve for MTZ plotted using the data listed in Table 2.6

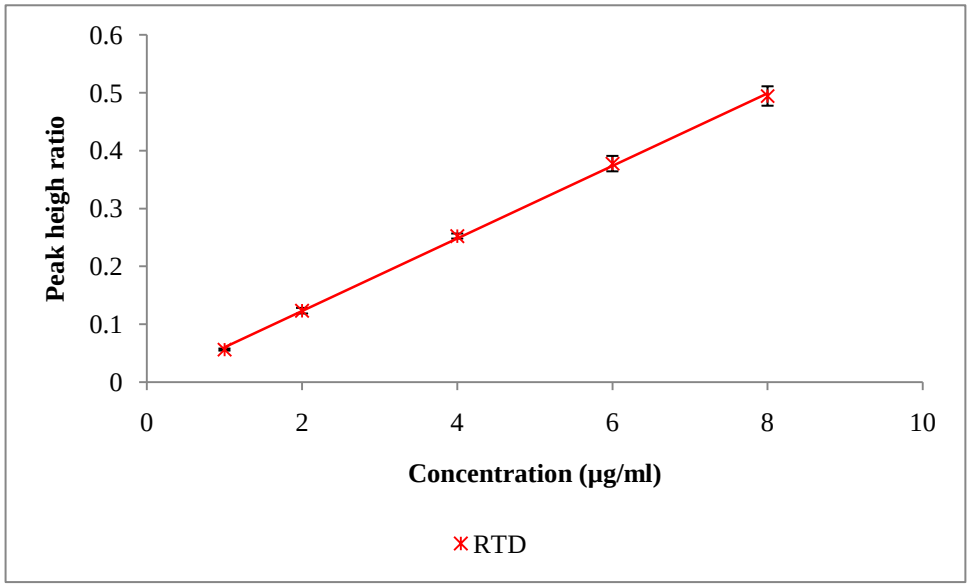

Figure 2.7 Range and linearity curve for RTD plotted using the data listed in Table 2.6

2.5.3 Precision

The precision of an analytical method is the closeness of agreement of the test results obtained following multiple analyses of the same homogenous sample under the prescribed conditions [96,129]. Precision can be further subdivided into repeatability, intermediate precision and reproducibility [96,128]. Precision is usually reported as the percent of relative standard deviation (% RSD). In this study a %RSD of <5 was set as the tolerance limit.

2.5.3.1 Repeatability

Repeatability is also known as intra-assay precision and is the precision of an analytical method used under the same operating conditions over a short time interval [129]. These types of studies are performed to test instrument performance [96]. A minimum of nine determinations covering the specified range for the procedure are required for repeatability studies [96,128,130]. Repeatability was determined following triplicate injection of three concentrations covering the calibration range at low, medium and high levels. The repeatability data generated within the previously determined calibration range on Day 1 are summarized in Table 2.7.

Table 2.7 Repeatability and intermediate precision data for the simultaneous analysis of MTZ and RTD

	MTZ			RTD		
DAY	**Concentration (µg/ml)**	**Mean concentration determined (µg/ml)**	**(% RSD)**	**Concentration (µg/ml)**	**Mean concentration determined (µg/ml)**	**(% RSD)**
1	2.50	2.52 ± 0.026	1.04	1.00	1.01 ±0.005	0.56
	10.00	9.69 ± 0.135	1.40	4.00	3.83 ± 0.045	1.17
	20.00	20.16 ± 0.533	2.64	8.00	8.00 ± 0.066	0.83
2	2.50	2.70 ± 0.070	2.59	1.00	1.19 ± 0.017	1.45
	10.00	10.05 ± 0.270	2.68	4.00	3.91 ± 0.070	1.81
	20.00	20.35 ± 0.350	1.72	8.00	7.87 ± 0.115	1.47
3	2.50	2.59 ± 0.117	4.55	1.00	0.94 ± 0.450	2.97
	10.00	9.75 ± 0.387	3.97	4.00	3.86 ± 0.119	3.08
	20.00	19.95 ± 0.560	2.80	8.00	7.79 ± 0.231	2.97

2.5.3.2 Intermediate precision

The intermediate precision of an analytical method expresses the precision of that method under various laboratory conditions [96]. These studies test the impact of different days or the use of different analysts or equipment on the analytical method [96,130]. Intermediate precision of the method was determined on two additional consecutive days. The analysis was performed in triplicate at the three concentrations covering the determined range at low, medium and high levels. The intermediate precision data for Days 2 and 3 are summarized in Table 2.7.

2.5.3.3 Reproducibility

The reproducibility of an analytical method is the precision of that method when analyses are conducted using the same method in different laboratories. These studies are usually performed if standardization of an analytical procedure is required [96,130]. However, for this study standardization of the analytical procedure was not necessary since the analysis was undertaken using the same equipment and analyst in the same laboratory.

2.5.4 Accuracy

Accuracy is defined as the closeness of agreement between a measured value and a value which is accepted as the conventional true value or accepted reference value for a sample undergoing analysis [130]. Usually accuracy is determined by use of recovery studies although analyte standard addition, reference standard comparison and spiked blank matrix analyte recovery studies have also been used for accuracy determination [96]. The FDA recommends accuracy studies to be performed at 80%, 100% and 120% levels of the product label claim [123] and these studies should be performed at levels within the expected final product concentration range [96,130]. Accuracy was performed in triplicate at three levels *viz.* high, medium and low in order to cover the necessary range of concentration that were to be investigated (§ 2.5.2). A tolerance of 5% was set for the % RSD and a % bias of <5% for the bias and the results of accuracy assessment are summarized in Table 2.8.

Table 2.8 Accuracy results for the simultaneous analysis of MTZ and RTD

MTZ				RTD			
Concentration (µg/ml)	**Mean concentration determined (µg/ml) (n=3)**	**Precision (% RSD)**	**% Bias**	**Concentration (µg/ml)**	**Mean concentration determined (µg/ml) (n=3)**	**Precision (% RSD)**	**% Bias**
2.50	2.52 ± 0.026	1.04	-0.90	1.00	1.01 ± 0.005	0.56	-1.75
10.00	9.60 ± 0.135	1.40	3.27	4.00	3.83 ± 0.040	1.17	4.18
20.00	20.16 ± 0.533	2.64	-0.82	8.00	8.00 ± 0.006	0.83	-0.06

2.5.5 Limits of quantitation (LOQ) and detection (LOD)

The limit of quantitation (LOQ) is the lowest concentration of an analyte that can be quantitated with acceptable precision and accuracy under the prescribed experimental conditions [96,123,130]. The limit of detection (LOD) of an analyte is the lowest concentration of an analyte that produces a measurable response but cannot accurately be quantitated under the stated experimental conditions [96,123,130]. The USP recommends the use of signal to noise ratio for the determination of LOQ and LOD of an analytical [129]. Signals of samples with known low concentration of the analyte(s) are compared to signals of blank samples in order to establish the analyte concentration that produces a signal to noise ratio of 10:1 for LOQ and 3:1 for LOD [129] as listed in Table 2.9. However the application of this method requires analytical methods that exhibit substantial baseline noise. Further, this method is detector specific, thus analyses of the same sample performed on different

detectors may produce different signal noise ratios and consequently different results for the LOQ and LOD may be observed. An alternate approach for the determination of LOQ and LOD of an analytical method may be the use of the standard deviation (σ) of the response and the slope of the line. A calibration curve in the range of LOQ or LOD is constructed followed by determination of the slope and standard deviation of the y-intercept of the resultant equation of the line. The relationship between the slope and the standard deviation in determination of LOQ and LOD is described in Table 2.9.

Table 2.9 Methods for the determination of LOQ and LOD

Method	**LOD**	**LOQ**	**Reference**
Signal to noise ratio	3 or 2: 1	10: 1	[96,130,131]
Based on standard deviation of the response and the slope	$\frac{3.3\sigma}{Slope}$	$\frac{10\sigma}{Slope}$	[130,131]
Based on precision value.	Not stated	% RSD > 3	[96]

The LOQ and LOD for this method were established by use of the signal to noise ratio method. Both MTZ and RTD had similar LOQ and LOD values *viz*. 0.3 µg/ml and 0.1 µg/ml respectively.

2.5.6 Specificity

The specificity of an analytical method is the ability of the method to accurately quantitate an analyte in the presence of compounds such as impurities, excipients and matrix materials that may interfere with the analysis [128,132]. In method development studies the establishment of specificity is vital since the reliability, accuracy, precision and linearity of a method are dependent on the specificity of the method [96].

The specificity of the method was established by assessing the resolution of MTZ and RTD in a mixture spiked with potential formulation excipients in the same ratio as they would be used in a product. Furthermore, commercial tablets of MTZ and RTD were used for specificity studies. Both MTZ and RTD were well resolved from the excipients tested, which suggesting that the method is specific when used for the simultaneous analysis of both compounds.

2.5.7 Forced Degradation Studies

Most regulatory authorities have adopted the ICH guidelines for method validation that require analytical methods for drug product analyses to be stability indicating. The guideline requires that an analytical method shows discrimination between an analyte and degradation products that may occur following forced degradation studies [52]. Furthermore forced degradation studies should be performed under a variety of environments including light, oxidative, acidic, basic and heat conditions [133]. In addition the ICH guidelines require the analysis of individual degradation products qualitatively and quantitatively, however qualitative analyses of degradation products only were used for this research.

2.5.7.1 Method

Analysis of degradation studies was performed by comparing chromatograms generated during forced degradation studies and those following analysis of a freshly prepared standard solution of MTZ and RTD.

2.5.7.1.1 Sample preparation

Approximately 1 mg of MTZ and RTD were weighed separately and quantitatively transferred into 10 ml A-grade volumetric flasks. With the exception of oxidative studies, the drug substance was dissolved and made up to volume with a medium specific for that degradation study, to yield a solution at a concentration of 100 µg/ml.

2.5.7.1.1.1 Oxidative degradation

MTZ and RTD exhibit poor solubility in H_2O_2. It has been reported that an appropriate solvent may be used to improve drug solubility in the degradation medium [134]. Thus each drug substance was dissolved in 4 ml of MeOH:water (80:20) and the resultant solutions were made up to volume (10 ml) with a 10% v/v H_2O_2 (Allied Drug Company Ltd, Durban, KwaZulu-Natal, South Africa) after which each sample was refluxed for 8 h at 50±0.5°C. Sample aliquots (2 ml) were collected prior to refluxing and after every hour during refluxing. Aliquots (2 ml) of IS that had been prepared as described in § 2.3.2.3 were added

to each sample and the resultant solution was made up to volume (10 ml) with MeOH:water (80:20) and analyzed using HPLC.

2.5.7.1.1.2 Acid degradation studies

The drug substances were dissolved and made up to volume (10 ml) using 0.1 M HCl and the solutions were refluxed for 8 h at 50±0.5°C. Sample aliquots (2 ml) were collected prior to refluxing and after every hour during refluxing and transferred to a 10 ml A-grade volumetric flask followed by addition of 2 ml of IS that had been prepared as per method in § 2.3.2.3. The resultant solution was made up to volume using MeOH:water (80:20) prior to analysis by HPLC.

2.5.7.1.1.3 Alkali degradation studies

The drug substances were dissolved and made up to volume (10 ml) using 0.1 M NaOH and the solutions were refluxed for 8 h at 50±0.5°C. Sample aliquots (2 ml) were collected prior to refluxing and hourly after refluxing had commenced and transferred to a 10 ml A-grade volumetric flask followed by addition of 2 ml of IS that had been freshly prepared as described in § 2.3.2.3 and the resultant solution made up to volume with MeOH:water (80:20) prior to analysis by HPLC.

2.5.7.1.1.4 Photolysis

The drug substances were dissolved and made up to volume (10 ml) with distilled water and the resultant solutions were exposed to sunlight for 8 h. Sample aliquots (2 ml) were collected prior to exposure and hourly following the commencement of exposure and transferred to a 10 ml A-grade volumetric flask followed by dilution with 2 ml of IS that had been prepared as described in § 2.3.2.3, and the resultant solution made up to volume with MeOH:water (80:20) prior to analysis by HPLC.

2.5.7.2 Results and Discussion

2.5.7.2.1 Oxidative degradation

Both compounds did not exhibit appreciable degradation when they were incubated in a 10% v/v H_2O_2 solution at room temperature, however significant degradation was detected for RTD samples in comparison to MTZ samples after 1 h of refluxing. MTZ and RTD produced peaks at 3.7 and 4.6 min respectively as shown in Figure 2.8 (I) but the analyses of degradation samples revealed a decrease in the peak height for RTD peak at 4.6 min and the appearance of a new peak at 1.8 min after 1 h of refluxing as depicted in Figure 2.8 (II). The total disappearance of the peak for RTD was observed at the end of the second hour of refluxing (Figure 2.8 III). This may be due to degradation of RTD to rantidine S-oxide. Similar results following incubation of RTD syrup in 3% H_2O_2 have been reported [14].

Unlike RTD, MTZ is relatively stable in a 3% v/v H_2O_2 solution and the chromatogram revealed neither a change in R_t nor the peak characteristics for MTZ. Similar results following 6 h incubation of MTZ in 3% v/v H_2O_2 solution have been reported although 30% degradation was detected following incubation in a 30% H_2O_2 solution [111].

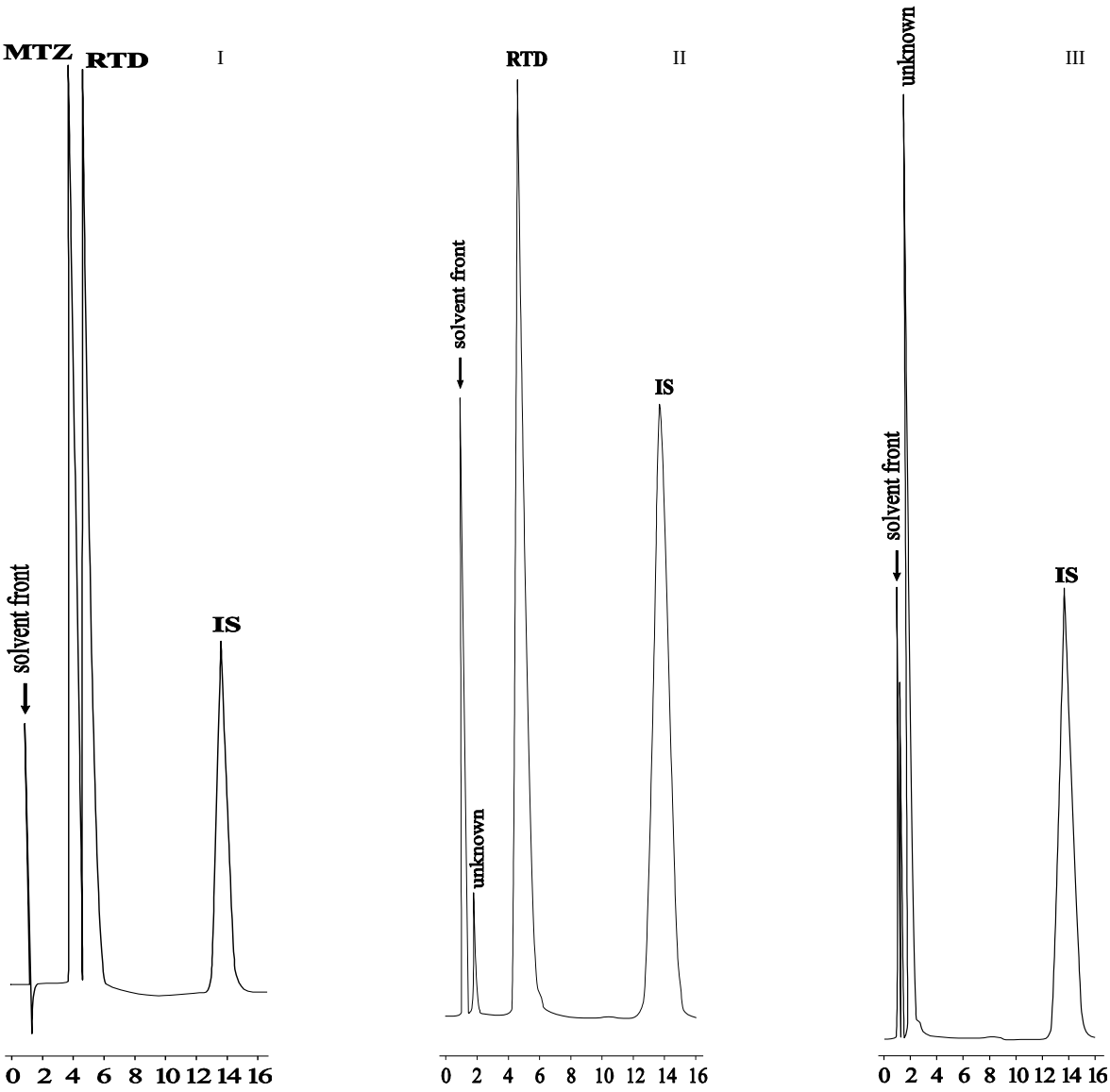

Figure 2.8 Chromatograms of standard solution each at a concentration of 20 µg/ml (I) and oxidative degradation of RTD after 1 h (II) and 2 h (III) of reflux

2.5.7.2.2 Acid degradation

Analyses performed following acid hydrolysis of RTD revealed no degradation under these conditions. The peak characteristics and R_t of RTD were similar to those of the standard solution. These results are in agreement with those observed following incubation of RTD in 0.1 N HCl [14]. Similarly no degradation was detected following the analysis of MTZ samples. However, these results did not agree with those of Bakshi *et al.* [111], where 20% degradation of MTZ was recorded when heated in 0.1 M HCl. The lack of degradation observed for MTZ may be ascribed to short refluxing time, *viz.* 8 h, and low heating temperature, *viz,* 50°C.

2.5.7.2.3 Alkali degradation

Both RTD and MTZ were observed to degrade when exposed to alkaline degradation. The chromatograms observed following exposure of MTZ to alkali conditions revealed a new peak at 6.9 min as can be seen in Figure 2.9 (I). The periodic sample analyses over the first 3 h showed appearance of new peak at 1 min, and both peaks *viz.* peak at 1 and 6.9 min existed at the expense of the parent peak at 3.7 min (Figure 2.9 II) and there was total disappearance of both peaks following 5 h of refluxing (Figure 2.9 III). This may be due to the formation of non-chromorphic degradants since MTZ degrades under alkali conditions to produce acetic acid and ammonia [52,111]. Furthermore 95% degradation of MTZ and the presence of non-chromorphic degradants following incubation of the drug in 0.1 M NaOH at 80°C has been reported [111].

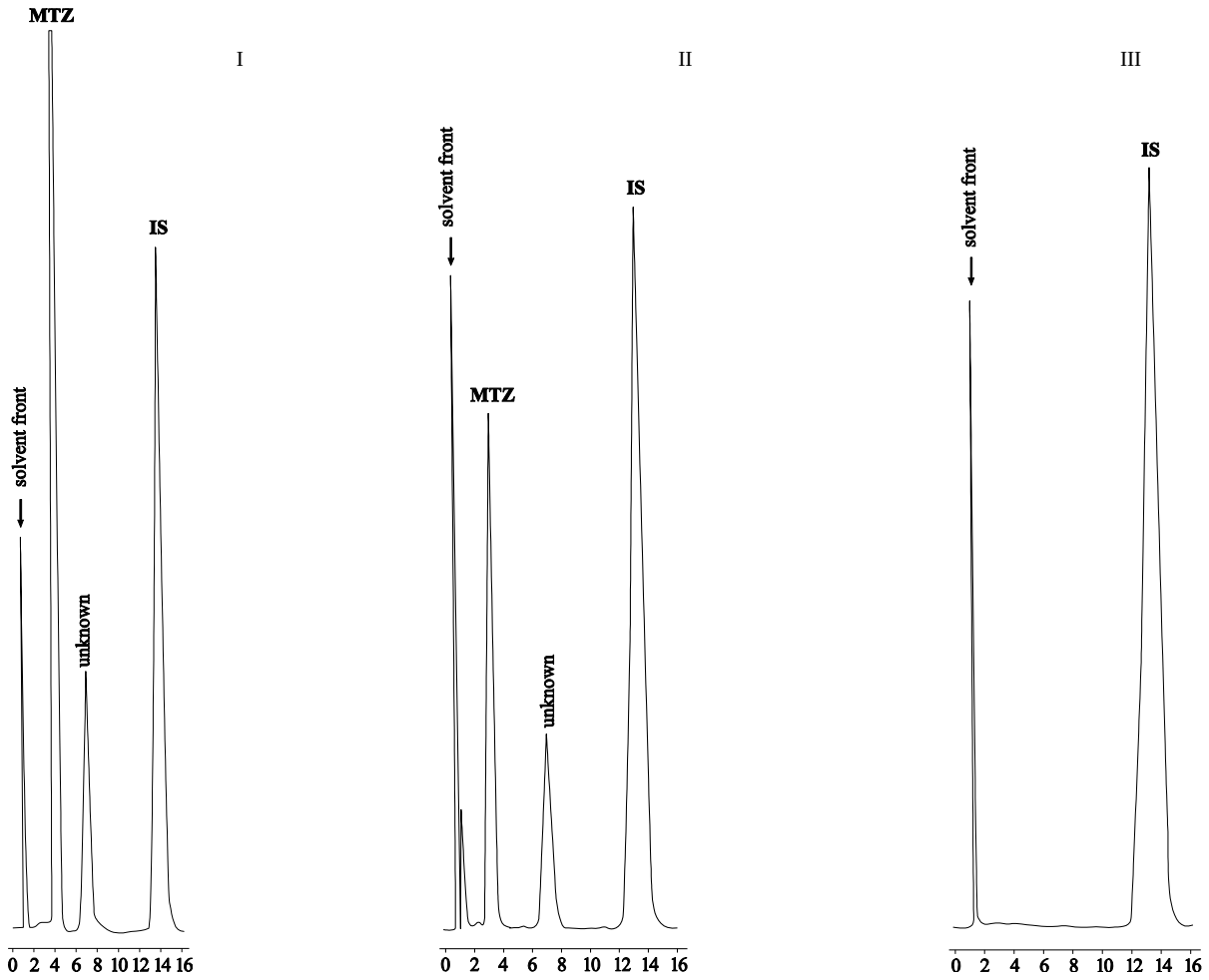

Figure 2.9 Chromatograms of alkali degradation of MTZ at 0 h (I), 3 h (II) and 5 h (III)

Similarly analyses of RTD following alkali degradation revealed the presence of two new peaks at 6.9 min prior to commencement of refluxing (Figure 2.10 I) and the presence of a second peak at 2.0 min after 1 h of refluxing (Figure 2.10 II). Subsequent analyses of samples showed that the two peaks existed with a decrease of the parent peak at 4.6 min (Figure 2.10 III) followed by complete disappearance of the drug and degradant peaks after 5 h of refluxing. These results were in agreement with those previously reported following incubation of rantidine syrup in 0.1 N NaOH [14].

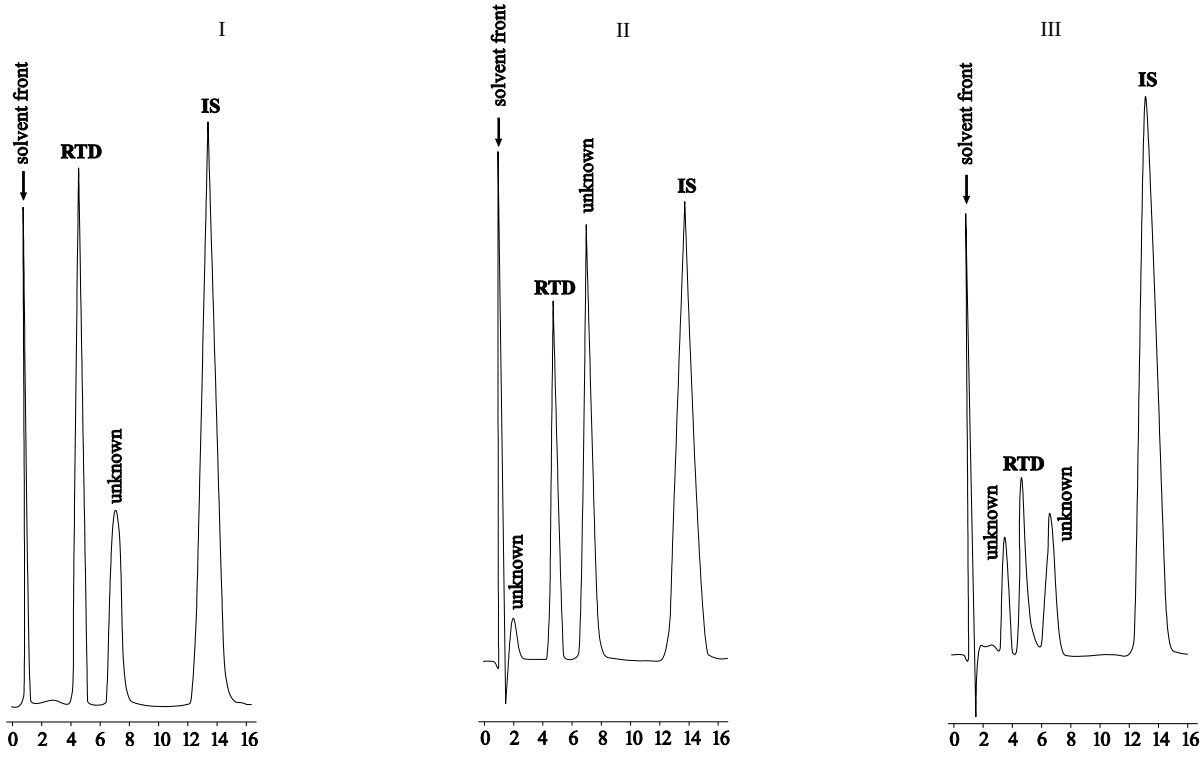

Figure 2.10 Chromatograms of alkali degradation of RTD at 0 h (I); 1 h (II) and 3 h (III)

2.5.7.2.4 Photo degradation

The analyses of samples following exposure to light revealed that both compounds are susceptible to photolysis. The peaks heights of MTZ and RTD decreased as refluxing continued when the solutions were compared to those of a standard solution of the same concentration. The lack of detection of the degradants may be due to the formation of non-chromorphic degradants or degradants with different λ_{max} in comparison to the parent compound. These results were similar to the reported photodegradation studies of MTZ and RTD respectively [14,111].

2.6 CONCLUSIONS

The use of an appropriate and validated analytical technique is essential for the generation of reliable data in the analysis of raw materials, intermediate and finished pharmaceutical products. A suitable analytical method must ensure that the compound(s) of interest is well resolved and free from interference from excipients used in the formulation and the IS. A successful chromatographic resolution is dependent on a variety of factors and these include suitable column and mobile phase composition, buffer concentration and pH, flow rate and temperature.

An HPLC method has been developed that has the necessary specificity, precision and accuracy for the simultaneous assessment of RTD and MTZ. The method was found to be linear within the range of 2.5–20 µg/ml and 1–8 µg/ml for MTZ and RTD respectively and the coefficient of determination of 0.9995 for both compounds *viz.* MTZ and RTD. Furthermore the method can also be used for the assessment of individual compounds in solid dosage forms and raw materials. In addition the separation of degradation products of the two compounds has been achieved using the same chromatographic conditions.

Furthermore MTZ and RTD can be used as an IS for the analysis of the other compound in analyses with analytical run times of <10 min.

The method is stability indicating, however additional instrumentation such as mass spectrometer and photodiode array detection must be used in order to detect and identify more degradation products.

CHAPTER THREE
PREFORMULATION AND POWDER ASSESSMENT

3.1 INTRODUCTION

Pharmaceutical dosage forms are usually mixtures of several excipients that are included in a formulation to facilitate the manufacturing process and ensure drug delivery to the systemic circulation. The mode of action of excipients is fairly well understood, however each excipient has a specific function(s) in a formulation and together they ensure optimal dosage form performance. The choice and use of an excipient in a dosage form depends on the type of dosage form to be produced and on the physiochemical and mechanical properties of the API. The preferred choice of an excipient(s) depends on the experience of a formulation scientist and access to relevant scientific data that describe the effect(s) of the excipient(s) in a formulation. The data that describes the effect of excipient(s) on a formulation is usually obtained from a series of tests or studies performed on the excipients with and without the API. These studies that are used to characterize the physiochemical and mechanical properties of an API and the excipients are known as preformulation studies [135].

Preformulation studies gained popularity in the 1950s where the use of this approach was aimed at reducing the trial and error approach that had to that point been used in the design of formulations. In the pharmaceutical industry, preformulation studies is a multidisciplinary study approach that involves different research teams in the areas of quality control, basic pharmaceutics, dosage form development and analytical research, amongst others [136,137].

There are myriads of tests that are performed during preformulation studies, however, commonly performed evaluations include but are not limited to establishing the pK_a, particle size, aqueous solubility, pH solubility profile, dissolution rate of pure drug substance (intrinsic dissolution), polymorphism and excipient compatibility with the chemical moiety.

RTD and MTZ have been used for the clinical management of different pathological conditions as mentioned in § 1.2.1.9.2 and § 1.2.2.8.4 respectively and the physiochemical properties have been described in Chapter One *vide infra.* Preformulation data for RTD and MTZ has also been well documented [8,42]. In this chapter, the influences of the molecular

properties and the physiochemical properties of these API and excipients on tablet dosage form development are discussed.

3.1.1 Physiochemical properties

3.1.1.1 Particle size and shape

The content uniformity of tablets is markedly influenced by the particle size and shape of an API and excipients. For a low dose formulation, the attainment of blend homogeneity can be a particularly challenging issue. Spherical particles have a low contact surface area in comparison to acicular or prism shaped materials and consequently they pose fewer mixing problems compared to the alternate shaped materials. Spherical particles have better flow properties resulting in minimal weight variation of tablets during compression. However, the concept of blend homogeneity and powder flow properties does not entirely depend on particle shape: other factors such as particle density, surface and size have been reported to exert significant effects [138,139].

Particle size has a significant influence on the dissolution rate of a material. Small particles exhibit better dissolution rates than larger particles as a consequence of their larger apparent surface area. The effect of surface area on dissolution rate has been documented [140] and the interrelation of other contributing factors on the dissolution rate can be described mathematically using Equation 3.1.

$$\frac{dC}{dt} = A \cdot \frac{D}{h} \cdot \frac{(C_s - C)}{V} \qquad \textbf{Equation 3.1}$$

Where

$\frac{dC}{dt}$ = Dissolution rate
A = Surface area of the dissolving particles
D= Diffusion coefficient of the solute
h = Hydrodynamic layer thickness
C_s= Equilibrium solubility
C = Solute concentration in the bulk of the solution
V = Volume of medium

It is evident that an increase in the surface area of the particles results in an increase in the dissolution rate (Equation 3.1), however increased surface area can cause blend

heterogeneity. Mixing properties of powders may be compromised as the particle size decreases since smaller particles have the potential to acquire a surface charge and consequently adhere to particles that have an opposite charge on their surfaces. In addition, segregation with a consequence of poor blend uniformity is inevitable when powders of different particles sizes are blended [141]. Therefore the determination of the properties of powders and particles provides preliminary data that can be used to guide a formulation scientist during the selection of an appropriate manufacturing method. Nonetheless the choice of a manufacturing process should take into account the molecular and physiochemical properties of a drug substance and potential excipients to be used since the selection of an inappropriate manufacturing process may alter the molecular and physiochemical properties of the drug and/or excipient(s) [142]. A summary describing the effects of manufacturing processes on drug molecular properties is described in Table 3.1.

Table 3.1 The effect of manufacturing processes on molecular properties of drugs. Adapted and modified from [135].

Processing step	Purpose of step	Possible solid-state transformation	Implication on tablet formulation
Milling	Size reduction; to improve powder flow and content uniformity	Polymorphic conversion, dehydration, amorphous phase transformation	Chemical stability, dissolution rate and bioavailability.
Roller compaction	Dry granulation, size increase; to improve powder flow and content uniformity	Polymorphic conversion, dehydration and amorphous phase transformation	Chemical stability, dissolution rate and bioavailability.
Wet massing	Wet granulation, size increase to improve powder flow and content uniformity	Polymorphic conversion, hydrate formation, salt to free acid/base conversion; amorphous phase transformation	Chemical and physical stability and dissolution rate

3.1.1.2 Powder density

In formulation development the density of individual powder components and blends may contribute to the behavioural characteristics of the material during the manufacturing process. The compressibility, compactability and flow properties of powders depend on or are closely associated with the density of the individual material or its behaviour when placed in a mixture [138,139]. The determination of the density of powders is a complicated procedure due to the nature of the material being evaluated. Powders are comprised of an infinite number of discrete particles that impart different types of density to a material, depending on

the equipment and conditions used for the evaluation process. However, in solid dosage form development the true, bulk and tapped densities of powders are the most important characteristics that must be evaluated.

3.1.1.2.1 Bulk density

The bulk density of a powder is the ratio of the mass of that powder to the volume that the mass of powder occupies. The volume of the powder includes the interparticle volume and envelope volume of the particles of the powder [143,144]. The bulk density of a powder has often been thought to have a direct relationship to the flowability of the material. However the inter-particulate interaction that influences the bulk properties of a powder are the same interactions that interfere with the flow properties of the material [145]. Therefore the determination of the bulk density of a powder provides valuable information pertaining to equipment requirements with respect to fill capacity of the equipment required for a particular method of manufacture [143]. In addition the bulk density of the powder is usually used to establish Carr's Index (CI) that describes the flow properties of a powder system. The interpretations of CI values are described in Table 3.2.

Table 3.2 Interpretation of Carr's index values

Carr's index (%)	**Flow**
5 – 15	Excellent
12 – 16	Good
18 – 21	Fair
23 – 35	Poor
33 – 38	Very poor
> 40	Very very poor

3.1.1.2.2 Tapped density

The tapped density of a powder is in effect the bulk density of a powder that is established after tapping or vibrating the powder in a specific manner for a period of time. Different types of instruments can be used to determine the tapped density of powders; they exhibit similarity in that the use of a fixed weight or volume of powder for the determination of tapped density is required. A given mass or volume of powder is dropped (tapped) from a set distance at a specified frequency for a fixed period of time until the equilibrium volume of the powder is reached, and the tapped density is then calculated mathematically [143]. The relationship between bulk density and tapped density of powders provides useful information

relating to properties of the powders such as flowability and compactability. Materials with a high compressibility value exhibit poor flow properties and *vice versa* [146,147]. The Hausner ratio (HR), that is, the ratio of tapped bulk density and aerated bulk density, provides information that describes the relationship between the cohesiveness of powder particles and powder flowability. Powders with a HR ≥ 1.4 are considered to be cohesive and difficult to fluidize and those with ratios ≤ 1.25 are characterized as free flowing [144,148].

3.1.1.2.3 True density

The true density of a substance is the average mass per unit volume of that material with all voids that are not a fundamental part of the molecular packing arrangement having been excluded [139]. The true density of powders translates to the average mass per unit volume of a unit powder particle, and is a critical parameter in the characterization of the mechanical properties, porosity and fluidization characteristics of a powder. The true density of powders has been used to calculate the porosity of a tablet on which tablet hardness and strength are dependent [139,149]. There are a variety of ways to determine the true density of powders, however, helium pycnometry is a commonly used method despite its lack of accuracy in samples containing loosely bound solvents [139,149]. In addition the mass of a powder compact has also been used to establish the true density of materials [150].

3.1.2 Molecular properties of powders

3.1.2.1 Polymorphism and solvatomorphism

It is not uncommon for organic compounds to exhibit the same elemental composition in different crystalline structures and hydration states. Compounds exhibiting these properties are considered to be polymorphs and this phenomenon is defined as polymorphism [151]. In addition, the solvation or hydration state of different crystal forms of a material may differ and the existence of crystal forms with different hydration states is defined as solvatomorphism [151-153].

The presence of polymorphs and solvatomorphs may have a significant effect on the solid state properties of a particular system in which the material is located. Different crystal forms of a compound may exhibit different solubilities, intrinsic dissolution rates and sometimes

different bioavailabilities [151]. Furthermore, different crystal forms of a solid system may exhibit different stability in a formulation and consequently behave differently during manufacture [151,154,155].

The identification of polymorphs and solvatomorphs of a compound is usually achieved using X-Ray Powder Diffraction (XRPD) in combination with other techniques. The techniques that are commonly used include polarizing light microscopy, differential scanning calorimetry (DSC) and thermogravimetric analysis (TGA), solid-state vibrational spectroscopy and/or solid-state NMR spectrometry [151]. IR spectroscopy also has been used for identification of polymorphic forms of materials [154].

RTD has been reported to exist in two major polymorphic forms, *viz.* polymorph 1 and polymorph 2, in addition to pseudo-polymorphic forms [8,9,153,155]. Despite the differences in aqueous solubility, physical stability and melting point, the two polymorphs are therapeutically equivalent and both are used in the manufacture of commercial formulations [156]. The two forms have been reported to undergo inter-conversion during certain manufacturing processes and under specific storage conditions [154]. Form 2 is the most stable polymorph of RTD and the two forms of RTD have been distinguished by IR spectroscopy [8].

The use of thermal analytical techniques to elucidate the properties of a compound is well known and, in such methods, materials are subjected to linear increases in temperature applied from an external source whilst evaluating heat flow (DSC) or weight change (TGA) continuously as analysis takes place [151,157]. Thermal analysis has been used for more than eleven decades in different disciplines for a variety of purposes that are listed in Table 3.4 In the pharmaceutical industry interest in the use of thermal analysis commenced during the 1960s [157].

Table 3.3 Applications of thermal analysis. Adapted from [158]

Application field	Applied techniques
Forming reaction and its kinetics	Thremogravimetry (TG), differential thermal analysis (DTA), evolve gas analysis (EGA), microscopic observation, emanation thermal analysis
Crystalline transition	DTA, thermo-dilatometry
Melting and glass transition	DTA, microscopic observation
Oxygen content	TG (Temperature program reduction) EGA
Non-stoichiometry	TG, EGA, temperature program reduction
Sintering and crack formation	Thermodilatometry
Matching of thermal expansion in thin-film formation	Thermodilatometry
Critical temperature	Thermo-electrometry
Phase diagram for single-crystal formation	DTA
Vapour pressure and volatilization for metal organic chemical vapour deposition	TG, EGA, evolve gas detection (EGD)
Heat capacity	Differential scanning calorimetry (DSC)

In addition to the identification of polymorphs and solvatomorphs of drug substances, thermal analysis (DSC) has often been used to establish the purity of compounds. The differences in behaviour of eutectic mixtures of a drug substance and/or excipient and its impurities form the foundation for the assessment of purity [151,157]. The prediction of potential interactions and instability of an API during manufacturing has also been performed using thermal analysis [157]. Thermal analysis has proven to be a vital tool in screening for API excipient incompatibilities [157,159] and the detection of a physical changes in a dosage form such as the conversion of a molecule from the anhydrous to hydrous state, for example anhydrous lactose to lactose monohydrate [157].

The thermal stability of RTD polymorphs has been studied [153,160]. Polymorph 2 degrades at 156°C whereas polymorph 1 undergoes degradation at 166°C [8,160]. MTZ does not exhibit polymorphism and therefore it poses fewer challenges in formulation development than RTD. The determination of the thermal stability of a drug substance provides useful information that can guide the formulation scientist in the selection of a suitable method of manufacture and formulation composition.

3.1.3 Drug-excipient compatibility

Excipients have been described as inert components of a formulation that are added to APIs to facilitate the production of dosage forms, enhance drug stability and absorption and to improve taste and other sensory requirements for the patient. However, reports on interactions between API and excipients are abundant [161-163] and excipients are better defined as enabling rather than inert substances [159]. The interaction between drug and excipients may be classified as physical, chemical, and/or physiological or biopharmaceutical that may be either beneficial or detrimental [142,159,164].

3.1.3.1 Beneficial drug-excipient interactions

Beneficial drug-excipient interactions have been used to facilitate the manufacturing of drug delivery technologies. Such interactions include, for example, the addition of magnesium stearate to powder blends for lubrication purposes. Magnesium stearate is a fine powder that is hydrophobic in nature and adheres to the surfaces of equipment and powders during blending. However, excessive blending following addition of magnesium stearate is not recommended since it results in abrasion of the magnesium stearate particles with a consequent increase in surface coverage of the blend, leading to poor tablet performance and drug dissolution [159,164].

Another example of a beneficial interaction occurs in certain dry powder inhalers and explores the differences in particle size between the drug and excipient to facilitate drug delivery. A carrier material, usually lactose, is used to facilitate delivery of small API of 2.9 μm mean diameter into deep tissues of the lung [165,166]. This delivery technology uses the variation in air velocity and relative humidity, amongst other factors, to facilitate and dislodge the drug particle from the carrier in order to deposit the API in the alveolar regions of the lungs [165,167].

Aqueous pharmaceutical preparations such as liquids and semi-solids are usually susceptible to microbial degradation unless preservatives are incorporated into the formulations. Penetration enhancers such as laurocapram, cylcodextrins and a variety of encapsulating systems have been used in transdermal products to promote drug delivery in the systemic circulation [164,168]. The interaction between sodium bicarbonate and citric acid in an

aqueous environment has been explored to facilitate the disintegration of tablets through the use of effervescence [164,169].

3.1.3.2 Detrimental drug-excipient interactions

Detrimental interactions between API and excipients include the commonly occurring Maillard reaction [170]. Compounds with a primary amine interact with the glycosidic hydroxyl group of a reducing sugar resulting in the formation of an imine and ultimately an amadori compound that has a characteristic yellow-brown colour. Several factors such as water activity, heating time and temperature, oxygen, light, presence of metal ions, pH and the type and the concentration of buffer have been reported to catalyse this reaction [164,171,172]. Nonetheless the Maillard reaction is not limited to primary amines only and secondary amines also undergo this reaction without the yellow-brown discolouration as the reaction does not proceed to the formation of an amadori compound in these cases [164].

Acetylsalicylic acid is an ester drug that is susceptible to hydrolysis in the presence of alkaline metal or earth salts. The degradation of acetylsalicylic acid in a suspension containing magnesium stearate was attributed to the alkaline environment that is formed following the formation of a buffer system comprised of the magnesium stearate acetylsalicylic acid salt and acetylsalicylic acid [164,173].

Primary amines may also undergo a reaction analogous to the Michael addition reaction with excipients that contain α-β unsaturated ketone [174] such as sodium stearyl fumarate and sorbitan monooleate. Such reactions have also been reported between flovoxamine maleate and maleic acid counter ions [164].

A further detrimental interaction occurs due to proximity between a heteroatom and active hydrogen resulting in the formation of lactones in benezapril molecule. Oxidative interactions between atovarstatin, cytidine nucleoside analogues and fumed metal oxides of silica, titania or zicornia have also been reported [164].

These examples of drug-excipient interactions are just a few of many that have been reported. For a new drug molecule, drug-excipient interaction data must be generated and screening for drug/excipient compatibilities constitutes an important part of preformulation studies

[164,175]. Well-known molecules have, on the other hand, been investigated, but due to differences in environmental conditions and synthetic procedures for an API, may behave differently necessitating the drug-excipient compatibility testing. Screening for excipient compatibility provides the formulation scientist with useful information pertaining to the suitability of excipients(s) that may be included in a formulation of a specific drug [164,175].

There are several techniques that may be used to screen materials for potential drug-excipient incompatibility. However, thermal techniques such as isothermal stress testing (IST) and DSC are frequently used although FT-IR spectroscopy has also been successfully applied to screening for physical or chemical reactions associated with drug-excipient interactions [164,176,177]. IR spectroscopy analysis results in the generation of peaks due to bending, stretching, twisting, wagging, rocking and scissoring (vibration) of the bonds in a molecule [178]. Furthermore each functional group in the molecule has a specific vibrational frequency and therefore the appearance of a peak at particular vibrational frequency is an indication of a presence of a particular functional group in the molecule and *vice versa* [178,179]. Therefore this property of specificity in vibrational frequency constitutes the basis for detecting potential drug-excipient incompatibility.

3.2 METHODS

3.2.1 SEM

The determination of particle size and morphology was performed using a Vega© Scanning Electron Microscope (Tescan, Vega LMU, Czechoslovakia Republic). Small amounts of MTZ, RTD, microcrystalline cellulose (MCC) pH 102 and dibasic calcium phosphate (DCP) were dusted onto a graphite plate separately after which gold coating was applied for 20 min under vacuum. The samples were visualized using SEM at an accelerated voltage of 20 kV.

3.2.2 Powder density

The tapped density of the materials was determined using a Model SVM 203 (Erweka GmbH, Heuseastamm, Germany) at rate of 220 taps per minute for 2 min. Approximately 10 g of MTZ, RTD, MCC and DCP were passed separately through a 850 µm sieve and filled

into individual tarred 100 ml graduated measuring cylinders. The bulk and tapped volume V_{bk} and V_{tp} were established. The test was performed in triplicate for each material investigated. The bulk density and the tapped density were calculated using Equation 3.2 and the powder porosity (ε), CI and HR were calculated using Equations 3.3, 3.4 and 3.5 respectively.

$$\boldsymbol{\rho = \frac{m}{v}} \qquad \textbf{Equation 3.2}$$

Where,

m = mass
v = volume
ρ = true density
ρ_{bk}= bulk density where $v = V_{bk}$
ρ_{tp}= tapped density where $v = V_{tp}$

$$\boldsymbol{\varepsilon = \left(1 - \frac{\rho_{tp}}{\rho}\right) \times 100} \qquad \textbf{Equation 3.3}$$

$$\boldsymbol{CI = \left[\frac{\{\rho_{tp} - \rho_{bk}\}}{\rho_{tp}}\right] \times 100} \qquad \textbf{Equation 3.4}$$

$$\boldsymbol{HR = \frac{\rho_{tp}}{\rho_{bk}}} \qquad \textbf{Equation 3.5}$$

Where,

ε = Powder porosity
CI = Carr's index
HR = Hausner ratio

The true density was established using a compacted mass of the powder. MTZ, RTD, MCC and DCP were separately filled manually into the dies and compressed to a steady state compact mass of 400 mg tablets using Manesty® B3B rotary tablet press (Manesty, Knowsley, Merseyside, England) fitted with six 12.00 mm flat punches that was operated manually. The true density of each material was calculated from the average weight and volume of the respective tablets (n=6) using the Equation 3.2.

3.2.3 IR spectroscopy

The IR spectra of individual components and 1:1 mixture of API and excipients *viz.* MCC, DCP, sodium starch glycolate (SSG), corscarmellos sodium (CCS), povidone-K30 (PVP-K30) and magnesium stearate were generated using a Spectrum 100 FT-IR ATR Spectrophotometer (Perkin Elmer® Ltd Beaconsfield, England). The powders were prepared

by mixing the components using a mortar and pestle. A small amount of the powder blend was placed on the diamond crystal and analyzed (n=4 scans) between 4000-650 cm^{-1} wave number range and resolution of 4 cm^{-1}.

3.2.4 Thermogravimetric analysis

TGA was performed using a Model TGA 7 Thermogravimetric analyzer (Perkin Elmer ®Norwalk, Conneticut, USA). Approximately 1 mg of each material was used and the measurements were performed in a nitrogen atmosphere at a flow rate 20 ml/min in a temperature range of 30°C to 200°C and 70°C to 220°C for RTD and MTZ respectively. The heating rate was set at 10°C/min.

3.2.5 DSC

Approximately 3 mg samples of the individual components and mixtures of API and excipient in a binary 1:1 mixture were used for DSC analyses. The DSC scans were generated between 25-350°C using a Model DSC 7 (Perkin Elmer®, Norwalk, Connecticut, USA) with equipment and PC control unit TAC 7 (Perkin Elmer®, Norwalk, Connecticut, USA) at a heating rate of 10°C/min and nitrogen at a flow rate of 20 ml/min. Data analysis was performed using Pyris™ Manager software.

3.3 RESULTS AND DISCUSSION

3.3.1 SEM

SEM images depicting the particle morphology and sizes of RTD, MTZ, DCP, and MCC are shown in Figures 3.1 and 3.2 respectively.

SEM images of RTD dry powder reveal the presence of sub-angular particles of medium sphericity (Figure 3.1 I) as reported [180] with equivalent spherical diameters of between 317.22 µm and 554.70 µm as shown in Figure 3.2 I. MTZ was shown to exist as prism (polyhedral) shaped particles (Figure 3.1 II) with the width of the particles (Feret's diameter) ranging between 90.29 µm and 539.16 µm as shown in Figure 3.2 II, and the polyhedral particle morphology is indicative that butanol was the recrystallization medium [181]. DCP

and MCC exhibited particles of high sphericity and angular with medium sphericity respectively as shown in Figures 3.1 III and IV. DCP exhibits better flowability and has smoother particles compared to MCC [182-186].

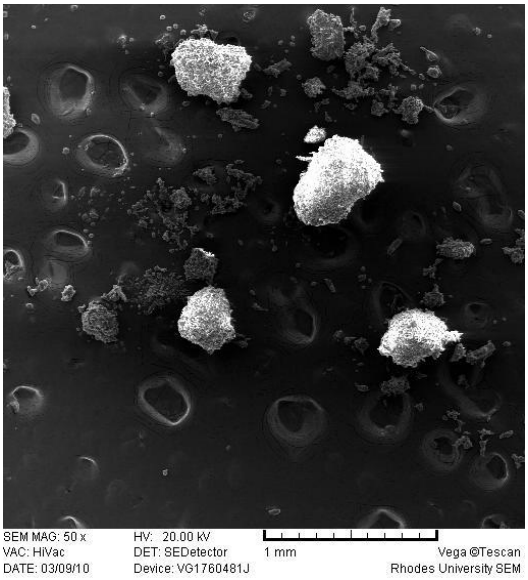

I

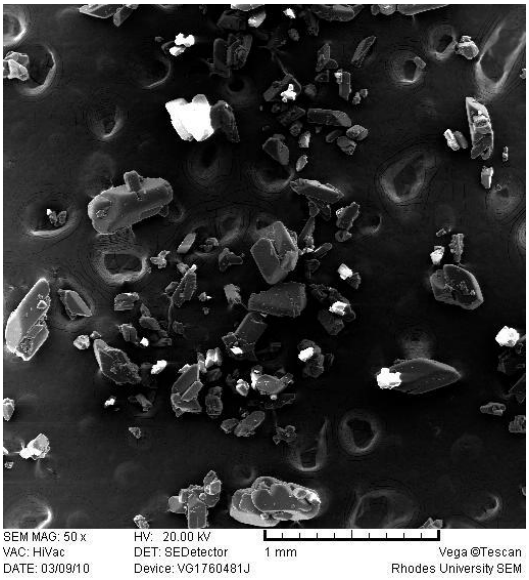

II

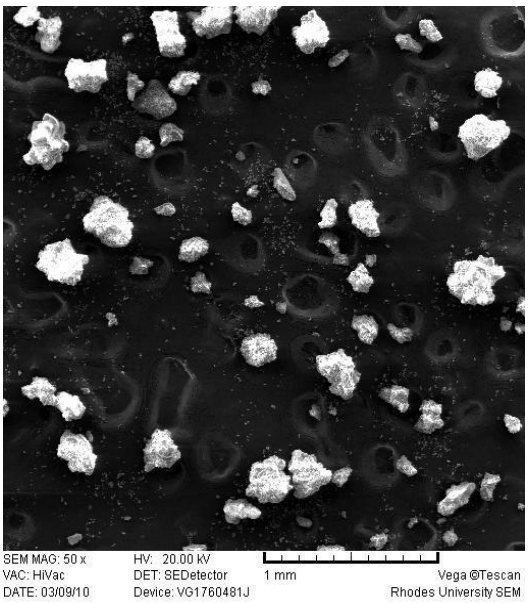

III

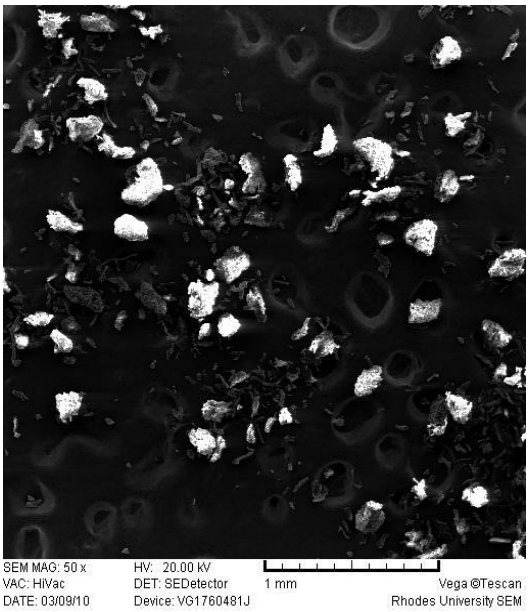

IV

Figure 3.1 Typical SEM showing particle morphology of RTD (I); MTZ (II); DCP (III) and MCC (IV)

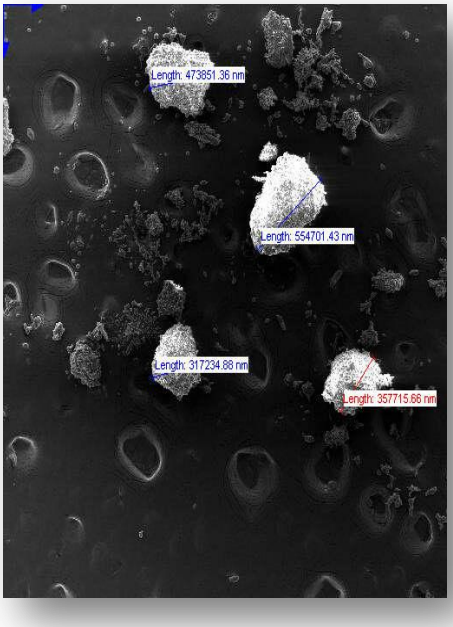

I

II

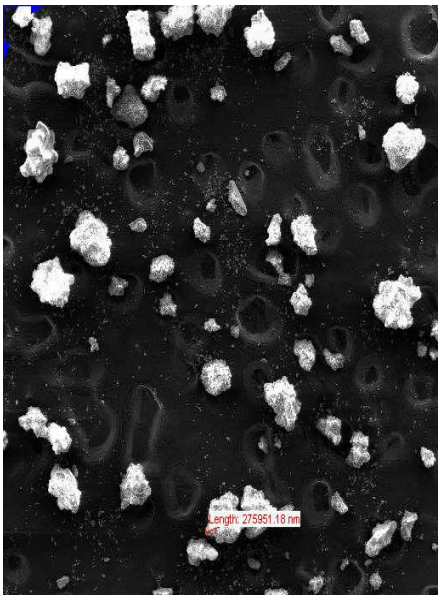

III

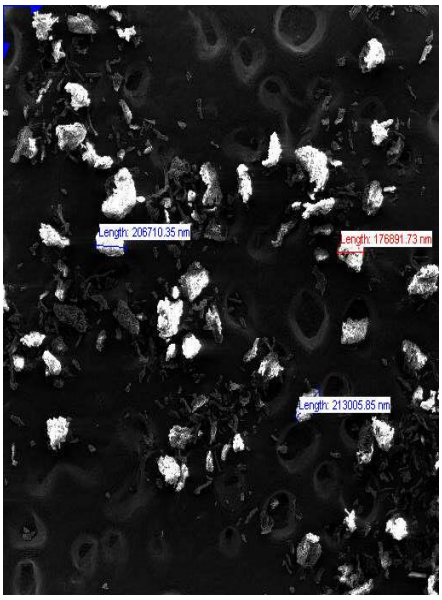

IV

Figure 3.2 Typical SEM image showing the particle size range of RTD (I), MTZ (II), DCP (III) and MCC (IV)

As can be seen in the SEM images MTZ powder may exhibit poor flow properties as a consequence of the shape and wide particle size distribution of the powder, therefore to improve flowability and subsequent manufacture, particle size reduction may be considered as a means for improvement of particle sphericity and size distribution. RTD exists as large

particles but with better sphericity, therefore particle size reduction may also be useful for the prevention of blend segregation as a consequence of particle size distribution differences.

The SEM images of DCP and MCC depict that both excipients exhibit similar particle size as seen in Figures 3.2 III and IV. This similarity is likely to facilitate the comparison of the physiochemical properties of the resultant tablets and consequently selection of an appropriate excipient for future optimization studies.

3.3.2 Powder density

3.3.2.1 True density

A summary of the reported and actual true density values determined in these studies are summarized in Table 3.4. The true density determined using the compacted mass of respective powders was in disagreement with those reported and that are usually established using helium pycnometry. This may be attributed to the use of different instrumentation or material characteristics that are a consequence of differences in the synthetic processes used to manufacture the API.

Table 3.4 True density values for raw materials

Raw material	Actual value (g/ml)	Literature value (g/ml)	Reference
RTD	1.23	Not stated	
MTZ	1.32	1.44-1.52	[181,188]
DCP	2.17	2.35	[182,189,190]
MCC	1.36	1.41-1.66	[182,187,190-192]

The true density of powders provides useful information that can be used for characterization of the mechanical properties of powders on which tablet hardness, tensile strength and elastic modulus are dependent [139]. The true density was used for determination of the porosity of the powders in which the compressibility of the powder material is dependent.

3.3.2.2 Bulk and tapped density

The bulk and tapped density of RTD, MTZ, DCP and MCC are summarized in Table 3.5.

Table 3.5 A list of raw materials bulk and tapped density values

Material	Bulk density			Tapped density		
	Actual (g/ml)	**Literature (g/ml)**	**Reference**	**Actual (g/ml)**	**Literature (g/ml)**	**Reference**
RTD	0.55	0.68	[193]	0.76±0.012	Not stated	
MTZ	0.72	0.60	[181]	0.86±0.001	0.81	[181]
DCP	1.05	0.94	[182,189,190]	1.19±0.008	1.10	[182,190]
MCC	0.35	0.36	[182,190,192]	0.46±0.004	0.41	[182,190,192]

The values for CI and HR of MCC shown in Table 3.6 indicate that MCC has good compressibility and flow properties compared to DCP. This may be due to irregular shape of the MCC particles compared to particles of DCP.

Table 3.6 Powder porosity, Carr's Indices and Haussner Ratios for raw materials

Material	CI	HR	Powder porosity (%)
RTD	27.63	1.38	38.21
MTZ	25.92	1.35	34.84
DCP	14.54	1.17	45.16
MCC	12.19	1.12	66.17

Spherical particles exhibit poor compressibility properties in comparison to irregularly shaped particles [194]. Spherical particles give rise to symmetrically opposite forces on particle contact points on compression, and consequently compressive deformation of particles results. However, unlike spherical particles, irregular particles develop asymmetrical opposite forces that lead to shear deformation [194]. Although the HR value indicates that MCC may exhibit better flow properties than DCP, previous studies indicate that DCP exhibits better flow properties [182]. The apparent difference in the results may be attributed to hygroscopic properties of MCC since it absorbs moisture from the atmosphere, resulting in an initial increase in the true density of the material followed by a decrease in the true density of the material, ultimately affecting the bulk and tapped density and HR for this powder [191].

It is evident that MCC is the most porous of the materials tested and consequently more compressible than DCP, as shown in Table 3.6. These results indicate that blends produced with MCC may exhibit better compressibility compared to those produced using DCP as a

diluent. Similar results were also observed following investigation of the tableting behaviour of pellets comprised of DCP and MCC in different compositions [195].

3.3.3 Polymorphism

The occurrence of the two polymorphs of RTD is a result of the space orientation, *viz.* cis/trans of the methylamine and nitro group in the molecule, and is also dependant on the polarity of the recrystallization solvent used during the manufacture of the raw material [153,196]. Less polar or non-polar crystallization solvents favour the formation of polymorph 1, whereas polymorph 2 is the major end product when polar crystallization solvents are used [196-198].

Polymorph 2 of RTD has a characteristic absorption band at 1045 cm^{-1} and polymorph 1 exhibits a band at wave number of 1551 cm^{-1} [153].

The infrared absorption scan of RTD depicted in Figure 3.3 shows the characteristic absorption band at 1045 cm^{-1} which suggests that this RTD sample is comprised primarily of polymorph 2.

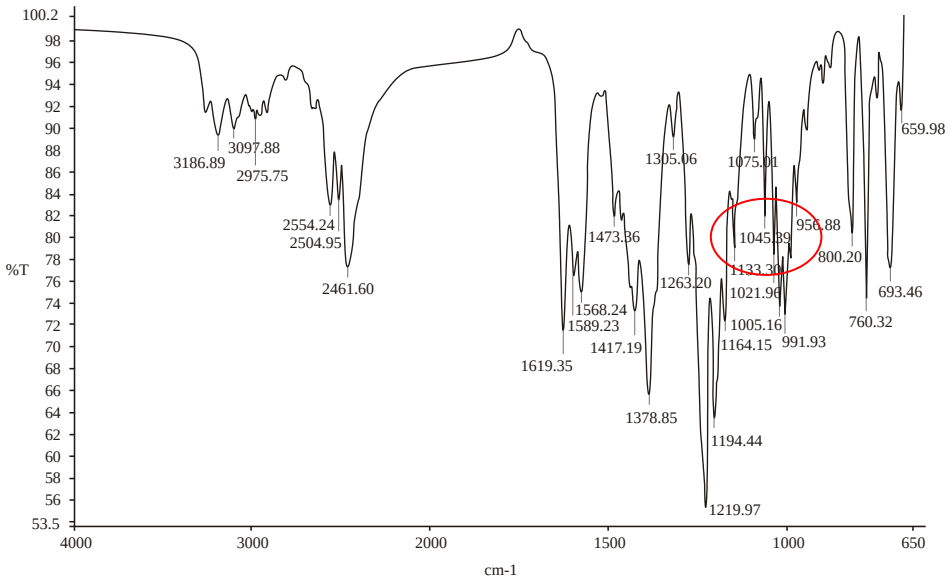

Figure 3.3 Typical IR spectrum of RTD generated at 4 scans and 4cm^{-1} resolution

The differences in intramolecular hydrogen bonds determine the occurrence of the characteristic absorption bands for each polymorph [153,196]. Polymorph 1 has strong

intramolecular hydrogen bonds compared to polymorph 2. The low water content of a less polar solvent used during crystallization favours the formation of intramolecular hydrogen bonds, whereas the presence of water in polar solvents favours the formation of both intramolecular and intermolecular hydrogen bonds. As a result, weak intramolecular hydrogen bonds with low vibrational frequency (1045 cm^{-1}) are formed in polar solvents [153,196]. These findings were confirmed using DSC analyses of the RTD samples and the DSC thermogram depicts a melting point of 147.83°C which is in close agreement with that of 145.3°C [160].

3.3.4 Thermogravimetric analysis

The thermogram depicted in Figure 3.4, generated following TGA of RTD, indicates that the drug is stable to approximately 153°C followed by 20% decomposition at 200°C.

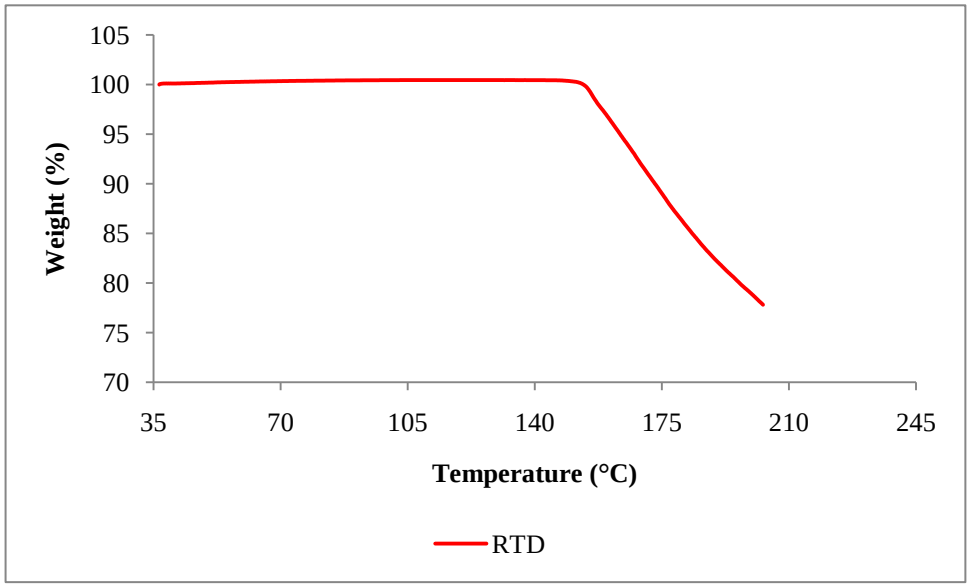

Figure 3.4 A typical TGA plot of RTD at 10°C/min heating rate

This value is in slight disagreement to the previously reported decomposition temperature of 156°C [160]. The difference in degradation temperature between the experimental and reported values may be due to the use of different synthetic pathways in drug synthesis and may perhaps be due to difference in instrumentation. Therefore since RTD exhibits thermo stability up to 153°C it may be inferred that the "normal" temperature range, *viz.* 50-80°C, used during manufacturing processes would have a negligible effect on the stability of RTD.

The thermogravimetric analysis curve for MTZ depicts a 2.76% decrease in weight of the drug following heating from 80°C to approximately 162°C that may be a consequence of dehydration. Following dehydration there is a drastic decline in the curve up to a temperature of 209°C that correlates with 97.22% loss in weight of the drug as a result of degradation as shown in Figure 3.5. Similar results were observed following heating of MTZ to 900°C [199,200].

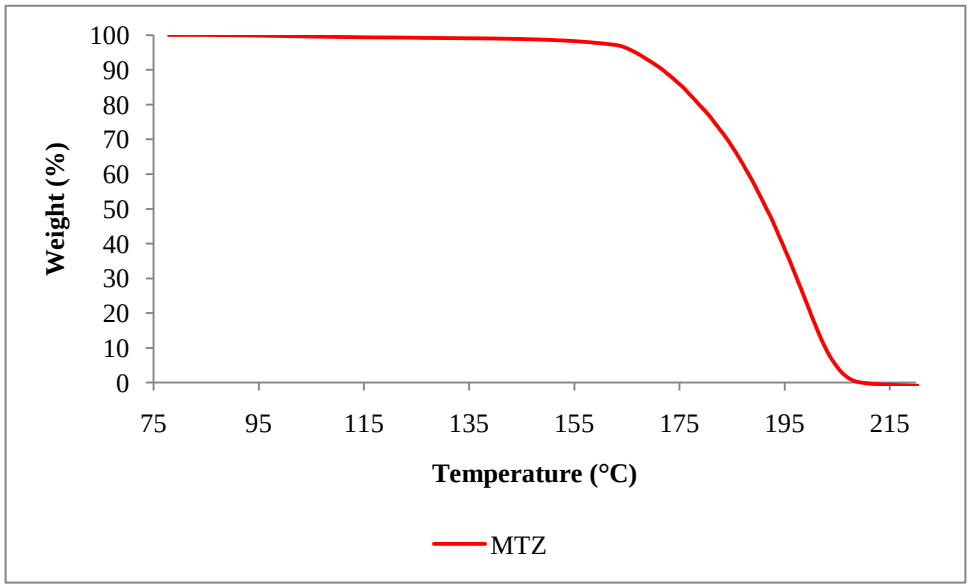

Figure 3.5 A typical TGA plot of MTZ at 10°C/min heating rate

3.3.5 DSC

MTZ and RTD exhibit melting endotherm peaks at 161.5°C (ΔH= 171.7437 J/g) Figure 3.6 I and 147.83°C (ΔH= 102.8577 J/g) Figure 3.6 II respectively with an evaporation endotherm peak for MTZ at 273.67°C.

These results are in close agreement with the previously reported analyses by Kiss *et al.* [201,202] and Mimehrabi *et al.* [153] following thermal analysis of MTZ and RTD respectively. However, in this study RTD exhibited a higher melting point compared to the reported 137.8°C [153] but is in close agreement to that of 145.3°C [8,160]. Thus the melting point exhibited by RTD suggests that the sample is primarily made up of polymorph 2.

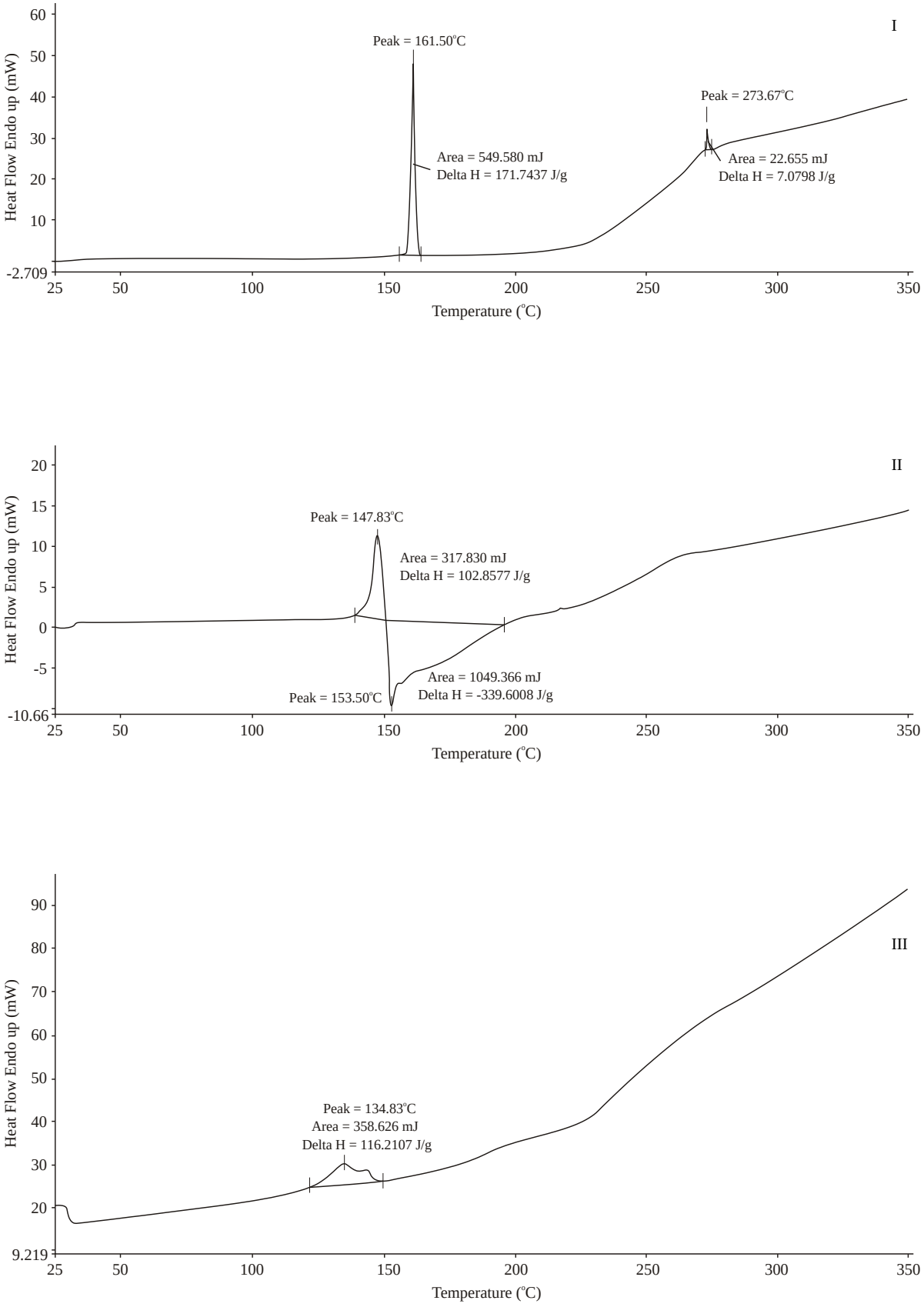

Figure 3.6 Typical DSC thermograms of MTZ (I) RTD (II) and binary mixture of MTZ and RTD (III) at a heating rate of 10°C/min

The thermogram for a binary mixture of RTD and MTZ depicts a broad endotherm peak at 137°C and none reflecting the endotherm for MTZ or RTD at 161.5°C and 147.83°C respectively (Figure 3.6 III). This suggests that RTD and MTZ exhibit an interaction at high temperature that results in the formation of a eutectic mixture. However the IR scan of the binary mixture of these compounds depicts the characteristic bands of both drugs as described in § 3.3.6. Therefore, due to the evidence of a potential interaction using thermal analysis, long term stability testing may be necessary for dosage forms in which therapeutic amounts of MTZ and RTD are included.

DCP exhibited a melting endotherm at 194°C (ΔH=436.3717 J/g) as shown in Figure 3.7 and this may be attributed to the loss of water of crystallization. DCP loses water of crystallization in two stages, *viz.* between 120-160°C and between 250-300°C, that correlates with the loss of 0.5 and 1.5 moles of crystalline water respectively [201].

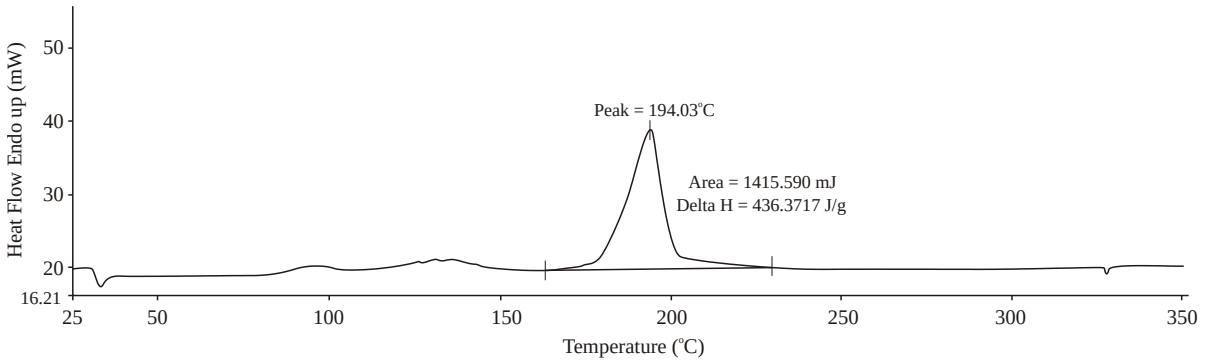

Figure 3.7 A typical DSC thermogram of DCP at a heating rate of 10°C/min

Similarly, thermograms of MCC, PVP-K30, SSG and CCS reveal no significant thermal events for the temperature ranges scanned in Figures 3.8-3.11.

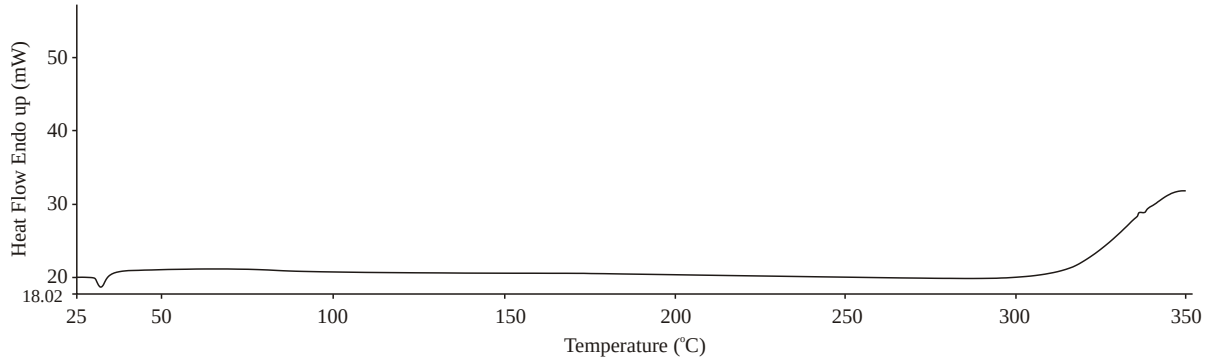

Figure 3.8 A typical DSC thermogram of MCC at a heating rate of 10°C/min

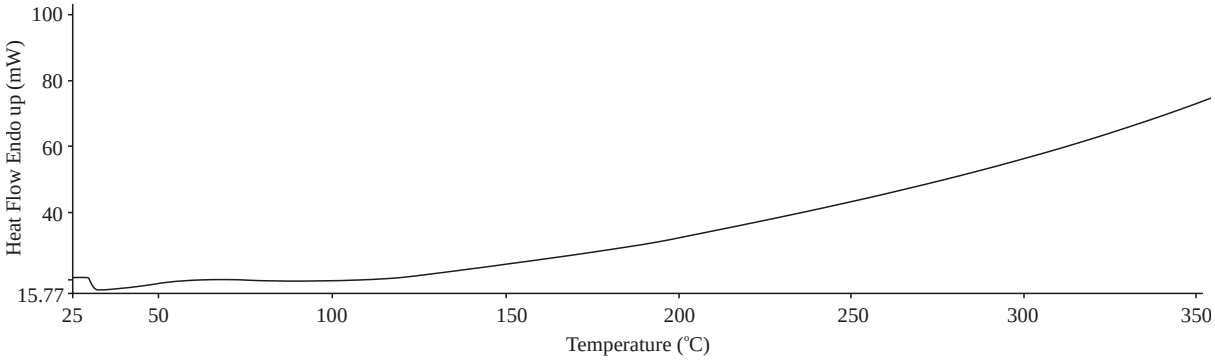

Figure 3.9 A typical DSC thermogram of PVP-K30 at a heating rate of 10°C/min

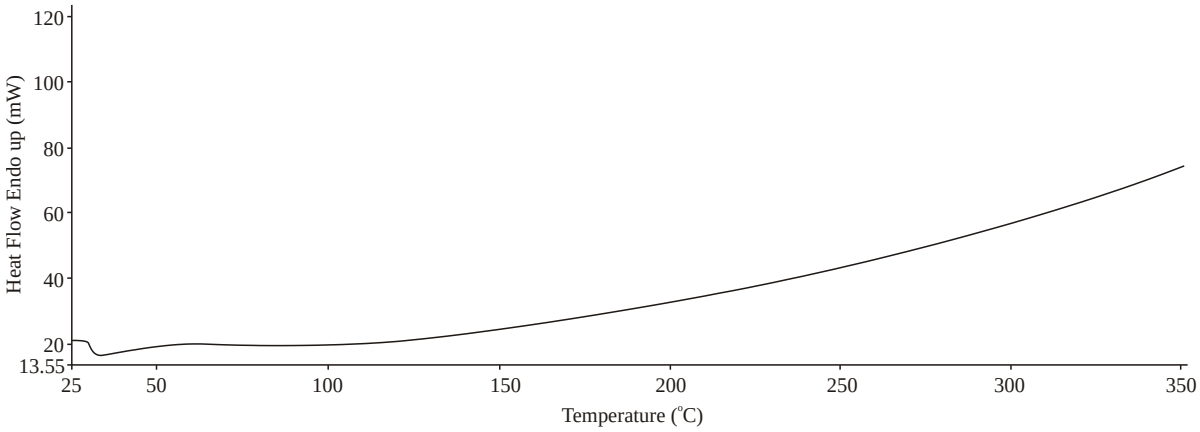

Figure 3.10 A typical DSC thermogram of SSG at a heating rate of 10°C/min

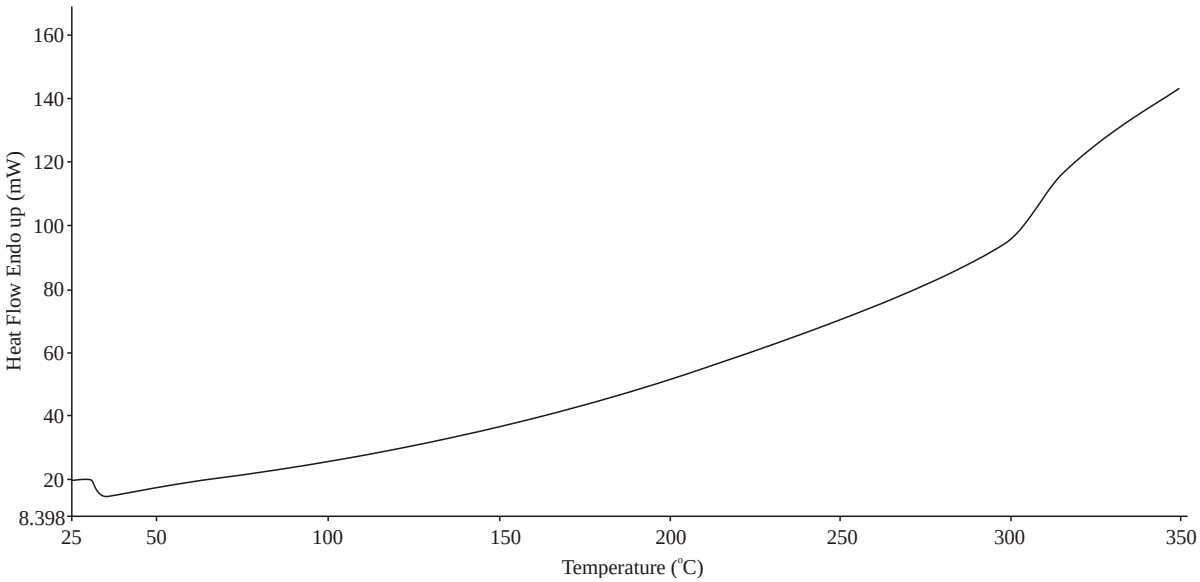

Figure 3.11 A typical DSC thermogram of CCS at a heating rate of 10°C/min

The thermogram of a binary mixture of MTZ and DCP depicted in Figure 3.12 reveals one endotherm peak at temperature of 161.37°C which is due to the melting of MTZ, and the endotherm peak due to loss of crystalline water by DCP is not present.

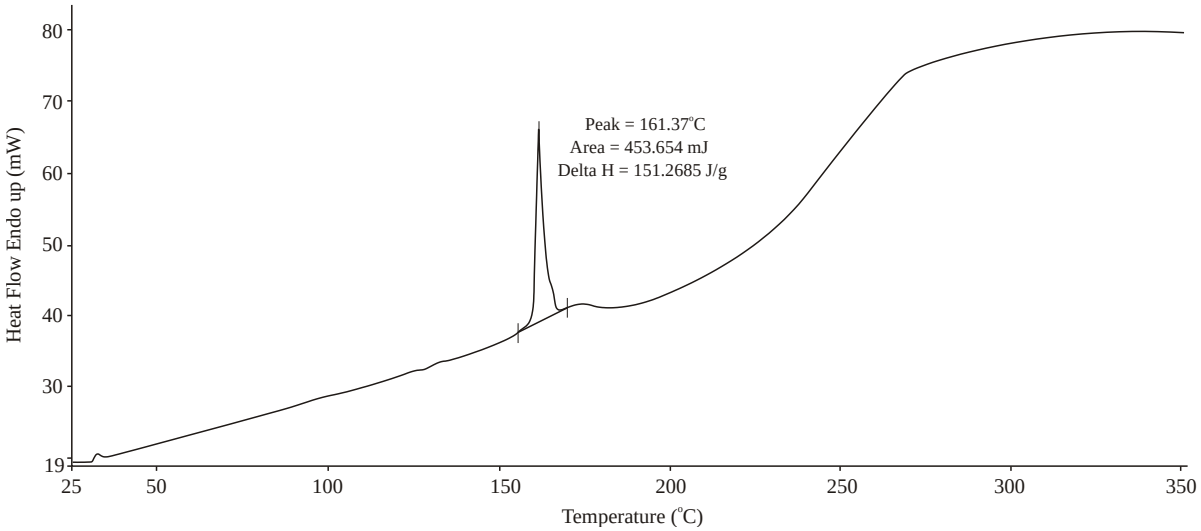

Figure 3.12 A typical binary mixture DSC thermogram of MTZ and DCP at a heating rate of 10°C/min

This suggests an interaction between the two compounds, and incompatibility between MTZ and other pharmaceutical excipients has been reported [201]. However the IR scan of a binary mixture of MTZ and DCP did not indicate a potential incompatibility since the characteristic peaks for both compounds were evident. This suggests exposure to a high temperature facilitates an interaction between MTZ and DCP.

The thermogram for the mixture of MTZ and MCC revealed a slight increase in the melting temperature for MTZ as depicted in Figure 3.13. The 1.3°C increase in the melting point of MTZ may be attributed to the shielding effect of MCC on MTZ. It has been reported that a 3°C increase in the melting point temperature of MTZ was observed following thermal compatibility studies of nitroimidazole and pharmaceutical excipients [203].

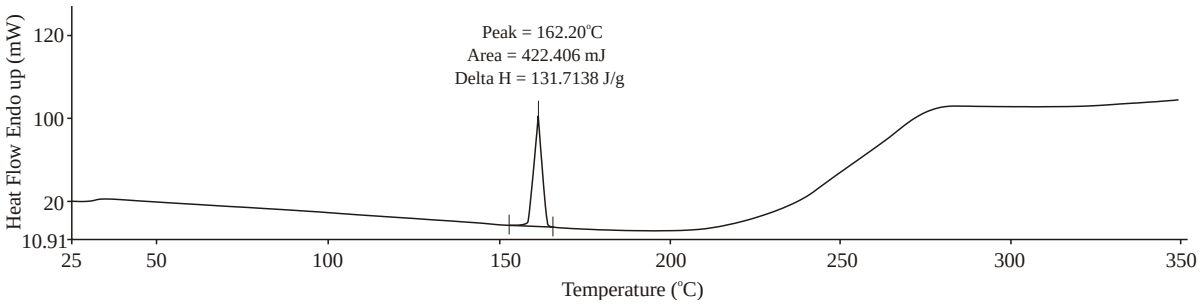

Figure 3.13 A typical binary mixture DSC thermogram of MTZ and MCC at a heating rate of 10°C/min

The analysis of a binary mixture of MTZ and PVP-K30 shown in Figure 3.14 exhibited an insignificant change in the melting temperature of MTZ, however the decomposition endotherm peak of MTZ between 250-300°C occurred in triplet in comparison to the singlet observed in the pure component. This may be attributed to the shielding effect of PVP-K30 on MTZ although this is not as effective as that observed for MCC and DCP.

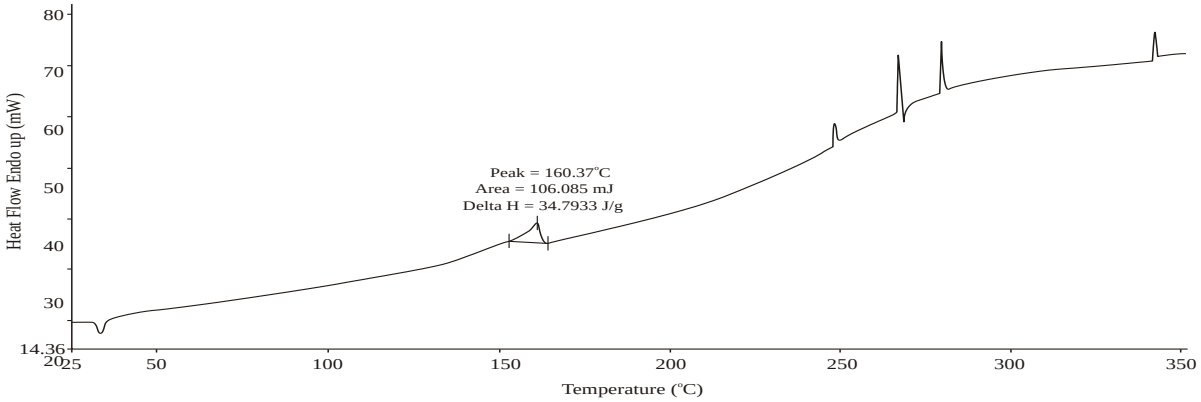

Figure 3.14 A typical DSC thermogram for binary mixture of MTZ and PVP-K30 at a heating rate of 10°C/min

A slight change in the melting temperature of RTD was observed in binary mixtures comprised of RTD: MCC (Figure 3.15), RTD:DCP (Figure 3.16) and RTD: PVP-K30 (Figure 3.17).

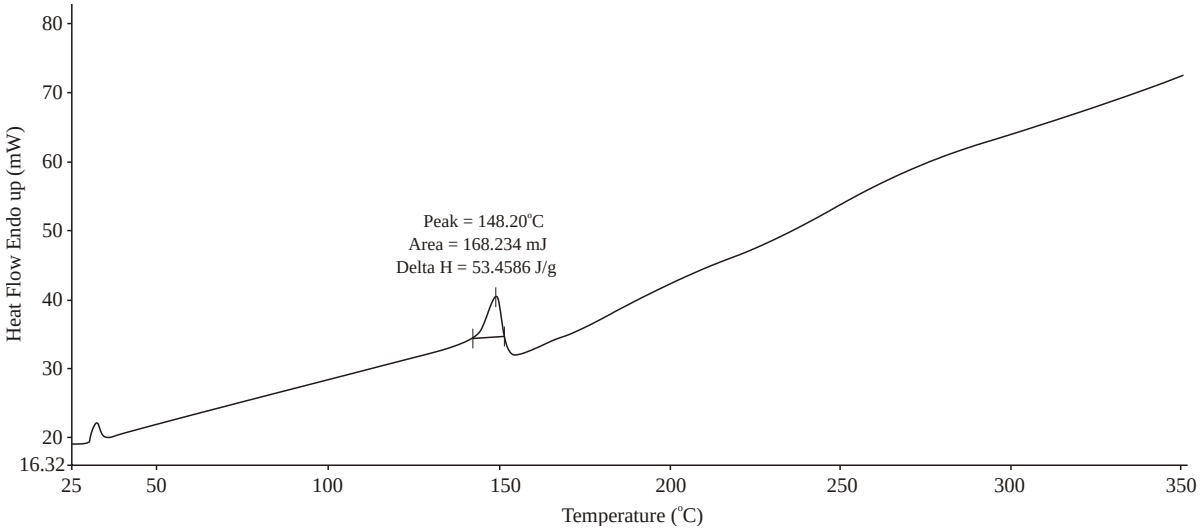

Figure 3.15 A typical binary mixture DSC thermogram of RTD and MCC at a heating rate of 10°C/min

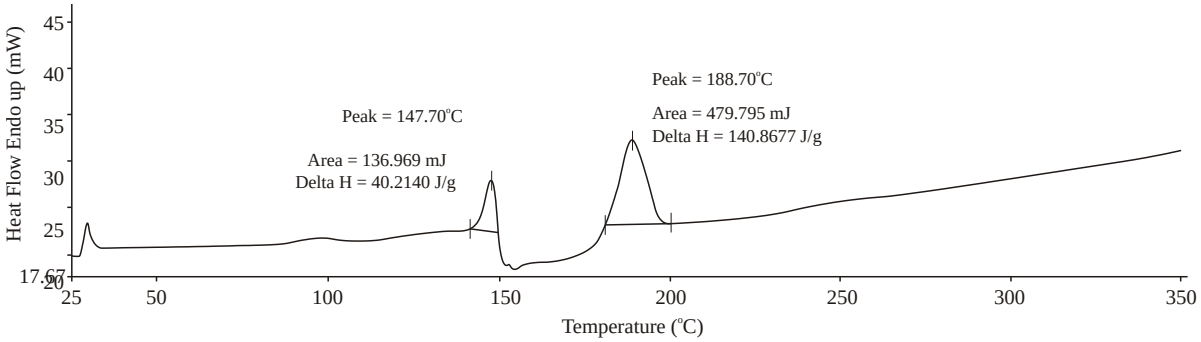

Figure 3.16 A typical binary mixture DSC thermogram of RTD and DCP at a heating rate of 10°C/min

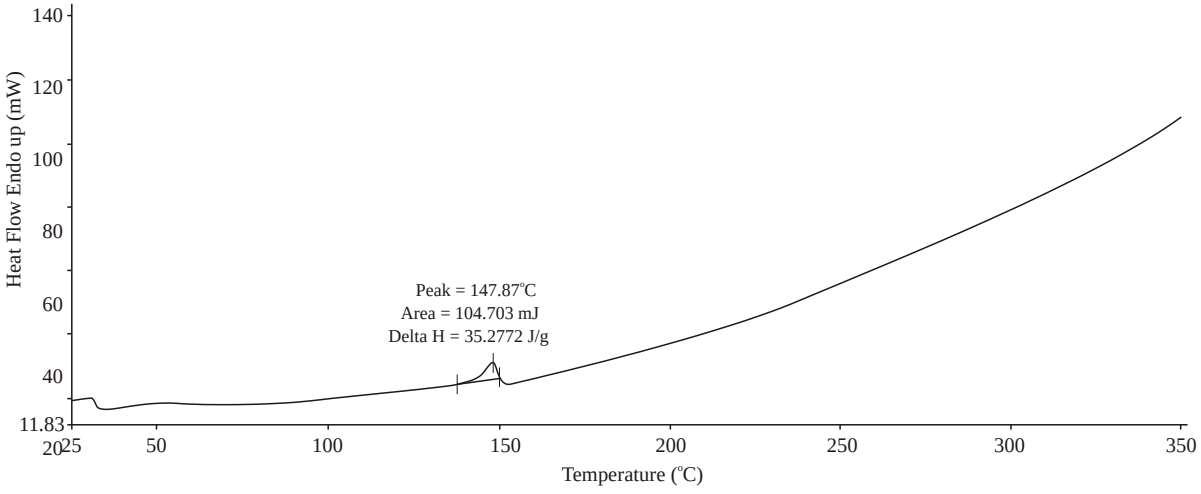

Figure 3.17 A typical DSC thermogram of binary mixture of RTD and PVP-K30 at a heating rate of 10°C/min

However, these changes were not significant and did not support a conclusion relating to the presence of incompatibilities. Furthermore, the broad melting endotherm observed for RTD in all binary mixtures may be attributed to the low sample mass and a change in reaction kinetics as consequence of the dilution effect of the excipients. It has been reported that sample mass, heating rate and reaction enthalpy significantly affect the peak height in DSC analyses [204].

With the exception of the binary mixture of MTZ:magnesium stearate that exhibited a 3.2°C increase in the melting temperature of MTZ (Figure 3.18), similar results to other binary mixtures with RTD were observed for RTD:magnesium stearate mixture as depicted in Figure 3.19.

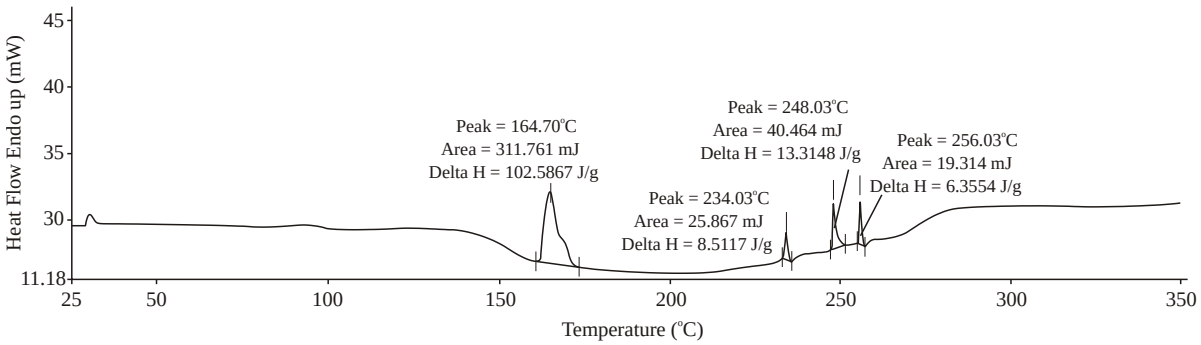

Figure 3.18 A typical DSC thermogram for a binary mixture of MTZ and magnesium stearate at a heating rate of 10°C/min

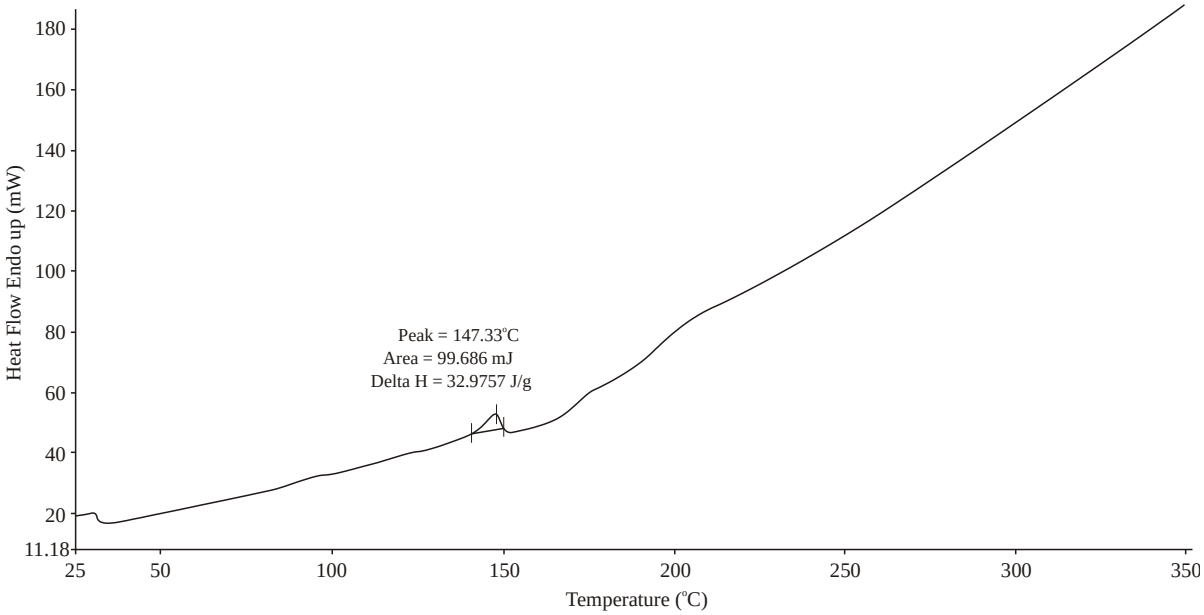

Figure 3.19 A typical binary DSC thermogram of a binary mixture of RTD and magnesium stearate at a heating rate of 10°C/min

DSC analyses of the mixtures comprised of drug substance and MCC in combination with all excipients revealed two endotherms at 142.87°C and 160.2°C which may be due to the melting of RTD and MTZ respectively (Figure 3.20). However no significant thermal activity was noted in their respective counterpart mixture of DCP as depicted in Figure 3.21. This may be attributed to shielding and dilution effect of the excipients on each other and on MTZ and RTD.

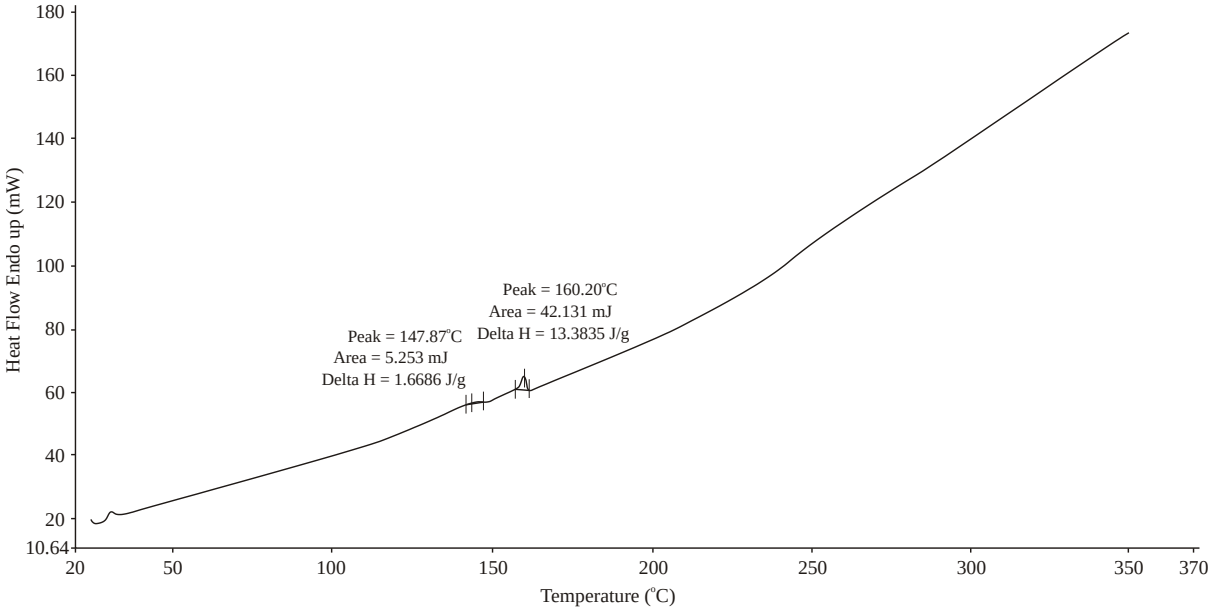

Figure 3.20 A typical DSC thermogram of MCC, MTZ and RTD in combination with all excipients at heating rate of 10°C/min

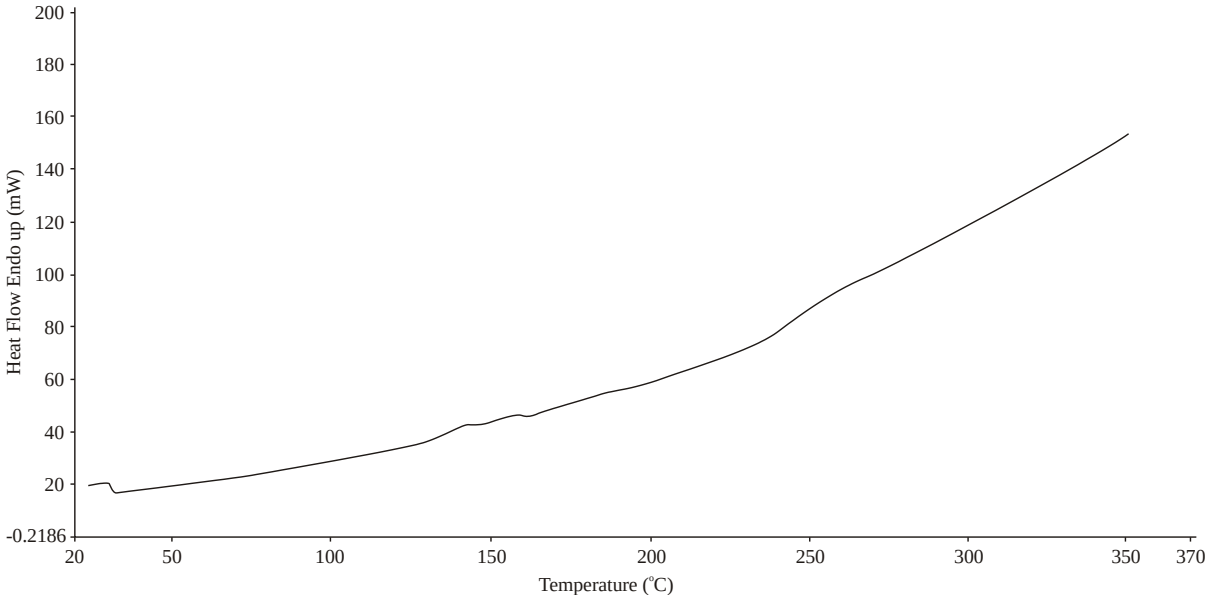

Figure 3.21 A typical DSC thermogram of DCP, MTZ and RTD in combination with all excipients at heating rate of 10°C/min

3.3.6 IR spectroscopy

The absorption band frequencies used for the interpretation of the IR spectra are described in Table 3.3 and have been reported [8,205].

Table 3.3 IR absorption band assignments. Adapted and modified from [8,205].

Wave number (cm^{-1})	**Group assignment**
3100-3260	NH and OH stretch
3105	C=CH; C-H stretch
3017-3066	C-H; stretch furane
2908-2970	C-H; stretch aliphatic
2560-2653	$H\text{-}N^{+}R_3$; N-H stretch
1670-1820	C=O
1500-1620	N-H; bending
1590	$=C\text{-}NO_2$; C-N stretch
1538, 1350	NO_2;N-O stretch
1570	NH
1350-1480	C-H; bending
1380	$=C\text{-}NO_2$; C-N stretch; N-O stretch
1137-1226	C-N stretch
1078	C-OH; C-O stretch
760-990	CH

The IR spectrum of a binary mixture of RTD and MTZ depicted in Figure 3.22 III revealed the presence of the typical band characteristics for both compounds.

The spectrum showed the tertiary amine N-H stretch absorption band of RTD at 2553^{-1}cm as well as the hydroxyl band of MTZ at 3201^{-1}cm. Furthermore the N-O stretch vibrational frequency at 1354 cm^{-1} and 1534 cm^{-1} due to the nitro group in MTZ (Figure 3.22 II) was clearly visible, indicating the absence of hydrogen bonding interactions. In addition the spectrum revealed peaks at 1589 cm^{-1} and 1164 cm^{-1} that are a characteristic of N-H stretch and at 1133 cm^{-1} that is a characteristic band of aliphatic C-N stretch absorption. However, the intensity of these bands decreased compared to the band intensity of their respective pure components (Figure 3.22 I and II) which may be due to the dilution effect that one component has on the other.

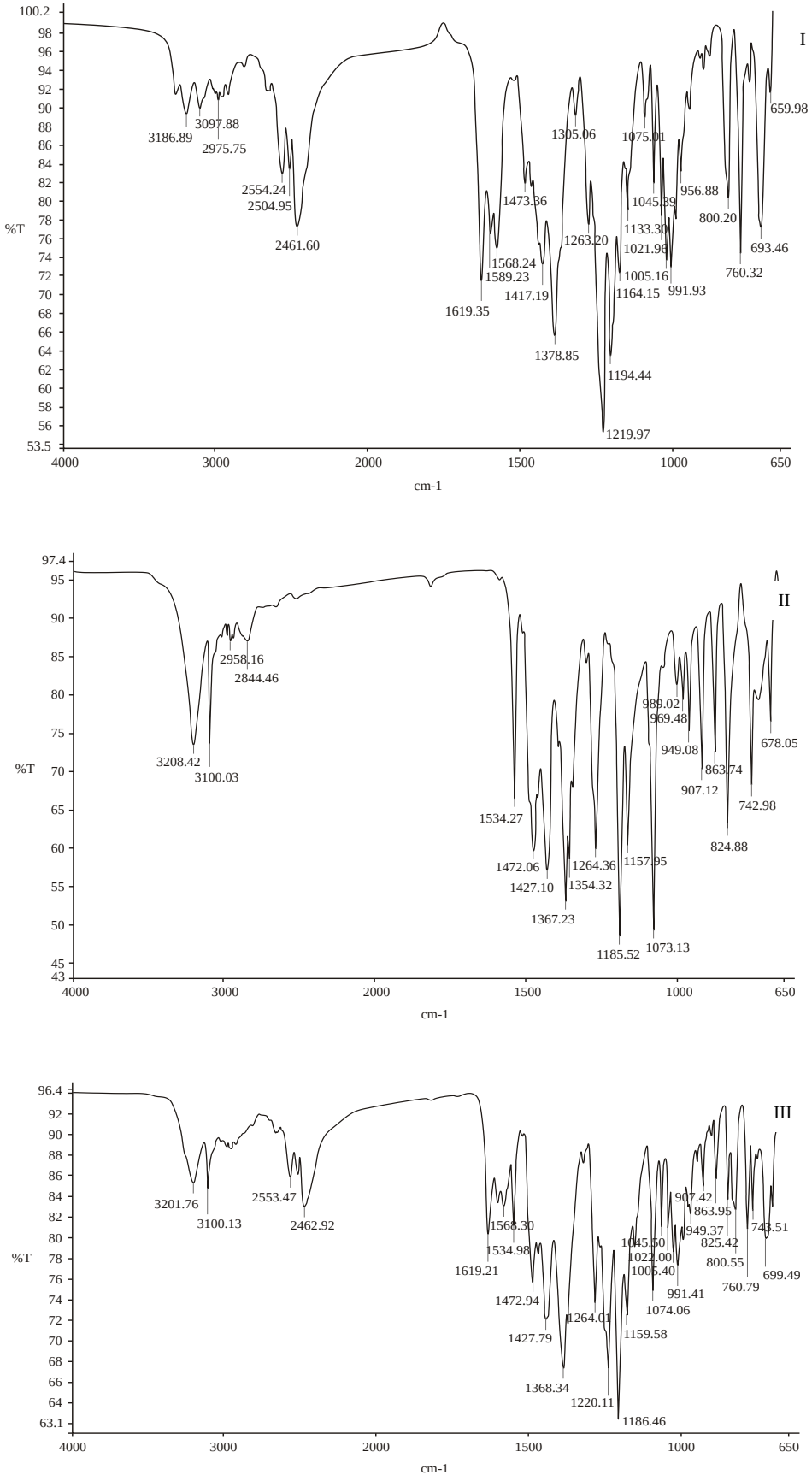

Figure 3.22 Typical IR spectrum of RTD (I), MTZ (II) and binary mixture of RTD and MTZ (III) generated at 4 scans and 4 cm^{-1} resolution

The IR spectrum of a binary mixture of RTD and PVP-K30 shown in Figure 3.23 II revealed characteristic peaks of RTD at 1220 cm^{-1}, 1620 cm^{-1} and 2552 cm^{-1} that are due to C-N stretch, N-H bending and N-H stretch vibrational frequency. However, the absorption band frequency at 1652 cm^{-1} due to ketone group in the PVP-K30 was not present. This may be attributed to hydrogen bonding between the carbony-carbon oxygen in PVP-K30 and the amine-hydorgen in RTD that resulted in a change in absorption frequency of the ketone group from 1652 $cm^{-1}$to 1620 cm^{-1}. A close examination of the absorption band at 1620 cm^{-1} in Figure 3.23 II, a broad band is observed at the peak base that gradually tapers at the top which suggest consolidation of the two absorption bands *viz.* C=O stretch and N-H stretch as shown in the spectrum. As has been reported hydrogen bonding causes redshift in absortion frequencies [206].

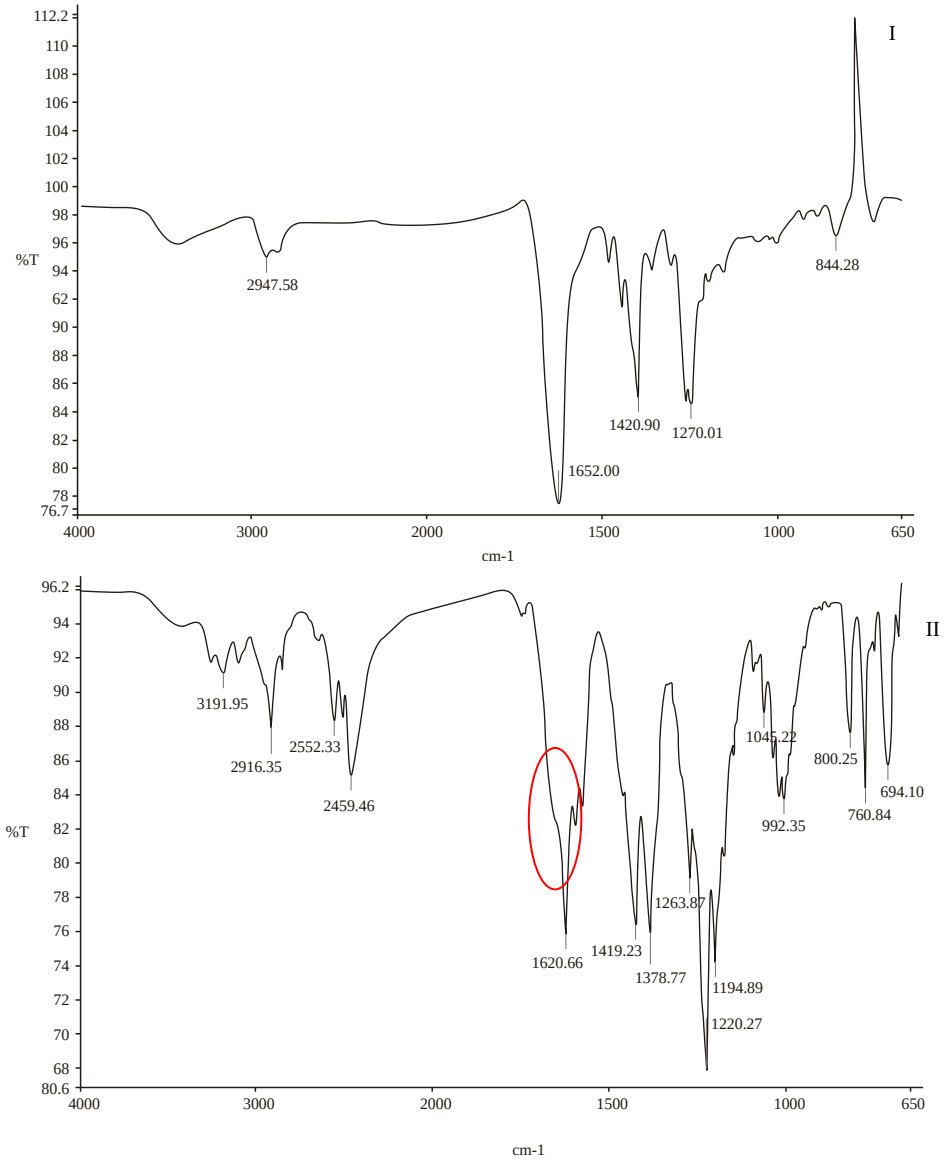

Figure 3.23 Typical IR spectrum of PVP-K30 (I) and RTD PVP-K30 binary mixture (II) generated at 4 scans and 4 cm^{-1} resolution

The IR spectra of binary mixtures of MTZ and MCC (Figure 3.24 II) and RTD and MCC (Figure 3.24 III) were similar to those of the individual components. However, the O-H absorption peak at 3217 cm^{-1} in the binary mixture of MTZ and MCC was slightly broader compared to that of pure MTZ and this again may be due to intermolecular hydrogen bonding interactions between MTZ and MCC.

Similarly the IR spectrum of a binary mixture of MTZ and DCP (Figure 3.25 II) revealed similar absorption peaks to those of the individual components in Figures 3.22 II and Figure 3.25 I respectively. However the disappearance of the O-H bending vibrational frequency of DCP at 1646 cm^{-1} depicted in Figure 3.25 I was noted in RTD and DCP binary mixture spectrum as shown in Figure 3.25 III. The cause for this disappearance could not be established since the binary mixture spectrum exhibited all characteristic peaks for RTD depicted in Figure 3.22 I. It may be concluded that there is interaction/incompatibility between RTD and DCP since the DSC analysis of the same mixture revealed the loss of DCP crystalline water at 188.7°C for DCP (Figure 3.16) instead of 194.03°C (Figure 3.7) that was previously recorded for the pure component.

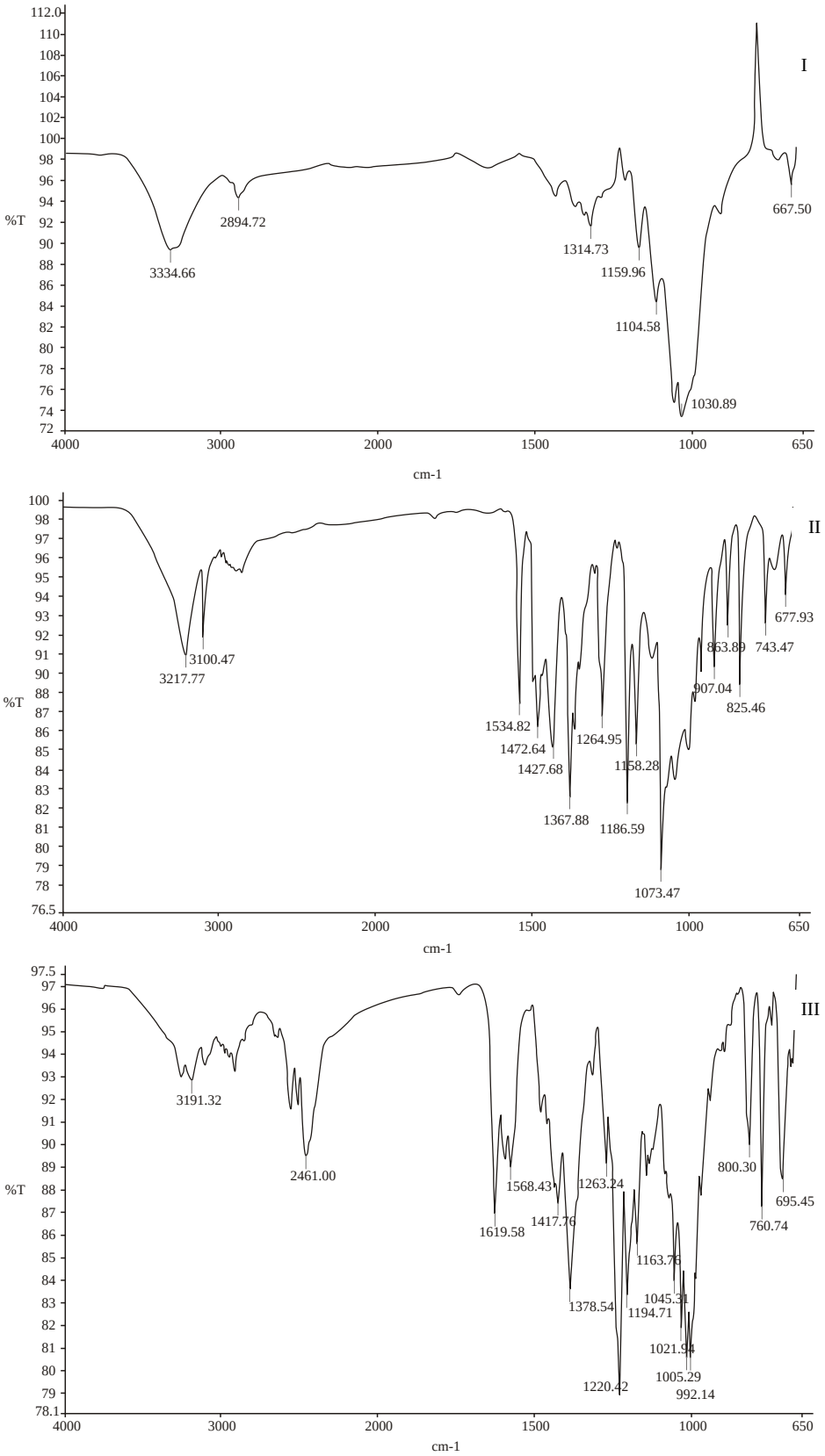

Figure 3.24 Typical IR spectra of MCC (I) MCC MTZ binary mixture (II) and MCC RTD binary mixture (III) generated at 4 scans and 4 cm^{-1} resolution

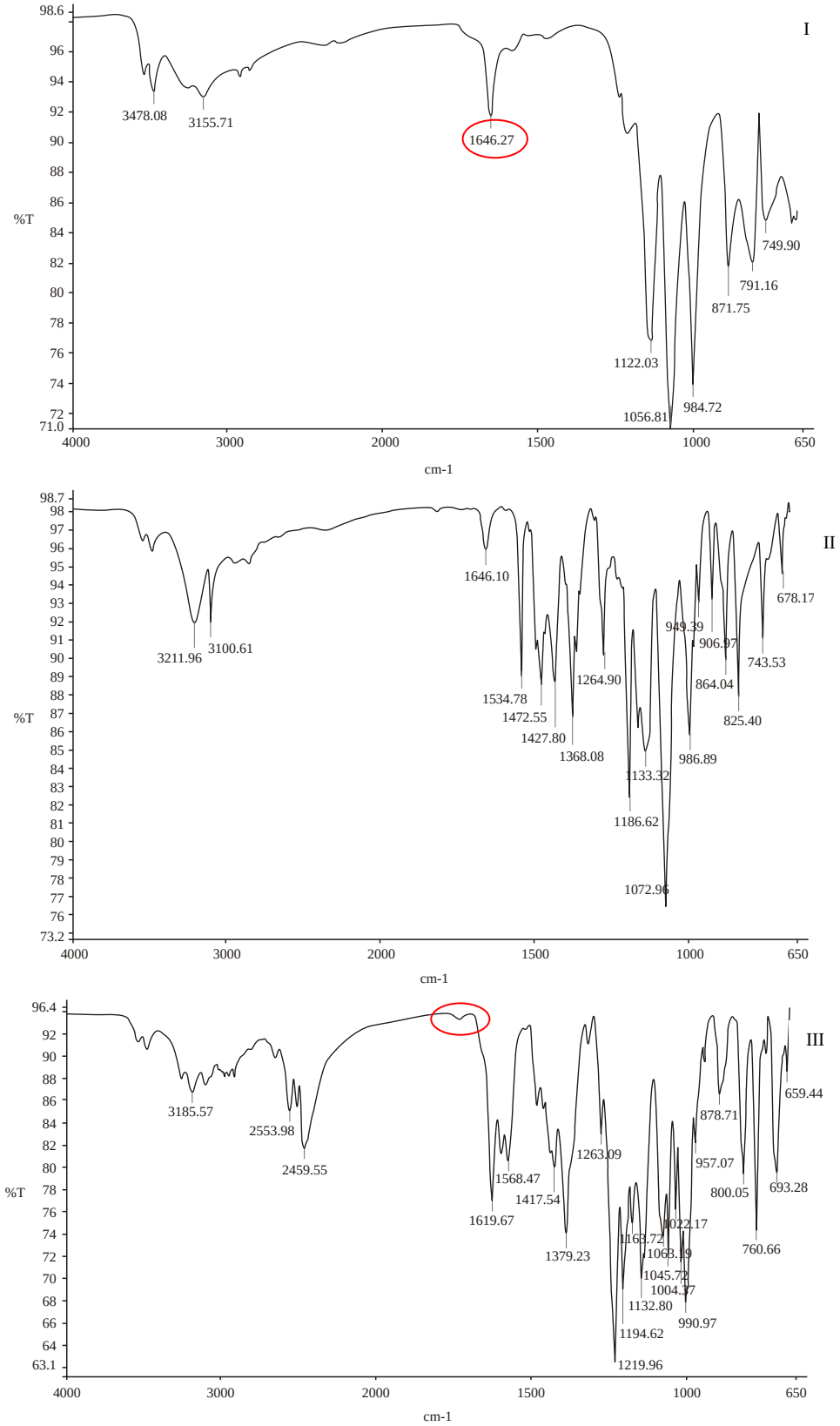

Figure 3.25 Typical IR spectrum of DCP (I) MTZ DCP binary mixture (II) and RTD DCP binary mixture (III) generated at 4 scans and 4 cm^{-1} resolution

The IR spectra of binary mixtures of MTZ and SSG, MTZ and magnesium stearate, and MTZ and CCS revealed all the characteristic peaks of MTZ and the respective excipients as depicted in Figures 3.26-3.28.

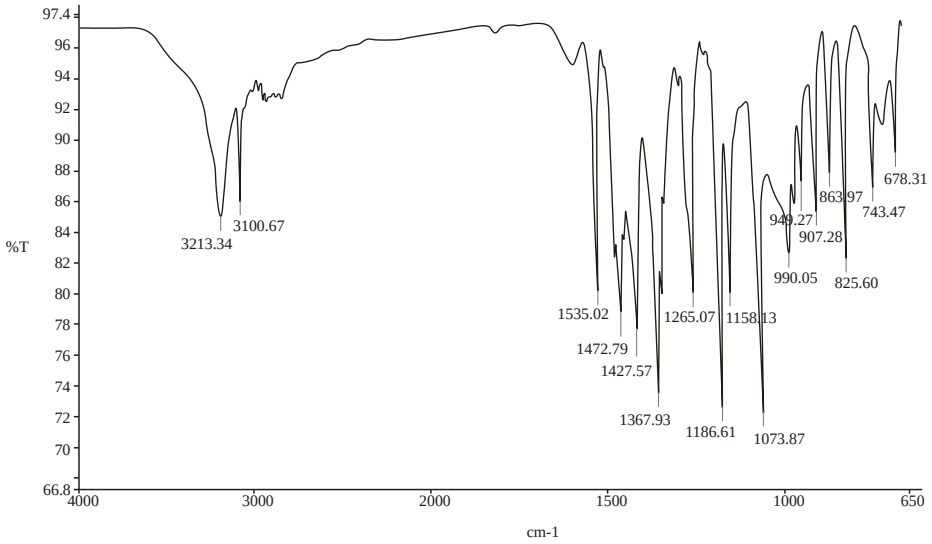

Figure 3.26 Typical IR spectrum MTZ and SSG binary mixture generated at 4 scans and 4 cm^{-1} resolution

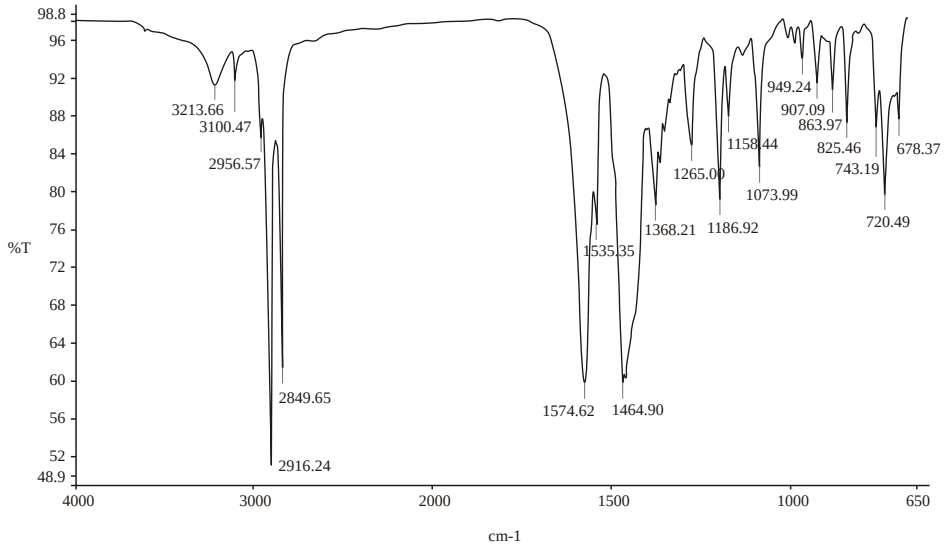

Figure 3.27 Typical IR spectrum of MTZ and magnesium stearate binary mixture generated at 4 scans and 4 cm^{-1} resolution

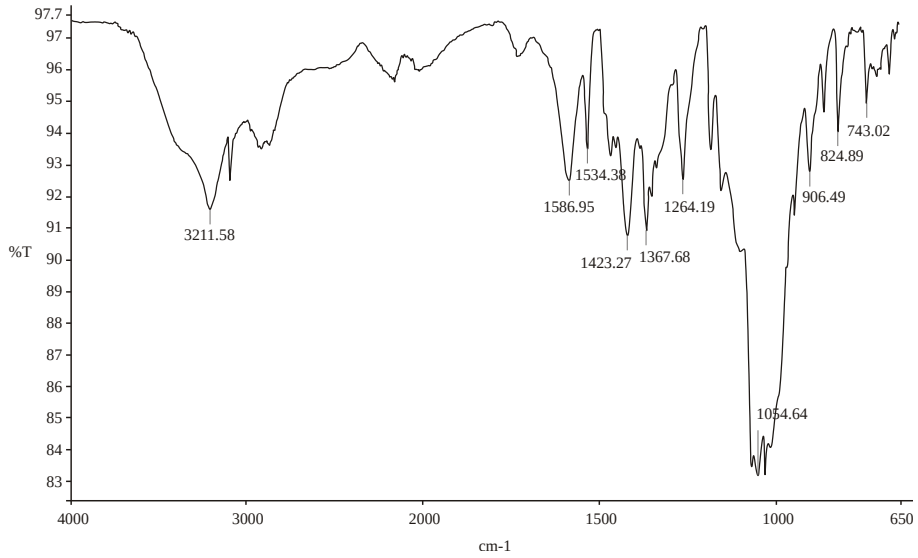

Figure 3.28 Typical binary mixture IR spectrum of MTZ and CCS generated at 4 scans and 4 cm^{-1} resolution

Similarly the IR absorption spectra of binary mixtures of RTD and SSG, RTD and magnesium stearate, RTD and CCS shown in Figures 3.29-3.31 revealed all the characteristic peaks of the drug and the respective excipients.

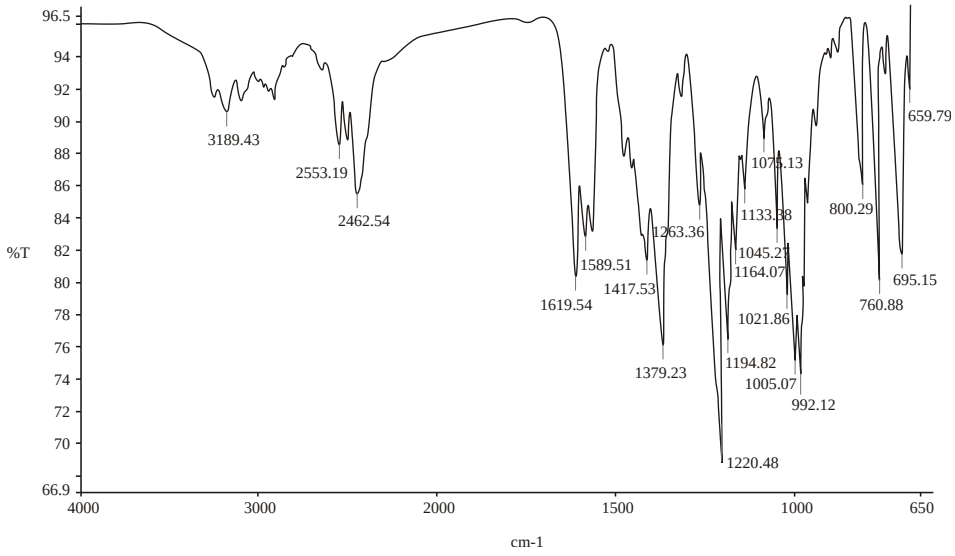

Figure 3.29 Typical IR spectrum of RTD and SSG binary mixture generated at 4 scans and 4 cm^{-1} resolution

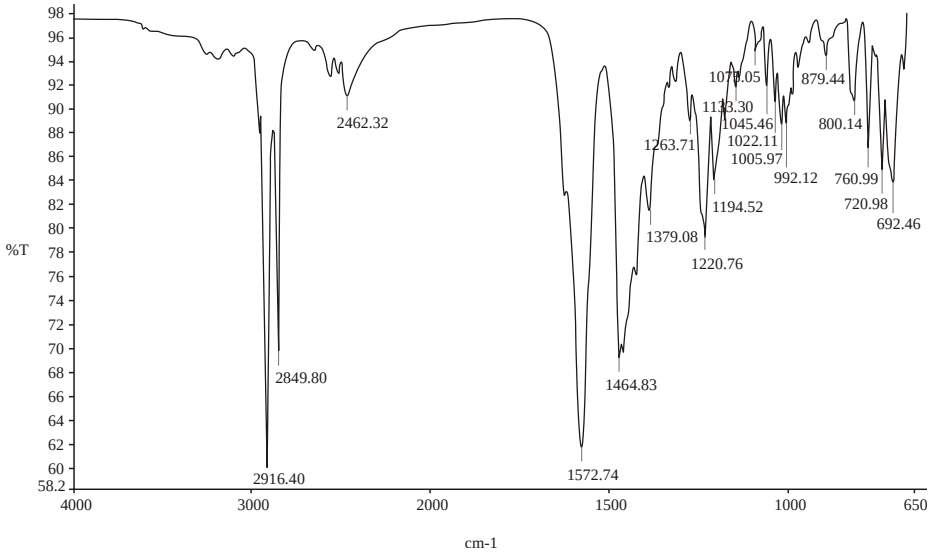

Figure 3.30 Typical IR spectrum of RTD and magnesium stearate binary mixture generated at 4 scans and 4 cm^{-1} resolution

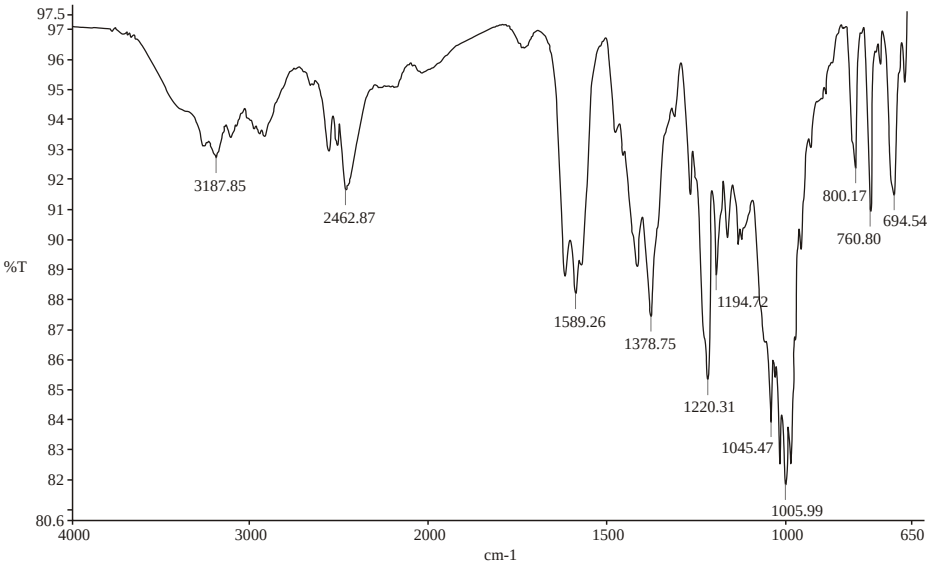

Figure 3.31 Typical binary mixture IR spectrum of RTD and CCS generated at 4 scans and 4 cm^{-1} resolution

A change in the absorption frequency for the N-H stretch to a higher wave length was observed for the IR spectrum of MCC in combination with MTZ, RTD and all the excipients with exclusion of DCP as shown in Figure 3.32. The shift in the absorption band from 1589 and 1164 cm^{-1} to 1575 and 1158 cm^{-1} respectively can be ascribed to hydrogen bonding. A similar observation was made for the spectrum of DCP in combination with MTZ, RTD and all the excipients as depicted in Figure 3.33.

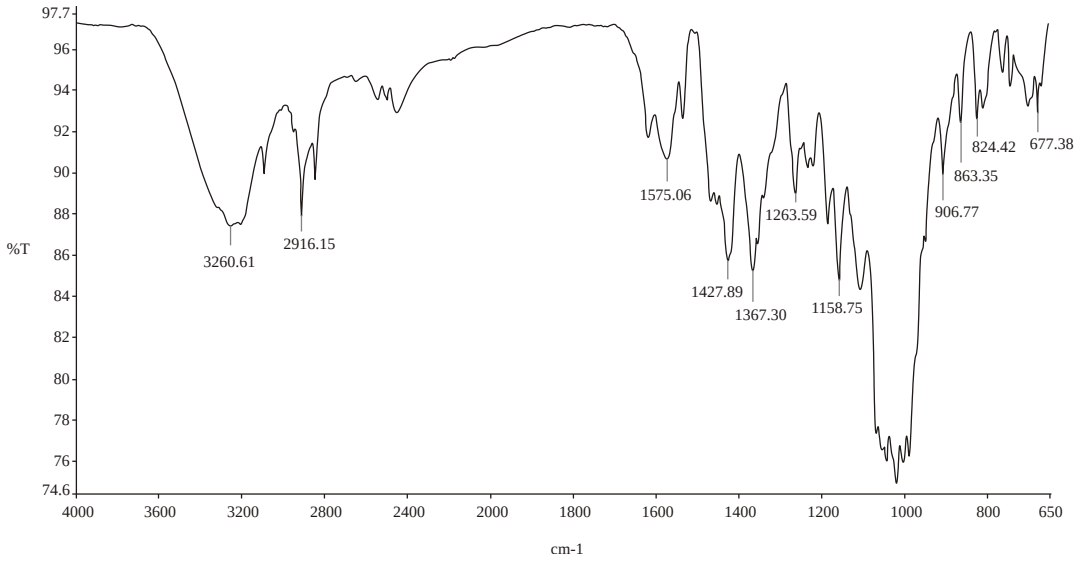

Figure 3.32 Typical IR spectrum of MTZ, RTD MCC and all the excipients generated at 4 scans and 4 cm^{-1} resolution

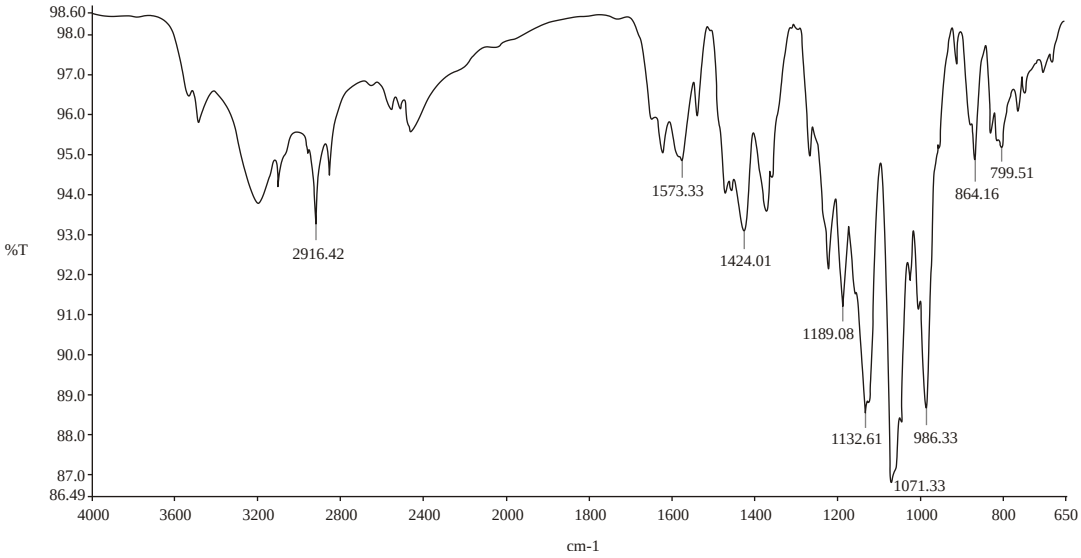

Figure 3.33 Typical IR spectrum of a mixture of MTZ, RTD, DCP and all the excipients

3.4 CONCLUSIONS

Preformulation studies are of great importance in formulation development since they provide a formulation scientist with relevant data that facilitates the prediction and the behaviour of a product during manufacturing and on long-term storage. Although the data offers no certainty, these studies form the foundation of building quality into a pharmaceutical product.

The DSC data has demonstrated that interactions between the drug substances and the excipients may occur. MTZ and RTD have shown interaction under the influence of high temperature but not incompatibility as has been evidenced following IR analysis. Furthermore, it can be concluded that the RTD sample studied is comprised of polymorph 2 as can be seen by the melting temperature and the enthalpy change. In addition, an interaction between RTD and DCP was noted in the DSC and IR analyses of RTD and DCP binary mixture, however it was not conclusive for incompatibility.

Based on the IR spectra, MTZ and RTD showed all the characteristic peaks in binary mixtures. Therefore it can be concluded that MTZ and RTD are compatible with most of the excipients tested despite the interactions that are hydrogen-bonding related. However, RTD interaction with DCP is of major concern and further investigation is warranted before the conclusion of incompatibility can be categorically reached. Furthermore, the IR spectrum for RTD has revealed the characteristic peak at 1045 cm^{-1} that is ubiquitous to polymorph 2. It can be concluded that the possibility of polymorphic change during manufacturing is minimal since form two is a stable polymorph.

Thermogravimetric analyses of RTD and MTZ have clearly confirmed the stability of both compounds under potential manufacturing conditions, and the degradation temperatures for both drugs have been confirmed following DSC analysis of the same material.

The physical characteristics of MCC and DCP indicate that both compounds possess suitable flowability and compressibility properties as evidenced by their respective CI, HR and ε values. Furthermore SEM indicates that size reduction for MTZ and RTD may be required in order to attain homogenous powder blend following blending with the potential excipients

It can be concluded that these studies have provide significant data on the suitability of formulating a fixed dose combination of MTZ and RTD with the aforementioned excipients.

CHAPTER FOUR
FORMULATION DEVELOPMENT AND MANUFACTURE OF FIXED DOSE COMBINATION TABLETS

4.1 INTRODUCTION

4.1.1 Overview

Active Pharmaceutical Ingredients (APIs) can be delivered to the body using a variety of different approaches. The choice of a specific route of administration is dependent on a number of factors including but not limited to the nature of the API, site and onset time of action, frequency of administration and age of the patient. The oral route of administration is considered the most convenient route for drug delivery as it is an acceptable and convenient route of administration for patients and solid dosage forms are relatively easy to manufacture [207]. Drug delivery systems for oral administration include tablets, capsules, syrups, solutions, elixirs, suspension, gels and powders. However solid oral dosage forms (SODF), *viz.* tablets and capsules, are the most frequently administered technology for adult patients whereas liquid oral dosage forms are primarily used for paediatric and geriatric patients [208,209]. Tablets and capsules are further categorized into formulation types as summarized in Table 4.1

Table 4.1 Tablet and capsule formulation types adapted from [209]

Formulation Type	Description
Immediate release tablet/capsule	The drug is released immediately following administration
Delayed release tablet/capsule	A physical event determines the when drug will be released
Sustained release tablet/capsule	The drug is released slowly over an extended period of time
Soluble tablet	The tablet is dissolved in water prior to administration
Dispersible tablet	The tablet is added to water to form suspension prior to administration
Effervescent tablet	The tablet is added to water to form an effervescent solution following release of carbon dioxide
Chewable tablet	The tablet is chewed and swallowed
Chewable gum	The formulation is chewed for a specified time and then removed from the mouth
Buccal and sublingual tablet	The tablet is placed in oral cavity for local or systemic action
Orally disintegrating tablet	The tablet dissolves or disintegrates in mouth without water
Lozenge	The tablet is designed to be sucked and dissolves slowly
Pastille	The tablet is comprised of gelatine and glycerine and is designed to dissolve slowly in the mouth
Hard gelatine capsule	A two-piece capsule shell filled with powder, granulate, semi-solid or liquid materials
Soft gelatine capsule	A single shell capsule containing a liquid or semi-solid material

Tablets have been used as a drug delivery technology since the nineteenth century with the earliest form used, *viz.* the pill, resembling manually rolled gum [209,210]. The pill was manufactured manually by mixing a gum with a herbal extract known to possess pharmacological activity. The manual production of pills was not efficient to meet the growing demand for this type of SODF and therefore the development of a mechanized manufacturing procedure was undertaken [210]. Further improvement of the pill manufacturing process was achieved by use of a piston to drive a punch in a die to compress mixtures of drug substance(s) and excipients leading to the production of tablets [210].

During the early stages of tablet development the application of pressure to an API did not always result into the formation of a suitably compacted mass. With the addition of binding agents and other excipients the compressibility and flow properties of the material were significantly improved, and the good compressibility and flowability exhibited following the addition of excipients led to the establishment of parameters that describe the quality of a suitable tablet and which are continuously reviewed during and after manufacture [210]. These parameters include but are not limited to appearance, dissolution, disintegration, weight variation, content uniformity, thickness, hardness and friability of the SODF [209].

4.1.2 Manufacture of compressed tablets

In general the simplest tablet formulation is usually an uncoated product manufactured by direct compression or by use of a wet or dry granulation process [209]. A suitable tablet formulation is uniform in content, exhibits drug stability and an optimal dissolution rate, and ensures that drug is available for absorption [208,209]. A typical manufacturing process for tablets includes weighing, milling, granulation and drying, blending and lubrication, compression and/or coating [211,212]. Each processing step may itself involve a number of processes that facilitate the production of robust tablets with suitable characteristics [209]. The manufacturing process of tablets can be further classified into three methods, *viz.* direct compression, wet and dry granulation which are discussed in the subsequent sections of this chapter.

The successful manufacture of compressed tablets is also dependent on the presence and appropriate use of excipients in a formulation. These additives facilitate the manufacture of dosage form by masking inadequate characteristics of a drug substance with respect to

compressibility, stability and ultimately absorption of that API [211]. Powder blends that are compressible and free flowing are readily compressed into tablets since their free-flowing nature ensures smooth and continuous uniform die filling for high-speed compression [211]. However, blends that exhibit poor flowability and/or compressibility pose difficulties during compression since inadequate flowability results in variable die filling, ultimately leading to the production of tablets that vary in weight and strength and that usually exhibit poor tensile strength [212]. Granulation is usually used in these instances to improve the flow properties, material density and powder compressibility of formulations [211,212]. The choice of excipients, equipment and process parameters used for the manufacture of tablets are usually determined during preformulation and process development studies.

4.1.3 Excipients

An excipient is a material that is added to pharmaceutical formulations to facilitate the manufacture of dosage forms and, where appropriate, to ensure drug delivery to the systemic circulation. Commonly used excipients in tablet manufacture include but are not limited to binders, diluents, disintegrants, lubricants, glidants, antiadherents, adsorbents, moistening agents, flavourants and colourants.

4.1.3.1 Binders

A binder is a substance that facilitates the adhesion of particles ultimately leading to the formation of cohesive agglomerates of granules that in due course form cohesive compacts following compression of the granular or powder mass. Binding agents are usually added in dry or liquid form depending on the method of tablet manufacture used to produce the material for compression. The addition of a binder in the dry state is common practice when tablets are manufactured by direct compression, whereas in a wet granulation process the binder is added to the powder blend in a liquid form [212]. Commonly used binders for wet granulation manufacture include polyvinylpyrrolidone (PVP), starch, gelatine, alginic acid derivatives, cellulose derivatives, glucose and sucrose amongst others, whilst microcrystalline cellulose and silicified microcrystalline cellulose have been reported to be effective binders for direct compression manufacturing [190,212].

4.1.3.2 Diluents

A diluent is a substance that is added to formulations to increase the mass of product, in particular for low-dose API, to a practical size for compression [213] and to improve the mechanical and physiochemical properties of the tablet [182]. Tablets with a mass of $\geq$ 50 mg are considered to be convenient to handle [212], thus very low dose drugs such as digoxin require bulking agents or diluents to increase the overall tablet mass to a size that is easy for patients to handle. In addition a diluent may also be added to an API to improve the flowability and compressibility of the resultant powder system to form tablets. Furthermore, a diluent may also be used to facilitate dissolution of an API known to possess poor aqueous solubility and it is usual that a water-soluble diluent is used for this purpose [208]. Some examples of commonly used diluents for the manufacture of SODF include lactose, dibasic calcium phosphate, starches, microcrystalline cellulose, dextrose, sucrose, mannitol, sorbitol and sodium chloride [190,212].

4.1.3.3 Disintegrants

A disintegrant is substance that is added to a blend prior to compression to facilitate the disintegration of a tablet once it comes into contact with the gastrointestinal tract fluids. Tablet disintegration results in an increase in the effective surface area of the material and is necessary to ensure effective dissolution of the API contained in the tablet [212]. Disintegration occurs by a number of mechanisms but usually involves wicking and swelling of the disintegrant following exposure to a liquid, with a consequence of disruption of the bonds that hold the tablet together, ultimately leading to tablet breakage. This mechanism of disintegration is exhibited by disintegrants that are derived from cellulosic material such as CCS [212,214]. Furthermore, tablet disintegration can be achieved through the production of a gas such as carbon dioxide following reaction of an organic acid with an inorganic base. By way of example, this mechanism of disintegration is used in effervescent tablets that are comprised of calcium carbonate or sodium bicarbonate in combination with an organic acid such as citric acid [215]. When placed in an aqueous environment the acid and base react through molecular movement and contact between the reactants and consequently liberation of carbon dioxide that causes fragmentation of the tablet [216].

4.1.3.4 Anti-frictional agents

Anti-frictional agents are used in SODF formulation to overcome the frictional forces that powders or the compressed tablets are exposed to during tablet manufacture. These agents are classified according to their primary anti-frictional activity and take the form of lubricants, anti-adherents and glidants.

4.1.3.4.1 Lubricants

Tablets may sometimes abrade due to friction occurring between the edges of the tablet and walls of the die cavity during the tablet ejection process following compression. In order to minimize friction, wear of punches and dies and to facilitate the production of tablets with smooth and high sheen appearance, lubricants are added to the powder blends [212]. The most commonly used lubricants are hydrophobic in nature and are comprised of fragile and fine particles that fragment easily and adhere to powder particles in a blend during the mixing process [159,164]. Lubricants can be categorized into two groups, *viz.* hydrophilic and hydrophobic. Typical examples of hydrophilic lubricants include magnesium and sodium lauryl sulphate, sodium benzoate, polyethyleneglycols and sodium chloride, whereas hydrophobic lubricants are materials such as magnesium stearate, stearic acid and hydrogenated vegetable oil [190,208].

4.1.3.4.2 Glidants

Powder flowability is a critical property that impacts tablet weight uniformity during compression. As most powders and blends do not flow readily, the addition of glidants to a formulation to reduce the interparticulate friction and improve powder flow properties is essential [212]. In general, good glidants usually exhibit poor lubricant properties [217]. However some glidants also possess lubricant properties and are able to serve a dual function in a formulation. Glidants, with the exception of talc, are frequently used at low concentrations (usually $\leq$ 1% w/w) and are often added to a powder blend immediately prior to compression. An excipient such as talc exhibits glidant, lubricant and anti-adherent properties. Other commonly used glidants include fumed or colloidal silica and starch [190,208].

4.1.3.4.3 Anti-adherents

Some powder blends may be produced with materials that have a tendency to adhere to the surfaces of punches and dies due to their sticky nature. This property may be a consequence of poor drying of a granulation or a high equilibrium moisture content of the material [209]. This effect usually results in the production of tablets with rough surfaces and this may exhibit sticking and/or picking. In general the addition of a lubricant to a formulation is sufficient to prevent adherence, however, in extreme cases the addition of an anti-adherent to overcome this defect may be necessary [218]. Commonly used anti-adherents include starch, talc and colloidal silicon dioxide at concentrations of between 1-2% w/w [190].

4.1.3.5 Adsorbents

Adsorbent are excipients that are capable of holding liquids and maintaining the appearance of an apparent dry state [212]. The addition of an adsorbent is useful in formulations that require the addition of a semi-solid or semi-liquid material, such as for example a volatile flavouring agent or fluid extract, or is useful in formulations that contain hygroscopic excipients and/or APIs. However, the addition of an adsorbent is not without its challenges and often abrasive tablets are produced, therefore the use of a fine and grit-free grade adsorbent is essential [212,218]. Examples of commonly used adsorbents include but are not limited to kaolin, bentonite, Fuller's earth, magnesium carbonate and microcrystalline cellulose.

4.1.3.6 Solvents

There are different types of liquids (solvents) that are used for wet granulation, *viz.* water, isopropanol and ethanol, however, due to safety and environmental concerns the use of organic liquids such as alcohol in pharmaceutical formulation has largely been surpassed by use of aqueous based systems. These liquids have a dual function, *viz.* solvation of the binder and wetting of the powder blend. During wet granulation wetting of the powder blend is of paramount importance since the resultant compactability of the resultant granular material is dependent, in part, on the residual moisture content of the granules following drying. A moisture content of ≤2% w/w for a granulation mass has been reported to offer a good

compromise between compactability and adherence of the powder blend to the punch surfaces [212].

4.1.3.7 Dyes and flavourants

Flavouring and colouring agents are added to a formulation to enhance the palatability and aesthetic appearance of the dosage form. Sweeteners have a dual role in a formulation, *viz.* bulk volume reduction and taste improvement. The use of dyes in a formulation is not without its challenges and patients may exhibit allergic reactions. Allergic reaction in patients may manifest as asthma or asthma-like symptoms or anaphylaxis following the use of a pharmaceutical product that has yellow or blue dyes, for example Sunset Yellow and Brilliant Blue [219]. Furthermore azo dye dermatitis has been observed in subjects who are sensitive to para-amino compounds [220]. This cross-reaction may be attributed to structural affinities or to metabolic conversion of these materials in tissues following consumption of the causative agent [221].

4.1.4 Wet granulation

Wet granulation is the oldest approach for the manufacture of materials suitable for compression and has been used by pharmaceutical industry for the manufacture of tablets for longer than the use of dry granulation or the direct compression approach [211,222]. Wet granulation involves the wetting of a powder blend with a granulation liquid that is either sprayed onto the powder as fine droplets or is poured slowly onto the powder bed. The formulation of a granulation liquid is usually comprised of a binder or wetting agent that is dissolved in an aqueous solvent, however, alcoholic and hydro-alcoholic solvents have also been used for the granulation of powders containing an API that is susceptible to hydrolysis [222]. The use of aqueous granulation fluids is preferred as they are economical, safe and versatile with respect to use in a variety of different equipment.

The characteristics of granules such as pore structure, particle size and distribution are dependent on the conditions and the method of granulation. Furthermore the experience of a formulator may also contribute significantly to the ultimate properties of the granules that are produced [211,222]. It is challenging to predict the properties of granules due to the complexity of interrelating factors such as granulation conditions, method of granulation and

experience of the formulation scientist. The mechanism of granule formation has been thoroughly studied and reported [223-227] as a three-step process and this is discussed in § 4.1.4.1 *vide infra.*

4.1.4.1 Granule formation

4.1.4.1.1 Wetting and nucleation

The formation of granules is commonly viewed as a combination of three rate processes that involve coalescence and breakage of particles [224]. In the initial stages of granule formation, *viz.* wetting and nucleation, a liquid binder is distributed on the surfaces of dry powder particles resulting in the formation of nuclei as shown in Figure 4.1. There is limited information pertaining to the processes that control nucleation, however the thermodynamics of wetting and binder dispersion have been reported to significantly influence the size of the initial nuclei that are formed [224,225].

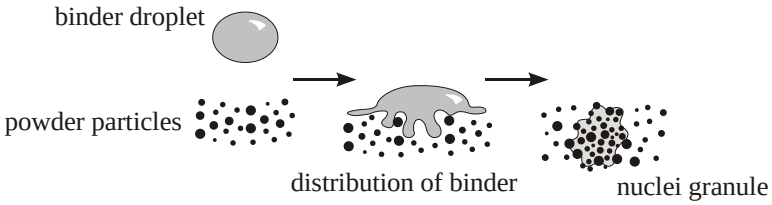

Figure 4.1 Wetting and nucleation stage of granule formation. Adapted and modified from [224]

4.1.4.1.2 Growth and consolidation

The growth and consolidation of granules is determined by the rate of collision of the nuclei granules, *viz.* coalescence, pre-existing granules and fine powder, *viz.* layering and/or granule and equipment surfaces [228]. Granule growth occurs as soon as a liquid binder solution is added to the agitated powder mass and growth may continue following completion of binder addition. In some cases granule growth is significantly influenced by nucleation conditions. In these systems the incorporation of limited amounts of binder solution is usually sufficient to produce conditions that favour the optimal growth of granules by nucleation [224].

Granule growth is also dependent on the mechanical properties of the material used to manufacture the granules in addition to properties of the binder solution. During agitation of

the wet powder mass, granules may exist in different states of liquid saturation, *viz.* pendular, funicular, capillary and droplet, and each state is differentiated from the other by the degree of granule saturation as shown in Figure 4.2 [224,229].

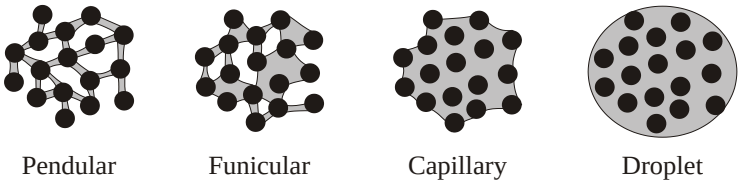

Figure 4.2 Different stages of saturation of liquid-bound granules. Adapted from [224]

In the pendular state, particles are bound together at their contact points by liquid bridges that occur as a result of the presence and addition of binder. The addition of further binder solution leads to the formation of the funicular state in which agglomeration of particles occurs, and this is followed by the formation of liquid bridges between the agglomerates in the capillary and droplet states. The strength of the resultant liquid-bound granule is attributed to two categories of forces, *viz.* liquid bridge and inter-particle frictional forces. These forces are interrelated in a complex manner that ultimately determine the mechanical properties of the resultant granules [224,230].

The properties of a binder solution such as content of binding agent, viscosity and surface tension have a significant effect on the consolidation of powder to form granules, as shown in Figure 4.3.

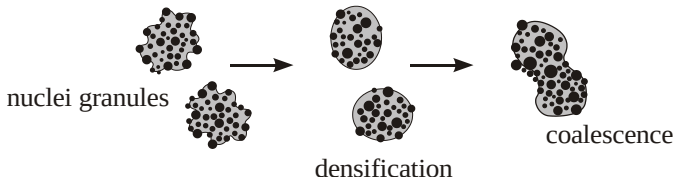

Figure 4.3 Granule growth as function of consolidation and coalescence. Adapted and modified from [224]

It has been reported that a high concentration of low-viscosity binder increases the initial rate and extent of powder consolidation to form granules due to increased particle mobility [224,227], whereas an increase in viscosity of the binder solution decreases the rate of granule consolidation due to reduced particle mobility. However, this relationship between the viscosity of a binder solution and the rate of consolidation has a critical value for binder viscosity, below which the viscosity has no effect on the rate of consolidation. The effect of

surface tension of the binder solution on granule consolidation is dependent on the type of equipment used in the granulation process. A non-significant change in the rate of granule consolidation was observed following an increase in the surface tension of binder solution when used in a high shear mixer [231]. However, in a tumbling drum mixer a decrease in surface tension of a binder resulted in an increase in the rate of consolidation but a decrease in the extent of consolidation [232].

4.1.4.1.3 Attrition and breakage

The attrition and breakage of granules depicted in Figure 4.4 shows two scenarios, *viz.* the breakage of wet granules as result of collision with other granules and/or the wall of the granulator, or attrition of dry granules in the granulator or dryer due to subsequent handling due to brittleness of the agglomerates [224,233].

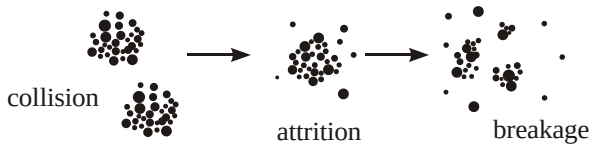

Figure 4.4 Attrition and breakage of granules. Adapted and modified from [224]

There is a dearth of information pertaining to granule breakage and attrition during granulation, nonetheless, it appears that attrition and breakage is extensive in high intensity mixers and hybrid granulators [233]. During granulation the control of wet granule breakage favours the production of granules with a narrow particle size distribution since the attrition of granulation is exhibited at the limit of granule breakage following the initial growth of the granules. The impact of the velocity of an impeller and chopper in a granulator and the turnover of granules through a high impact region in the manufacturing bowl are contributing factors that determine the size distribution of the granules produced during granulation [224,233,234].

4.1.4.2 Screening and drying of wet powder mass

The resultant wet mass produced following granulation is usually forced through a screen of pore size between 2380 and 3360 µm to produce relatively uniform granules, and different screen sizes may also be used depending on the properties of the wet material [211].

Alternatively uniform granules may be manufactured by extruding the damp mass through a screen with perforations of a predetermined size using an extruder to produce pellets that are subsequently spheronized to produce spherically-shaped particles [235].

The granules are dried following screening by use of thermostatically controlled ovens or fluidized bed dryers. The drying time and the final moisture content of the granule blend is usually established with due consideration of the stability of an API, the effect of moisture content on compressibility of the granules, and the equilibrium moisture content of the material equilibrated to the relative humidity of the manufacturing environment [222].

4.1.4.3 Dry screening, lubrication and tablet compression

The dried granules are once again passed through a screen of aperture size between 354 and 841 µm. The extent of granule size reduction is usually dependent on the size of the tablet to be produced and the physical characteristics of the tooling used during the compression process. Resizing of the granules facilitates the rapid and complete filling of die cavities and the production of tablets that are uniform in weight and thickness. The compression of large granules is not recommended due to their potential to create voids or air spaces within die cavities and consequently the production of tablets of uneven dimension and variable dose content following compression [211].

Lubricants are often passed through a fine screen of pore size between 149 and 250 µm prior to blending with the granules using a process known as bolting. The blending process is usually much shorter and is often between 2-5 min in duration, however, on rare occasions 10 min may sometimes be required depending on the nature of the lubricant, *viz.* particle surface area and aqueous solubility [208,236].

Following the addition of lubricant to the granules the powder blend is then compressed into tablets using a rotary tablet press fitted with multiple punches and dies or, on rare occasions, a single punch press. Despite the differences in the number of stations on the tablet presses, they are all operated in a similar manner and usually differ in the output in terms of number of units produced per hour [211]. Tablet compression occurs using a stainless steel (grade 316) die cavity and as a result of pressure exerted by the movement of two stainless steel

punches located above and below the die. The type of tooling to be used is usually established during preformulation studies.

4.1.5 Dry granulation

API and other materials that are sensitive to heat and/or moisture are best manipulated for compression by a dry granulation process, if the material exhibits poor flowability and compressibility properties that do not permit the use of a direct compression approach to manufacture and if the API or other excipients are cohesive in nature [212]. The dry granulation process entails force-feeding a powder blend into the die cavity of a tablet press and compacting the materials to form slugs by a process called slugging, or alternatively the powder blend may be forced between rollers and compacted into ribbons by a process called roller compaction [211,212,237]. The resultant slugs or ribbons are milled and screened prior to lubrication and the lubricated granules are then compressed into tablets.

4.1.6 Direct compression

The compression of powder blends into tablets without prior modification of the physical nature of the material, is defined as direct compression tableting [208]. Formerly this method was reserved for the manipulation of a few materials that were crystalline in nature and that possessed physical characteristics such as flowability and cohesiveness that are necessary for the application of this approach to tablet production [208]. Such materials included potassium salts such as chlorate, bromide, iodide, nitrate and permanganate, ammonium chloride and methenamine [208,211]. Due to advances in excipient and manufacturing technology there are far fewer limitations in the use of direct compression for the large scale production of SODF. This is primarily due to the availability of excipients that exhibit good compressibility and flowability properties and that lend themselves to the application of direct compression to a wide range of drug substances.

In general the manufacture of tablets by direct compression consists of three unit operations, *viz.* sizing or milling, blending and compression [212]. Resized excipients and API are mixed using an appropriate blender and the resultant homogenous blend is then lubricated prior to compression into tablets. Excipients that are commonly used for direct compression formulations include diluents such as spray-dried lactose, microcrystalline cellulose and

dibasic calcium phosphate and disintegrants including sodium carboxymethylcellulose, cross-linked polyvinylpyrrolidone and cross-linked carboxymethylcellulose fibres. The lubricants that are used include magnesium stearate and talc, and fumed silicone dioxide is often used as a glidant [190,211].

4.2 METHODS

4.2.1 Study design for the development of a method of manufacture

The initial stages of developing FDC tablets involved screening for an appropriate method of manufacture. Tablets were manufactured using wet granulation and direct compression using the formulae described in Table 4.2 (Batches RM 001 and 002). The success of the method of manufacture was determined by assessing the suitability of the resultant granules/powder blends in terms of CI, HR and the physico-mechanical properties of the resultant tablets, *viz.* weight uniformity, disintegration time and friability to compendial specifications.

Table 4.2 Formulae used for the manufacture of FDC tablets by direct compression and wet granulation

Raw material	**Direct compression (% w/w) Batch RM 001**	**Wet granulation (% w/w) Batch RM 002**
RTD	16.8	16.8
MTZ	50.0	50.0
MCC	28.0	27.0
PVP- K30	-	1.0
SSG	4.0	4.0
Colloidal silicone dioxide	0.2	0.2
Magnesium stearate	1.0	1.0

Following this initial evaluation, optimization of the selected method of manufacture was undertaken. The optimization studies were aimed at establishing a blending time that would produce a homogenous blend of API with the excipients of choice using the standard formulation composition summarized in Table 4.2. The success of the optimization procedure was determined by assessing the content uniformity of powder blends using the HPLC method described in Chapter Two.

The content of API was established and limits of 100±15% and a RSD of <5% were adopted as the acceptance criteria for the blend uniformity assessment. Tablets from these blends were

subjected to content uniformity analysis, assay and physico-mechanical tests to establish the optimal manufacturing conditions.

4.2.2 Materials

RTD and MTZ were purchased from Changzhou Longcheng Medicine Raw Material Co., Ltd (Changzhou City, Jiangsu, China) and Huanggang Hongya Pharmaceutical Co. Ltd (Huanggang, Hubei, China) respectively. MCC, DCP, SSG, CCS, colloidal silicon dioxide and magnesium stearate were purchased from Aspen Pharmacare (Port Elizabeth, Eastern Cape, South Africa).

4.2.3 Manufacturing equipment

All raw materials were weighed using a top-loading analytical balance Model PM4600 (Mettler Instruments, Zurich, Switzerland) with a sensitivity of 0.01g. Blending and granulation was performed in a Saral® vertical axis high-shear mixer granulator fitted with a 3.5 l bowl (Saral Engineering Company, Vapi, India). A model 7521-001 Cole Palmer peristaltic pump (Cole-Palmer Instruments Co., Barrington, Illinois, USA) consisting of a spray gun fitted with a pressure gauge was used for the addition of binder solution. The granules were dried using a Memmert® dry heat oven (Memmert GmbH Co., Schwabach, Germany) and tablet compression was performed on Manesty® B3B rotary tablet press (Manesty, Speke, Liverpool, England) tooled with six 12 mm flat-faced punches. All materials were sieved using wire cloth sieves conforming to DIN 4188 standards.

4.2.4 Method of manufacture

4.2.4.1 Direct compression

4.2.4.1.1 Manufacturing procedure

RTD, MTZ and MCC, were weighed and passed through a screen of aperture size 850 µm and blended for 5 min with 50% of the SSG at an impeller speed of 100 rpm. The resultant blend was then mixed for a further 3 min with colloidal silicone dioxide, magnesium stearate and the balance of the SSG that had been sieved through a screen of aperture size 315 µm.

The powders were then tested for bulk and tapped densities as described in § 3.2.2. The lubricated blend was transferred to the tablet press and compressed into 500 mg tablets at a turret speed of 25 rpm to a target hardness of 80-120 N. An example of a typical executed batch manufacturing record used to record the manufacturing process is included in Appendix 1. The formulation used for direct compression manufacture of tablets is summarized in Table 4.2 and schematic diagram of the manufacturing method is depicted in Figure 4.5.

4.2.4.2 Wet granulation

4.2.4.2.1 Preparation of binder solution

Approximately 12.5 g of PVP-K30 was accurately weighed and slowly added in a beaker that contained 100 ml of purified water. The solution was stirred gently until the PVP-K30 had dissolved to produce a solution of 12.5% w/v concentration.

4.2.4.2.2 Rheological studies of binder solutions

The viscosity of the binder solution was measured using a Model DV-II+ Brookfield viscometer (Brookfield Engineering Laboratories, Middleboro, Massachusetts, USA). The test was performed using 600 ml of binder solution that had been prepared as described in § 4.2.4.2.1. The viscometer was fitted with a RV spindle and operated at 100 rpm for 5 min prior to data collection. The test was performed in triplicate at a temperature 20±0.5°C.

4.2.4.2.3 Manufacturing procedure

Prior to addition of the granulation fluid the powders were dry blended as described in § 4.2.4.1.1. The resultant blend was granulated with 40 ml of PVP-K30 solution (12.5% m/v) delivered at a rate of 36 g/min using a pump speed of 25 rpm and a spray pressure of 52 psi. The blend was mixed with an impeller and chopper speed of 100 and 1000 rpm respectively. The granulation was mixed for a further minute after completion of wetting of the powder mass and the power consumption of the equipment was used to establish the endpoint of granulation prior to drying in oven at 50±0.5°C for 24 h. The dried granules were passed through a screen of aperture size 350 µm and lubricated for a further 3 min with the previously screened colloidal silicone dioxide, magnesium stearate and the balance of the

SSG (10 g). The granules were then assessed for bulk and tapped densities as described in § 3.2.2. The lubricated granules were compressed into 500 mg tablets at speed of 25 rpm to get a hardness of 80-120 N. The formulation used for the wet granulation manufacture of tablets is summarized in Table 4.2. The schematic diagram of the manufacturing method is depicted in Figure 4.5 and an example of a typical batch manufacturing record used to record the manufacturing processes is included in Appendix 1.

4.2.5 Physical characterization of tablets

4.2.5.1 Weight uniformity

The individual weight of 10 randomly selected tablets was measured using a top-loading electronic balance Model AG 135 (Mettler Instruments, Zurich, Switzerland) with a sensitivity of 0.1 mg and the average weight calculated.

4.2.5.2 Crushing strength and diameter

The crushing strength and diameter of the tablets was determined using a Model PTB 311 E hardness tester (Pharma Test AG, Hainburg, Germany). Each tablet was placed in the tester to facilitate horizontal application of the crushing force and the crushing strength and diameter of 10 randomly selected tablets was established simultaneously.

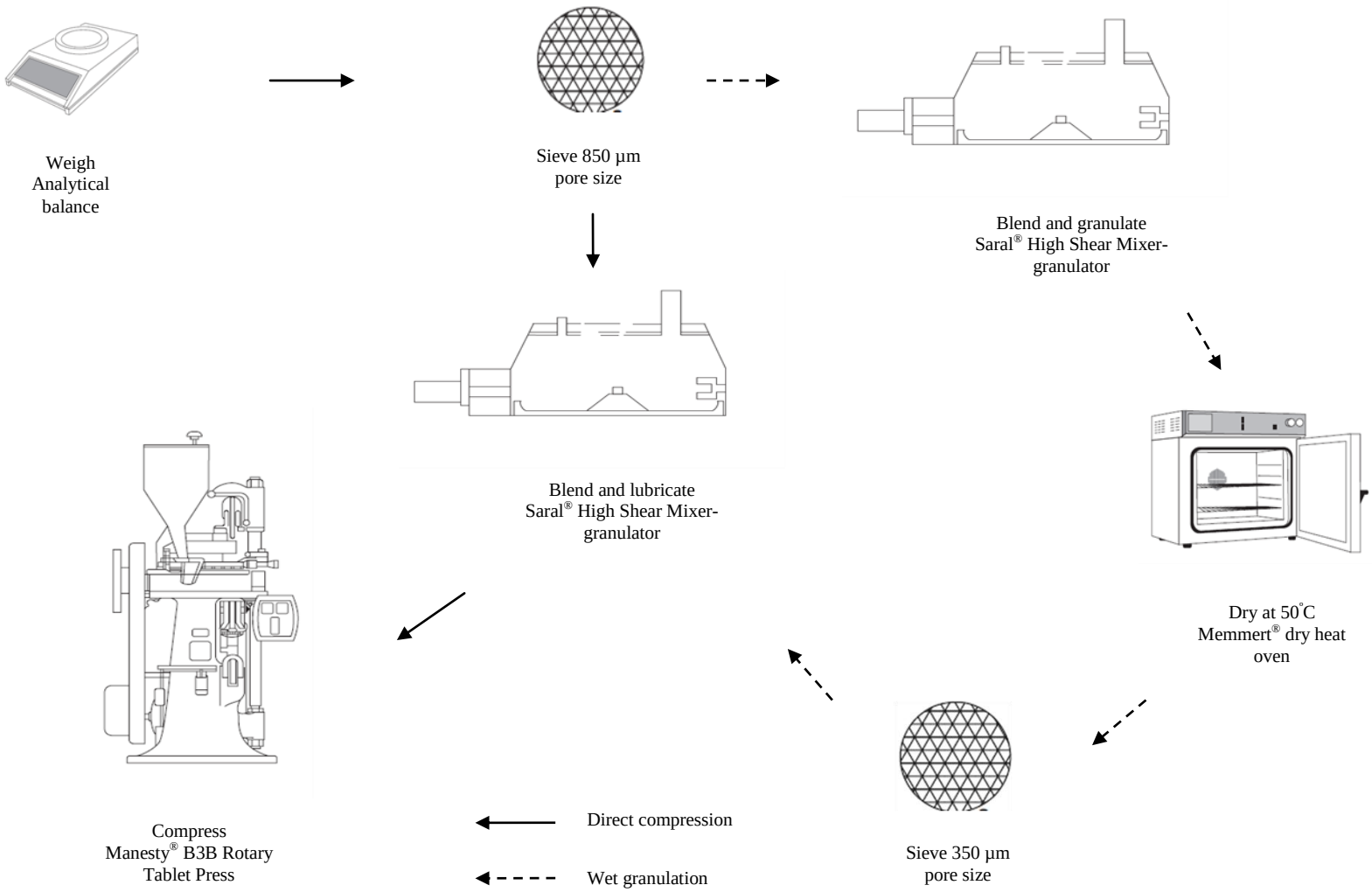

Figure 4.5 Schematic diagram of the methods of manufacture of tablets

4.2.5.3 Friability

The friability of 20 randomly selected tablets was established using a Model TA3R friabilator (Erweka GmbH, Heusenstamm, Germany). The compressed tablets were de-dusted and weighed using a top-loading balance Model PM 4600 (Mettler Instruments, Zurich, Switzerland). The tablets were allowed to tumble at 25 rpm for 4 min (100 drops), removed and de-dusted and then reweighed. The friability was then calculated using Equation 4.1

$$Fr = \left(\frac{w_1 - w_2}{w_1}\right) \times 100 \qquad \textbf{Equation 4.1}$$

Where,

w_1 = weight prior to tumbling
w_2 = weight after tumbling
Fr = friability

4.2.5.4 Tensile strength

The tensile strength of the resultant tablets was calculated using data generated in the diametral-compression test using Equation 4.2.

$$\sigma_0 = \frac{2F}{\pi dT} \qquad \textbf{Equation 4.2}$$

Where,

F = crushing strength, N
T = tablet thickness, mm
d = tablet diameter, mm
σ_o = tensile strength, MPa

4.2.5.5 Disintegration test

The disintegration time of the manufactured tablets was established using a Model ZT 61 tablet disintegration apparatus (Erweka GmbH, Heusenstamm, Germany). Six tablets were used for the determination of disintegration time. Each tablet was placed into a cylinder of the basket-rack and covered with a disc. The basket was set to oscillate vertically inside a beaker containing 700 ml of distilled water maintained at 37±0.2°C at a speed of 30 cycles/min and the time for disintegration of each tablet was recorded automatically on completion of the test.

4.2.5.6 Tablet assay

Twenty randomly selected tablets were crushed into a powder using a mortar and pestle. An aliquot equivalent to the weight of one tablet (approximately 500 mg) was weighed using a top-loading analytical balance Model AG 135 (Mettler Instruments, Zurich, Switzerland) and quantitatively transferred into a100 ml A-grade volumetric flask. The granules were dissolved in MeOH:water (80:20) followed by sonication for 5 min using a Model B-12 Ultrasonic bath (Branson Cleaning Equipment Co., Shelton, Connecticut, USA). The resultant solution was made up to volume using MeOH:water (80:20) and filtered through an ashless S &S round filter paper (Schleicher & Schüll GmbH, Postfach, Dassel, Germany) of 12 µm pore size and 125 mm diameter. A 1 ml aliquot of the filtrate was transferred into 100 ml A-grade volumetric flask and filled to mark with MeOH:water (80:20). Aliquots of 1 ml were collected and transferred into a 5ml A-grade volumetric flask followed by addition of 2 ml of the IS and filled to mark using MeOH:water (80:20). The resultant solution was filtered through 0.22 µm Acrodisc® PSF syringe filter (Pall Corporation, Port Washington, New York, USA) and injected into the HPLC. The analysis was performed in triplicate and the results were expressed as the mean ± SD.

4.2.6 Blend homogeneity studies

A blending time of 2-10 min has been reported to be ideal for processing of powders [238] although times of 10-20 min and even 60 min have also been used [239]. The optimal blending time was determined by assessing the homogeneity of the powder blend at different mixing time intervals as summarized in Table 4.3 using the validated HPLC method described in Chapter Two.

Table 4.3 Mixing times used to prepare blends for homogeneity analysis

Batch number	Mixing time
RM 003	5
RM 004	10
RM 005	15
RM 006	2
RM 007	3
RM 008	7
RM 009	9

Aliquots of powder of approximately 1±0.05 g (n=6) were collected for HPLC analysis using the spoon end (length of 2.54 cm) of a nickel/stainless steel laboratory spatula. Initially samples from batches RM 003, RM 004 and RM 005 were collected at 5, 10 and 15 min respectively after commencement of blending. In order to characterize the blend uniformity further, samples for analysis were collected from batches RM 006, RM 007, RM 008 and RM 009 following 2, 3, 7 and 9 min after the commencement of blending respectively and the content of API established.

4.2.7 Optimisation of tablet manufacturing process

4.2.7.1 Manufacture of tablets

Blend uniformity was found to be satisfactory following 9 min of mixing and therefore tablets from blends mixed following 8, 9, 10 min were manufactured using the methods described in § 4.2.4.2.3 as shown in Table 4.4.

Table 4.4 Batches of tablets manufactured

Batch	Mixing time (min)
RM 010	8
RM 011	9
RM 012	10

4.2.7.2 Content uniformity of tablets

Content uniformity analysis of tablets was performed on batches that were manufactured, *viz.* Batches RM 010, RM 011 and RM 012 respectively as shown in Table 4.4. Ten tablets from each batch were selected and then crushed individually using a mortar and pestle. Approximately 100 mg of each tablet was accurately weighed and transferred into a 100 ml A-grade volumetric flask. The powders were dissolved in MeOH:water (80:20) and the mixture was sonicated for 5 min using a Model B-12 Ultrasonic bath (Branson Cleaning Equipment Co., Shelton, Connecticut, USA). The resultant solution was made up to volume using MeOH:water (80:20) and filtered through an ashless S &S round filter paper (Schleicher & Schüll GmbH, Postfach, Dassel, Germany) of 12 µm pore size and 125 mm diameter. Aliquots (0.05 ml) of the filtrate were collected and transferred into a 5 ml A-grade volumetric flask followed by addition of 2 ml of the IS solution that had been prepared as

described in § 2.3.2.3 and the solution made up to volume using MeOH:water (80:20) and filtered through 0.22 µm Acrodisc® PSF syringe filter (Pall Corporation, Port Washington, New York, USA) prior to HPLC analysis.

4.3 RESULTS AND DISCUSSION

4.3.1 Micromeretic analysis of granules

Information obtained about the relationship between bulk and tapped density provides data that infers the compressibility and flow properties of a powder as described in § 3.1.1.2.1 and § 3.1.1.2.2. The CI and HR for the blends that are reported in Table 4.5 suggest that the wet granulation method of manufacture is likely to be the most suitable method of manufacture of these tablets since granules with good compressibility and flow properties were produced.

Table 4.5 Carr's index and Hausner ratio values of powder and granules following blending for direct compression and wet granulation prior to compression

Batch number	CI	HR
RM 001*	18.36	1.22
RM 002	15.12	1.17
RM 003	14.98	1.16
RM 004	15.55	1.18
RM 005	15.53	1.18
RM 006	15.42	1.17
RM 007	15.12	1.17
RM 008	14.14	1.16
RM 009	13.11	1.15

* Indicates powder blend obtained following direct compression method of tablet manufacture

4.3.2 Physico-mechanical properties of the tablets

The tablets manufactured by wet granulation appeared to be better than those manufactured by direct compression method when evaluating the data summarized in Table 4.6.

Table 4.6 Physico-mechanical properties of the tablets

Parameter	Method of manufacture	
	Direct compression	**Wet granulation**
Appearance	Off-white coloured tablets with capping	Cream coloured and sheen tablets
Weight variation (mg)	483.47±5.53	496±4.11
Diameter (mm)	11.83±0.03	11.93±0.05
Thickness (mm)	3±0.08	3.28±0.02
Disintegration (min.)	4.08±0.20	13.61±0.29
Crushing strength (N)	41.5±2.91	165.4±8.01
Tensile strength* (MPa)	0.74	2.77
Friability (%)	2.05	0.31

*The mean values of crushing strength, diameter and thickness of the tablets were used to compute for tensile strength.

The tablets manufactured by direct compression capped following compression and this may be a consequence of the relatively high content of MTZ (≈ 50% w/w) in the formulation and the poor compressibility properties exhibited by MTZ [240]. These results are similar to those reported by Odeniyi *et al*. [188] following investigations in which the effect of the diluent concentration on compressibility, porosity and flow properties of MTZ binary mixtures were evaluated. The tablets manufactured by direct compression also exhibited a low crushing strength and were friable in comparison to those manufactured by wet granulation. This may also be due to the intrinsic nature and poor compressibility of MTZ crystals [181,241].

Tablets manufactured by wet granulation exhibited better friability and crushing strength, however disintegration was slower compared to the tablets manufactured by direct compression (Table 4.6). This may be attributed to the compactability and compressibility of the granules that led to the production of tablets with a high crushing strength. It has been reported that granulation improves blend porosity and densification of granules on compression and the mechanical strength of tablets is dependent on this occurring [181]. The long disintegration times observed in tablets manufactured by wet granulation may be attributed to poor medium penetration as a consequence of the high tensile strength of the tablets.

4.3.3 Blend homogeneity

The USP recommends that blend uniformity analysis (BUA) be performed on a drug product that contains 50 mg of an API per dosage unit or if the API content is <50% w/w of content

of the dosage unit [242]. The acceptance criteria set by the USP for BUA is 100±10% of the expected quantity of the active ingredient with a RSD of no more than 5% [243].

The API content of powder blends prepared after blending between 3 and 15 min is shown in Figure 4.6 which shows that the optimal dry blending time was found to be 9 min, where the API content is within the USP tolerance limits for both RTD and MTZ.

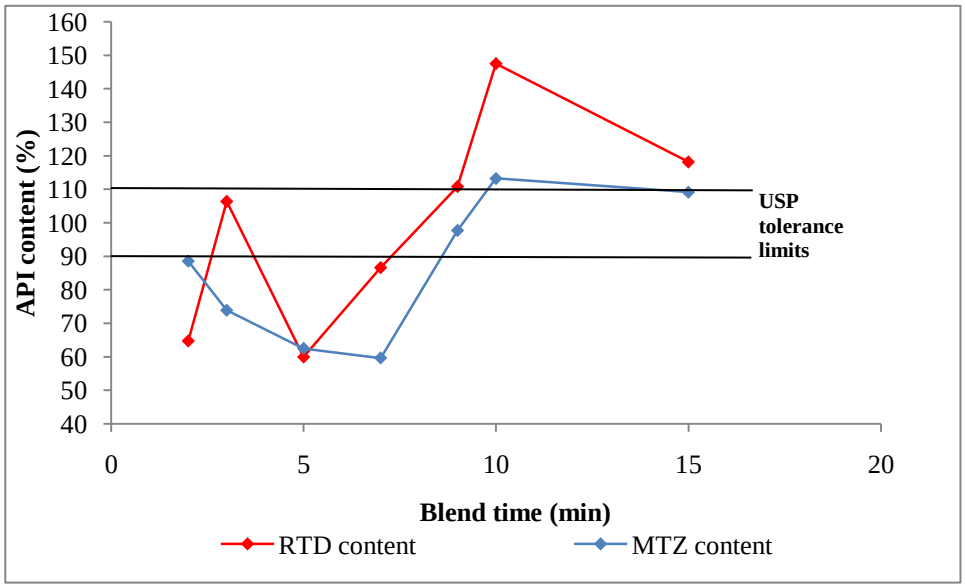

Figure 4.6 The variation in the content of MTZ and RTD in the sample aliquots of the blend as function of blending time

HPLC analysis of the aliquots of powder collected following 9 min of dry blending revealed that the content of MTZ and RTD were 97.73±7.08% (RSD=7.24%) and 110.82±10.14% (RSD=9.15%) respectively as shown in Table 4.7 and Figure 4.6.

Table 4.7 The actual content of MTZ and RTD determined in the powder blends of batches that underwent different dry blending time intervals

Batch number*	Blend time	Actual amount (mg) per g n = 6		Precision (% RSD)		% Bias	
		MTZ	RTD	MTZ	RTD	MTZ	RTD
RM 006	2	442.78 ± 83.39	108.79 ± 16.06	18.83	14.76	11.44	35.24
RM 007	3	369.38 ± 19.63	178.74 ± 16.96	5.31	9.49	26.12	-6.39
RM 003	5	312.50 ± 40.25	100.75 ± 14.34	14.23	12.88	37.49	40.02
RM 008	7	298.18 ± 50.42	145.54 ± 77.97	53.57	16.91	40.36	13.36
RM 009	9	488.66 ± 35.41	186.19 ± 17.04	7.24	9.15	2.26	-10.82
RM 004	10	566.18 ± 30.54	247.79 ± 16.53	5.38	6.67	-13.23	-47.49
RM 005	15	545.80 ± 530.82	198.51 ± 179.81	97.25	90.58	-9.16	-18.16

* Indicates MTZ (500 mg per g) and RTD (168 mg per g)

These results are in close agreement with the compendial specifications for these compounds despite the slight blend heterogeneity that may be attributed to differences in the particle size

and other properties of the blend constituents [244]. The properties of particles such as particle size and shape, adhesive and cohesive interactions, surface energy and electrostatics play a significant role in ensuring that there is a homogenous distribution of components in a powder mixture [245-248]. In addition material characteristics such as particle shape and size that tend to facilitate manufacturing processes are the same characteristics that compromise dose and content uniformity of powder blends and tablets [249,250]. Furthermore, the sampling techniques used to harvest powders for analysis may have also contributed to content heterogeneity. The use of a sample thief or any device may introduce sampling errors due to channelling and segregation as a consequence of perturbation of powder blends [251,252].

4.3.4 Content uniformity of tablets

Initially dose uniformity was a term used to describe weight uniformity of SODF. In 1970 the terminology gained a broader meaning and the definition was modified to include content uniformity as an additional parameter [253]. The USP and the International Pharmacopoeia (IP) require an assessment of the content uniformity of single-dose formulations and a limit of ±15% w/w of the average amount of the API is expected to be present in the tablets [254,255].

HPLC analysis of 10 individual tablets of batches RM 010, RM 011 and RM012 revealed that a significant variation in the content of API was evident and the resultant data are summarized in Table 4.8.

Table 4.8 Variation of tablet content uniformity and assay as function of blending time

Batch number	Blend time (min)	Label claim (mg)		Tablet content (%) n=10		Assay (%)		%Bias	
		MTZ	RTD	MTZ	RTD	MTZ	RTD	MTZ	RTD
RM 010	8	250.00	84.00	79.83±7.51	83.57±6.49	72.95±6.10	68.67±9.84	27.05	31.33
RM 011	9	250.00	84.00	94.90±13.16	97.58±13.85	85.19±3.14	84.41±8.23	14.81	15.59
RM 012	10	250.00	84.00	79.57±27.78	102.68±18.53	87.32± 6.1	77.06±6.67	20.43	22.94

The use of a blending time of 9 min during the dry mixing of powders resulted in the production of tablets with better content uniformity (% bias MTZ = 14.81, RTD =15.59) and the results are in close agreement with compendial specifications when compared to the tablets produced when either 8 or 10 min of dry blending was used for manufacture. The uniformity of content of dose units is attributed to a variety of factors including blending

time, load of blender and impeller and chopper speed as these factors can and do influence blend homogeneity [256]. In addition the design of equipment is also implicated [257]. The variation in content uniformity of tablets following the use of an optimal blending time may be attributed to segregation of material that is induced as a consequence of subsequent processing steps. The effect of air-induced segregation has been reported to be more pronounced in blends that exhibit variations in particle size of the constituents [258]. Furthermore variations in powder properties often affect the behaviour of a powder blend during handling and processing and usually leads to a variation in the final dose content of a finished product [259,260].

4.4 CONCLUSIONS

The formulation of a FDC of a clinically relevant drug combination is challenging when a low-dose API is to be incorporated into the dosage form. The variation of dose content in a final product is not an uncommon phenomenon in FDC, with a variety of factors, such as the characteristics and compatibility of formulation constituents, suitability of the equipment and processing methods used, contributing significantly to the final product dose content [257,258,260].

Blending time is one of the critical parameters that determines dose homogeneity in a final product, nonetheless, subsequent processing and formulation constituents properties have also been reported as contributing factors [257-259]. The determination of a blending endpoint depends on the accurate determination of blend homogeneity which in turn is dependent on the sampling technique used. The blending time established for use in these studies has the necessary accuracy for the manufacture of suitable quality FDC tablets of RTD and MTZ.

Direct compression is a convenient and cost effective method used for the manufacture of tablets, however the use of wet granulation method resulted in the production of tablets of better quality as can be seen from the data reported in Table 4.6. Therefore a wet granulation method of manufacture was adopted for the production of FDC tablets since the resultant powder characteristics of the batch manufactured by direct compression shown in Table 4.5 did not favour the production of tablets of suitable quality.

CHAPTER FIVE
THE APPLICATION OF RESPONSE SURFACE METHODOLOGY AND IN-VITRO RELEASE OF METRONIDAZOLE AND RANITIDINE

5.1 INTRODUCTION

5.1.1 Response surface methodology

Statistical design of experiments (DOE) have been used in pharmaceutical industry for optimization of processes and formulations for over three decades [261,262]. DOE permit formulation scientists to study the effects of multiple factors that determine product quality during the optimization process simultaneously [263,264]. Furthermore DOE may be used to generate mathematical equations that can be modelled and used to produce graphical representations that describe the variability of responses of a system as a function of predetermined input factors [263]. The application of statistical design and mathematical equations in the development, improvement or optimization of pharmaceutical processes is defined as response surface methodology (RSM) [159,264-266].

The use of RSM in the optimization of pharmaceutical processes is usually performed in three steps, *viz.* performing a series of statistically designed experiments, development of mathematical models that describe the relationship between input and output variables through multiple linear regression, and finally identification of the experimental parameters that are critical for the production of a desired response(s) [267].

5.1.1.1 Statistically designed experiments in formulation development

The optimization of formulations and manufacturing processes requires the identification of variables that can affect dosage form performance and the definition of an appropriate range in which the desired response can be expected to fall. There are two types of variables, *viz.* independent and dependent variables. Independent variables are those variables that affect the final characteristics of a product and that are easily manipulated by a formulation scientist, whereas dependent variables are the responses that may be observed following alteration of the independent variables [263,265].

Classes of excipient such as diluents, binders and disintegrants and manufacturing parameters such as compression force are independent variables and their influence on dependent variables has been studied extensively and has been well documented [190,209]. However the appropriate ranges required to produce the desired response(s) are only determined from preliminary studies. In DOE the effect of input factors on response variables is assessed at three levels, *viz.* high, medium and low, with the levels coded +1, 0, and -1 respectively [263,265]. For immediate release formulations, typical independent variables may include but are not limited to disintegrant, lubricant, diluent, binder (type and composition) compression force, blending time, impeller and chopper speed. Response variables may include disintegration time, crushing strength, granule size distribution, and rate and extent of dissolution amongst others.

In the pharmaceutical industry setbacks in the manufacture of products such as tablets include raw material shortages, equipment and facility breakdown that may well be inevitable, however the existence of an alternate validated method of manufacture may help to reduce disruption in production. The alternate manufacturing method may entail the use of different types of equipment and/or facility and raw materials. Due to these possible challenges the FDA have set guidelines that indicate permissible changes to a manufacturing process, formulation and site of manufacture that can be made following regulatory approval for market authorization [268]. However the determination of an outcome following changes in a formulation composition or process variables requires that a series of experiments are performed and these in most cases are time and resource intensive. Therefore the use of RSM for the determination of an outcome following changes in the method of manufacture or formulation may be beneficial, since less time and resources may be consumed. Thus following the manufacture of an oral FDC of MTZ and RTD as described in § 4.2.4.2, the effect of varying the disintegrant, lubricant and binder content on tablet disintegration time and the rate and extent of *in vitro* release of MTZ and RTD were investigated. Furthermore, level two changes in component and compositions as described in Scale Up and Post Approval Changes for Immediate Release (SUPAC-IR) of solid oral dosage form guidelines [268] were used as the experimental domain.

The DOE commonly used in the pharmaceutical industry for the optimization of formulations include factorial [269], central composite design (CCD) [270], Box-Behnken [271] and D-optimal design [272] approaches.

5.1.1.2 Mathematical models

The mathematical or polynomial equations that describe the relationship between independent and dependent variables may be first, second or third order in nature depending on how the output variables or responses react to changes in the input variables [273]. The relationship between the input and output variables exhibited in pharmaceutical systems is most often described by first and second order mathematical models [273].

Pharmaceutical systems with response variables that are significantly affected by a small change in the input factors and exhibit little or no interaction between the input variables are best described using first order mathematical models similar to that shown in Equation 5.1. Second order models are used to generate linear and quadratic equations in pharmaceutical systems that exhibit interactions between the input factors, and those that ultimately affect the response variable are best described using equations of the type shown in Equation 5.2. It has been reported that second order models are also applicable to input factors that exhibit extensive variation over an experimental domain and these relationships are best described by equations of the form shown in Equation 5.3 [265].

$$\boldsymbol{y = \beta_0 + \beta_1 x_1 + \beta_2 x_2 + \ldots + \varepsilon} \qquad \textbf{Equation 5.1}$$

$$\boldsymbol{y = \beta_0 + \beta_1 x_1 + \beta_2 x_2 + \beta_{12} x_{12} + \ldots + \varepsilon} \qquad \textbf{Equation 5.2}$$

$$\boldsymbol{y = \beta_0 + \beta_1 x_1 + \beta_2 x_2 + \beta_{12} x_1 x_2 + \beta_{11} x_1^2 + \beta_{22} x_2^2 + \ldots + \varepsilon} \qquad \textbf{Equation 5.3}$$

Where,

y = estimated response
χ_i = input factors
β_0 = constant that represent the intercept
β_i = coefficient of first order term
β_{ii} = coefficient of second order term
β_{ij} = coefficient of second order interaction

The values of the coefficients in the model are generated through multiple linear least squares regressions analysis of empirical data. A coefficient with a positive value is indicative of an agonistic effect of the factors on the measured response, whereas coefficients with a negative value indicate the opposite. The response variables that exhibit dependence on at least two independent variables can be illustrated in a three-dimensional manner that depicts the

variation of dependent factor(s) as a function of variation of the independent factors within an experimental domain [265]. The three-dimensional illustration of the variables is known as response surface plot. Alternatively a two-dimensional illustration of the independent variables plotted against one another produce contour plots that may also be used to describe the relationship between input factors and response variables [265].

5.1.1.3 Optimization

The use of DOE in pharmaceutical systems is aimed at identification of the input variable levels within an experimental domain that would lead to the production of a single value or range of values for a response variable. The determination of levels or experimental domain that facilitates the production of the desired value of a measured response is usually achieved by the use of the response surface plots [265].The achievement of a successful optimization for a process is dependent on the properties of the variable(s) under investigation and the experimental design must be continuous and controllable in an experiment with negligible error [273].

5.1.1.4 Advantages of response surface methodology

Statistical design of experiments that use RSM are time- and cost-effective techniques for the optimization of formulations or processes since precise information is generated from a small number of experiments that have been conducted in a systematic manner. Furthermore RSM provides the formulation scientist with insight into formulation development with respect to composition and product behaviour through the use of suitable mathematical models [263].

RSM is useful for the identification of input factors that are critical for the production of a high quality pharmaceutical product, and the detection of potential interactions and synergies between input variables that are critical for the optimization of a formulation [263]. In addition RSM provides a thorough understanding of the process factors that are significant for the successful scale up of batches to a manufacturing scale.

5.1.1.5 Limitations of response surface methodology

A limitation of using RSM is that relationships between input factors and measured response variables in which complex interactions exist between the variables under investigation may not be adequately described. Therefore the usefulness of RSM in optimization of a system becomes limited since a thorough investigation of the complex interactions requires an immense amount of resources and time.

The experimental design approach used for RSM, *viz.* Box-Behnken, full factorial and CCD, are useful for the evaluation of a small number of input variables, since the number of experiments increases dramatically as the number of variables required to be investigated increases. In addition, the resultant polynomial relationships estimated by linear regression analysis would also become too complex, as the number of factors investigated increases resulting in complication of the optimization procedure [263].

5.1.2 *In vitro* drug release testing

Dissolution testing for the characterization of release rate profiles of compounds with low aqueous solubility has been reported [274,275]. Dissolution testing is used to assess the ability of a dosage form, *viz.* tablet or capsule, to release an API in a specific test medium and it plays a major role in drug-product development and manufacturing since an API must be in solution in order to be absorbed [222]. The test is primarily a quality control tool that is used to measure batch-to-batch consistency in drug release and to show the impact of inherent variability in formulation excipients or manufacturing procedures on the dissolution of an API from a SODF [222,276].

The dissolution properties of a solid dosage form may be tested in an artificial physiological environment, which is termed *in vitro* release testing, or in a physiological environment, which is termed *in vivo* release testing. Samples are usually analyzed with an appropriately validated analytical method. The test media commonly used for *in vitro* drug release studies include water, buffered systems that are at a pH of 1.2 (0.1 M HCl), 4.6, 6.5 or 7.5 [268]. *In vivo* dissolution studies are complex and expensive to perform but are critical for the determination of bioavailability and formulation suitability. In general, *in vivo* studies involve

the analysis of an API and/or metabolite(s) in whole blood, serum or some other appropriate biological fluids after collection at specific times following oral administration [277,278].

The USP requires IR dosage forms to release 85% of an API from the dose unit into a medium at 37±0.5°C within 45 min using either USP Apparatus 1 or Apparatus 2 operated at 100 rpm and 50 rpm respectively [279]. This is a general requirement and provides guidance for the development of acceptance criteria for the dissolution of an API in an IR solid dosage form and does not constitute an approach to the testing of a product that is alternative to that required in the product monograph.

The acceptance criterion for the dissolution of MTZ and RTD tablets differs from compendium to compendium. The USP requires that no less than 85% of the label claim of MTZ is released within one hour when tested in 0.1 M HCl using USP Apparatus 1 at 100 rpm and at a medium temperature of 37± 0.5°C [280]. For RTD tablets the USP requires that no less than 90% of the label claim is released within 45 min in water using USP Apparatus 2 operated at 50 rpm and at a medium temperature of 37± 0.5°C [281].

The FDA suggests that for a rapidly dissolving drug substance no less than 85% of the label claim should dissolve within 30 min in solution of different pH made up across the pH range [282]. MTZ and RTD are considered to be Class I or highly soluble highly permeable and Class III or highly soluble and poorly permeable compounds respectively [282-284] and according to the Biopharmaceutics Classification System (BCS) they are classified as rapidly dissolving drugs. The high solubility of MTZ and RTD prevents the use of 30 min as a discriminatory sampling time point to determine the effect of formulation variables on drug release in any critical manner, therefore it was decided to adopt 10 min as the discriminatory sampling point for determination of the effect of formulation variables on drug release from tablets manufactured in laboratories that contained these compounds.

5.1.2.1 Factors that influence dissolution of drugs

There are several steps that a solid dosage form undergoes prior to dissolution of an API in that dosage form, *viz.* wetting, dissolution medium penetration, swelling, disintegration of components into granules, deaggregation of the granules to form fine particles, and ultimately dissolution of the API [285]. Nonetheless the dissolution process is complex and is

dependent on a variety of factors of which the formulation, composition and intrinsic properties of the API play a critical role.

5.1.2.1.1 Properties of the API

The solubility of an API in the test medium plays a significant role in the control of dissolution rate of that API from a SODF. The factors that influence the solubility of an API include, but are not limited to, the particle size, crystalline nature, amorphic and/or hydration state, free acid or base, salt form, eutectic and polymorphic form of the API. These are factors that must be controlled in order to achieve an optimal dissolution rate of an API from a dosage form [285,286].

5.1.2.1.2 Formulation properties

The dissolution rate of an API may be influenced by the type and amount of the excipients used in a formulation in addition to the manufacturing procedure used to produce the dosage form [286].

The type and amount of a disintegrant that is incorporated into a formulation controls the dissolution rate of an API from a SODF significantly [285]. In general the dissolution rate of an API from a dosage form is increased with an increase in the amount of disintegrant included in the formulation as a result of an increase in surface area of the API available for dissolution [286-288].

The effect of diluents on the dissolution rate of an API is dependent of the properties of the diluent and the API, *viz.* hydrophilicity and hydophobicity respectively. The use of a hydrophilic diluent in a formulation comprised of a hydrophobic API has been reported to facilitate the dissolution of that API due to increased wetting of the dosage form and improved hydrophilicity of the API [286,287]. The diluent facilitates the formation of a fine hydrophilic surface layer around the API that promotes solvation of the API [286,287].

The type and concentration of binder or granulating agent may also have a significant impact on the dissolution rate of an API from a SODF. The incorporation of high concentrations of a binder in a formulation may result into the production of hard and compact tablets that do not

disintegrate easily, resulting in slower dissolution due to the presence of low surface area for the dissolution [286,287]. A typical example of the effect of binder on API dissolution has been encountered in phenobarbital tablets that are comprised gelatine as a binding agent. The use of gelatine solution for the manufacture of phenobarbital tablets has been reported to facilitate the dissolution of phenobarbital compared to when a sodium carboxymethylcellulose solution was used [286,287,289].

The effect of lubricants on the dissolution rate of an API is dependent on the physical properties of the lubricant, *viz.* hydrophilicity and hydrophobicity and their respective concentrations. Most of the lubricants used in SODF formulations are hydrophobic and consequently decrease the dissolution rate of an API from the dosage form. Hydrophobic lubricants form a thin hydrophobic film around the dosage form that prevents the penetration of dissolution medium, thereby reducing the dissolution rate of the API [236,286,287]. Hydrophilic lubricants, on the other hand, facilitate the dissolution of an API from a dosage form. However the effect of hydrophilic lubricants on the dissolution rate are more apparent when incorporated in a formulation comprised of a hydrophobic API, whereby the lubricant facilitates the wetting of the API and consequently increases the dissolution rate of the API [286,287].

5.1.2.1.3 Manufacturing processes and conditions

Manufacturing processes, *viz.* milling, granulation, drying and tableting, may affect the physicochemical properties of an API and consequently may affect the dissolution rate of the drug [290]. APIs that exhibit polymorphism may undergo polymorphic change in certain manufacturing processes such as milling and/or granulation that may lead to a change in the properties of the API that facilitate dissolution [290].

During tablet compression the use of a high compression force often results in a decrease in the dissolution rate of the drug from that tablet. The use of high compression forces facilitates particle bonding that subsequently causes an increase in tablet hardness and the formation of a firmer and more effective sealing layer by the lubricant, consequently decreasing the penetration of dissolution medium into the tablet [286,291].

Another example of a process condition that affects the dissolution of drug from a SODF is that of extensive blending during lubrication following addition of lubricant to the formulation. The duration of lubrication of powder or granule blends using hydrophobic lubricants is critical to the dissolution performance of a dosage form. Over blending of powder or granule blends with magnesium stearate or hydrophobic lubricant may result in formation of a hydrophobic film on the surface of dosage form that acts as barrier to penetration of dissolution medium [164].

5.1.2.1.4 Dissolution apparatus

There are seven official apparatus listed in the USP for use in dissolution testing, and these are USP apparatus 1 *viz.* rotating basket, USP apparatus 2 *viz.* paddle, USP apparatus 3 *viz.* reciprocating cylinder, USP apparatus 4 *viz.* flow-through cell, USP apparatus 5 *viz.* paddle over disk, USP apparatus 6 *viz.* rotating cylinder, and USP apparatus 7 *viz.* reciprocating holder [276]. The dissolution rate of an API from a SODF is also dependent on the type of dissolution apparatus used when conducting the dissolution test. However for SODF, USP apparatus 1 and USP apparatus 2 are the most commonly recommended apparatus in regulatory guidelines [292]. USP apparatus 3 has also been used for SODF in cases where dissolution results generated from USP apparatus 1 or 2 become unreliable due to shaft wobble, location, centring and coning [293]. Furthermore, due to the single container nature of USP apparatus 1 and 2, variations in medium parameters such as pH, change in sink conditions and saturation during an experiment are inevitable. Therefore the use of USP apparatus 3 may facilitate the generation of precise dissolution results in cases where the variation in medium parameters may exert a significant effect on the reliability of the dissolution results [292].

In addition the precise set-up of a dissolution apparatus contributes to the generation of accurate and reliable dissolution measurements since reproducibility of dissolution test results are dependent on the consistency of medium flow patterns and the hydrodynamic properties of a dissolution medium. It has been documented that most of the automated dissolution apparatus may produce erroneous dissolution data as result of disruption of system hydrodynamics due to continuous immersion of sample probes [285].

5.1.2.1.5 Dissolution test parameters

The reproducibility of dissolution rate testing results are affected by several test parameters including pH, the nature, composition, volume and viscosity of the dissolution medium in which the test is conducted [286]. Inconsistent production of dissolution media may lead to increases or decreases in the dissolution rate of an API, and dissolved air in the dissolution medium is another major source of error in dissolution rate testing. Temperature changes may result in the release of air that is dissolved in the dissolution medium and the bubbles could adhere to the surface of the dosage unit. As a consequence a barrier may be formed between the medium and the dosage unit under investigation, leading to a reduction in the dissolution rate of an API as a result of reduced surface area of tablet medium interface [285].

5.2 EXPERIMENTAL

5.2.1 Proposed evaluation design

The successful optimization of a formulation is dependent on the composition of the formulation whereby incorporation of suitable excipients in the formulation is of paramount importance in order to achieve optimal performance of the dosage form. The suitability of an excipient is usually determined through screening of potential excipients known to have the appropriate tableting characteristics. MCC and DCP, *viz.* diluents CCS and SSG, *viz.* disintegrants, are commonly used excipients that are usually included in formulation for the manufacture of tablets and their impact on a dosage form is well documented [182,288,294-297]. Therefore to screen for a suitable diluent and disintegrant that may be used in the optimization process in these studies, batches RM 013, RM 014 and RM 015 were manufactured according to the method described in § 4.2.4.2.3 and the formulae described in Table 5.1, which is similar to the formula described in Table 4.2.

Table 5.1 Formulation composition of batches manufactured for preliminary studies

Excipient	RM 011 (% w/w)	RM 013 (% w/w)	RM 014 (% w/w)	RM 015 (% w/w)
API*				
MCC	27	27	-	-
DCP	-	-	27	27
SSG	4	-	-	4
CCS	-	4	4	-
PVP-K30	1	1	1	1
Colloidal silicon dioxide	0.2	0.2	0.2	0.2
Magnesium stearate	1	1	1	1

*MTZ (50% w/w) and RTD (16.8% w/w)

The selection of a suitable diluent and disintegrant for response surface studies was performed by evaluation of physicochemical characteristics such as weight, disintegration time, assay, dissolution, friability, tensile strength and the crushing strength of the resultant tablets. Further, the physicochemical characteristics of the tablets comprised of MCC and SSG were generated from batch RM 011 that had also been manufactured using the method described in § 4.2.4.2.3 and the formula described in Table 4.2 *vide infra*.

Following the preliminary studies, the effect of input variables, *viz.* binder, disintegrant and magnesium stearate composition, on the response variables D_t and % drug released in 10 min (Q_{10}) of MTZ and RTD were investigated using a Box-Behnken experimental design approach.

5.2.2 Materials and equipment

All the materials and equipment that were used were the same as those reported in § 4.2.2 and § 4.2.3 respectively *vide infra.*

5.2.3 Experimental design

5.2.3.1 Box-Behnken design

An evaluation of the main effects, interaction and quadratic effects of the input and response variables was performed using a Box-Behnken statistical screening design that had three centre points. The mathematical relationship between the input and output variables was

generated using Design Expert® 8.0.4 software (Stat-Ease Inc, Minneapolis, Minnesota, USA). The independent variable levels were established based on level two formulation and composition changes that have been described in SUPAC-IR [268] and were studied at three levels, *viz.* high, medium and low. The levels of the independent variables and the constraints of the responses used in optimization studies are described in Table 5.2.

Table 5.2 Actual content of factors used and respective codes (independent variables) and constraints of response (dependent) variables used in Box-Behnken design

Independent variables	**Levels used, Actual (Coded)**		
	Low (-1)	**Medium (0)**	**High (+1)**
x_1**= CCS (% w/w)**	15	20	25
x_2**= PVP-K30 (% w/w)**	0	5	10
x_3**= Magnesium stearate (% w/w)**	2.5	5	7.5
Dependent variables		**Constraints**	
y_1**= D_t**		Minimize	
y_2**= MTZ Q_{10}**		$80 > y_2 < 90$	
y_3**= RTD Q_{10}**		$80 > y_3 < 90$	

A summary of the composition of the independent variables used for the manufacture of tablets following the Box-Behnken design are listed in Table 5.3.

Table 5.3 Combination sequence of independent variable levels generated using a Box-Behnken design of experiment

Batch number [a]	**Independent variables**		
	x_1	x_2	x_3
RM 016	15.00	0.00	5.00
RM 017	25.00	0.00	5.00
RM 018	15.00	10.00	5.00
RM 019	25.00	10.00	5.00
RM 020	15.00	5.00	2.50
RM 021	25.00	5.00	2.50
RM 022	15.00	5.00	7.50
RM 023	25.00	5.00	7.50
RM 024	20.00	0.00	2.50
RM 025	20.00	10.00	2.50
RM 026	20.00	0.00	7.50
RM 027	20.00	10.00	7.50
RM 028	20.00	5.00	5.00
RM 029	20.00	5.00	5.00
RM 030	20.00	5.00	5.00

[a] Indicates arrangement in standard order

5.2.3.2 Statistical analysis of the data

The significance of the model and model terms that were generated were analyzed using analysis of variance (ANOVA) type three (partial sum of squares) at a 5% level of

significance using the statistical package, Design Expert® 8.0.4 (Stat-Ease Inc, Minneapolis, Minnesota, USA) . The predicted residual error sum of squares (PRESS) was used to assess which of the input factors had a significant impact on the measured response. A backward elimination procedure was used to fit data into the different predictor equations and the negligible effect of omission of non-significant factors was confirmed following comparison of the predicted and adjusted R^2 values of the full and reduced model. Furthermore, predicted *vs*. actual data diagnostic plots were used to determine the goodness of fit of the proposed model to the experimental data and these results are shown in Appendix 2.

5.2.4 Preparation and rheological studies of binder solutions

Binder solutions were prepared using PVP-K30 at concentrations of 12.5% w/v and 25% w/v as described in § 4.2.4.2.1. Rheological studies of the resultant binder solutions were performed as described in § 4.2.4.2.2.

5.2.5 Characterization of granules

The impact of viscosity of the binder solution on granule particle size following granulation has been reported [227,260,298]. MCC exhibits properties of a binder in addition to its use as a diluent and its effect as a binder was investigated by comparing the particle size distribution of the granules that were produced using a binder solution comprised of PVP-K30 and purified water.

The particle size distribution of the granules was established using a Model VT sieve shaker (Erweka, GmbH, Heussenstam, Germany) fitted to a Model UPE drive unit (Kraemer Elektronik GmbH, Dramstadt, Germany) and a sieve stack comprised of sieves with 315, 800, 1250 and 2000 µm apertures that conformed to DIN 4188 standards. A 100 g sample of the dried granulation was weighed and placed in the sieve stack that was then closed and set to shake for 10 min at an oscillation speed rpm of 200. The amount of granulation retained on the sieves was then weighed and the results were expressed as % w/w of the dry granules retained on the sieves.

5.2.6 Physical properties of tablets

The tablets were subjected to dissolution, assay, disintegration, friability, crushing strength, tensile strength, thickness, diameter and weight testing and these procedures were performed as described in § 4.2.5.

5.2.7 *In vitro* release

In vitro release studies of the FDC were performed using USP Apparatus 2 (Hanson Research SR 8 PLUS, Chartsworth, California, USA) fitted with an Autoplus™ Multifill™ and Maximizer Syringe Fraction Collector. Six tablets were dropped into the dissolution vessels each containing 900 ml of degassed 0.1 M HCl (pH 1.2). The paddles were set to rotate at 75 rpm since this speed represented a suitable compromise between the 50 and 100 rpm specifications described in the USP for RTD and MTZ respectively. The temperature of the dissolution media was maintained at 37±0.5°C and 5 ml aliquots were collected for analysis at intervals of 10, 20, 30 and 45 min with replacement of an equal volume of fresh medium after each sample collection. Aliquots of 0.1 ml of the samples were collected using an electronic pipette (Boeckel & Co. GmbH, Hamburg, Germany) and transferred into a 5 ml A-grade volumetric flask followed by addition of 2 ml of IS that had been prepared as described in § 2.3.2.3. The resultant solution was made up to volume using MeOH:water (80:20) and filtered through 0.22 µm Acrodisc® PSF syringe filter (Pall Corporation, Port Washington, New York, USA) prior to analysis using the HPLC method described in Chapter Two *vide infra.*

5.3 RESULTS AND DISCUSSION

5.3.1 Rheological studies

The viscosities of the resultant PVP-K30 binder solutions in purified water listed in Table 5.4 were in close agreement to the reported values [299].

Table 5.4 The viscosity of PVP-K30 binder solution

PVP-K30 concentration in purified water %w/v	**Viscosity (n=3) cP**
0	1.0 ± 0.01
12.5	8.1 ± 0.01
25.0	25.8 ± 0.01

5.3.2 Physical properties of tablets

The tablets that were produced were cream in colour and had a smooth surface without evidence of chipping or lamination. The resultant tablet weight, thickness, diameter, assay, crushing strength, tensile strength and friability data of all manufactured batches are summarized in Table 5.5.

The weight of the tablets ranged between 494 and 510 mg with the average diameter ranging between 12.00 and 12.07 mm and thickness ranging between 3.31 and 3.40 mm.

Table 5.5 Physicochemical properties of the resultant tablets (preliminary and experimental design formulations)

Batch number	Weight (n=10) mg	Thickness (n=10) mm	Diameter (n=10) mm	Crushing strength (n=10) N	Tensile strength MPa	Friability (%)	D_t (n=6) min	Assay (n=3) %	
								MTZ	RTD
RM 011	495.86±1.78	3.31±0.00	12.02±0.02	158±17.2	2.52	0.20	13.05±1.55	85.19 ± 3.14	84.41 ± 8.23
RM 013	496.80±1.58	3.32±0.00	12.02±0.00	101±5.30	1.61	0.10	11.49±1.15	83.49 ± 4.13	81.30 ± 4.70
RM 014	501.34±7.35	3.35±0.02	12.03±0.03	67.1±11.00	1.06	0.20	4.61±1.26	68.53 ± 2.53	78.92 ± 1.68
RM 015	498.02±3.17	3.30±0.01	12.02±0.00	77.8±10.10	1.24	0.09	8.56±1.81	74.70 ± 4.43	73.69 ± 2.27
RM 016	509.90±3.21	3.37±0.03	12.04±0.02	99.4±09.50	1.56	0.30	8.71±0.75	85.60 ± 1.60	86.09 ± 2.05
RM 017	508.83±2.95	3.39±0.03	12.05±0.02	88.5±07.00	1.37	0.19	3.58±0.49	84.28 ± 2.01	81.89 ± 1.77
RM 018	494.19±3.15	3.31±0.03	12.03±0.00	88.7±06.80	1.41	0.20	10.32±1.54	87.78 ± 6.41	85.34 ± 3.68
RM 019	508.47±4.85	3.40±0.00	12.05±0.02	102.4±12.40	1.59	0.09	6.08±0.20	105.19 ± 1.85	81.51 ± 1.58
RM 020	500.42±5.33	3.35±0.02	12.02±0.00	99.5±13.40	1.57	0.19	9.58±0.91	84.96 ± 2.67	89.05 ± 1.81
RM 021	502.56±3.27	3.34±0.01	12.03±0.00	92.7±05.20	1.46	0.19	5.50±0.54	105.78 ± 4.42	99.79 ± 3.77
RM 022	506.96±3.06	3.39±0.01	12.01±0.00	100.9±0.58	1.57	0.29	11.41±0.20	89.56 ± 3.36	91.32 ± 2.93
RM 023	503.76±7.18	3.38±0.03	12.02±0.00	86.8±04.10	1.36	0.29	7.33±0.25	85.87 ± 1.49	88.74 ± 3.94
RM 024	507.98±6.35	3.38±0.03	12.02±0.00	115.5±04.8	1.81	0.09	5.33±1.22	110.23 ± 2.11	86.81 ± 1.40
RM 025	496.83±3.40	3.37±0.02	12.01±0.00	124.4±10.7	1.95	0.10	8.50±1.01	90.18 ± 2.25	86.06 ± 1.32
RM 026	500.81±2.46	3.31±0.02	12.05±0.02	83.9±11.80	1.33	0.27	6.38±0.87	96.98 ± 2.70	94.56 ± 2.13
RM 027	498.28±2.10	3.32±0.02	12.04±0.01	91.3±07.00	1.45	0.27	9.81±0.77	88.67 ± 1.18	84.71 ± 2.24
RM 028	500.21±4.17	3.32±0.02	12.03±0.00	95.6±06.20	1.52	0.29	7.55±0.28	84.92 ± 5.87	85.01 ± 2.79
RM 029	499.18±3.14	3.31±0.02	12.07±0.07	94.7±08.70	1.50	0.30	7.21±0.87	87.31 ± 3.84	90.47 ± 3.30
RM 030	503.43±4.10	3.34±0.02	12.06±0.07	93.5±07.50	1.47	0.19	6.93±0.51	87.27 ± 7.20	86.93 ± 6.53

5.3.3 Preliminary screening formulations

5.3.3.1 Physical properties of tablets

The data summarized in Table 5.5 reveals that formulations that were manufactured using DCP, *viz.* batches RM 014 and 015, resulted in the production of soft tablets of between 67-77 N compared to the formulation in which MCC, *viz.* batches RM 011 and RM 013, was used. These tablets exhibited crushing strength of between 101 and 158 N.

All tablets were not friable as all the values for this parameter were ≤0.3% and all tablets had a D_t <15 min. Furthermore, formulations in which CCS was used produced tablets with shorter D_t compared to those which were manufactured using SSG.

The content of MTZ:RTD in tablets manufactured in these preliminary studies was low, with a drug content of < 80% for tablets in which DCP was used and >80% for tablets in which the diluent was MCC. Therefore all subsequent batches were manufactured using MCC and the MTZ and RTD content for these was between 83-110% and 81-99% respectively. On this basis MCC and CCS were considered to be the most suitable diluent and disintegrant respectively for the response surface studies.

5.3.3.2 *In vitro* release

The dissolution profiles of MTZ and RTD from tablets that were manufactured in the preliminary studies, *viz.* batches RM 011, RM 013, RM 014 and RM 015, are shown in Figures 5.1 and 5.2 respectively. For ease of understanding the qualitative impact of the diluents, *viz.* MCC and DCP, on the Q_{10} for MTZ and RTD, the dissolution profiles of the tablets comprised of a similar disintegrant, *viz.* batches RM 011 and RM 015, RM 013 and RM 014, were compared. A similar approach was also used to evaluate the qualitative impact of the disintegrant, *viz.* CCS and SSG, on the Q_{10} for MTZ and RTD.

5.3.3.2.1 In vitro release of metronidazole

The dissolution profiles of batches RM 013 and RM 014 shown in Figure 5.1 indicate a burst release of MTZ with a Q_{10} value of 82% for tablets that are comprised of MCC and CCS, *viz.*

formulation RM 013, whereas those comprised of DCP and CCS, *viz.* formulation RM 014, exhibited a Q_{10} value of 55%. The high Q_{10} value for MTZ observed for the tablets in formulation RM 013 may be attributed to the hydrophilicity of MCC as it facilitates wetting of the tablet and consequently rapid dissolution of the drug from the tablet whereas DCP is hydrophobic and therefore may delay the wetting process [286,287].

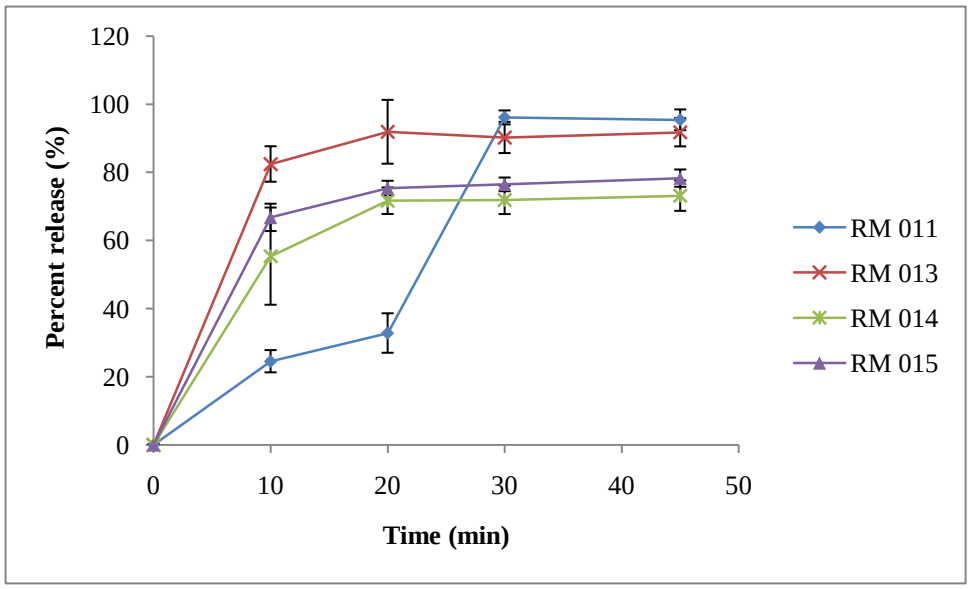

Figure 5.1 *In vitro* dissolution profiles of MTZ from preliminary batches

The Q_{10} for MTZ observed for the tablets comprised of SSG and MCC, *viz.* formulation RM 011, and CCS MCC, *viz.* formulation RM 013, revealed large variability in the rate of drug release. CCS appears to have a greater effect in facilitating the release of MTZ as evidenced by the Q_{10} value of 82% compared to the Q_{10} value of 24% exhibited in formulation RM 011. The release of MTZ in formulation RM 011 appears to be slow with only 32% released within the first 20 min of dissolution testing after which a burst release of MTZ occurs.

In contrast to the effect of SSG on the Q_{10} value for MTZ in formulation RM 011 a relatively minor change was observed for the Q_{10} value of MTZ in formulations RM 014 and RM 015. Substitution of SSG for CCS in tablets comprised of DCP resulted in a change in the Q_{10} value for MTZ from 66% to 55%. This observation suggests that the combination of SSG and DCP in a formulation may result in the production of tablets with better dissolution characteristics for MTZ compared to a formulation in which a combination of CCS and DCP are used.

5.3.3.2.2 Dissolution of ranitidine

Drug release from formulation RM 013 exhibited a burst release of RTD with a Q_{10} value of 89% and 95% observed for RTD within 30 min of the commencement of dissolution testing as shown in Figure 5.2.

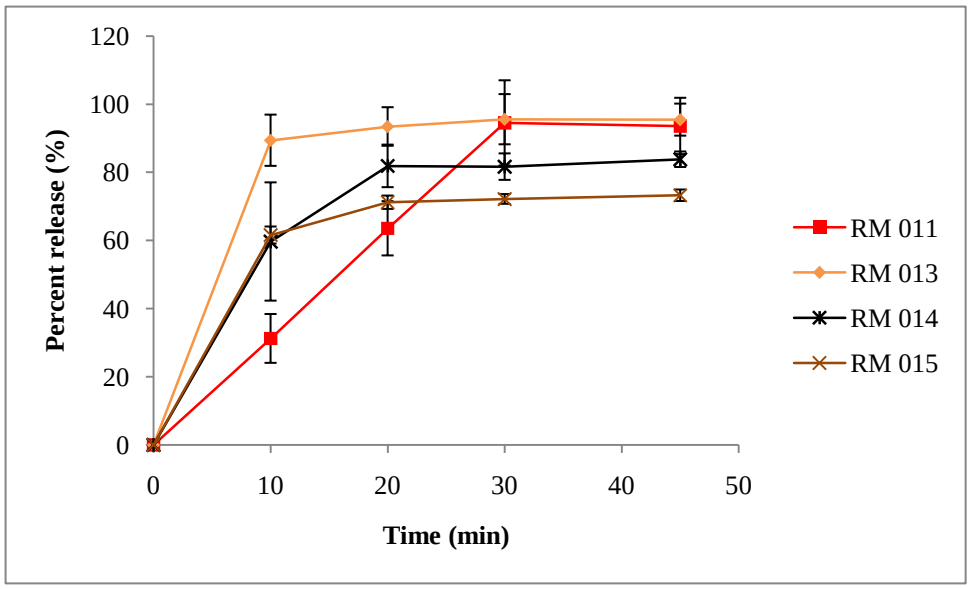

Figure 5.2 *In vitro* release profiles of RTD form preliminary formulations

In contrast to the effect of CCS on the Q_{10} for RTD in formulation RM 013, tablets comprised of DCP, *viz.* formulation RM 014, exhibited a Q_{10} value of 59% for RTD followed by 83% release within 45 min of dissolution testing. These results suggest that MCC facilitates the dissolution of RTD to greater extent than DCP.

The substitution of CCS for SSG in formulation RM 011 resulted in a drastic decline in the Q_{10} value for RTD with only 31% being released compared to the Q_{10} value of 89% observed when CCS was used in formulation RM 013. The dissolution of RTD from formulation RM 011 appears to be slow, achieving ≥90% with 30 min of dissolution testing. Conversely a minor change was observed for the Q_{10} value for RTD following the substitution of CCS for SSG in formulations comprised of DCP, *viz.* formulations RM 014 and RM 015. Tablets in which SSG and DCP were used, *viz.* formulation RM 015, exhibited a Q_{10} of 59% for RTD whereas a Q_{10} of 61% was observed for the formulation comprised of CCS and DCP, *viz.* RM 014. Therefore it may be concluded that a combination of MCC and CCS results in the production of tablets with better Q_{10} values compared to those produced with DCP.

5.3.4 Box-Behnken design formulations

5.3.4.1 Micromeretic analysis of granules

Granulation is a commonly used process to enlarge the particle size of a material [300] during the manufacture of tablets for the purposes of improving flowability, compressiblity and homogeneity of the powder blends and to reduce dust and possible cross-contamination [230,301].

The particle size distribution of the granulation depicted in Figure 5.3 reveals some degree of similarity between the granule size distribution observed when using 12.5% w/v PVP-K30 solution with a viscosity of 8.1±0.01 cP and those produced using water of 1.0±0.01 cP viscosity.

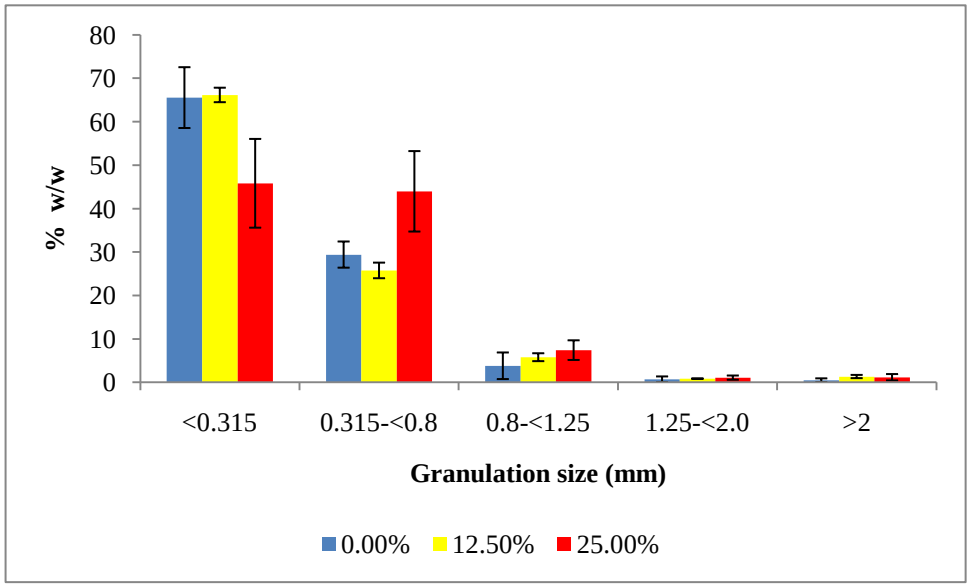

Figure 5.3 Granulation size distribution of formulations comprised of 0.00%, 12.50% and 25.00% (w/v)
of PVP-K30

Approximately 66% w/w of the granulation in the formulations manufactured using 0% and 12.5% w/v PVP-K30 were <315 µm in diameter, 27.5% w/w were sized ≥315≤800 µm and only 4.7% w/w were sized ≥800≤1250 µm. The granulation produced using a 25% w/v PVP-K30 solution and viscosity of 25.8±0.01 cP was mostly comprised of two categories of granule size as shown in Figure 5.3. Approximately 45% w/w of the granulation was <315 µm in size and ≥315≤ 800 µm, whereas 7.3% w/w was sized ≥800≤1250 µm.

The difference in the size of the granules observed following granulation using the binder solution of 25% w/v PVP-K30 may well be due to the high viscosity of the binder solution. An increase in the viscosity of a binder solution is known to facilitate granule growth as a consequence of increased cohesivity of the binder solution and granule-break threshold [260,302]. Similar results were also reported by Becker *et al*. [298] following an investigation into the effect of use of different binding agents in wet granulation procedures. In contrast to the results observed when 25.8±0.01 cP PVP-K30 solution was used, the effect of viscosity on granule size distribution was not apparent for granules produced when water or 12.5% w/v PVP-K30 solution was used as the granulation fluid.

5.3.4.2 Disintegration time (D_t)

The impact of formulation variables on the D_t of the tablets was investigated using RSM to determine which of the input variables may have a significant impact on the D_t of the tablets. The quadratic model shown in Equation 5.4 describes the quantitative effect of CCS (x_1), PVP-K30 (x_2) and magnesium stearate (x_3) on the D_t of the resultant tablet.

$$y_1 = 7.21 - 2.15x_1 + 1.21x_2 + 0.66x_3 + 0.50x_1^2 - 0.62x_2^2 + 0.74x_3^2 \qquad \textbf{Equation 5.4}$$

It is evident from Equation 5.4 that an increase in the amount of CCS used in the formulation resulted in a decrease in the D_t whereas an increase in the content of magnesium stearate and PVP-K30 leads to an increase in the D_t.

The effect of the amount of CCS on the D_t of the tablets has been investigated and the decrease in D_t observed as function of an increase in the content of CCS is ascribed to increased wicking and the swelling capacity of the disintegrant [294,303]. An increase in the wicking and swelling capacity of CCS following exposure to water results in an increase in the rate of fragmentation of the tablet which is dependent on the concentration of CCS in the tablet [304]. Similar results were observed following the use of statistical optimization of an IR formulation of a water soluble drug [305].

In contrast magnesium stearate has been reported to delay the disintegration of tablets [306,307]. Magnesium stearate is hydrophobic in nature and is comprised of fine particles that easily abrade and adhere to the surfaces of other components of a formulation, leading to

the formation of a hydrophobic film on that surface [164]. The resultant hydrophobic film acts as a barrier and delays the penetration of water into the formulation, delaying wetting of the tablet and ultimately leading to a delay in disintegration. The concentration of magnesium stearate and the duration of lubrication blending have a profound effect on tablet disintegration [136]. However, since the blending time following the addition of the lubricant was constant for all the batches, the variation in D_t can be attributed to the amount of magnesium stearate in the formulation. Similar results were observed following formulation optimization studies of fast disintegrating tablets [306].

In general the quantity and type of binder used in wet granulation has an effect on the ultimate characteristics of a compressed tablet. The use of excess or a strong binder during granulation results in the production of tablets that are very hard and that do not disintegrate readily [286,299]. The increase in D_t observed as a result of an increase in binder content in the formulation may be attributed to an increase in the mechanical strength of the resultant tablets. Binders are cohesive in nature and facilitate the agglomeration of powder particles to form granules, resulting in improved compactability of the granules and improved mechanical strength of the tablets [308]. Although the evidence of a direct effect of PVP-K30 on the disintegration of tablets has not been reported, the increase in D_t of these tablets may be attributed to a reduced permeability of the tablet to water, therefore the increase in mechanical strength of the tablets as a result of an increase in binder content confers resistance to penetration of water, consequently prolonging the disintegration time of the tablets.

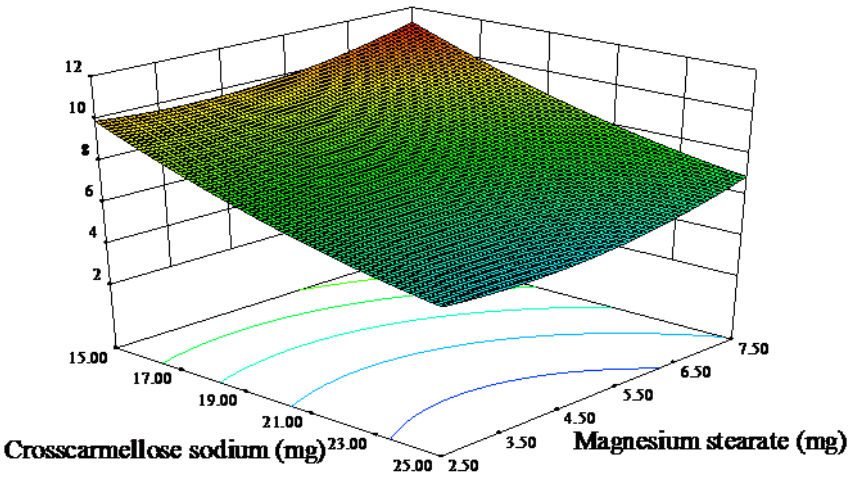

Figure 5.4 A three-dimensional response surface plot showing the relationship between CCS, magnesium stearate and D_t with PVP-K30 maintained at medium level

It is evident in Figure 5.4 that CCS has a profound effect on the D_t of the tablets compared to the effects of magnesium stearate. Tablets with the shortest D_t are produced when the content of CCS is at a high level, *viz.* ≥25 mg, and longer D_t are observed when the levels of CCS are low, *viz.* ≤15 mg. The effect of magnesium stearate and PVP-K30 on D_t are significantly dependent on the amount of CCS in the formulations. A significant decrease in D_t is observed when the content of magnesium stearate is decreased from 7.5 mg to 5.0 mg and a further decrease in content of this lubricant to <5.0 mg did not result in a further significant change in D_t.

The response surface plot in Figure 5.5 shows that the effect of PVP-K30 on D_t is also dependent on the CCS content. However, the effect of variation in levels of PVP-K30 on D_t is more pronounced when the content of CCS is ≥15≤21 mg and becomes less significant at high levels of CCS, *viz.* >21 mg of CCS, as shown in Figure 5.5. This may be due to increased wicking and swelling capacity of CCS as a consequence of an increase in concentration, as has been reported [294,303]. At low levels of CCS, *viz.* <20 mg per tablet, the mechanical strength of the tablet is determined by the content of PVP-K30 and resistance to fragmentation predominates whereas at high levels, *viz.* >20 mg of CCS, the mechanical

strength of the tablet is not sufficient to resist fragmentation induced as a result of wicking and swelling of the CCS irrespective of the levels of PVP-K30.

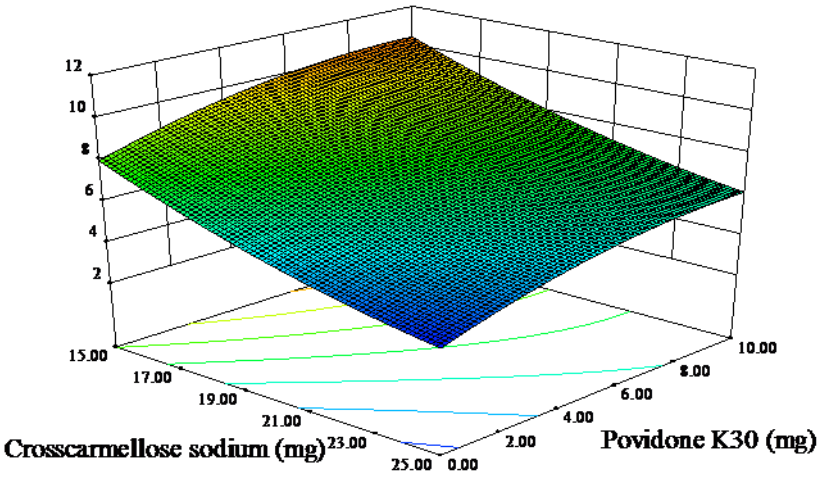

Figure 5.5 A three-dimensional response surface plot showing the relationship between CCS, PVP-K30 and D_t with magnesium stearate maintained at medium level

The contour plot depicted in Figure 5.6 visually describes the relationship between PVP-K30, CCS and the D_t with the content of magnesium stearate held constant at intermediate level.

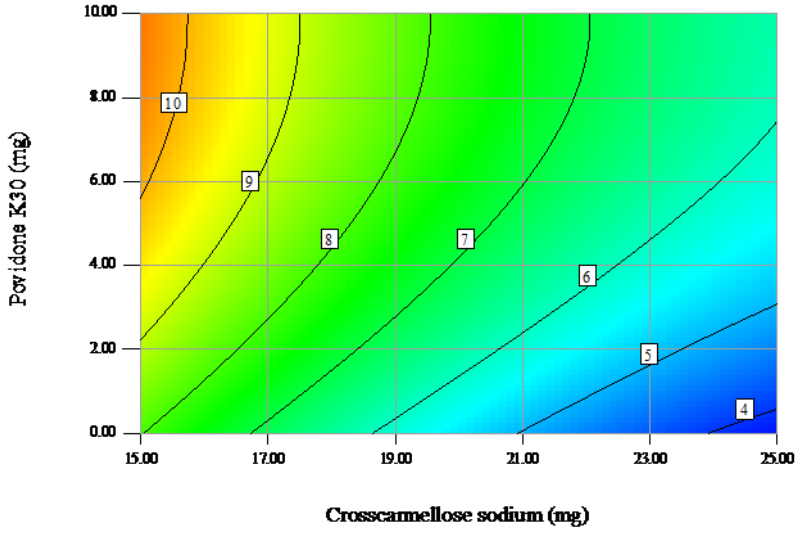

Figure 5.6 Contour plot showing the relationship between CCS, PVP-K30 and D_t at intermediate levels of magnesium stearate

A variation in the content levels of magnesium stearate and PVP-K30 has a relatively minor effect on the D_t when the concentration of CCS is held constant at intermediate levels, as shown in Figure 5.7.

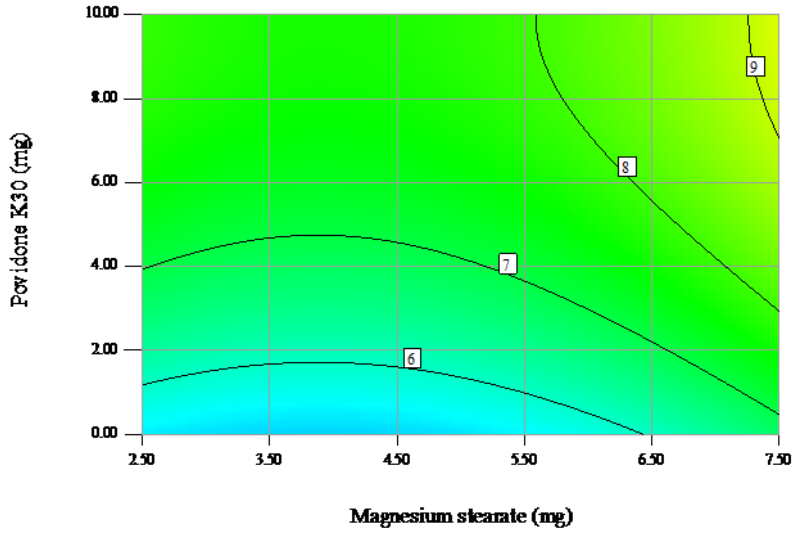

Figure 5.7 Contour plot showing the relationship between PVP-K30, magnesium stearate and disintegration time at intermediate levels of CCS

Tablets with a long D_t, *viz.* 9 min, are produced when the content of magnesium stearate and PVP-K30 are at high levels, *viz.* 7.5 mg and 10.0 mg respectively. However a reduction in the content of both PVP-K30 and magnesium stearate to lower levels results in a relatively minor decrease in D_t to 6 min. The long D_t observed at high levels of magnesium stearate and PVP-K30 may be attributed to increased hydrophobicity and formation of a viscous film that reduce wetability of the resultant tablets [136,286].

5.3.4.3 In vitro release of tablets manufactured using a Box-Behnken design

For ease of determination of the quantitative and qualitative effects of factor on drug release, the Q_{10} for MTZ and RTD from formulations manufactured with different levels of input factors were compared with those from formulations manufactured with intermediate levels of excipient composition, *i.e.* the centre formulations. The notation used to depict the formulations uses the ratios of CCS:PVP-K30:magnesium stearate and this convention has been adopted for the following discussion. By way of example, the centre point formulation is denoted 40:10:10.

5.3.4.4 In vitro release of formulations with low levels of factors

The effect of low levels of CCS, PVP-K30 and magnesium stearate in different ratios on the dissolution of MTZ and RTD are depicted in Figure 5.8 and Figure 5.9 respectively.

5.3.4.4.1 In vitro release of metronidazole

The centre formulation exhibited 71% release within 10 min for MTZ and 100% of the compound is released within 20 min of the commencement of dissolution testing as shown in Figure 5.8.

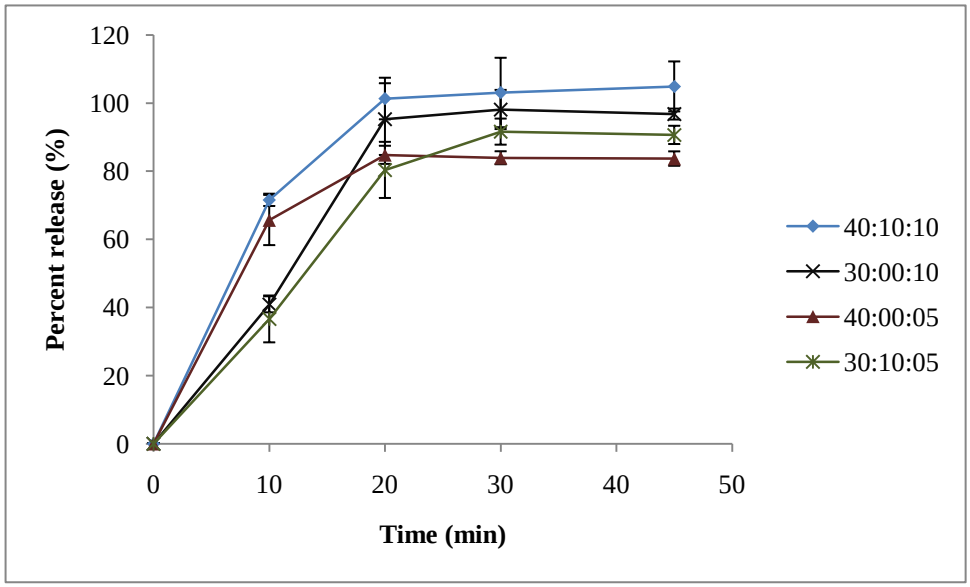

Figure 5.8 *In vitro* release profiles of MTZ for formulations that contain CCS, PVP-K30 and magnesium stearate at lower levels of composition compared to the centre formulation

A reduction in the levels of CCS and the exclusion of PVP-K30 in formulation 30:00:10 resulted in a significant effect on the Q_{10} for MTZ, *viz.* 40% released, however the total amount of MTZ released was unaffected. Formulation 40:00:05 exhibited a relatively minor decrease in Q_{10} for MTZ, *viz.* 65%, when PVP-K30 was excluded and magnesium stearate was included at low levels, however the overall amount of MTZ released was unaffected with 84% MTZ released after 45 min of test. A reduction in CCS and magnesium stearate to minimum levels, *viz.* formulation 30:10:05 resulted in a dramatic reduction in the Q_{10} for MTZ to 36%, however approximately 100% MTZ was released within 20 min of commencing dissolution testing. It is evident that the Q_{10} for MTZ is dependent on the content of CCS. Furthermore the exclusion of PVP-K30 and the use of low levels of

magnesium stearate have a relatively minor effect on the release of MTZ as evidenced by the changes in Q_{10}.

5.3.4.4.2 In vitro release of ranitdine

Similarly to the release of MTZ, the centre formulation exhibited a burst release of RTD with a Q_{10} for the drug of 67% and 89% drug release within 20 min of commencement of dissolution testing as shown in Figure 5.9. The exclusion of PVP-K30 and the reduction of CCS to a lower level in formulation 30:00:10 resulted in a decrease in Q_{10} for RTD to 50%.

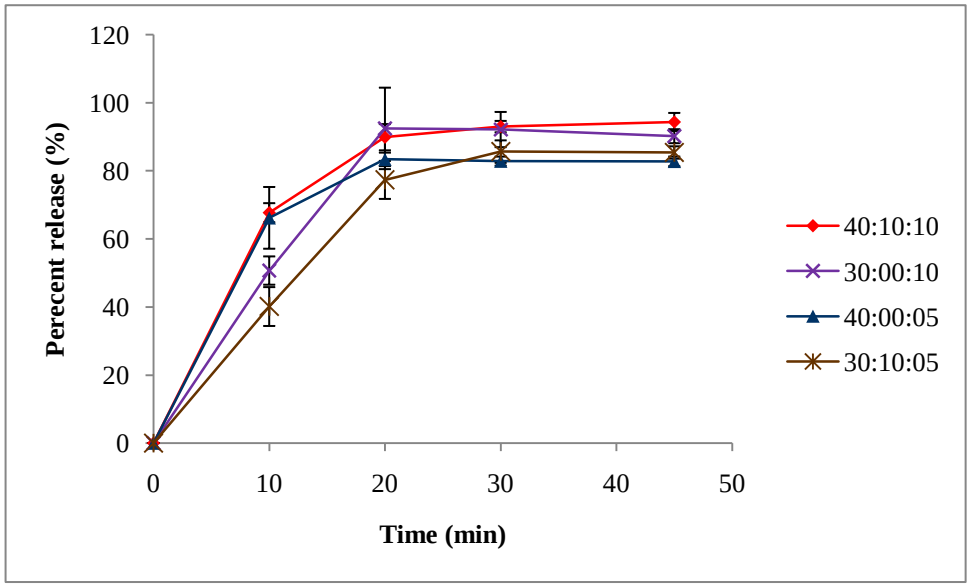

Figure 5.9 *In vitro* release profile of RTD for formulations that contain CCS, PVP-K30 and magnesium stearate at lower levels of composition compared with centre formulation

However, the total drug released was unaffected since 92% RTD was released within 20 min. The reduction of magnesium stearate to 2.5 mg per tablet and the exclusion of PVP-K30 in formulation 40:00:05 had a relatively minor effect on the Q_{10} for RTD compared to that observed for the centre formulation. Formulations 40:00:05 exhibited a Q_{10} of 66% for RTD and 83% of RTD was released within 20 min of commencement of the test. The reduction of both CCS and magnesium stearate to low levels, *viz.* 15 mg and 2.5 mg respectively, in formulation 30:10:05 resulted in a significant reduction in the initial amount of RTD released. Low levels of CCS and magnesium stearate in formulation 30:10:05 resulted in a Q_{10} of 40% for RTD and an almost two fold increase in the extent of drug released to a value of 77% after 20 min compared to the Q_{10}, and 85% release was achieved with 30 min of commencement of the dissolution test. Therefore it is clear that the dissolution of RTD is dependent on the concentration of CCS in the formulation. Furthermore magnesium stearate

and PVP-K30 exhibited relatively minor effects on the dissolution of RTD compared to that observed for the centre formulation. However at low levels of CCS, *viz.* 15 mg, in formulations 30:00:10 and 30:10:05 the dissolution profiles suggest that PVP-K30 has a greater retardation effect on the dissolution of RTD compared to the effect observed for magnesium stearate when using this Q_{10} approach to evaluate the data.

5.3.4.5 In vitro drug release of formulations with high levels of factors

The effects of high levels of CCS, PVP-K30 and magnesium stearate on the release of MTZ and RTD are depicted in Figures 5.10 and Figure 5.11 respectively.

5.3.4.5.1 In vitro release of metronidazole

Formulation 50:20:10 in which high concentrations of CCS and PVP-K30 were used exhibited a burst release for MTZ with the resultant Q_{10} of 82% and 97% of MTZ released after 20 min as shown in Figure 5.10. High concentrations of CCS and magnesium stearate, *viz.* 50:10:15, had a relatively minor effect on the Q_{10} for MTZ compared to that observed for the centre formulation. In contrast, increasing the PVP-K30 and magnesium stearate content of the tablet to 10 mg and 7.5 mg respectively, *viz.* formulation 40:20:15, resulted in a decrease in Q_{10} for MTZ by a factor of 1.5 (46%) when compared to 71% for the centre formulation.

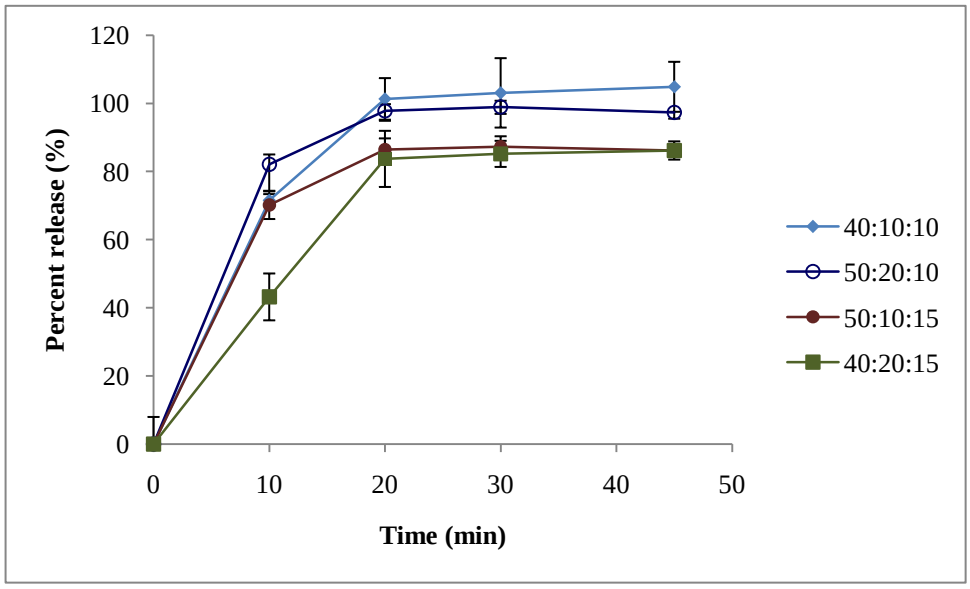

Figure 5.10 *In vitro* release profile of MTZ for formulations that contain CCS, PVP-K30 and magnesium stearate at high levels of composition compared with centre formulation

It is apparent that the Q_{10} for MTZ is dependent on the amount of CCS used in the formulation. Moreover the effects of PVP-K30 and magnesium stearate on the Q_{10} of MTZ are also dependent on the CCS content. At high concentrations of CCS, *viz.* 25 mg per tablet, variations in the amount of PVP-K30, *viz.* formulation 50:20:10, and magnesium stearate, *viz.* formulation 50:10:15, exert relatively minor effects on the Q_{10} of MTZ. When the content of CCS is held constant at 20 mg per tablet, *viz.* formulation 40:20:15, an increase in the PVP-K30 and magnesium stearate content results in a significant decrease for the Q_{10} of MTZ. The effect of varying the amount of binder on dissolution at constant levels of disintegrant has been reported [309]. The decrease in the value for Q_{10} observed following an increase in the content of PVP-K30 and magnesium stearate may be ascribed to the effect of a combination of factors, *viz.* formation of viscous film and hydrophobic film formation respectively. The inclusion of a high concentration of binder in a formulation may result in a formation of a viscous film on the surface of the tablet, with a consequent retardation in dissolution of the API [310].

5.3.4.5.2 In vitro release of ranitidine

The *in vitro* dissolution profile of formulation 50:20:10 which is comprised of high amounts of CCS and PVP-K30, *viz.*25 and 10 mg per tablet respectively, is depicted in Figure 5.11 and reveals a Q_{10} of 62% for RTD and a total of 86% release was observed within 20 min of commencement of dissolution testing. A similar profile was also observed for formulation 50:10:15 in which an increase in the content of CCS and magnesium stearate resulted in a Q_{10} of 72% and 90% of RTD was released within 20 min of commencement of the test. It is apparent that intermediate levels of PVP-K30, *viz.* 5 mg per tablet, and high levels of magnesium stearate and CCS facilitate the release of RTD. This observation indicates that a possible synergistic interaction between CCS and magnesium stearate exists which promotes the release of RTD. In contrast an increase in the content of magnesium stearate and PVP-K30 and constant level of CCS, *viz.* formulation 40:20:15, results in the opposite effect being observed. The Q_{10} for RTD was reduced to 40% compared to that of 67% observed for the centre formulation. The low Q_{10} of 40% observed may be attributed to the high content of PVP-K30 and magnesium stearate as has been discussed [310,311].

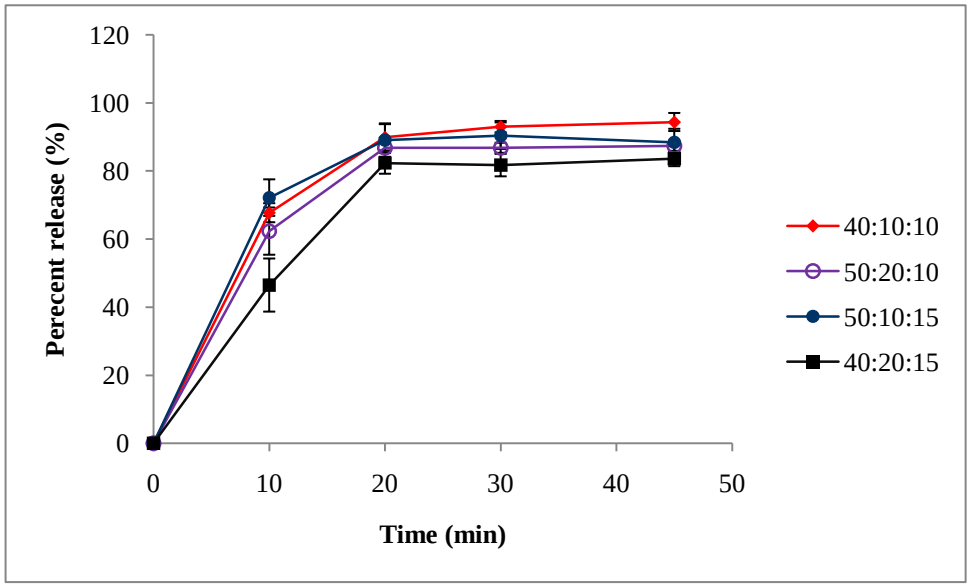

Figure 5.11 *In vitro* release profile of RTD for formulations that contain CCS, PVP-K30 and magnesium stearate at high levels of composition compared with centre formulation

It is apparent that the overall Q_{10} for formulations that contain high and low amounts of CCS are similar, which suggests that CCS has a significant impact on the rate of drug release from these dosage forms. Further the impact of PVP-K30 and magnesium stearate on drug release is dependent on the content of CCS, which validates the fact that CCS is an important formulation factor that determines the rate of drug release. However the relationship between the factors and their levels in their impact on the rate of drug release is complex and involves some degree of interaction, as shown for formulation 50:10:15 depicted in Figure 5.11. The use of RSM may be valuable to investigate and explore the nature of this relationship and its potential impact on the release of MTZ and RTD.

5.3.5 Response surface modelling

The Q_{10} for MTZ and RTD are best described by use of a quadratic equation. The polynomial models used for the investigation of the relationship between the input factors and *in vitro* release profiles of MTZ and RTD are summarized in Equations 5.5 and 5.6.

$$y_2 = 72 + 22.94x_1 - 5.98x_2 - 3.88x_3 - 9.72x_1^2 - 4.76x_2^2 - 10.83x_3^2 \quad \textbf{Equation 5.5}$$

$$y_3 = 65.16 + 14.78x_1 - 7.64x_2 - 1.17x_3 + 5.16x_1x_3 - 8.65x_1^2 - 6.19x_3^2 \quad \textbf{Equation 5.6}$$

Where,

x_1= CCS
x_2= PVP-K30
x_3= Magnesium stearate
y_2= Q_{10} of MTZ
y_3= Q_{10} of RTD

Coefficients with more than one factor represent an interaction between factors and coefficients with second order terms are indicative of the quadratic nature of that relationship and are used to simulate the curvature of the design space of the sample.

From Equation 5.5 it is evident that CCS has synergistic effect on the release of MTZ whereas PVP-K30 and magnesium stearate have an opposite effect. These results are supported by the *in vitro* release profiles depicted in Figures 5.8 and 5.10. Similar results were also observed following an investigation into the effect of disintegrant, filler ratio and lubricant levels on the *in vitro* release of propranolol hydrochloride [289].

Similarly CCS has a synergistic effect on the release of RTD whereas PVP-K30 and magnesium stearate have an antagonistic effect as described by Equation 5.6. Furthermore, CCS and magnesium stearate exhibit a synergistic interaction on the release of RTD, as can be seen from the positive value of the coefficient for this factor.

The impact of independent factors, *viz.* CCS, PVP-K30 and magnesium stearate, at different levels on the *in vitro* release rate of MTZ and RTD is shown on contour and three-dimensional response surface plots in Figures 5.12-5.18 and 5.19-5.21 respectively.

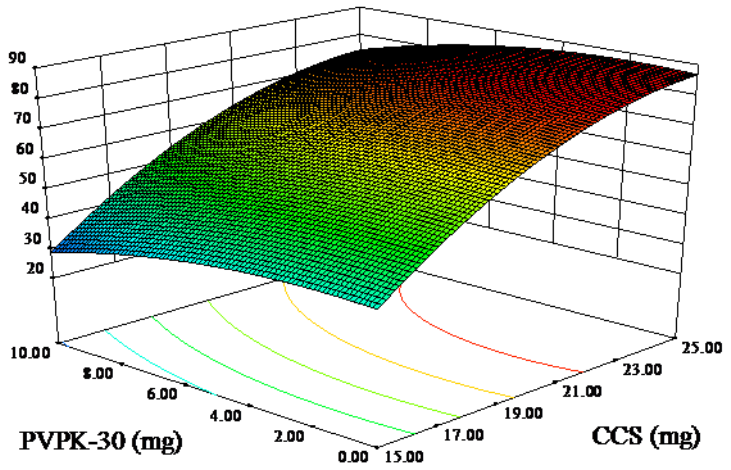

Figure 5.12 A three-dimensional response surface plot showing the impact of CCS and PVP-K30 on Q_{10} of MTZ at intermediate levels of magnesium stearate

The three-dimensional response surface plot in Figure 5.12 reveals that the highest Q_{10} for MTZ ≥80% is achieved when the levels of CCS are high and those for PVP-K30 are between a low and intermediate level. In addition ≥80% of MTZ is released when the amount of CCS and PVP-K30 per tablet are >21 mg and <8 mg respectively. However, it is evident that the antagonistic effect of PVP-K30 in the attainment of a Q_{10} of ≥80% for MTZ is achieved when the content of PVP-K30 per tablet is >8 mg at which point an increase in the content of CCS to maximum levels of 25 mg per tablet resulted in <80% drug release. A similar antagonistic effect was also observed when the amount of CCS per tablet was >15<21 mg and a decrease in the Q_{10} for MTZ was exhibited when the content of PVP-K30 was >8 mg per tablet as seen in response surface plot in Figure 5.13. Therefore it may be concluded that the high Q_{10} of ≥80% for MTZ may be achieved when the amount of CCS and PVP-K30 per tablet is >23 mg and <6 mg respectively and when an intermediate level of magnesium stearate is included in the formulation.

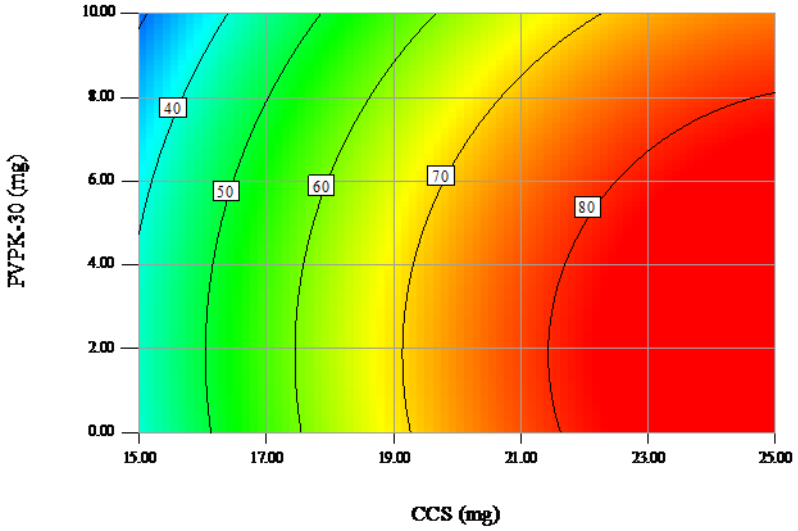

Figure 5.13 Contour response surface plot showing the impact of CCS and PVP-K30 on Q_{10} of MTZ at intermediate levels of magnesium stearate

In general the impact of magnesium stearate and PVP-K30 on the Q_{10} for MTZ is minor in comparison to that of CCS, as can be seen in Figure 5.14. It is clear that both factors have an antagonistic effect on drug release and an increase in the amount of either factor resulted in a decrease in the value of Q_{10} for MTZ. This effect is apparent when the amount of PVP-K30 is > 6 mg per tablet and may in part be attributed to the high hydrophilicity of MTZ which would require high concentrations of PVP-K30 to retard drug release by creating a viscous film on the tablet surface. A Q_{10} of ≥70% for MTZ is achieved when the content of magnesium stearate per tablet is >2.5<6.5 mg and that of PVP-K30 is <6 mg with CCS at an intermediate of 20 mg per tablet.

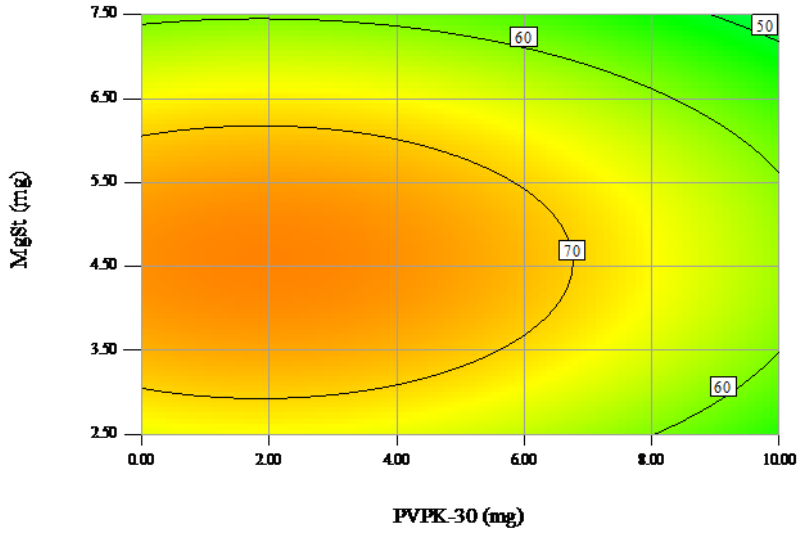

Figure 5.14 Contour response surface plot depicting the impact of magnesium stearate and PVP-K30 on Q_{10} of MTZ at intermediate levels of CCS

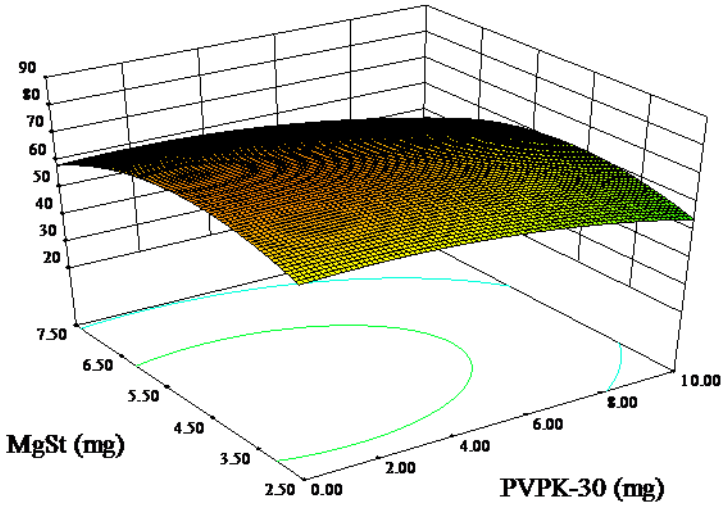

Figure 5.15 A three-dimensional response surface plot depicting the impact of magnesium stearate and PVP-K30 on Q_{10} of MTZ at intermediate levels of CCS

It evident that magnesium stearate exhibits an antagonistic effect similar to the effects observed with PVP-K30 on the dissolution of MTZ as shown in Figures 5.14 and 5.15. However this effect is marked when the content of magnesium stearate per tablet is > 5.5 mg. These results are supported by the *in vitro* release profile of formulation 40:20:15 depicted in Figure 5.10. The decrease in drug release observed at concentrations of magnesium stearate > 5% w/w can be ascribed to the high degree of hydrophilicity of MTZ, whereby high levels

of magnesium stearate are required to create an hydrophobic film that retards drug dissolution.

It evident that an increase in the levels of CCS resulted in an increase in drug release, however a high Q_{10} of ≥80 for MTZ was observed when the content of CCS and magnesium stearate per tablet was >22 mg and <6.5 mg respectively as shown in the response surface plots in Figures 5.16 and 5.17.

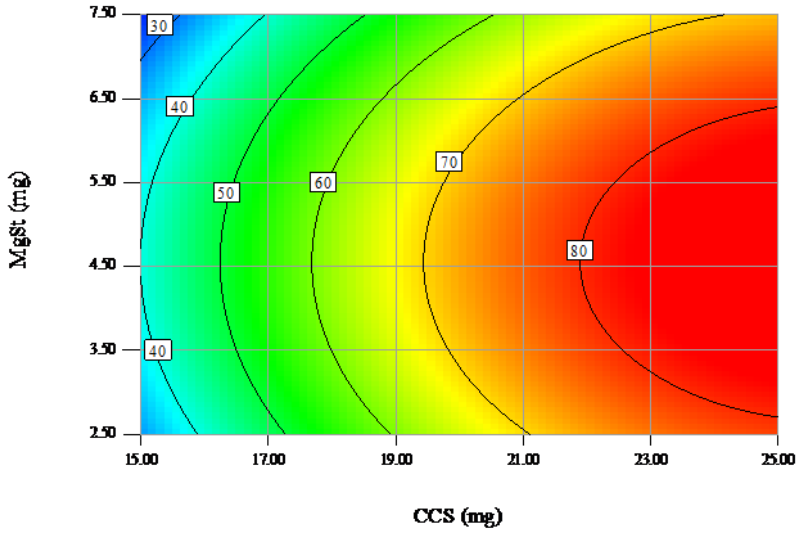

Figure 5.16 Contour response surface plot of the impact of magnesium stearate and CCS on the Q_{10} of MTZ at intermediate levels of PVP-K30

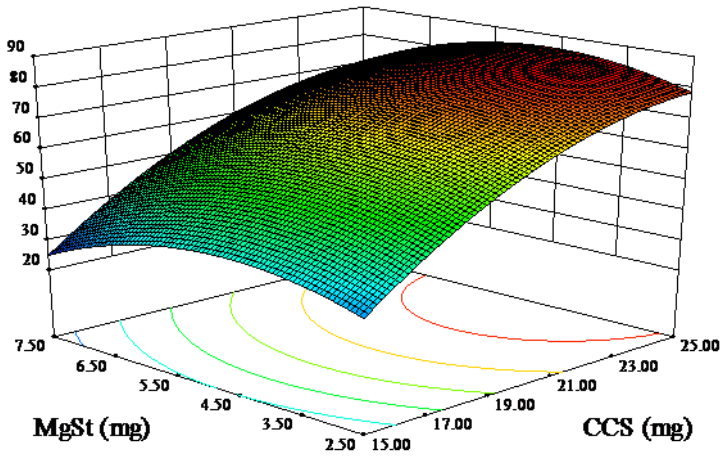

Figure 5.17 A three-dimensional response surface plot showing the impact of magnesium stearate and CCS on Q_{10} of MTZ at intermediate levels of PVP-K30

The three-dimensional response surface plot for the Q_{10} for RTD depicted in Figure 5.18 is curvilinear in nature for the relationship of this parameter with the CCS input factor, whereas a linear relationship is observed for PVP-K30. As with the MTZ formulations it is clear that CCS has a profound effect on the release of RTD and it is clearly evident that an increase in the content of CCS results in an increase in the value of Q_{10} for RTD, and where there is a decrease in CCS concentration the converse is true. In contrast PVP-K30 appears to exert an antagonistic effect on the value for Q_{10} for RTD and the impact is greater when the amount of CCS per tablet is <17 mg per tablet. At low levels of CCS the D_t of the tablets is increased as a consequence of the low content of CCS [312]. The increase in D_t, of the tablets results in a lower Q_{10} value for RTD since the total surface area necessary for dissolution is smaller and therefore the impact of PVP-K30 on D_t is more apparent. The response surface plot depicted in Figure 5.19 shows that a high Q_{10} value of ≥78 is achieved when the amount of CCS is >23 mg per tablet and when PVP-K30 is omitted from the tablet formulation and intermediate levels of magnesium stearate are used.

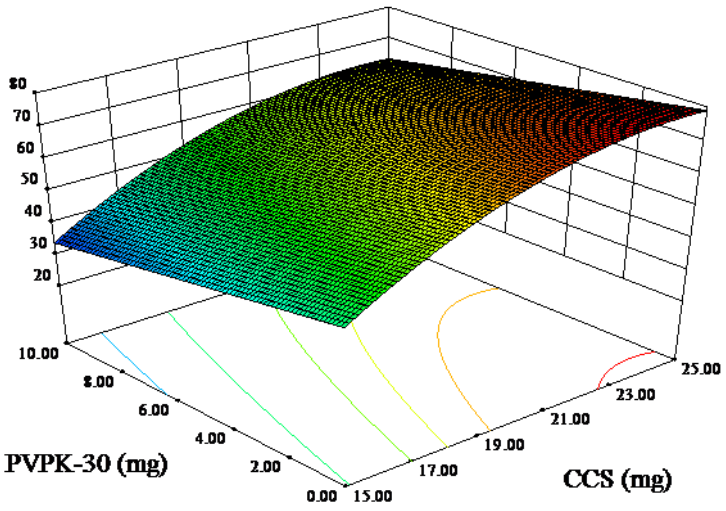

Figure 5.18 A three-dimensional response surface plot showing the impact of PVP-K30 and CCS on the Q_{10} of RTD at intermediate levels of magnesium stearate

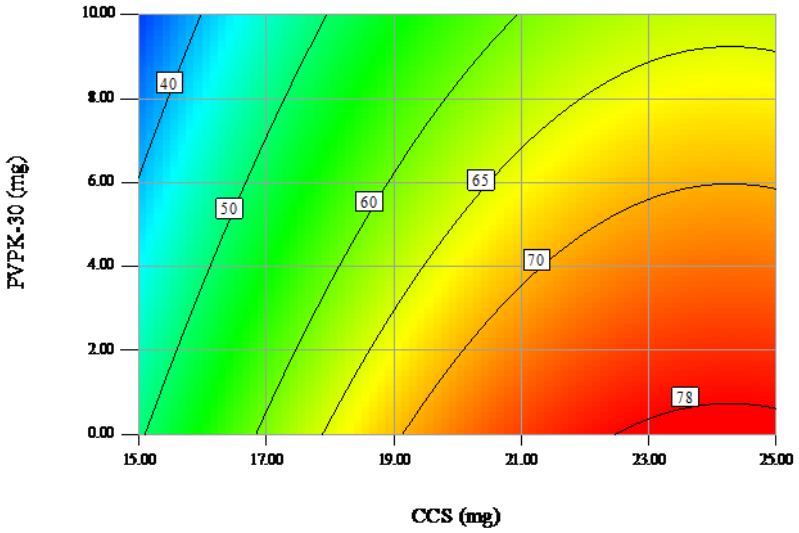

Figure 5.19 Contour response surface plot showing the impact of PVP-K30 and CCS on the Q_{10} of RTD at intermediate levels of magnesium stearate

In contrast to the effect of magnesium stearate on the value of Q_{10} for MTZ, different results are observed when evaluating the Q_{10} value for RTD. A curvilinear relationship is exhibited for the effect of CCS and magnesium stearate on the Q_{10} of RTD and a region corresponding to maximum value for $Q_{10} \geq 70\%$ is located between intermediate levels of magnesium stearate and high levels of CCS, as depicted in Figure 5.20. These results suggest that a synergistic interaction exists between CCS and magnesium stearate at these levels, *viz.* ≥ 23 mg per tablet and $\geq 4.5 \leq 6.5$ mg per tablet respectively, as shown in Figure 5.21. Although this synergistic interaction has not been reported, the results are in agreement with those reported by Wang *et al*. [236] after an investigation of drug and excipient interaction with lubricants. Close inspection of the *in vitro* release profile for formulation 50:10:15 as shown in Figure 5.11 and evaluation of the resultant model equation for parameter y_3 shows that a synergistic interaction between CCS and magnesium stearate is clearly evident.

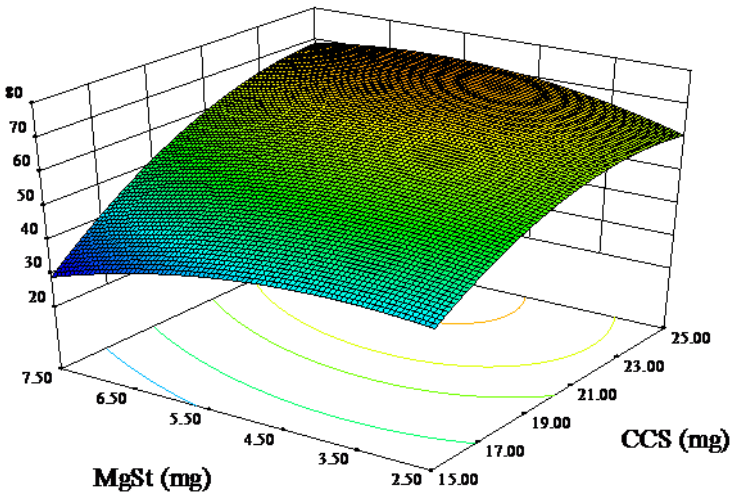

Figure 5.20 A three-dimensional response surface plots of the impact of magnesium stearate and CCS on the Q_{10} of RTD at intermediate levels of PVP-K30

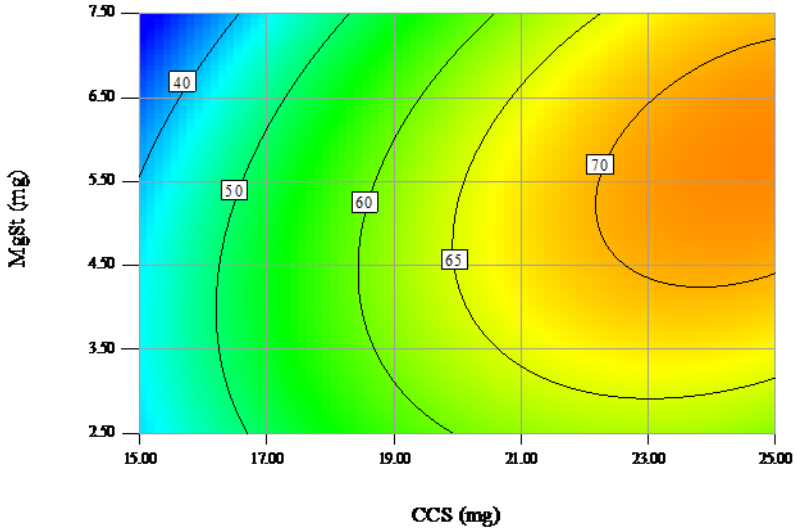

Figure 5.21 Contour response surface plot of the impact of magnesium stearate and CCS on the Q_{10} of RTD at intermediate levels of PVP-K30

The response surface plot depicted in Figure 5.22 reveals a linear antagonistic relationship between PVP-K30 and magnesium stearate on the Q_{10} value for RTD. It is clear that PVP-K30 exerts a greater effect on the Q_{10} value than magnesium stearate and consequently the Q_{10} value is not affected with an increase in the levels of magnesium stearate in the formulation. The effect of magnesium stearate is more apparent at low levels of PVP-K30,

viz. < 2 mg per tablet, as indicated by a Q_{10} of < 70% for RTD when the amount of lubricant per tablet is ≥ 6.5 mg and where intermediate levels of CCS are used as shown in Figure 5.23.

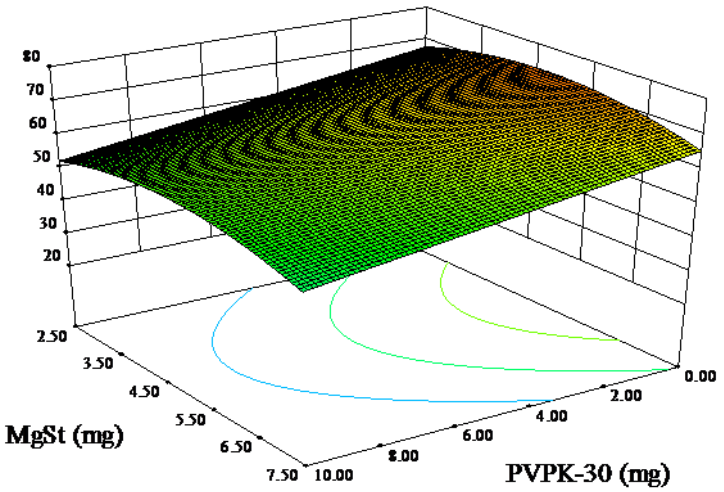

Figure 5.22 Athree-dimensional response surface plot depicting the impact of PVP-K30 and magnesium stearate on the Q_{10} for RTD at intermediate levels of CCS

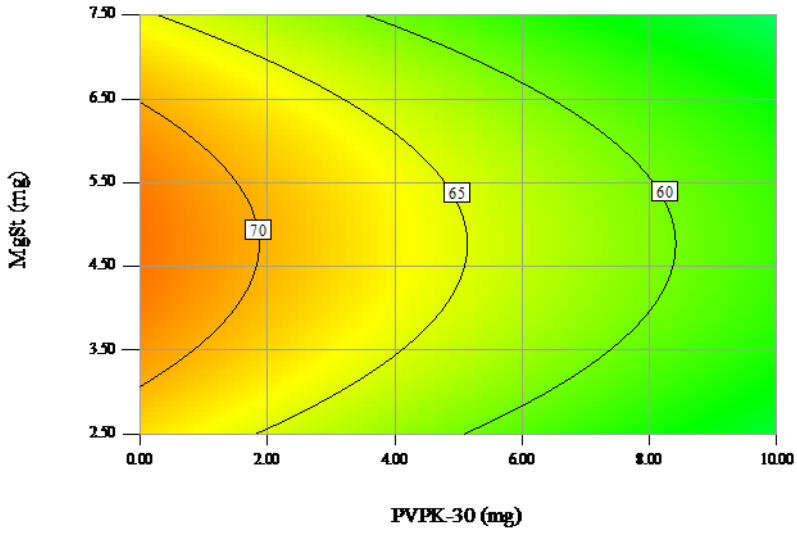

Figure 5.23 Contour response surface plot showing the impact of PVP-K30 and magnesium stearate on the Q_{10} for RTD at intermediate levels of CCS

5.3.6 Formulation optimization

A numerical optimization technique using the desirability approach was used for the development of a new formulation that would ensure the desired responses were achieved. The constraints set for the designated responses are described in Table 5.2 in § 5.2.3.1 The predicted response values and respective factor compositions are summarized in Table 5.6.

Table 5.6 Predicted values for input variables and the respective response variables

Factor composition (mg)			**Response**			**Desirability**
x_1	x_2	x_3	y_1	y_2	y_3	0.98
25.0	0.0	5.70	3.96 min	84.85%	79.57%	

The physical characteristics of the tablets manufactured using the optimized formulation composition are summarized in Table 5.7.

Table 5.7 Physical characteristics of the resultant tablets manufactured following numerical optimization

Parameter	**Results**
Weight mg	505.25 ± 3.01
Thickness mm	3.40 ± 0.01
Diameter (mm)	12.00 ± 0.00
Crushing strength (N)	92 ± 1.39
Tensile strength (MPa)	1.43
Friability (%)	0.3
Disintegration (min)	3.82 ± 0.36

The tablets that were produced were cream in colour and had a smooth appearance without any evidence of chipping or cracking. The physicochemical and mechanical parameters also comply with general compendial specifications for these variables. Furthermore the Q_{10} values for MTZ and RTD observed in Figure 5.24 are in close agreement with the predicted values for this parameter. The percent error of the prediction (PE) observed for the optimum responses, *viz.* D_t, and the Q_{10} values for MTZ and RTD summarized in Table 5.8, indicate that the mathematical models generated have the necessary accuracy in the estimation of responses since the PE is < 5%.

Table 5.8 Experimental and predicted response values with percent error for prediction for the optimized formulation composition

Response	Experimental value	Predicted value	Percent prediction error
y_1	3.82 ± 0.46	3.96	-3.66
y_2	83.66 ± 5.23	84.85	-1.42
y_3	80.11 ± 4.10	79.57	0.67

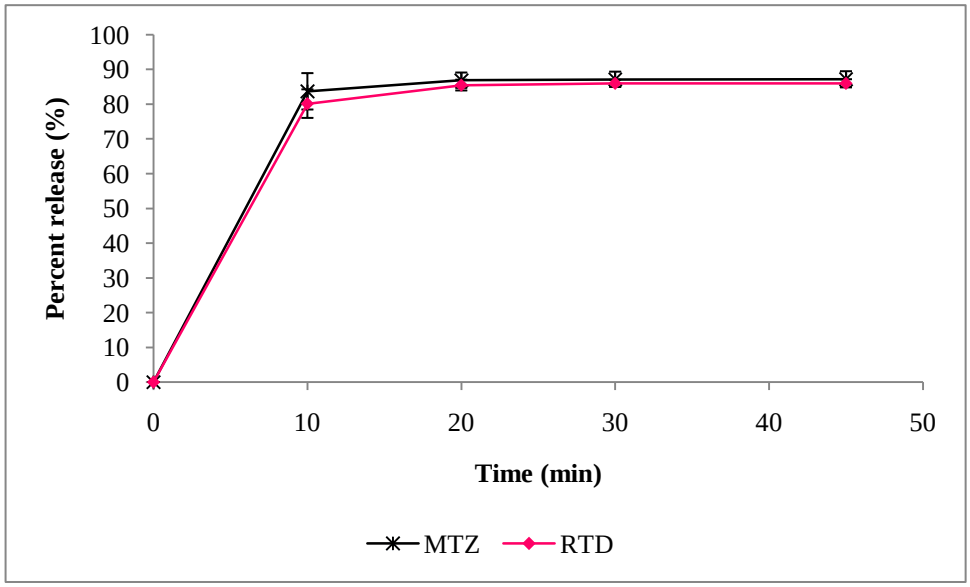

Figure 5.24 *In vitro* release profiles of the tablets manufactured following numerical optimization

5.4 CONCLUSIONS

The impact of viscosity on granulation particle size distribution has been revealed. The use of PVP-K30 at 25% w/v results in the production of granules with wide particle size distribution compared to the use of 12.5% w/v PVP-K30 solution. In addition purified water has a similar impact to the solution comprised of 12.5% w/v PVP-K30 on the granule particle size distribution. Therefore it can be concluded that purified water and PVP-K30 solution at 12.5% w/v have a similar effect on granulation particle size distribution when the conditions described in § 4.2.4.2.3, and the formula in Table 5.1 that is comprised of MCC and CCS are used.

Response surface methodology has many applications in the development and optimization of pharmaceutical systems, including the optimization of formulation, manufacturing processes and analytical methods. However, the application of RSM requires that accurate, precise and reproducible experimental conditions are used for the generation of reliable data.

Therefore the potential wide application of RSM is limited, due to the sensitivity of the technique to experimental variability.

There are several statistical designs of experiment approaches that use RSM and these include but are not limited to Box-Behnken, CCD and D-Optimal designs. A Box-Behnken design was selected for this optimization since fewer experiments are required to generate data for the same number of factors compared to a CCD approach. Furthermore the Box-Behnken approach has specific design points where factors are changed over three levels that facilitate the expansion of the experimental domain, whereas a D-Optimal approach establishes the design points algorithmically. The excipients that were selected as variables for evaluation and their impact on D_t and *in vitro* release of MTZ and RTD were CCS (disintegrant), PVP-K30 (binder) and magnesium stearate (lubricant). Furthermore the experimental domain was selected in accordance with level two formulation and composition changes described in the SUPAC-IR guideline, in order to determine the impact of these factors on the measured responses selected for monitoring.

Three-dimensional and contour response surface plots clearly demonstrated the impact of the different levels of CCS, PVP-K30 and magnesium stearate on the D_t and the *in vitro* release of MTZ and RTD. It is clear from the response surface plots that CCS is the most significant factor that affects the measured responses and that the exclusion of PVP-K30 had no significant impact on tablet crushing strength or friability. Moreover it has been shown that magnesium stearate has a synergistic interaction with CCS, thereby promoting the *in vitro* release of RTD. The use of RSM has facilitated the determination of the impact of level two SUPAC for IR dosage forms on the D_t and Q_{10} values for MTZ and RTD. In addition this approach permitted the identification of significant factors in the formulations under investigation. Furthermore the development of a predicted optimal formulation which subsequently led to the production of tablets with the desired specifications summarized in Table 5.6 has been achieved by the use of RSM.

Therefore the use of RSM has facilitated the assessment of the impact of level two SUPAC changes for IR formulations in a rapid and efficient manner with minimum waste of resources compared to the use of a change of single factor at a time (COST) approach.

CHAPTER SIX
CONCLUSIONS

The oral route of administration is the most convenient route for drug delivery to the body. Although it is widely acceptable to patients, adherence to oral drug therapy becomes a challenge when prolonged use of multiple drug products is required to achieve an optimal therapeutic outcome. The use of FDC has the potential to improve adherence in the management of pathological conditions such as diabetes, hypertension, tuberculosis, heart failure and HIV/AIDS, amongst others, that require long-term therapy and that may use multiple drug products [7,313-316]. FDC have proved effective in reducing the risk of the emergence of drug-resistant strains of causative agents in infectious disease, and have also been shown to reduce the cost of treatment and risk of medication errors [315]. Thus, as with other pathological conditions that require multiple drug agents to achieve therapy, the use of FDC tablets for the management of ulcers may well reduce morbidity and mortality due to the disease and therefore FDC tablets of MTZ and RTD were manufactured for this purpose.

An HPLC method was developed and validated in accordance to ICH guidelines for the simultaneous quantitation of MTZ and RTD [130]. The method was found to be sensitive, accurate, precise and linear over the concentration range 2.5-20 µg/ml and 1-8 µg/ml for MTZ and RTD respectively. The precision and accuracy of the HPLC method was confirmed by use of % RSD and % bias and the results of these parameters were < 5% for both compounds of interest. The HPLC method was also found to be stability-indicating and both MTZ and RTD were well resolved from degradants, using the same chromatographic conditions.

Preformulation studies constitute an integral part of any formulation development process since they form the foundation of building quality into a product [317]. Preformulation studies require a wide scope of investigation of the compound(s) of interest and potential excipients that may be used in a formulation in order to ensure the development of a quality pharmaceutical product that will perform consistently following manufacture and in clinical use. The identification of the polymorphic nature of RTD was achieved by use of DSC and IR spectroscopy. These techniques are accurate and precise and have been used extensively for the identification of the polymorphic nature of many drug compounds. The melting temperature of RTD, determined using DSC, indicated that the raw material compound was

primarily comprised of polymorph 2 and this was confirmed by evaluation of the IR spectrum of this material. Thermal gravimetric analysis of MTZ and RTD indicated that both compounds exhibited thermal stability following heating to temperatures of approximately 169°C and 143°C respectively.

The use of MCC and/or DCP as diluents in tablet formulations is common, since their intrinsic physicochemical characteristics facilitate the tablet manufacturing process. There is a wealth of information with respect to the properties and application of MCC and DCP in the manufacture of SODF and therefore these materials were selected as potential diluents for the manufacture of FDC tablets containing MTZ and RTD. Both compounds, *viz.* MTZ and RTD, exhibited compatibility with MCC when assessed using DSC and IR spectroscopy whereas DCP revealed a potential interaction with MTZ at high temperature, however IR spectroscopy revealed that there was unlikely to be an interaction. Similarly MTZ and RTD exhibited a potential interaction at high temperatures but the interaction was not apparent following IR analysis which indicated that MTZ and RTD could be incorporated into a FDC formulation.

SEM images of the materials revealed that MTZ and RTD exhibited particles that are larger in size when compared to the particle size of MCC and DCP. Therefore, for ease of processing, the materials of both compounds, *viz.* MTZ and RTD, were forced through a sieve of aperture size of 850 μm, in order to narrow the particle size distribution of the powders.

Evaluation of the micromeretic results revealed that direct compression manufacture of the FDC was not feasible. The CI and HR values for both compounds indicated that MTZ and RTD exhibited poor flow and compressibility properties which further indicate that it was necessary to include a diluent in the formulation to facilitate the manufacturing process. MCC and DCP exhibit good flow properties and compressibility and were consequently used in the formulation of FDC tablets. MCC is frequently incorporated in tablet formulations since it confers suitable mechanical strength to tablets, whereas DCP is commonly used in the manufacture of tablets since it imparts suitable flow properties to a formulation.

The suitability of a method of manufacture for a tablet formulation is dependent on the physicochemical properties of the formulation constituents which include thermal stability,

moisture sensitivity, particle size, shape and distribution amongst others. Furthermore the crystal properties of the solid system will also define the suitability of a method of manufacture. FDC tablets of MTZ and RTD were manufactured by direct compression and wet granulation. The tablets produced by direct compression exhibited physico-mechanical properties that did not meet compendial specifications for SODF. The tablets were friable, had a low crushing strength and exhibited capping, whereas those produced by wet granulation had a better appearance and met compendial specifications for SODF. Therefore, a wet granulation method of manufacture was adopted to produce a FDC of RTD and MTZ. In addition the blending process was optimized in order to ensure tablets that contained a uniform dose of both compounds were produced.

Blend homogeneity is one of the critical parameters that ensures therapeutic efficiency of a dosage unit and is usually established through the analysis of multiple samples of a powder blend, sampled from different sites, in blending equipment, following mixing of the materials for different periods of time. The blend uniformity analyses revealed that blend homogeneity was achieved following 9 min of mixing and this was confirmed when the results of content uniformity testing were evaluated.

Optimization of the manufacturing process by use of DOE required the selection of appropriate factors that are known to impart an optimal effect on selected measured response(s). The identification of factors and their combinations is usually achieved in two stages, *viz.* a review of literature and then undertaking screening studies. The information extracted from the literature is used to guide the formulation scientist in the screening process to identify suitable factors and their respective combinations that would be necessary to produce tablets that exhibit the desired response(s). The screening studies revealed that MCC and CCS produced tablets that appeared to have better physico-mechanical properties compared to those that were produced using DCP alone. The Q_{10} for MTZ and RTD from tablets comprised of MCC and CCS, *viz.* formulation RM 013, were 82% and 89% respectively, whereas for formulation RM 014 that was comprised of DCP and CCS the Q_{10} for MTZ and RTD were 55% and 59% respectively. Although formulation RM 014 produced tablets that disintegrated in < 4 min, the Q_{10} values for MTZ and RTD from the tablets of batch RM 013 were used as the criterion for the selection of this formulation composition for the optimization, and evaluation of the impact of level two formulation and composition changes on product performance.

A Box-Behnken statistical design approach was selected to optimize the FDC formulation. The compositions of CCS, PVP-K30 and magnesium stearate were selected as the factors to be varied, in order to establish their impact on the D_t and *in vitro* release of MTZ and RTD from the tablet formulations that were manufactured. Level two formulation and composition changes, described in the SUPAC Guideline for IR, were used to establish the experimental domain. Contour and three-dimensional response surface plots were generated to examine the nature of the relationship between the levels of input factors on the measured responses.

The results of the optimization studies revealed that the responses D_t, the Q_{10} for MTZ and RTD are strongly dependent on the levels of CCS in the formulation. The D_t exhibited an inverse linear relationship with variations in the concentration of CCS whereas the Q_{10} showed a linear agonistic relationship for the same raw material. The effects of PVP-K30 and magnesium stearate on the measured responses were also dependent on the concentration of CCS in the formulation. An increase in the content of PVP-K30 and magnesium stearate resulted in an increase in the D_t when the content of CCS was maintained at low levels. A similar effect was observed for the Q_{10} for MTZ where an increase in the content of PVP-K30 and magnesium stearate resulted in a decrease in the Q_{10} value at low concentrations of CCS, whereas increasing the concentration of CCS revealed that the converse is true. The effect of amount of PVP-K30 on the Q_{10} for RTD was also dependent on the content of CCS in the formulation, where increasing the content of PVP-K30 whilst using low levels of CCS resulted in a decrease in the Q_{10} value for RTD and decreasing the content of PVP-K30 in the formulation had the opposite effect. In contrast magnesium stearate exhibited a synergistic interaction with CCS on the Q_{10} value for RTD. A high value for the Q_{10} for RTD, *viz.* > 70%, was achieved when the amount of CCS and magnesium stearate in the formulation was at high and intermediate levels, respectively.

The numerical optimization technique using the desirability approach was used to predict a formulation composition that would produce tablets that exhibit measured responses values within the predetermined constraints listed in Table 5.2. A formulation composition that included CCS, PVP-K30 and magnesium stearate at concentrations of 25.0, 0.0 and 5.7% w/w respectively was subsequently predicted. The predicted response values were in close agreement with the experimental values with a percent prediction error (PE) of 3.66, 1.42 and 0.67 for the D_t, Q_{10} for MTZ and Q_{10} for RTD, respectively, indicating that the model was accurate for the prediction of the values of measured responses due to the small PE values,

viz. < 5%. In general, the accuracy of a model is usually expressed as the prediction error and a small PE value represents accurately estimated parameter(s) [318].

A FDC of MTZ and RTD has been developed and manufactured by use of wet granulation. The manufacturing process was optimized and the impact of changes in formulation composition on dosage form performance has been evaluated using DOE. In addition RSM was used to optimize the tablet formulation with respect to disintegration and *in vitro* release of MTZ and RTD, and the formulation has the potential to be adapted to commercial manufacture.

Future studies that are essential would include stability testing of the FDC tablets and the development of an alternative formulation that would permit the incorporation of MTZ and RTD in cases where potential incompatibilities between these compounds may exist. Furthermore, investigation of variation of process parameters such as impeller and chopper speed and the rate of binder addition by the use of RSM may be necessary in order to establish their impact on the disintegration and tensile strength of the tablets, and *in vitro* release of MTZ and RTD from the dosage form. Risk assessment studies would be necessary for the investigation of factors *viz.* qualitative and quantitative that may have detrimental effects on the product quality and to facilitate the establishment of a design space in which the quality of the product would be assured and maintained.

APPENDIX 1
BATCH MANUFACTURING RECORDS

Templates of batch manufacturing records used in the manufacture of FDC tablets of MTZ and RTD indicating the quantities of excipients that were used and the procedure that were followed are included in the thesis. The records of all formulation batches that were manufactured are available on request.

Rhodes University
Faculty of Pharmacy
Department of Pharmaceutics
Grahamstown 6140

BATCH MANUFACTURING RECORD

DIRECT COMPRESSION

Product	Ranimetro
Date of manufacture	
Temperature and humidity	
Formulator	King'ori L D
Batch number	RM 001
Batch size	500 g
Target weight	500 mg
Granulating fluid	-

FORMULA

Material	Unit Dose (mg)	Batch (g)	% w/w	Raw Material number
Ranitidine hydrochloride	84.0	84.0	16.8	RM 000244
Metronidazole	250.0	250.0	50.0	RM 000247
Microcrystalline cellulose pH 102	140.0	140.0	28.0	X061882
Sodium starch glycolate	20.0	20.0	4.0	X070074
Povidone K30	-	-	-	X062448
Colloidal silicone dioxide	1.0	1.0	0.2	X069339
Magnesium Stearate	5.0	5.0	1.0	X052015
TOTAL WEIGHT	**500.0**	**500.0**	**100**	

EQUIPMENT VERIFICATION

Description	Type	Verified By	Confirmed
Balance	Mettler Model PM 4600		
Sieves	DIN 4418		
Blender	Saral® 3.5 L		
Tablet Press	Manesty® B3B		
Tooling	12.00 mm flat faced punches		
Oven	Memmert®		

MANUFACTURING DIRECTIONS

Step	Procedure	Equipment	Settings	Done by	Checked by
1	Separately weigh the material and screen through a 850 µm sieve Ranitidine hydrochloride Metronidazole Microcrystalline cellulose Sodium starch glycolate	Mettler Model PM 4600 Sieve type DIN 4I88	Unit (g)		
2	Place the material in (1) in a high-shear mixer granulator and blend for 9 min.	Saral® high-shear mixer granulator	Impeller speed 100 rpm Chopper speed 0 rpm		
3	Weigh and screen the following material separately through a 315 µm sieve Colloidal silicone dioxide Magnesium stearate	Sieve Type DIN 4188			
4	Mix blends (1) and (3) in the high-shear mixer granulator for3 min.	Saral® high shear mixer granulator	Impeller speed 100 rpm Chopper speed 0 rpm		
5	Discharge the blend (4) in a tarred stainless steel bowl and weigh the blend	Mettler Model PM 4600	Unit (g)		
6	Compress the blend in (5) into 500mg tablets. Sample 5 tablets every 90 s and record the weight, and hardness	Mansety®B3B Mettler Model PM 4600 Pharmatest PTB 311E	Speed 25rpm Target hardness 80-120 N Weight (mg)		

OBSERVATION AND DEVIATIONS

Rhodes University
Faculty of Pharmacy
Department of Pharmaceutics
Grahamstown 6140

BATCH MANUFACTURING RECORD

WET GRANULATION

Product	Ranimetro
Date of manufacture	
Temperature and humidity	
Formulator	King'ori L D
Batch number	RM 002
Batch size	500 g
Target weight	500 mg
Granulating fluid	12.5% w/v Povidone K30 solution

FORMULA

Material	Unit Dose (mg)	Batch (g)	% w/w	Raw Material number
Ranitidine hydrochloride	84.0	84.0	16.8	RM 000244
Metronidazole	250.0	250.0	50.0	RM 000247
Microcrystalline cellulose pH 102	135.0	135.0	27.0	X061882
Sodium starch glycolate	20.0	20.0	4.0	X070074
Povidone K30	5.0	5.0	1.0	X062448
Colloidal silicone dioxide	1.0	1.0	0.2	X069339
Magnesium Stearate	5.0	5.0	1.0	X052015
TOTAL WEIGHT	**500.0**	**500.0**	**100**	

EQUIPMENT VERIFICATION

Description	Type	Verified By	Confirmed
Balance	Mettler Model PM 4600		
Sieves	DIN 4418		
Blender	Saral® 3.5 L		
Tablet Press	Manesty® B3B		
Tooling	12.00 mm flat faced punches		
Oven	Memmert®		

MANUFACTURING DIRECTIONS

Step	Procedure	Equipment	Settings	Done by	Checked by
1	Separately weigh the material and screen through a 850 µm sieve Ranitidine hydrochloride Metronidazole Microcrystalline cellulose Sodium starch glycolate	Mettler Model PM 4600 Sieve type DIN 4I88	Unit (g)		
2	Place the material in (1) and 50% of the disintegrant in a high-shear mixer granulator and blend for 9 min.	Saral® high-shear mixer granulator	Impeller speed 100 rpm Chopper speed 0 rpm		
3	Weigh and screen the following material separately through a 315 µm sieve Colloidal silicone dioxide Magnesium stearate	Sieve Type DIN 4188			
4	Granulate the blend in (2) with a Povidone K30 binder solution	Saral® high shear mixer granulator Cole- Palmer® Peristaltic pump	Impeller speed 100 rpm Chopper speed 1000 rpm Pump speed 25 rpm Air pressure 52 PSI		
5	After the addition of the binder solution continue mixing the wet granules in (4) for an additional minute	Saral® high shear mixer granulator	Impeller speed 100 rpm Chopper speed 1000 rpm		
6	Dry the wet granules in (5) in a dry heat oven	Memmert®	Temperature 50°C Time 24 h		
7	Pass the dry granules through a 350 µm sieve and add the granules in the blender and mix for 3 min with the balance of the disintegrant and the lubricants in (3)	Sieve Type DIN 4188 Saral ® high shear mixer granulator	Impeller speed 100 rpm Chopper speed 0 rpm		
8	Compress the blend in (9) into 500 mg tablets. Sample 5 tablets every 90 s and record the weight, and hardness	Mansety®B3B Mettler Model PM 4600 Pharmatest PTB 311E	Speed 25 rpm, Target hardness 80-120 N Weight (mg)		

OBSERVATION AND DEVIATIONS

APPENDIX 2

RESPONSE SURFACE METHODOLOGY STATISTICS

DISINTEGRATION

Table 7.1 Model fit comparison for disintegration of tablets

Model	PRESS
Linear	12.99
Quadratic	6.5

Table 7.2 Backwards elimination results quadratic model for tablet disintegration

Factor	Coefficient	Standard deviation	p value	Significance
Intercept	7.21	0.29	0.0013	Significant
x_1- CCS	-2.15	0.18	< 0.0001	Significant
x_2- PVP-K30	1.21	0.18	0.0011	Significant
x_3- Magnesium stearate	0.66	0.18	0.0144	Significant
x_1x_2	0.30	0.20	0.2900	Not significant
x_1x_3	-5×10^{-003}	0.25	0.9850	Not significant
x_2x_3	-0.11	0.25	0.6759	Not significant
x_1^2	0.5	0.26	0.1174	Not significant
x_2^2	-0.62	0.26	0.0660	Not significant
x_3^2	0.74	0.26	0.0385	Significant

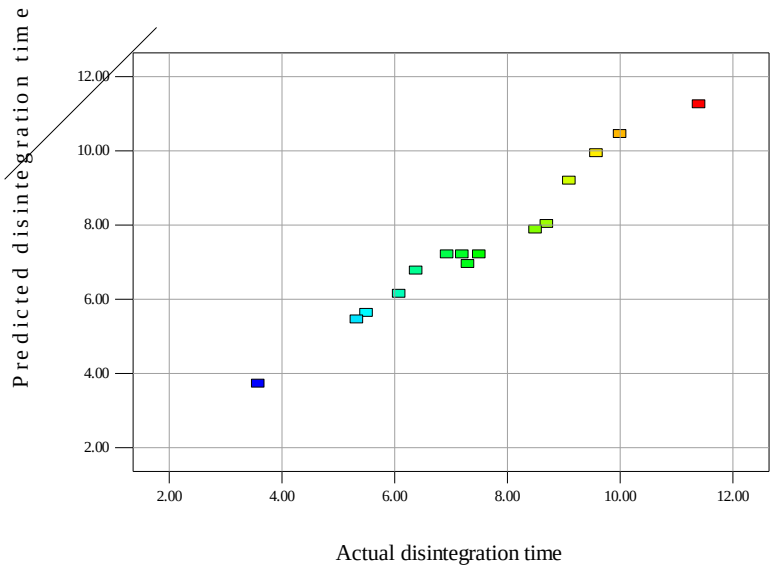

Figure 7.1 Predicted vs. Actual diagnostic plot for D_t.

Q_{10} FOR MTZ

Table 7.3 Model fit comparison for *in-vitro* release of MTZ

Model	PRESS
Linear	1463.31
Quadratic	682.17

Table 7.4 Backward elimination results quadratic model for the Q_{10} value for MTZ

Factor	Coefficient	Standard deviation	p value	Significance
Intercept	72.35	2.73	< 0.0001	Significant
x_1- CCS	22.94	1.67	< 0.0001	Significant
x_2- PVP-K30	-5.98	1.67	0.0073	Significant
x_3- Magnesium stearate	-3.88	1.67	0.0491	Significant
x_1x_2	3.62	2.18	0.1579	Not significant
x_1x_3	1.58	2.18	0.5014	Not significant
x_2x_3	-2.37	2.18	0.3271	Not significant
x_1^2	-9.72	2.46	0.0043	Significant
x_2^2	-4.76	2.27	0.0894	Not significant
x_3^2	-10.83	2.46	0.0023	Significant

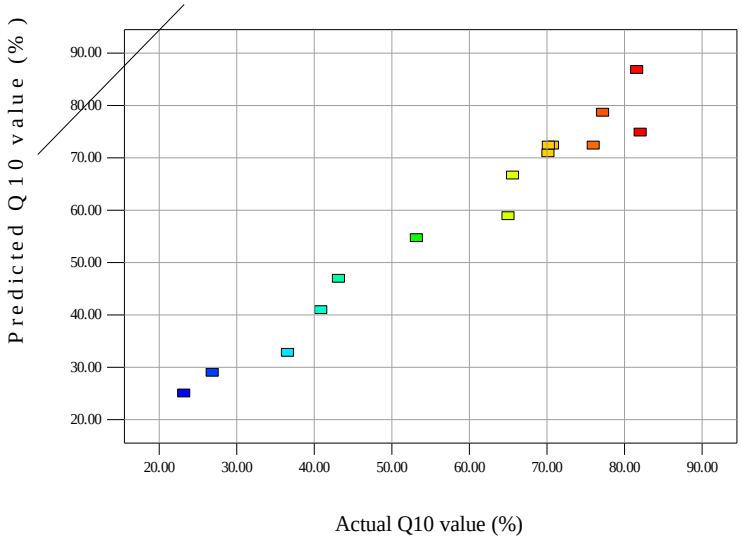

Figure 7.2 Predicted vs. Actual diagnostic plot for the Q_{10} value of MTZ.

Q_{10} FOR RTD

Table 7.5 Model fit comparison for *in vitro* release for RTD

Model	PRESS
Linear	1000.83
Quadratic	367.24

Table 7.6 Backward elimination results quadratic model for the Q_{10} value for RTD

Factor	Coefficient	Standard deviation	p value	Significance
Intercept	65.16	1.56	< 0.0001	Significant
x_1- CCS	14.78	1.15	< 0.0001	Significant
x_2- PVP-K30	-7.64	1.15	0.0002	Significant
x_3- Magnesium stearate	-1.17	1.15	0.3381	Not significant
x_1x_2	0.66	1.72	0.7195	Not significant
x_1x_3	5.16	1.62	0.0131	Significant
x_2x_3	-1.98	1.72	0.3020	Not significant
x_1^2	-8.65	1.69	0.0009	Significant
x_2^2	-4.76	2.27	0.4609	Not significant
x_3^2	-6.19	1.69	0.0063	Significant

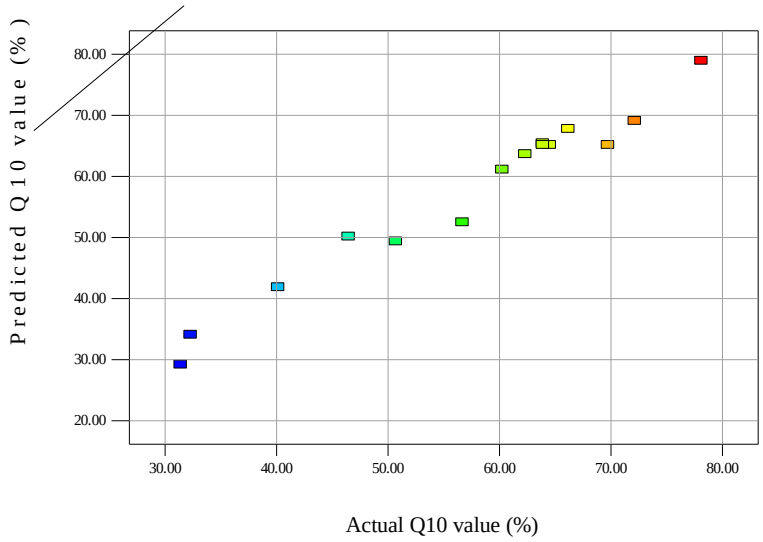

Figure 7.3 Predicted vs. Actual diagnostic plot for the Q_{10} value of RTD.

APPENDIX 3
BATCH RECORD SUMMARY

Only four batch record summaries indicating the quantities of excipients used and the physical tests that were conducted are included in the thesis. The records for all the formulation that were manufactured are available on request.

BATCH SUMMARY RECORD

Product	Ranimetro
Date of manufacture	9th June 2010
Formulator	King'ori LD
Batch number	RM 011
Batch size	1000 tablets
Target weight	500 mg
Granulating fluid	12.5% w/v Povidone K30 solution
Temperature	19±0.5°C
Humidity	50±3%

FORMULA

Material	Unit Dose (mg)	Batch (g)	% w/w	Raw Material number
Ranitidine hydrochloride	84.0	84.0	16.8	RM 000244
Metronidazole	250.0	250.0	50.0	RM 000247
Microcrystalline cellulose pH 102	140.0	140.0	28.0	X061882
Sodium starch glycolate	20.0	20.0	4.0	X070074
Povidone K30	-	-	-	X062448
Colloidal silicone dioxide	1.0	1.0	0.2	X069339
Magnesium Stearate	5.0	5.0	1.0	X052015
TOTAL WEIGHT	**500.0**	**500.0**	**100**	

TABLET PARAMETER

	Mean±SD
Weight (mg)	496±1.78
Diameter (mm)	12.02±0.02
Thickness (mm)	3.31±0.00
Crushing strength (N)	158±17.2
Disintegration time (min)	13.05±1.55

IN VITRO RELEASE

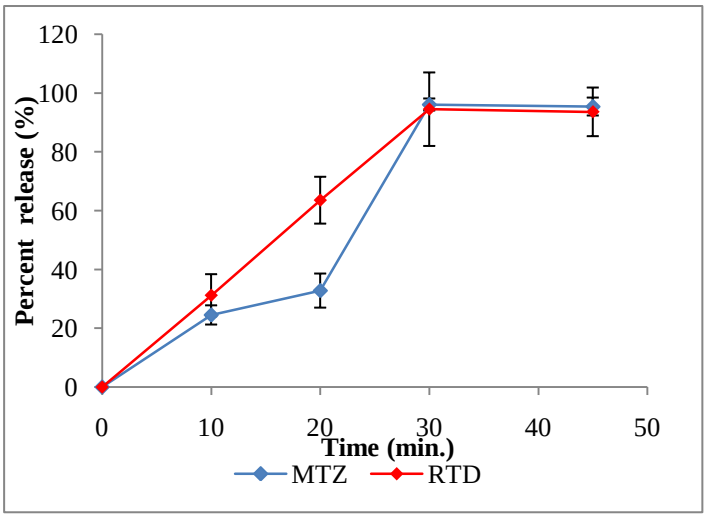

Figure 8.1 *In vitro* release of MTZ and RTD of formulation RM 011

BATCH SUMMARY RECORD

Product	Ranimetro
Date of manufacture	10th June 2010
Formulator	King'ori LD
Batch number	RM 013
Batch size	1000 tablets
Target weight	500 mg
Granulating fluid	12.5% w/v Povidone K30 solution
Temperature	20.±0.5°C
Humidity	51±3%

FORMULA

Material	Unit Dose (mg)	Batch (g)	% w/w	Raw Material number
Ranitidine hydrochloride	84.0	84.0	16.8	RM 000244
Metronidazole	250.0	250.0	50.0	RM 000247
Microcrystalline cellulose pH 102	135.0	135.0	27.0	X061882
Croscarmellose sodium	20.0	20.0	4.0	X070074
Povidone K30	5.0	5.0	1.0	X062448
Colloidal silicone dioxide	1.0	1.0	0.2	X069339
Magnesium Stearate	5.0	5.0	1.0	X052015
TOTAL WEIGHT	**500.0**	**500.0**	**100**	

TABLET PARAMETER

	Mean±SD
Weight (mg)	496.80±1.58
Diameter (mm)	12.00±0.00
Thickness (mm)	3.32±0.00
Crushing strength (N)	101±5.3
Disintegration time (min)	11.49±1.15

IN VITRO RELEASE

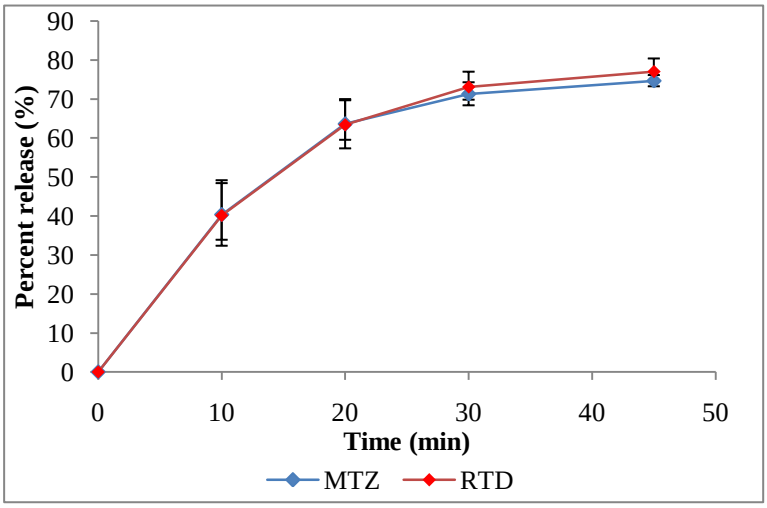

Figure 8.2 *In vitro* release of MTZ and RTD of formulation RM 013

Rhodes University
Faculty of Pharmacy
Department of Pharmaceutics
Grahamstown 6140

BATCH SUMMARY RECORD

Product	Ranimetro
Date of manufacture	11th June 2010
Formulator	King'ori LD
Batch number	RM 014
Batch size	1000 tablets
Target weight	500 mg
Granulating fluid	12.5% w/v Povidone K30 solution
Temperature	19±0.5°C
Humidity	50±3%

FORMULA

Material	Unit Dose (mg)	Batch (g)	% w/w	Raw Material number
Ranitidine hydrochloride	84.0	84.0	16.8	RM 000244
Metronidazole	250.0	250.0	50.0	RM 000247
Dibasic calcium Phosphate	135.0	135.0	27.0	X061882
Croscarmellose sodium	20.0	20.0	4.0	X070074
Povidone K30	1.0	1.0	1.0	X062448
Colloidal silicone dioxide	1.0	1.0	0.2	X069339
Magnesium Stearate	5.0	5.0	1.0	X052015
TOTAL WEIGHT	**500.0**	**500.0**	**100**	

TABLET PARAMETER

	Mean±SD
Weight (mg)	501.34±7.35
Diameter (mm)	12.03±0.03
Thickness (mm)	3.35±0.02
Crushing strength (N)	67.1±11.00
Disintegration time (min)	4.61±1.26

IN VITRO RELEASE

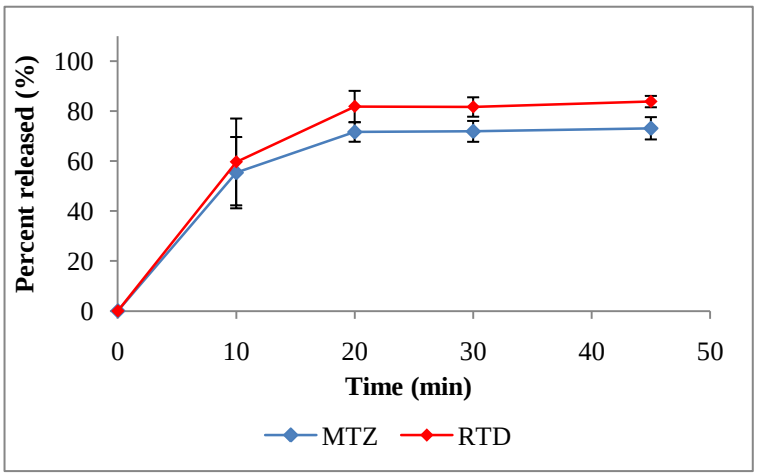

Figure 8.3 *In vitro* release of MTZ and RTD of formulation RM 014

Rhodes University
Faculty of Pharmacy
Department of Pharmaceutics
Grahamstown 6140

BATCH SUMMARY RECORD

Product	Ranimetro
Date of manufacture	12th June 2010
Formulator	King'ori LD
Batch number	RM 015
Batch size	1000 tablets
Target weight	500 mg
Granulating fluid	12.5% w/v Povidone K30 solution
Temperature	19±0.5°C
Humidity	50±3%

FORMULA

Material	Unit Dose (mg)	Batch (g)	% w/w	Raw Material number
Ranitidine hydrochloride	84.0	84.0	16.8	RM 000244
Metronidazole	250.0	250.0	50.0	RM 000247
Dibasic calcium phosphate	135.0	135.0	27.0	X061882
Sodium starch glycolate	20.0	20.0	4.0	X070074
Povidone K30	1.0	1.0	1.0	X062448
Colloidal silicone dioxide	1.0	1.0	0.2	X069339
Magnesium Stearate	5.0	5.0	1.0	X052015
TOTAL WEIGHT	**500.0**	**500.0**	**100**	

TABLET PARAMETER

	Mean±SD
Weight (mg)	498.02±3.17
Diameter (mm)	12.02±0.00
Thickness (mm)	3.30±0.01
Crushing strength (N)	77.8±10.10
Disintegration time (min)	8.56±1.81

IN VITRO RELEASE

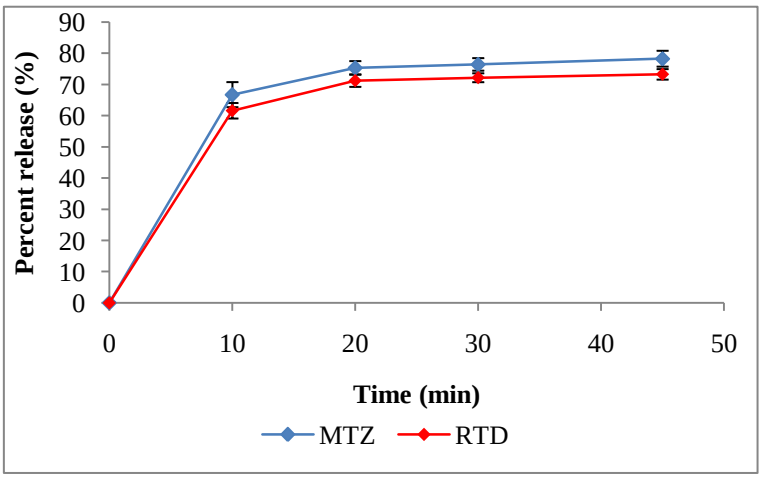

Figure 8.4 *In vitro* release of MTZ and RTD of formulation RM 015

References

1. Anderson, W. A. D. and Scotti, T. M., "Alimentary tract," *Synopsis of Pathology*, Ninth ed. The C.V Mosby Company, Saint Louis, 1976, pp. 773-788.

2. Malfertheiner, P., Chan, F. K., and McColl, K. E., "Peptic ulcer disease," *The Lancet*, Vol. 374, No. 9699, 2009, pp. 1449-1461.

3. Mou, S. M., "The relationship between helicobacter infection and peptic ulcer disease," *Primary Care Update for Obstetrics/Gynaecology*, Vol. 5, No. 5, 1998, pp. 229-232.

4. Ma, L., Chow, J. Y. C., and Cho, C. H., "Mechanistic study of adverse actions of cigarette smoke exposure on acetic acid-induced gastric ulceration in rats," *Life Sciences*, Vol. 62, No. 3, 1997, pp. 257-266.

5. Green, R. J. and Harris, N. D., "Gastrointestinal and liver disease," *Pathology and Therapeutics for Pharmacists*, 2nd ed. Pharmaceutical Press, London, 2000, pp. 320-331.

6. Drugs of Acid Related Disorders. Baren, K. I. South Africa Medicine Formulary. 8th[A02], 39-44. 2008. Cape Town, Health and Medical Publishing Group.
Ref Type: Serial (Book,Monograph)

7. Melikian, C., White, T. J., Vanderplas, A., Dezii, C. M., and Chang, E., "Adherence to oral antidiabetic therapy in a managed care organization: A comparison of monotherapy, combination therapy, and fixed-dose combination therapy," *Clinical Therapeutics*, Vol. 24, No. 3, 2002, pp. 460-467.

8. Marijan, H., Kuftinec, J., Malnar, M., Skreblin, M., Kajfez, F., Nagl, A., and Blazevic, N., "Ranitidine," *Analytical Profile of Drug Substances*, edited by K. Florey Academic Press, Orlando, 1986, pp. 535-561.

9. Agatonovic-Kustrin, S., Rades, T., Wu, V., Saville, D., and Tucker, I. G., "Determination of polymorphic forms of ranitidine hydrochloride by DRIFTS and XRPD," *Journal of Pharmaceutical and Biomedical Analysis*, Vol. 25, No. 5-6, 2001, pp. 741-750.

10. "Gastrointestinal drugs," *Martindale: The Complete Drug Reference*, edited by S. C. Sweetman, 35th ed. Pharmaceutical Press, China, 2007, pp. 1590-1591.

11. Meloun, M., Syrový, T., and Vrána, A., "The thermodynamic dissociation constants of ambroxol, antazoline, naphazoline, oxymetazoline and ranitidine by the regression analysis of spectrophotometric data," *Talanta*, Vol. 62, No. 3, 2004, pp. 511-522.

12. Degim, T., Zaimoglu, V., Akay, C., and Degim, Z., "pH-Metric log-K calculations of famotidine, naproxen, nizatidine, ranitidine and salicylic acid," *Il Farmaco*, Vol. 56, No. 9, 2001, pp. 659-663.

13. El-Bary, A., El-Gazayerly, O. N., and El-Timimy, M., "Solid state and bioavailability of ranitidine hydrochloride capsule," *Al-Azhar Journal of Pharmaceutical Sciences*, Vol. 24, 1999, pp. 167-186.

14. Shah, R. B., "Development of a validated stability indicating HPLC method for ranitidine hydrochloride syrup," *Clinical Research and Regulatory Affairs*, Vol. 23, No. 1, 2006, pp. 35-51.

15. Gomes de Pinho, R., Jesus, J., and Honda, M., "Study of ranitidine stability in dosage forms. Determination of shelf life," *Revista Brasileira de Famacia*, Vol. 77, No. 4, 1996, pp. 142-145.

16. Katzung, B. G., "Histamine, serotonin and the ergot alkaloids," *Basic and Clinical Pharmacology*, edited by B. G. Katzung, Eigth ed. McGraw Hill, San-Fransico, 2001, pp. 275-277.

17. Royer, J. E. and Triplett, R. G., "Effect of preoperative cimetidine and ranitidine on gastric secretion," *Journal of Oral and Maxillofacial Surgery*, Vol. 43, No. 12, 1985, pp. 956-957.

18. Gastrointestinal Disorders. Berkow, R. and Fletcher, A. J. 16th, 768-780. 1992. New Jersey, Merck Research Laboratories. The Merck Manual.
Ref Type: Serial (Book,Monograph)

19. Joyce, T. H., "Prophylaxis for pulmonary acid aspiration," *The American Journal of Medicine*, Vol. 83, No. 6, Supplement 1, 1987, pp. 46-52.

20. Vial, T., Goubier, C., Begeret, A., Cabrera, F., Evreux, J. C., and Descoted, J., "Side effects of ranitidine," *Drug safety:An International journal of medical toxicology and drug experience*, Vol. 6, No. 2, 1991, pp. 94-117.

21. Amir, I., Anwar, N., Baraona, E., and Lieber, C. S., "Ranitidine increases the bioavailability of imbibed alcohol by accelerating gastric emptying," *Life Sciences*, Vol. 58, No. 6, 1996, pp. 511-518.

22. Hiroki, I. and Toshiaki, N., "Ranitidine increase bioavailability of acetaminophen by inhibiting first-pass glucuronidation in man," *Pharmacy and Pharmacology Communication*, Vol. 6, No. 11, 2000, pp. 495-500.

23. Gill, S., O'Brien, L., and Koren, G., "The safety of histamine 2 (H2) blockers in pregnancy: A meta-analysis," *Digestive Diseases and Sciences*, Vol. 54, No. 9, 2009, pp. 1835-1838.

24. Mahadevan, U., "Gastrointestinal medications in pregnancy," *Best Practice & Research Clinical Gastroenterology*, Vol. 21, No. 5, 2007, pp. 849-877.

25. Grant, S. M., Langtry, S. D., and Brogden, R. M., "Ranitidine; An updated review of its pharmacodynamics and pharmacokinetics properties and therapeutic use in peptic ulcers disease and other allied diseases," *Drugs*, Vol. 37, No. 6, 1989, pp. 801-870.

26. Valuck, R. J. and Ruscin, J. M., "A case-control study on adverse effects: H2 blocker or proton pump inhibitor use and risk of vitamin B12 deficiency in older adults," *Journal of Clinical Epidemiology*, Vol. 57, No. 4, 2004, pp. 422-428.

27. Ireland, A., Gear, P., Jones, D. G. C., Golding, P. L., Ramage, J. K., Williams, J. G., Leicester, R. J., Smith, C. L., Ross, G., Bamforth, J., Degara, C. J., Gledhill, T., and Hunt, R. H., "Ranitidine 150 mg twice daily vs 300 mg nightly in treatment of duodenal ulcers," *The Lancet*, Vol. 324, No. 8397, 1984, pp. 274-276.

28. Koelz, H. R. and Halter, F., "Sucralfate and ranitidine in the treatment of acute duodenal ulcer : Healing and relapse," *The American Journal of Medicine*, Vol. 86, No. 6, Supplement 1, 1989, pp. 98-103.

29. Nishina, K., Katsuya, M., Nobuhiro, M., Yumiko, T., Makoto, S., and Hidefumi, O., "A comparison of Lansoprazole, Omeprazole, and Rantidine for reducing preoperative gastric secretion in adult patients undergoing elective surgery," *Anesthesia and Analgesia*, Vol. 82, 1996, pp. 832-836.

30. Baer, A. B. and Holstege, C. P., "Ranitidine," *Encyclopedia of Toxicology*, edited by P. Wexler Elsevier, New York, 2005, pp. 620-621.

31. Blumer, J. L., Rothstein, F. C., Kaplan, B. S., Yamashita, T. S., Eshelman, F. N., Myers, C. M., and Reed, M. D., "Pharmacokinetic determination of ranitidine pharmacodynamics in paediatric ulcer disease," *The Journal of Paediatrics*, Vol. 107, No. 2, 1985, pp. 301-306.

32. Schaiquevich, P., Niselman, A., and Rubio, M., "Comparison of two compartmental models for describing ranitidine's plasmatic profiles," *Pharmacological Research*, Vol. 45, No. 5, 2002, pp. 399-405.

33. Klotz, U. and Kroemer, H. K., "The drug interaction potential of ranitidine: An update," *Pharmacology & Therapeutics*, Vol. 50, No. 2, 1991, pp. 233-244.

34. Robert, C. J., "Clinical pharamacokinetics of ranitidine," *Clinical Pharmacokinetics*, Vol. 9, No. 3, 1984, pp. 211-221.

35. Lebert, P. A., "Ranitdine kinetics and dynamics.II.Intravenous dose study and comparison with cimetidine," *Clincal pharmacology and therapeutics*, Vol. 30, No. 4, 1981, pp. 545-550.

36. Yoshio, E., Yoshitaka, J., Yasuko, M., and Tetsuyoki, Y., "The Pharmacokinetic behaviour of rantidine: Absorption, distribution, and excreition of ranitidine after an intravenous,intramascular administration in rats," *Yakuri to Chiryo (1973-2000)*, Vol. 12, No. 8, 1984, pp. 3227-3247.

37. Kears, G. L., McConnell, R. F. J., Trang, J. M., and Kluza, R. B., "Appearance of ranitdine in breast milk following multiple dosing," *Clinical Pharmacy*, Vol. 4, No. 3, 1985, pp. 322-324.

38. Cross, D. M., Bell, J. A., and Wilson, K., "Kinetics of ranitidine metabolism in dog and rat isolated hepatocytes," *Xenobiotica*, Vol. 24, No. 5, 1995, pp. 365-375.

39. Sima, S. and Tajerzedeh, H., "Efficacy of urine sample in bioavailability study of ranitidine," *Journal of Faculty of Pharamacy*, Vol. 11, No. 2, 2003, pp. 52-57.

40. Koch, K. M. and Liu, M., "Pharmacokinetics and pharmacodynamics of ranitidine in renal impairment.," *European Journal of Clinical Pharmacology*, Vol. 52, No. 3, 1997, pp. 229-234.

41. Gladziwa, U. and Klotz, U., "Pharmacokinetics and pharmacodynamics of H-2 receptor antagonists in patients with renal insufficiency," *Clinical Pharmacokinetics*, Vol. 24, No. 4, 1993, pp. 319-332.

42. Wearley, L. L. and Anthony, G. D., "Metronidazole," *Analytical Profile of Drug Substances*, edited by K. Florey Academic Press, New Brunswick, New Jersey, 1976, pp. 329-344.

43. Sweetman, S. C., "Antiprotozoal," *Martindale: The Complete Drug Reference*, edited by S. C. Sweetman, 35th ed. Pharmaceutical Press, Peoples Republic of China, 2007, pp. 753-757.

44. Wu, Y. and Fassihi, R., "Stability of metronidazole, tetracycline HCl and famotidine alone and in combination," *International Journal of Pharmaceutics*, Vol. 290, No. 1-2, 2005, pp. 1-13.

45. Yang, S., "Determination of dissociation constant of metronidazole by UV-Spectrophotometry," *Huaxi Youxue Zazhi*, Vol. 14, No. 1, 1999, pp. 9-10.

46. Marciniec, B. and Bugaj, A., "Kinetics studies of photo degradation of nitroimidazole in solution," *Acta Poloniae Pharmaceutica*, Vol. 52, 1995, pp. 197-200.

47. Pfoertner, K. H. and Daly, J. J., "Photochemical rearrangement of N-1subsituted 2-methyl-5-nitro-1H imidazole," *Helvetica Chemica Acta*, Vol. 70, 1987, pp. 171-174.

48. Fink, W. S. and Fox, A., "Spectromphotometric determination of N-substituted and N-unsubstituted nitroimidazole," *Analytica Chemica Acta*, Vol. 106, 1979, pp. 389-393.

49. Shemer, H., Kunukcu, Y. K., and Linden, K. G., "Degradation of the pharmaceutical metronidazole via UV, fenton and photo-fenton processes," *Chemosphere*, Vol. 63, No. 2, 2006, pp. 269-276.

50. Jukka-Pekka, K. S.. Hydrolysis of tinidazole. 10-13. 3-8-2003. Finland, University of Helsinki.
Ref Type: Thesis/Dissertation

51. Baveja, S. K. and Rao, A. V. R., "Kinetics of metronidazole hydrolysis," *Indian Journal of Technology*, Vol. 11, 1973, pp. 311-312.

52. Bakshi, M. and Singh, S., "Development of validated stability-indicating assay methods critical review," *Journal of Pharmaceutical and Biomedical Analysis*, Vol. 28, No. 6, 2002, pp. 1011-1040.

53. Katzung, B. G., "Antiprotozoal drugs," *Basic and Clinical Phramacology*, edited by B. G. Katzung, Eighth ed. MacGraw Hill, San-Fransisco, 2001, pp. 882-902.

54. Menéndez, D., Rojas, E., Herrera, L. A., López, M. C., Sordo, M., Elizondo, G., and Ostrosky-Wegman, P., "DNA breakage due to metronidazole treatment," *Mutation Research/Fundamental and Molecular Mechanisms of Mutagenesis*, Vol. 478, No. 1-2, 2001, pp. 153-158.

55. Fung, H. B. and Doan, T. L., "Tinidazole: A nitroimidazole antiprotozoal agent," *Clinical Therapeutics*, Vol. 27, No. 12, 2005, pp. 1859-1884.

56. Johnson, P. J., "Metronidazole and drug resistance," *Parasitology Today*, Vol. 9, No. 5, 1993, pp. 183-186.

57. Church, D. L., Bryant, R. D., Sim, V., and Laishley, E. J., "Metronidazole susceptibility and the presence of hydrogenase in pathogenic bacteria," *Anaerobe*, Vol. 2, No. 3, 1996, pp. 147-153.

58. "Infectious diseases," *The Merck Manual*, edited by R. Berkow, 16th ed. Merck Research Laboratories, New Jersey, 1992, pp. 43-44.

59. Fang, H., Edlund, C., Hedberg, M., and Nord, C. E., "New findings in beta-lactam and metronidazole resistant *Bacteroides fragilis* group," *International Journal of Antimicrobial Agents*, Vol. 19, No. 5, 2002, pp. 361-370.

60. Liu, S. M., Brown, D. M., O'Donoghue, P., Upcroft, P., and Upcroft, J. A., "Ferredoxin involvement in metronidazole resistance of *Giardia duodenalis*," *Molecular and Biochemical Parasitology*, Vol. 108, No. 1, 2000, pp. 137-140.

61. Trend, M. A., Jorgensen, M. A., Hazell, S. L., and Mendz, G. L., "Oxidases and reductases are involved in metronidazole sensitivity in *Helicobacter pylori*," *The International Journal of Biochemistry & Cell Biology*, Vol. 33, No. 2, 2001, pp. 143-153.

62. Land, K. M. and Johnson, P. J., "Molecular basis of metronidazole resistance in pathogenic bacteria and protozoa," *Drug Resistance Updates*, Vol. 2, No. 5, 1999, pp. 289-294.

63. Bendesky, A., Menéndez, D., and Ostrosky-Wegman, P., "Is metronidazole carcinogenic?," *Mutation Research/Reviews in Mutation Research*, Vol. 511, No. 2, 2002, pp. 133-144.

64. "Antiparasitic products," *South Africa Medicine Formulary*, edited by C. J. Gibbon, Eighth ed. Health and Medical Publishing Group, Cape Town, 2008, pp. 492-493.

65. Groothoff, M. V. R., Hofmeijer, J., Sikma, M. A., and Meulenbelt, J., "Irreversible encephalopathy after treatment with high-dose intravenous metronidazole," *Clinical Therapeutics*, Vol. 32, No. 1, 2010, pp. 60-64.

66. Ostrosky-Wegman, P., Lares Asseff, I., Santiago, P., Elizondo, G., and Montero, R., "Metronidazole hprt mutation induction in sheep and the relationship with its

elimination rate," *Mutation Research/Fundamental and Molecular Mechanisms of Mutagenesis*, Vol. 307, No. 1, 1994, pp. 253-259.

67. Burtin, P., Taddio, A., Ariburnu, O., Einarson, T. R., and Koren, G., "Safety of metronidazole in pregnancy: A meta-analysis," *American Journal of Obstetrics and Gynaecology*, Vol. 172, No. 2, Part 1, 1995, pp. 525-529.

68. Kazy, Z., Puhó, E., and Czeizel, A. E., "Teratogenic potential of vaginal metronidazole treatment during pregnancy," *European Journal of Obstetrics & Gynaecology and Reproductive Biology*, Vol. 123, No. 2, 2005, pp. 174-178.

69. Carvajal, A., Sánchez, A., and Hurtarte, G., "Metronidazole during pregnancy," *International Journal of Gynaecology & Obstetrics*, Vol. 48, No. 3, 1995, pp. 323-324.

70. Murphy, P. A. and Jones, E., "Use of oral metronidazole in pregnancy : Risks, benefits, and practice guidelines," *Journal of Nurse-Midwifery*, Vol. 39, No. 4, 2007, pp. 214-220.

71. Kester, R. C., Antrum, R., Thornton, C. A., Ramsden, C. H., and Harding, I., "A comparison of teicoplanin versus cephradine plus metronidazole in the prophylaxis of post-operative infection in vascular surgery," *Journal of Hospital Infection*, Vol. 41, No. 3, 1999, pp. 233-243.

72. Meyer, N. L., Scott, K., Hosier, K., and Sibai, B., "Cefazolin versus cefazolin/ metronidazole for antibiotic prophylaxis at cesarean delivery," *Obstetrics & Gynaecology*, Vol. 95, No. 4, Supplement 1, 2000, pp. S74.

73. Zip, C. M., "Innovative use of topical metronidazole," *Dermatologic Clinics*, Vol. 28, No. 3, 2010, pp. 525-534.

74. Barco, D. and Alomar, A., "Rosacea," *Actas Dermo-Sifiliográficas*, Vol. 99, No. 4, 2008, pp. 244-256.

75. Brandt, M., Abels, C., May, T., Lohmann, K., Schmidts-Winkler, I., and Hoyme, U. B., "Intravaginally applied metronidazole is as effective as orally applied in the treatment of bacterial vaginosis, but exhibits significantly less side effects," *European Journal of Obstetrics & Gynaecology and Reproductive Biology*, Vol. 141, No. 2, 2008, pp. 158-162.

76. Ings, R., McFadzian, J., and Ormerod, W., "The action of metronidazole on DNA," *Xenobiotica*, Vol. 5, No. 4, 1975, pp. 223-235.

77. Lamp, K. C., Freeman, C. D., Klutman, N. E., and Lacy, M. K., "Pharmacokinetics and pharmacodynamics of the nitroimidazole antimicrobials," *Clinical Pharmacokinetics*, Vol. 36, No. 5, 1999, pp. 353-373.

78. Ings, R. M. J., Law, G. L., and Parnell, E. W., "The metabolism of metronidazole (1 - 2'-hydroxyethyl-2-methyl-5-nitroimidazole)," *Biochemical Pharmacology*, Vol. 15, No. 5, 1966, pp. 515-519.

79. Loft, S., Otton, V., Lennard, M. S., Tucker, G. T., and Poulsen, H. E., "Characterization of metronidazole metabolism by human liver microsomes," *Biochemical Pharmacology*, Vol. 41, No. 8, 1991, pp. 1127-1134.

80. Upadhyaya, P., Bhatnagar, V., and Basu, N., "Pharmacokinetics of intravenous metronidazole in neonates," *Journal of Paediatric Surgery*, Vol. 23, No. 3, 1988, pp. 263-265.

81. Jager-Roman, E., Doyle, P. E., Baird-Lambert, J., Cvejic, M., and Buchanan, N., "Pharmacokinetics and tissue distribution of metronidazole in the newborn infant," *The Journal of Paediatrics*, Vol. 100, No. 4, 1982, pp. 651-654.

82. Ostrow, B., "Pepticl ulcer disease: The impact of *Helicobacter pylori*," *International Journal of Epidemiology*, Vol. 30, 2001, pp. 13-17.

83. Ungan, M., Kulaçoglu, H., and Kayhan, B., "Cure rates obtained with five different *Helicobacter pylori* eradication protocols in patients with duodenal ulcer: a prospective, open-label randomized study in a primary care setting in Turkey," *Current Therapeutic Research*, Vol. 62, No. 6, 2001, pp. 462-472.

84. Igata, H. and Okabe, S., "Discovery and development of the proton pump inhibitor," *Japanese Journal of Clinical Medicine*, Vol. 50, No. 1, 1992, pp. 11-17.

85. Scarpignato, C., "New drugs to suppress acid secretion: Current and future developments," *Drug Discovery Today: Therapeutic Strategies*, Vol. 4, No. 3, 2007, pp. 155-163.

86. Lucas, L. M., Gerrity, M. S., and Anderson, T., "A practice-based approach for converting proton pump inhibitors to less costly therapy," *Effective Clinical Practice*, Vol. 4, No. 6, 2001, pp. 263-270.

87. Miller, M. J., "Impact of industrial and governmental regulatory practices on analytical chromatography," *Chromatography:Concepts and Contrasts*, Second ed. John Wiley and Sons, New Jersey, 2005, pp. 1.

88. Wixom, L. R., Gehrke, W. C., and Bayer, E., *The Beginings of Chromatography: The Pioneers (1900-1960)*, First ed. 2001, pp. 4-17.

89. Kazakevich, Y. and Brutto, R., "Introduction," *HPLC for Pharmaceutical Scientists* John Wiley and Sons, United States of America, 2007, pp. 6-11.

90. Braithwaite, A. and Smith, J. F., "Introduction," *Chromatographic Methods*, Fifth ed. Kluwer Academic Publishers, Netherlands, 1999, pp. 1-14.

91. Shabir, G. A., "Validation of high-performance liquid chromatography methods for pharmaceutical analysis: Understanding the differences and similarities between validation requirements of the US Food and Drug Administration, the US Pharmacopoeia and the International Conference on Harmonization," *Journal of Chromatography A*, Vol. 987, No. 1-2, 2003, pp. 57-66.

92. Snyder, R. L., Kirkland, J. J., and Dolan, W. J., *Introduction to Modern Liquid Chromatography*, 3rd ed., Vol. 1, John Wiley and Sons, United States of America, 2010.

93. Pryde, A. and Gilbert, M. T., *Application of High Performance Liquid Chromatography*, John Wiley and Sons 1979.

94. Parris A.N, "Bonded phase," *Instrumental Liquid Chromatography: A Practical Manual on High Performance Liquid Chromatography Methods*, Second ed. Elsevier Science Publishing Company, Netherlands, 1985, pp. 203-204.

95. Kenkel, J., *Analytical Chemistry for Technicnians*, 3rd ed. Lewis Publishers, 2003, pp. 374-376.

96. Snyder, R. L., Kirkland, J. J., and Glajch, L. J., *Practical HPLC Method Development.*, 2nd ed., John Wiley and Sons, United States of America, 1997.

97. Dong, M. W., *Modern HPLC for Practicing Scientists*, John Wiley and Sons, Hoboken, 2006.

98. Konishi, T., Kamada, M., and Nakamura, H., "Evaluation of ammonium acetate as a volatile buffer for high-performance hydrophobic-interaction chromatography," *Journal of Chromatography A*, Vol. 515, 1990, pp. 279-283.

99. Subirats, X., Bosch, E., and Rosés, M., "Retention of ionisable compounds on high-performance liquid chromatography XVII: Estimation of the pH variation of aqueous buffers with the change of the methanol fraction of the mobile phase," *Journal of Chromatography A*, Vol. 1138, No. 1-2, 2007, pp. 203-215.

100. Lough, J. W. and Wainer, W. I., *High Performance Liquid Chromatography: Fundamental Principles and Practice*, 1st ed., Blackie Academic and Professional, Glasgow, 1996.

101. Barth, G. H. and Boyes, E. B., "Size exclusion chromatography," *Analytical Chemistry*, Vol. 64, 1992, pp. 428-442.

102. Ricker, R. D. and Sandoval, L. A., "Fast, reproducible size-exclusion chromatography of biological macromolecules," *Journal of Chromatography A*, Vol. 743, No. 1, 1996, pp. 43-50.

103. Oliver, W. A. R., *HPLC of Macromolecules: A Practical Approach*, Second ed., Oxford University Press, New York, 1998.

104. Barth, G. H., "Size exclusion chromatography," *Handbook of HPLC*, edited by E. Katz Marcle Dekker, United States of America, 1998, pp. 273-292.

105. Van Der Borght, A., Vandeputte, G. E., Derycke, V., Brijs, K., Daenen, G., and Delcour, J. A., "Extractability and chromatographic separation of rice endosperm proteins," *Journal of Cereal Science*, Vol. 44, No. 1, 2006, pp. 68-74.

106. Sadao, M. and Howard, G. B., *Size Exclusion Chromatography*, Springer, Germany, 1999, pp. 11-24.

107. do Nascimento, T. G., de Jesus Oliveira, E., and Macédo, R. O., "Simultaneous determination of ranitidine and metronidazole in human plasma using high performance liquid chromatography with diode array detection," *Journal of Pharmaceutical and Biomedical Analysis*, Vol. 37, No. 4, 2005, pp. 777-783.

108. Munro, J. S. and Walker, T. A., "Ranitidine hydrochloride: Development of an isocratic stability-indicating high-performance liquid chromatographic separation," *Journal of Chromatography A*, Vol. 914, No. 1-2, 2001, pp. 13-21.

109. Flores, P. C., Juárez, O. H., Flores, P. J., Toledo, L. A., Lares, A. I., and Alvarez, G. C., "Reliable method for the determination of ranitidine by liquid chromatography using a microvolume of plasma," *Journal of Chromatography B*, Vol. 795, No. 1, 2003, pp. 141-144.

110. Lunn, G. and Schmuff, R. N., "Ranitidine," *HPLC Methods for Pharmaceutical Analysis* John Wiley and Sons, United States of America, 2000, pp. 1209.

111. Bakshi, M. and Singh, S., "ICH guidance in practice. Stress degradation studies on metronidazole and development of a validated stability-indicating HPLC assay method," *Pharmaceutical Technology*, Vol. 27, No. 10, 2003, pp. 148, 150, 152, 154, 156, 158, 160.

112. Lunn, G., "Metronidazole," *HPLC Methods for Pharmaceutical Analysis* John Wiley and Sons, United States of America, 2000, pp. 1354-1362.

113. Galmier, M. J., Frasey, A. M., Bastide, M., Beyssac, E., Petit, J., Aiache, J. M., and Lartigue-Mattei, C., "Simple and sensitive method for determination of metronidazole in human serum by high-performance liquid chromatography," *Journal of Chromatography B: Biomedical Sciences and Applications*, Vol. 720, No. 1-2, 1998, pp. 239-243.

114. Venkateshwaran, T. G. and Stewart, J. T., "Determination of metronidazole in vaginal tissue by high-performance liquid chromatography using solid-phase extraction," *Journal of Chromatography B: Biomedical Sciences and Applications*, Vol. 672, No. 2, 1995, pp. 300-304.

115. Emami, J., Ghassami, N., and Hamishehkar, H., "A rapid and sensitive HPLC method for the analysis of metronidazole in human plasma: Application to single dose pharmacokinetic and bioequivalence studies," *Daru, Journal of Faculty of Pharmacy, Tehran University of Medical Sciences*, Vol. 14, No. 1, 2006, pp. 15-21.

116. Bempong, D. K., Manning, R. G., Mirza, T., and Bhattacharyya, L., "A stability-indicating HPLC assay for metronidazole benzoate," *Journal of Pharmaceutical and Biomedical Analysis*, Vol. 38, No. 4, 2005, pp. 776-780.

117. Srtiegel, A. M., Wallace, W. Y., Kirkland, J. J., and Bly, D. D., *Modern Size Exclusion Liquid Chromatography: Practice of Gel Permeation and Gel Fitration Chromatogrphy*, Second ed., John Wiley and Sons, Hoboken, New Jersey, 2009.

118. Kastner, M., *Protein Liquid Chromatography*, 1st ed., Vol. 61, Elsevier science, Amsterdam, 2000.

119. Shimizu, M., Uno, T., Niioka, T., Yaui-Furukori, N., Takahata, T., Sugawara, K., and Tateishi, T., "Sensitive determination of omeprazole and its two main metabolites in human plasma by column-switching high-performance liquid chromatography: Application to pharmacokinetic study in relation to CYP2C19 genotypes," *Journal of Chromatography B*, Vol. 832, No. 2, 2006, pp. 241-248.

120. Hammarstrand, K., "Internal standard in gas chromatography," *Varian Instrument Application*, Vol. 10, No. 1, 1976, pp. 10-11.

121. Guichon, G. and Guillemin, L. C., *Quantitative Gas Chromatography: for Laboratory Analysis and On-line Process Control*, Vol. 42, Elsevier Science Publishers, Netherlands, 1988.

122. Leo, M. and Nollet, L., *Food Analysis by HPLC*, Second ed., Marcel Dekker, United States of America, 2000.

123. Center for Drug Evaluation and Research Control, "Validation of chromatographic methods," FDA, 3, Rockville, 1994.

124. Scholten, A. B., Claessens, H. A., de Haan, J. W., and Cramers, C. A., "Chromatographic activity of residual silanols of alkylsilane derivatized silica surfaces," *Journal of Chromatography A*, Vol. 759, No. 1-2, 1997, pp. 37-46.

125. Vervoort, R. J. M., Maris, F. A., and Hindriks, H., "Comparison of high-performance liquid chromatographic methods for the analysis of basic drugs," *Journal of Chromatography A*, Vol. 623, No. 2, 1992, pp. 207-220.

126. Roos, R. W. and Lau-Cam, C. A., "General reversed-phase high-performance liquid chromatographic method for the separation of drugs using triethylamine as a competing base," *Journal of Chromatography A*, Vol. 370, 1986, pp. 403-418.

127. Satinder, A. and Rasmussen, H., *HPLC Method Development for Pharmaceuticals*, 1st ed., Vol. 8, Academinc Press, London, 2007, pp. 78.

128. Green, M. J., "A Practical Guide to Analytical Method Validation," *Analytical Chemistry*, Vol. 68, 1996, pp. 305A-309A.

129. USP: Validation of Compendial Methods. [28], 2748-2751. 2005. Rockville, Maryland, United States Pharmacopoeia Convention.
Ref Type: Serial (Book,Monograph)

130. European Medicines Agency, "Validation of Analytical Procedures: Definitions and Methodology Q2 (R1)," European Medicines Agency, London, 1995.

131. Carr, G. P. and Wahlich, J. C., "A practical approach to method validation in pharmaceutical analysis," *Journal of Pharmaceutical and Biomedical Analysis*, Vol. 8, No. 8-12, 1990, pp. 613-618.

132. Gustavo, G. A. and Ángeles, H. M., "A practical guide to analytical method validation, including measurement uncertainty and accuracy profiles," *Trends in Analytical Chemistry*, Vol. 26, No. 3, 2007, pp. 227-238.

133. International Conference on Harmonisation of Technical Requiements for Registration of Pharmaceutical for Human Use, "Stability testing of new drug substance and product Q1A R2," European Medicine Agency, London, UK, 2006.

134. Bakshi, M., Singh, B., Singh, A., and Singh, S., "The ICH guidance in practice: Stress degradation studies on ornidazole and development of a validated stability-indicating assay," *Journal of Pharmaceutical and Biomedical Analysis*, Vol. 26, No. 5-6, 2001, pp. 891-897.

135. Augsburger, L. M. and Hoag, S. W., *Pharmaceutical Dosage Forms*, 3rd ed., Vol. 1, Informa Health Care, United States of America, 2008, pp. 465.

136. Ahuja, S. and Scypinski, S., *Handbook of Modern Pharmaceutical Analysis*, Vol. 3, Academic Press, London, 2001, pp. 173.

137. Gibson, M., *Pharmaceutical Preformulation and Formulation*, Interpharm CRC, United States of America, 2004, pp. 22.

138. Leuenberger, H., "The compressibility and compactibility of powder systems," *International Journal of Pharmaceutics*, Vol. 12, No. 1, 1982, pp. 41-55.

139. Sun, C. C., "A material-sparing method for simultaneous determination of true density and powder compaction properties: Aspartame as an example," *International Journal of Pharmaceutics*, Vol. 326, No. 1-2, 2006, pp. 94-99.

140. Mahato, R. I., "Biopharmaceutical and physiological concideration," *Pharmaceutical Dosage Forms and Drug Delivery* Taylor and Francis Group LLC, United States of America, 2007, pp. 29-46.

141. Ramirez-Dorronsoro, J. C., Jacko, R. B., and Kildsig, D. O., "Chargeability measurement of selected phramceutical dry powders to assess their electrostatic charge control capabilities," *AAPS PharmSciTech*, Vol. 4, No. 7, 2006, pp. E1-E8.

142. Lieberman, H. A., Leon, L., and Schwartz, J. B., *Pharmacetical Dosage Forms: Tablets*, 2nd ed., Vol. 1, Marcle Dekker, New York, 1989.

143. Swabrick, J., *Encylopedia of Pharmaceutical Technology*, 3rd ed., Vol. 6, Informa Healthcare, New York, 2007.

144. Abdullah, E. C. and Geldart, D., "The use of bulk density measurements as flowability indicators," *Powder Technology*, Vol. 102, No. 2, 1999, pp. 151-165.

145. USP. Bulk Density. [29], 2638. 2010. Rockville, Maryland, United States Pharmacopeial Convention. 16-9-2010.
Ref Type: Serial (Book,Monograph)

146. Carr, R., "Evaluating flow properties of solids," *Chemical Engineering Journal*, Vol. 72, 1965, pp. 163-168.

147. Sarraguça, M. C., Cruz, A. V., Soares, S. O., Amaral, H. R., Costa, P. C., and Lopes, J. A., "Determination of flow properties of pharmaceutical powders by near infrared

spectroscopy," *Journal of Pharmaceutical and Biomedical Analysis*, Vol. 52, No. 4, 2010, pp. 484-492.

148. Grey, R. O. and Beddow, J. K., "On the Hausner Ratio and its relationship to some properties of metal powders," *Powder Technology*, Vol. 2, No. 6, 1969, pp. 323-326.

149. Cao, X., Leyva, N., Anderson, S. R., and Hancock, B. C., "Use of prediction methods to estimate true density of active pharmaceutical ingredients," *International Journal of Pharmaceutics*, Vol. 355, No. 1-2, 2008, pp. 231-237.

150. Mahajan, R. R., Gill, M., Ahmed, S. U., and Chowdhury, T.. Estimation of true density of pharmaceutical powder material from the density of compacted mass. American Association of Pharmaceutical Scientist . 2002.
Ref Type: Abstract

151. Brittain, H. G., "Preparation and identification of polymorphs and solvatomorphs," *Preformulation in Solid Dosage Forms Development*, edited by C. M. Adeyeye and H. G. Brittain Informa Health Care, New York, 2008, pp. 185-228.

152. Agatonovic-Kustrin, S., Wu, V., Rades, T., Saville, D., and Tucker, I. G., "Ranitidine hydrochloride X-ray assay using a neural network," *Journal of Pharmaceutical and Biomedical Analysis*, Vol. 22, No. 6, 2000, pp. 985-992.

153. Mirmehrabi, M., Rohani, S., Murthy, K. S. K., and Radatus, B., "Characterization of tautomeric forms of ranitidine hydrochloride: Thermal analysis, solid-state NMR, X-ray," *Journal of Crystal Growth*, Vol. 260, No. 3-4, 2004, pp. 517-526.

154. Pratiwi, D., Fawcett, J. P., Gordon, K. C., and Rades, T., "Quantitative analysis of polymorphic mixtures of ranitidine hydrochloride by Raman spectroscopy and principal components analysis," *European Journal of Pharmaceutics and Biopharmaceutics*, Vol. 54, No. 3, 2002, pp. 337-341.

155. Chieng, N., Rades, T., and Saville, D., "Formation and physical stability of the amorphous phase of ranitidine hydrochloride polymorphs prepared by cryo-milling," *European Journal of Pharmaceutics and Biopharmaceutics*, Vol. 68, No. 3, 2008, pp. 771-780.

156. Raw, A. S., Furness, M. S., Gill, D. S., Adams, R. C., Holcombe, F. O., and Yu, L. X., "Regulatory considerations of pharmaceutical solid polymorphism in Abbreviated New Drug Applications (ANDAs)," *Advanced Drug Delivery Reviews*, Vol. 56, No. 3, 2004, pp. 397-414.

157. Giron, D., "Applications of thermal analysis in the pharmaceutical industry," *Journal of Pharmaceutical and Biomedical Analysis*, Vol. 4, No. 6, 1986, pp. 755-770.

158. Ozawa, T., "Thermal analysis review and prospect," *Thermochimica Acta*, Vol. 355, No. 1-2, 2000, pp. 35-42.

159. Adeyeye, C. M., "Drug-excipient interaction occurences during solid dosage form development," *Preformulation in Solid Dosage Form Development*, edited by C. M. Adeyeye and H. G. Brittain Informa Health Care, New York, 2008, pp. 357-436.

160. Madan, T. and Kakkar, A. P., "Preparation and characterization of ranitidine hydrochloride crystals," *Drug Development and Industrial Pharmacy*, Vol. 20, No. 9, 1984, pp. 1571-1588.

161. Wu, Y., Dali, M., Gupta, A., and Raghavan, K., "Understanding drug-excipient compatibility: Oxidation of compound a in a solid dosage form understanding drug-excipient compatibility," *Pharmaceutical Development and Technology*, Vol. 14, No. 5, 2009, pp. 556-564.

162. Cory, W. C., Harris, C., and Martinez, S., "Accelerated degradation of ibuprofen in tablets," *Pharmaceutical Development and Technology*, Vol. 15, No. 6, 2010, pp. 636-643.

163. Bãitan, M., Gafitan, E., Lionte, M., and Moisuc, L., "Formulation of creams with betamethasone dipropionate: Evaluation of chemical stability," *Revista medico-chirurgical*, Vol. 114, No. 2, 2010, pp. 600-604.

164. Katdare, A. and Chaubal, M. V., *Excipient Development for Pharmaceutical, Biotechonolgy and Drug Delivery Systems*, Vol. 8, Informa Health Care, New York, 2006.

165. Steckel, H. and Bolzen, N., "Alternative sugars as potential carriers for dry powder inhalations," *International Journal of Pharmaceutics*, Vol. 270, No. 1-2, 2004, pp. 297-306.

166. Thi, T. H. H., Danède, F., Descamps, M., and Flament, M. P., "Comparison of physical and inhalation properties of spray-dried and micronized terbutaline sulphate," *European Journal of Pharmaceutics and Biopharmaceutics*, Vol. 70, No. 1, 2008, pp. 380-388.

167. Chougule, M. B. and Padhi, B. K., "Development of dry powders inhalers," *Recent Patent on Drud Delivery and Formulaton*, Vol. 1, 2007, pp. 11-21.

168. Benson, H. E. A., "Transdermal drug delivery: Penetration enhancement technique," *Current Drug Delivery*, Vol. 2, 2005, pp. 23-33.

169. Lee, R. E., "Effervescent Tablets," CSC Publishing, United States of America, 2010.

170. Wirth, D. D., Baertschi, S. W., Johnson, R. A., Maple, S. R., Miller, M. S., Hallenbeck, D. K., and Gregg, S. M., "Maillard reaction of lactose and fluoxetine hydrochloride a secondary amine," *Journal of Pharmaceutical Sciences*, Vol. 87, No. 1, 1998, pp. 31-39.

171. Laroque, D., Inisan, C., Berger, C., Vouland, É., Dufossé, L., and Guérard, F., "Kinetic study on the Maillard reaction. Consideration of sugar reactivity," *Food Chemistry*, Vol. 111, No. 4, 2008, pp. 1032-1042.

172. Weenen, H., "Reactive intermediates and carbohydrate fragmentation in Maillard chemistry," *Food Chemistry*, Vol. 62, No. 4, 1998, pp. 393-401.

173. Harding, L., Qi, S., Hill, G., Reading, M., and Craig, D. Q. M., "The development of microthermal analysis and photothermal microspectroscopy as novel approaches to

drug-excipient compatibility studies," *International Journal of Pharmaceutics*, Vol. 354, No. 1-2, 2008, pp. 149-157.

174. Garcia-Raso, A., Garcia-Raso, J. A., Mestres, R., and Sinisterra, J. V., "Mechanism of Michael addition of ethyl acetoacetate to chalcone catalyzed by activated Ba(OH)₂" *Reaction Kinetics and Catalysis Letters*, Vol. 28, No. 2, 1985, pp. 365-371.

175. Swamivelmanickam, M., Valliappan, K., Reddy, P. G., Madhukar, A., and Manavalan, R., "Preformulation studies for amoxicillin trihydrate and dicloxacillin sodium as mouth dissolve tablets," *International Journal of ChemTech Research*, Vol. 1, No. 4, 2009, pp. 1032-1035.

176. Smith, R. J. and Webb, M. J., *Analysis of Drug Impurities*, Blackwell, Singapore, 2007.

177. Brittain, H. G., "Methodology for the evaluation of chemical and physical interaction between drug substances and excipients," *Preformulation in Solid Dosage Form Development*, edited by C. M. Adeyeye and H. G. Brittain Informa Healthcare, New York, 2008, pp. 437-476.

178. Stuart, B., *Infrared Spectroscopy; Fundamentals and Application*, John Wiley and Sons, Sussex, 2004.

179. Hartauer, K. J. and Guillory, J. K., "A comparison of Diffuse Refluctance FT-IR sectroscopy and DSC in the characterization of drug excipient-interaction," *Drug Development and Industrial Pharmacy*, Vol. 17, No. 4, 1991, pp. 617-630.

180. Powers, M. C., "A new roundness scale for sedimentary particles," *Journal of Sedimentary Petrol*, Vol. 23, 1953, pp. 117-119.

181. Di Martino, P., Censi, R., Ledjan, M., and Martelli, S., "Influence of metronidazole particle properties on granule preprared by high-shear mixer granulator," *Drug Development and Industrial Pharmacy*, Vol. 33, 2007, pp. 121-131.

182. Zhang, Y., Law, Y., and Chakrabarti, S., "Physical properties and compact analysis of commonly used direct compression binders," *AAPS PharmSciTech*, Vol. 4, No. 4, 2003.

183. Narayan, P. and Hancock, B. C., "The relationship between the particle properties, mechanical behavior, and surface roughness of some pharmaceutical excipient compacts," *Materials Science and Engineering A*, Vol. 355, No. 1-2, 2003, pp. 24-36.

184. Narayan, P., Hancock, B. C., Hamel, R., Bergstrom, T. S., Childs, B. E., and Brown, C. A., "Differentiation of the surface topographies of pharmaceutical excipient compacts," *Materials Science and Engineering: A*, Vol. 430, No. 1-2, 2006, pp. 79-89.

185. Oshima, T., Zhang, Y. L., Hirota, M., Suzuki, M., and Nakagawa, T., "The effect of the types of mill on the flowability of ground powders," *Advanced Powder Technology*, Vol. 6, No. 1, 1995, pp. 35-45.

186. Venables, H. J. and Wells, J. I., "Powder mixing," *Drug Development and Industrial Pharmacy*, Vol. 27, No. 7, 2001, pp. 599-612.

187. Sun, C. C., "True density of microcrystalline cellulose," *Journal of Pharmaceutial Sciences*, Vol. 94, 2005, pp. 2132-2334.

188. Odeniyi, M. A., Abobarin, T. O., and Itiola, O. A., "Compressibility of binary mixtures of metronidazole with lactose and microcrystalline cellulose," *FARMACIA*, Vol. 56, No. 6, 2008, pp. 625-638.

189. Kachrimanis, K., Karamyan, V., and Malamataris, S., "Artificial neural networks (ANNs) and modeling of powder flow," *International Journal of Pharmaceutics*, Vol. 250, No. 1, 2003, pp. 13-23.

190. Rowe, C. R., Sheskey, P. J., and Owen, S. C., *Handbook of Pharmaceutical Excipients*, 5th ed., Pharmaceutical Press, Great Britain, 2006.

191. Sun, C. C., "Mechanism of moisture induced variations in true density and compaction properties of microcrystalline cellulose," *International Journal of Pharmaceutics,* Vol. 346, No. 1-2, 2008, pp. 93-101.

192. Kumar, V., de la Luz Reus-Medina, M., and Yang, D., "Preparation, characterization, and tabletting properties of a new cellulose-based pharmaceutical aid," *International Journal of Pharmaceutics*, Vol. 235, No. 1-2, 2002, pp. 129-140.

193. Emshanova, S. V., Sadchikova, S. P., and Zuev, A. P., "Drug particle shape and size control: A necessary factor for high-quality drug production," *Pharmceutical Chemistry Journal*, Vol. 41, No. 1, 2007, pp. 41-49.

194. Fogagnolo, J. B., Ruiz-Navas, E. M., Robert, M. H., and Torralba, J. M., "The effects of mechanical alloying on the compressibility of aluminium matrix composite powder," *Materials Science and Engineering A*, Vol. 355, No. 1-2, 2003, pp. 50-55.

195. Nicklasson, F., Johansson, B., and Alderborn, G., "Tabletting behaviour of pellets of a series of porosities: A comparison between pellets of two different compositions," *European Journal of Pharmaceutical Sciences*, Vol. 8, No. 1, 1999, pp. 11-17.

196. Mirmehrabi, M., Rohani, S., Murthy, K. S. K., and Radatus, B., "Solubility, dissolution rate and phase transition studies of ranitidine hydrochloride tautomeric forms," *International Journal of Pharmaceutics*, Vol. 282, No. 1-2, 2004, pp. 73-85.

197. Trifkovic, M. and Rohan, S., "Polymorphic generation through solvent selection," *Organic Process Research and Development*, Vol. 11, No. 1, 2007, pp. 138-143.

198. McGoverin, C. M., Ho, L. C. H., Zeitler, J. A., Strachan, C. J., Gordon, K. C., and Rades, T., "Quantification of binary polymorphic mixtures of ranitidine hydrochloride using NIR spectroscopy," *Vibrational Spectroscopy*, Vol. 41, No. 2, 2006, pp. 225-231.

199. Antonilêni, F. D., Ana Flavía, O., and de Souza, F. S., "Thermal studies of preformulates of metronidazole obtained by spray drying technique," *Journal of Thermal Analysis and Calorimetry,* Vol. 89, No. 3, 2008, pp. 775-781.

200. Gomes, A. P., Correia, L. P., and da Silva, M. O., "Development of thermalgravimetric methods for quantitative determination of metronidazole," *Journal of Thermal Analysis and Calorimetry*, Vol. 88, No. 2, 2007, pp. 383-387.

201. Kiss, D., Zelkó, R., Nováík, C., and Éhen, Z., "Application of DSC and NIRS to study the compatibility of metronidazole with different pharmaceutical excipients," *Journal of Thermal Analysis and Calorimetry*, Vol. 84, No. 2, 2006, pp. 447-451.

202. Pinto, M. F., de Moura, E., de Souza, F. S., and Macêdo, R., "Thermal compatibility studies of nitroimidazoles and excipients," *Journal of Thermal Analysis and Calorimetry*, Vol. 102, No. 1, 2010, pp. 323-329.

203. Bruni, G., Amici, L., Berbenni, V., Marini, A., and Orlandi, A., "Drug-excipient compatibility studies. Search of interaction indicators," *Journal of Thermal Analysis and Calorimetry*, Vol. 68, No. 2, 2002, pp. 561-573.

204. Ceipidor, U. B., Brizzi, E., Bucci, R., and Magri, A. D., "Using thermoanalytical data. Part 7. DSC/DTA/DTG peak shapes depending on operational settings, equipment features, sample kinetic and thermodynamic parameters," *Thermochimica Acta*, Vol. 247, No. 2, 1994, pp. 347-356.

205. Jamrógieweciz, M. and Lukasiak, J., "Short term monitor of photodegradation process in ranitidine hydrochloride observed by ATR-FTIR," *Journal of Food and Drug Analysis*, Vol. 17, No. 5, 2009, pp. 342-347.

206. Magnes, B. Z., Pines, D., Strashnikova, N., and Pines, E., "Hydrogen-bonding interactions of photoacids: Correlation of optical solvatochromism with IR absorption spectra," *Solid State Ionics*, Vol. 168, No. 3-4, 2004, pp. 225-233.

207. Singh, B. N. and Kim, K. H., "Drug delivery: Oral route," *Encyclopedia of Pharmaceutical Technology* Informa Healthcare, 2006, pp. 1242-1265.

208. Rudnic, E. M. and Schwartz, J. B., "Oral solid dosage forms," *Remington: The Science and Practice of Pharmacy*, edited by D. B. Troy Lippincott Williams and Wilkins, Baltimore, 2006, pp. 889-928.

209. Shyne, C. G., *Pharmaceutical Manufacturing Handbook: Production and Processes*, Vol. 10, John Wiley and Sons, Hoboken, 2008, pp. 235-245.

210. Bennet, B. and Graham, C., *Pharmaceutical production: An Engineering Guide*, Institution of Chemical Engineering, Warwickshire, 2003.

211. Allen Jr, L. V., Popovich, N. G., and Ansel, H. C., *Pharmaceutical Dosage Forms and Drug Delivery Systems*, 8th ed., Lippincott Williams and Wilikins, United States of America, 2005.

212. Mahato, R. I., "Tablets," *Pharmaceutical Dosage Forms and Drug Delivery* Taylor and Francis, 2007, pp. 153-172.

213. Di Martino, P., Joiris, E., and Martelli, S., "Particle interaction of lubricated or unlubricated binary mixtures according to their particle size and densification mechanism," *Il Farmaco*, Vol. 59, No. 9, 2004, pp. 747-758.

214. Pesonen, T., Paronen, P., and Ketolainen, J., "Disintegrant properties of an agglomerated cellulose powder," *International Journal of Pharmaceutics*, Vol. 57, No. 2, 1989, pp. 139-147.

215. Tadros, M. I., "Controlled-release effervescent floating matrix tablets of ciprofloxacin hydrochloride: Development, optimization and in vitro-in vivo evaluation in healthy human volunteers," *European Journal of Pharmaceutics and Biopharmaceutics*, Vol. 74, No. 2, 2010, pp. 332-339.

216. Wells, M. L., Wood, D. L., Sanftleben, R., Shaw, K., Hottovy, J., Weber, T., Geoffroy, J. M., Alkire, T. G., Emptage, M. R., and Sarabia, R., "Potassium carbonate as a desiccant in effervescent tablets," *International Journal of Pharmaceutics*, Vol. 152, No. 2, 1997, pp. 227-235.

217. Ciullo, P. A., *Industrial Mineral and Their Uses: A Handbook and Formulary*, Noyes Publication, Westwood, New Jersey, 1996.

218. Banker, G. S. and Rhodes, C. T., *Modern Pharmaceutics*, 4th ed., Vol. 121, Marcel Dekker, New York, 2002.

219. Florence, A. T., "Excipients: Not always inert," *An Introduction to Clinical Pharmaceutics*, edited by A. T. Florence Pharmaceutical Press, London, 2010, pp. 27-40.

220. Seidenari, S., "Cross-sensitization between azo dyes and para-amino compounds: A study of 236 azo-dye-sensitive subjects," *Contact Dermatitis*, Vol. 36, 1997, pp. 91-96.

221. Johansen, D. J., Frosch, P. J., and Lepoittevin, J., "Allergens from european baseline series," *Contact Dermatitis*, edited by D. J. Johansen, P. J. Frosch, and J. Lepoittevin, 5th ed. Springer, Berlin, 2010, pp. 565.

222. Zheng, J., *Formulation and Analytical Development for Low-dose Oral Drug Products*, John Wiley and Sons, Hoboken, New Jersey, 2009.

223. Ennis, B. J. and Litster, J. D., "Particle size enlargment," *Perry's Chemical Engineering*, edited by R. Perry and D. Green, 7th ed. McGraw-Hill, New York, 1997, pp. 20-89.

224. Iveson, S. M., Litster, J. D., Hapgood, K., and Ennis, B. J., "Nucleation, growth and breakage phenomena in agitated wet granulation processes: a review," *Powder Technology*, Vol. 117, No. 1-2, 2001, pp. 3-39.

225. Grünewald, G., Westhoff, B., and Kind, M., "Fluidized bed spray granulation: Nucleation studies with steady-state experiments," *Drying Technology*, Vol. 28, No. 3, 2010, pp. 349-360.

226. Charles-Williams, H. R., Wengeler, R., Flore, K., Feise, H., Hounslow, M. J., and Salman, A. D., "Granule nucleation and growth: Competing drop spreading and infiltration processes," *Powder Technology*, Vol. 206, No. 1-2, 2011, pp. 63-71.

227. Smirani-Khayati, N., Falk, V., Bardin-Monnier, N., and Marchal-Heussler, L., "Binder liquid distribution during granulation process and its relationship to granule size distribution," *Powder Technology*, Vol. 195, No. 2, 2009, pp. 105-112.

228. Bouwman, A. M., Visser, M. R., Eissens, A. C., Wesselingh, J. A., and Frijlink, H. W., "The effect of vessel material on granules produced in a high-shear mixer," *European Journal of Pharmaceutical Sciences*, Vol. 23, No. 2, 2004, pp. 169-179.

229. Goldszal, A. and Bousquet, J., "Wet agglomeration of powders: From physics toward process optimization," *Powder Technology*, Vol. 117, No. 3, 2001, pp. 221-231.

230. Benali, M., Gerbaud, V., and Hemati, M., "Effect of operating conditions and physico-chemical properties on the wet granulation kinetics in high shear mixer," *Powder Technology*, Vol. 190, No. 1-2, 2009, pp. 160-169.

231. Ritala, M., Jungersen, O., and Kristernsen, H. G., "A comparison between binder in the wet phase of granulation in a high shear mixer," *Drug Development and Industrial Pharmacy*, Vol. 12, 1986, pp. 1685-1700.

232. Iveson, S. M. and Litster, J. D., "Fundamental studies of granule consolidation part 2: Quantifying the effects of particle and binder properties," *Powder Technology*, Vol. 99, No. 3, 1998, pp. 243-250.

233. Giry, K., Genty, M., Viana, M., Wuthrich, P., and Chulia, D., "Multiphase versus single pot granulation process: Influence of process and granulation parameters on granules properties," *Drug Development and Industrial Pharmacy*, Vol. 32, No. 5, 2006, pp. 509-530.

234. Nieuwmeyer, F. J. S., van der Voort Maarschalk, K., and Vromans, H., "Granule breakage during drying processes," *International Journal of Pharmaceutics*, Vol. 329, No. 1-2, 2007, pp. 81-87.

235. Galland, S., Ruiz, T., and Delalonde, M., "Twin product/process approach for pellet preparation by extrusion/spheronisation: Part I: Hydro-textural aspects," *International Journal of Pharmaceutics*, Vol. 337, No. 1-2, 2007, pp. 239-245.

236. Wang, J., Wen, H., and Desai, D., "Lubrication in tablet formulations," *European Journal of Pharmaceutics and Biopharmaceutics*, Vol. 75, No. 1, 2010, pp. 1-15.

237. Bozic, D. Z., Dreu, R., and Vrecer, F., "Influence of dry granulation on compactibility and capping tendency of macrolide antibiotic formulation," *International Journal of Pharmaceutics*, Vol. 357, No. 1-2, 2008, pp. 44-54.

238. Poux, M., Fayolle, P., Bertrand, J., Bridoux, D., and Bousquet, J., "Powder mixing: Some practical rules applied to agitated systems," *Powder Technology*, Vol. 68, No. 3, 1991, pp. 213-234.

239. Sucker, H., Fuchs, P., and Speiser, P., *Pharmazeutische Technologie*, 2nd ed., Thieme Verlag, Stuttgart, 1991.

240. Itiola, O. A. and Pilpel, N., "Tableting characteristics of metronidazole formulations," *International Journal of Pharmaceutics*, Vol. 31, No. 1-2, 1986, pp. 99-105.

241. Di Martino, P., Censi, R., Malaj, L., Capsoni, D., Massarotti, D., and Martelli, S., "Influence of solvent and crystallization method on the crystal habit of metronidazole," *Journal of Crystal Reseach and Technology*, Vol. 42, No. 8, 2007, pp. 800-806.

242. Center for Drug Evaluation and Research (CDER), "Guidance for Industry: Powder Blends and Finished Dosage Units-Stratified In-Process Dosage Unit Sampling and Assessment," 2003, pp. 1-15, http://www.fda.gov/OHRMS/DOCKETS/98fr/03d-0493-gdl0001.pdf.

243. Center for Drug Evaluation and Research (CDER), "Guidance for Industry ANDAs: Blend Uniformity Analysis," 1999, http://www.fda.gov/OHRMS/DOCKETS/98fr/992635gd.pdf .

244. Yanagida, T., Matchett, A. J., Asmar, B. N., Langston, P. A., Walters, J. K., and Coulthard, J. M., "Dynamic response of segregated two-phase systems subjected to low magnitude vibration and its application to non-invasive monitoring of a powder mixing transition process," *Advanced Powder Technology*, Vol. 14, No. 5, 2003, pp. 571-588.

245. Rhodes, M., *Introduction to Powder Technology*, John Wiley and Sons Ltd, West Sussex, 2008.

246. Jullien, R. and Meakin, P., "A mechanism for particle size segregation in three dimensions," *Nature*, Vol. 344, No. 6265, 1990, pp. 425-427.

247. Israelachvili, J., *Intermolecular & Surface Forces*, 2nd ed., Academic Press Ltd 1995.

248. Hausman, D. S., Cambron, R. T., and Sakr, A., "Application of Raman spectroscopy for on-line monitoring of low dose blend uniformity," *International Journal of Pharmaceutics*, Vol. 298, No. 1, 2005, pp. 80-90.

249. Huang, C. Y. and Sherry Ku, M., "Prediction of drug particle size and content uniformity in low-dose solid dosage forms," *International Journal of Pharmaceutics*, Vol. 383, No. 1-2, 2010, pp. 70-80.

250. Zhang, Y. and Johnson, K. C., "Effect of drug particle size on content uniformity of low-dose solid dosage forms," *International Journal of Pharmaceutics*, Vol. 154, No. 2, 1997, pp. 179-183.

251. Vergote, G. J., De Beer, T. R. M., Vervaet, C., Remon, J. P., Baeyens, W. R. G., Diericx, N., and Verpoort, F., "In-line monitoring of a pharmaceutical blending process using FT-Raman spectroscopy," *European Journal of Pharmaceutical Sciences*, Vol. 21, No. 4, 2004, pp. 479-485.

252. Muzzio, F. J., Robinson, P., Wightman, C., and Dean, B., "Sampling practices in powder blending," *International Journal of Pharmaceutics*, Vol. 155, No. 2, 1997, pp. 153-178.

253. Grady, L. T., " Overview of compendial standards for solid oral dosage forms," *Drug Development and Industrial Pharmacy*, Vol. 15, No. 6&7, 1989, pp. 1105-1117.

254. United States Pharmacopoeia. Uniformity of Dosage Units. [31], 363. 2008. Rockville, Maryland, United States Pharmacopoeia Convention.
Ref Type: Serial (Book,Monograph)

255. Method of analysis: Pharmaceutical technical procedure: Uniformity of content of single-dose preparations. Fourth[5]. 2008. World Health Organization. International Pharmacopoeia.
Ref Type: Serial (Book,Monograph)

256. Nash, R. A.. Validation of pharmaceutical processes. Encyclopedia of Pharmaceutical Technology. Encylopedia of Pharmaceutical Technology, 3rd. 3928-3940. 2006. Informa Healthcare.
Ref Type: Abstract

257. Berthiaux, H., Marikh, K., and Gatumel, C., "Continuous mixing of powder mixtures with pharmaceutical process constraints," *Chemical Engineering and Processing: Process Intensification*, Vol. 47, No. 12, 2008, pp. 2315-2322.

258. Deng, T., Paul, K. A., Bradley, M. S. A., Immins, L., Preston, C., Scott, J. F., and Welfare, E. H., "Investigations on air induced segregation of pharmaceutical powders and effect of material flow functions," *Powder Technology*, Vol. 203, No. 2, 2010, pp. 354-358.

259. Ely, D., Chamarthy, S., and Carvajal, M. T., "An investigation into low dose blend uniformity and segregation determination using NIR spectroscopy," *Colloids and Surfaces A: Physicochemical and Engineering Aspects*, Vol. 288, No. 1-3, 2006, pp. 71-76.

260. Schæfer, T., Johnsen, D., and Johansen, A., "Effects of powder particle size and binder viscosity on intergranular and intragranular particle size heterogeneity during high shear granulation," *European Journal of Pharmaceutical Sciences*, Vol. 21, No. 4, 2004, pp. 525-531.

261. Schwartz, J. B., Flamholz, J. R., and Press, R. H., "Computer optimization of pharmaceutical formulations I: General procedure," *Journal of Pharmaceutical Sciences*, Vol. 62, No. 7, 1973, pp. 1165-1170.

262. Fonner, D. E. Jr., Buck, R., and Banker, G. S., "Mathematical optimization techniques in drug product design and process analysis," *Journal of Pharmaceutical Sciences*, Vol. 59, No. 11, 1970, pp. 1587-1596.

263. Singh, B., Kumar, R., and Ahuja, N., "Optimizing drug delivery using systematic design of experiments Part I: Fundamental aspects," *Critical Reviews in Therapeutic Drug Carrier Systems*, Vol. 22, No. 1, 2004, pp. 27-105.

264. Aslan, N., "Application of response surface methodology and central composite rotatable design for modelling and optimization of multi-gravity separator for chromite concentration," *Powder Technology*, Vol. 185, No. 1, 2008, pp. 80-86.

265. Lewis, G. A., "Optimization methods," *Encylopedia of Pharmaceutical Technology*, edited by J.Swarbrick Informa Healthcare, London, 2002, pp. 1922-1937.

266. Myers, R. H., Montgomery, D. C., and Anderson-Cook, C. M., *Response Surface Methodology:Process and Product Optimization Using Designed Experiments*, 3rd ed., John Wiley and Sons, Hoboken, New Jersey, 2009.

267. Myers, R. H. and Montgomery, D. C., *Response surface methodology: Process and Product Optimization Using Designed Experiments*, 2nd ed., John Wiley and Sons, Hoboken, New Jersey, 2002.

268. U.S.Food and Drug Administration, "Guidance for industry: Immediate Release Solid Oral Dosage Forms Scale Up and Post Approval Changes," Center for Drug Evaluation and Research, Rockville, Maryland, 1995.

269. Bodea, A. and Leucuta, S. E., "Optimization of propranolol hydrochloride sustained release pellets using factorial design," *International Journal of Pharmaceutics*, Vol. 154, No. 1, 1997, pp. 49-57.

270. Mcleod, A. D., Lam, F. C., Gupta, P. K., and Hung, C. T., "Optimized synthesis of polyglutaraldehyde nanoparticles using central composite design," *Journal of Pharmaceutical Science*, Vol. 77, No. 8, 1988, pp. 704-710.

271. Bodea, A. and Leucuta, S. E., "Optimization of propranolol hydrochloride sustained release pellets using Box-Behnken design and desirability function," *Drug Development and Industrial Pharmacy*, Vol. 24, No. 2, 1998, pp. 145-155.

272. Bodea, A. and Leucuta, S. E., "Optimization of hydrophilic matrix tablets using D-optimal design," *International Journal of Pharmaceutics*, Vol. 153, No. 2, 1997, pp. 247-255.

273. Draper, N. R. and Lin, D. K. J., "Response surface methodology," *Design and Analysis of Experiments*, edited by S. Ghosh and C. R. Rao, 5th ed. North-Holland, Amsterdam, 1996, pp. 343-375.

274. Cohen, J. L., Hubert, L. J., Rhodes, C. T., Robinson, J. R., Roseman, T. J., and Shefter, E., "The development of USP dissolution and drug standards," *Pharmceutical Research*, Vol. 7, No. 10, 1990, pp. 983-987.

275. Zahirul, M. and Khan, I., "Dissolution testing for sustained or controlled release oral dosage forms and correlation with in vivo data: Challenges and opportunities.," *International Journal of Pharmaceutics*, Vol. 140, 1996, pp. 131-143.

276. Mansoor, M. A. and Sandman, J. B., "Dissolution phenomena," *Applied Physical Pharmacy* McGraw Hill and Companies, Inc., United States of America, 2003, pp. 311.

277. Ramchandani, M. and Robinson, D., "In vitro and in vivo release of ciprofloxacin from PLGA 50:50 implants," *Journal of Controlled Release*, Vol. 54, No. 2, 1998, pp. 167-175.

278. Waterbeemd, H. and Testa, B., *Drug Bioavailability: Estimation of Solubility, Permeability, Absorption and Bioavailability*, Wiley-VCH Verlag GmbH & Co KGaA, Weinheim, 2009.

279. O'Hara, T., Dunne, A., Butler, J., and Devane, J., "A review of the methods used to compare dissolution profile data," *Pharmacetuical Science and Technology*, Vol. 1, No. 5, 1998, pp. 214-223.

280. Metronidazole. [33], 3877. 2010. Rockville, Maryland, United States Pharmacopeia Convention. United States Pharmacopoeia.
Ref Type: Serial (Book,Monograph)

281. Ranitidine. [33], 4556. 2010. Rockville, Maryland, United States Pharmacopeia Convention. United States Pharmacopoeia.
Ref Type: Serial (Book,Monograph)

282. U.S.Food and Drug Administration, "Guidance for industry: Waiver of in vivo bioavailability and bioequivalence studies for immediate-release solid oral dosage forms based on a biopharmaceutics classification system," U.S Department of Health and Human Services, Food and Drug Administration, Center for Drug Evaluation and Research, Rockville, Maryland, 2000.

283. Ahmad, M., Pervaiz, K., Murtaza, G., and Razman, M., "Pharmacokinetic modelling of microencapsulated metronidazole," *Acta Pharmacologica Sinica*, Vol. 44, 2009, pp. 674-679.

284. Blume, H. H. and Schug, B. S., "The biopharmaceutics classification system (BCS): Class III drugs better candidates for BA/BE waiver?," *European Journal of Pharmaceutical Sciences*, Vol. 9, No. 2, 1999, pp. 117-121.

285. Jacobson, T. M. and Wertheimer, A. I., *Modern Pharmaceutical Industry: A Primer*, Jones and Bartlett Publisher, United States of America, 2010.

286. Kumar, V. and Tewari, D., "Dissolution," *Remington: The Science and Practice of Pharmacy*, edited by D. B. Troy Lippincott Williams and Wilkins, Baltimore, 2006, pp. 672-688.

287. Paradkar, A. R., *Biopharmaceutics and Pharmacokinetics*, 3rd ed., Nirali Prakashan, Pune, 2008.

288. Balasubramaniam, J. and Bee, T., "The influence of superdisintegrant choice on the rate of drug dissolution from oral solid dosage forms," *Pharmaceutical Technology Europe*, Vol. 21, No. 9, 2009.

289. Eddington, N. D., Ashraf, M., Augsburger, L. L., Leslie, J. L., Fossler, M. J., Lesko, L. J., Shah, V. P., and Rekhi, G. S., "Identification of formulation and manufacturing variables that influence in vitro dissolution and in vivo bioavailability of propranolol hydrochloride tablets," *Pharmaceutical Development and Technology*, Vol. 3, No. 4, 1998, pp. 535-547.

290. Zhang, G., Yihong, Q., and Chen, Y., *Developing Solid Oral Dosage Forms:Pharmaceutical Theory and Practice*, Academic Press, United States of America, 2009, pp. 328.

291. Delalonde, M. and Ruiz, T., "Dissolution of pharmaceutical tablets: The influence of penetration and drainage of interstitial fluids," *Chemical Engineering and Processing: Process Intensification*, Vol. 47, No. 3, 2008, pp. 370-376.

292. Aiache, J. M., Aoyagi, H., Blune, J., Dressman, H. D., Friedel, L. T., and Gray, V., "FIP guidance for dissolution testing of solid oral products," *Dissolution Technology*, Vol. 4, No. 4, 1997, pp. 5-14.

293. Borst, I., Ugwu, S., and Bekett, A., "New and extended application for USP drug release Apparatus 3," *Dissolution Technology*, Vol. 4, No. 1, 1997, pp. 11-16.

294. Gohel, M. C. and Jogani, P. D., "Functionality testing," *Pharmaceutical Technology North America*, Vol. 26, No. 3, 2002, pp. 64.

295. Wan, L. S. C. and Prasad, K. P. P., "Uptake of water by excipients in tablets," *International Journal of Pharmaceutics*, Vol. 50, No. 2, 1989, pp. 147-153.

296. Gordon, M. S., Rudraraju, V. S., Rhie, J. K., and Chowhan, Z. T., "The effect of aging on the dissolution of wet granulated tablets containing super disintegrants," *International Journal of Pharmaceutics*, Vol. 97, No. 1-3, 1993, pp. 119-131.

297. Bolhuis, G. K., Zuurman, K., and te Wierik, G. H. P., "Improvement of dissolution of poorly soluble drugs by solid deposition on a super disintegrant. II. The choice of super disintegrants and effect of granulation," *European Journal of Pharmaceutical Sciences*, Vol. 5, No. 2, 1997, pp. 63-69.

298. Becker, D., Rigassi, T., and Bauer-brandl, A., "Effectiveness of binders in wet granulation: A comparison using model formulations of different tabletability," *Drug Development and Industrial Pharmacy*, Vol. 23, No. 8, 1997, pp. 791-808.

299. Bühler, V., *Polyvinylpyrrolidone Excipients for Pharmaceuticals*, Springer-Verlag, Germany, 2005.

300. Chitu, T. M., Oulahna, D., and Hemati, M., "Wet granulation in laboratory scale high shear mixers: Effect of binder properties," *Powder Technology*, Vol. 206, No. 1-2, 2011, pp. 25-33.

301. Boerefijn, R., Juvin, P. Y., and Garzon, P., "A narrow size distribution on a high shear mixer by applying a flux number approach," *Powder Technology*, Vol. 189, No. 2, 2009, pp. 172-176.

302. Mills, P. J. T., Seville, J. P. K., Knight, P. C., and Adams, M. J., "The effect of binder viscosity on particle agglomeration in a low shear mixer/agglomerator," *Powder Technology*, Vol. 113, No. 1-2, 2000, pp. 140-147.

303. Ferrero, C., Muñoz, N., Velasco, M. V., Muñoz-Ruiz, A., and Jiménez-Castellanos, R., "Disintegrating efficiency of croscarmellose sodium in a direct compression formulation," *International Journal of Pharmaceutics*, Vol. 147, No. 1, 1997, pp. 11-21.

304. Guerrero Arevalo, C., Monedero Perales, M. C., and Muñäoz Ruiz, A., "Disintegrants and superdisintegrants. Study of disintegration mechanisms," *Ciencia y Tecnologia Pharmaceutica*, Vol. 15, No. 1, 2005, pp. 11-21.

305. Kyriacos, S. and Dimassi, H., "Formulation optimization study for an immediate-release tablet," *International Journal of Pharmaceutical Compounding*, Vol. 13, No. 3, 2009, pp. 259-261.

306. Late, S. G., Yu, Y. Y., and Banga, A. K., "Effects of disintegration-promoting agent, lubricants and moisture treatment on optimized fast disintegrating tablets," *International Journal of Pharmaceutics*, Vol. 365, No. 1-2, 2009, pp. 4-11.

307. Uzunovc, A. and Vranic, E., "Effect of magnesium stearate concentration on dissolution properties of ranitidine hydrochloride coated tablets," *Bosnian journal of basic medical sciences / Association of Basic Medical Sciences*, Vol. 7, No. 3, 2007, pp. 279-283.

308. Gibaldi, M., Lee, A., and Desai, A., "Oral drug delivery systems," *Gibaldi Drug Delivery Systems in Pharmaceutical Care*, edited by L. Mary and A. Desai American Society of Health System Pharmacists, 2007, pp. 23.

309. Gupta, A., Hunt, R., Shah, R., Sayeed, V., and Khan, M., "Disintegration of highly soluble immediate release tablets: A surrogate for dissolution," *AAPS PharmSciTech*, Vol. 10, No. 2, 2009, pp. 495-499.

310. Parmar, J. and Rane, M.. Tablet Formulation Design and Manufacture: Oral Immediate Release Application. Pharma Times 41[4], 21-29. 2009.
Ref Type: Abstract

311. Dilova, V., Miteva, Z., and Arnaudova, P., "Influence of lubricants on physicomechanical and kinetic parameters of tablets," *Pharmacia*, Vol. 53, No. 1, 2006, pp. 21-23.

312. Massimo, G., Catellani, P. L., Santi, P., Bettini, R., Vaona, G., Bonfanti, A., Maggi, L., and Colombo, P., "Disintegration propensity of tablets evaluated by means of disintegrating force kinetics," *Pharmaceutical Development and Technology*, Vol. 5, No. 2, 2000, pp. 163-169.

313. Cheong, C., Barner, J. C., Lawson, K. A., and Johnsrud, M. T., "Patient adherence and reimbursement amount for antidiabetic fixed dose combination products compared with dual therapy among texas medicaid recipients," *Clinical Therapeutics*, Vol. 30, No. 10, 2008, pp. 1893-1907.

314. Sapienza, S., Sacco, P., Floyd, K., DiCesare, J., and Doan, Q. D., "Results of a pilot pharmacotherapy quality improvement program using fixed dose, combination amlodipine/benazepril antihypertensive therapy in a long-term care setting," *Clinical Therapeutics*, Vol. 25, No. 6, 2003, pp. 1872-1887.

315. Agrawal, S., Kaur, K. J., Singh, I., Bhade, S. R., Kaul, C. L., and Panchagnula, R., "Assessment of bioequivalence of rifampicin, isoniazid and pyrazinamide in a four drug fixed dose combination with separate formulations at the same dose levels," *International Journal of Pharmaceutics*, Vol. 233, No. 1-2, 2002, pp. 169-177.

316. "Fixed Dose Combination Tablet for the Treatment of Tuberculosis," World Health Organization, WHO/CDC/TB/99.267, Geneva, 1999.

317. International Conference on Harmonisation of Technical Requirments for Registration of Pharmaceutical for Human Use, "Pharmaceutical Development Q8 (R2)," International Conference on Harmonization, Geneva, 2009.

318. Monteleon, P. R. J. and Duffull, B. S., "Analysis of simulations: Choice of best design," *Simulation for Designing Clinical Trial: Pharmacokinetic Pharmacodynamic Modelling Perspective*, edited by Hui C Kimko and Stephen C Duffull Marcel Dekker Inc, New York, 2003, pp. 171-183.